

Virus-like Particle Production Using Cowpea Mosaic Virus-based Vectors

by

Eva Christiane Thuenemann

This thesis is submitted in partial fulfilment of the requirements of the degree of
Doctor of Philosophy at the University of East Anglia

John Innes Centre, Norwich
September, 2010

© This copy of the thesis has been supplied on condition that anyone who consults it is understood to recognise that its copyright rests with the author and that no quotation from the thesis, nor any information derived therefrom, may be published without the author's prior, written consent.



The Green Vaccine Machine, © Eva Thuenemann, 2009

DECLARATION

I hereby certify that the work contained within this thesis is my own original work, except where due reference is made to other contributing authors. This thesis is submitted for the degree of Doctor of Philosophy at the University of East Anglia and has not been submitted to this or any other university for any other qualification.

Eva C. Thuenemann

ABSTRACT

Transient expression is fast becoming a widely used platform for the rapid expression of pharmaceutical proteins in plants. In order to fully exploit the high-level expression achieved from the Cowpea Mosaic Virus-based *HyperTrans* (CPMV-*HT*) transient expression system, the pEAQ vector series was developed. These vectors allow for easy and quick direct restriction cloning or high-throughput Gateway cloning into the CPMV-*HT* system. They are tailored for high-level transient expression through incorporation of a suppressor of gene silencing and gene of interest on the same T-DNA. Furthermore, the T-DNA region can accommodate multiple expression cassettes to ensure same-cell coexpression of multiple proteins. The pEAQ vectors are now a widely used toolbox for plant transient expression.

The pEAQ vectors have been used for the expression and assembly of virus-like particles (VLPs) of Hepatitis B core (HBcAg) and Bluetongue virus (BTV) in plants. The widely used epitope carrier HBcAg can be efficiently expressed using this system. The use of dimeric, tandem HBcAg (tHBcAg) constructs alleviates the steric constraints usually encountered upon display of large foreign polypeptides on the outer surface of HBcAg. Assembled tHBcAg particles displaying functional green fluorescent protein have been produced and purified to enable structural analysis. The expression of tHBcAg constructs for the display of two different, medically relevant polypeptides has also been achieved.

Efficient, high-level expression and assembly of the four main structural proteins of BTV using the pEAQ vectors has allowed for purification of high-quality VLP preparations for use in immunogenicity studies. Relative protein expression levels were modulated by codon optimization or selective use of the *HT* leader sequence. The heteromultimeric BTV VLP represents the most complex VLP to have been expressed in plants to date. This technology has also been used to produce Bluetongue VLPs encapsidating different fluorescent proteins – a useful tool for the study of BTV infection.

ACKNOWLEDGMENTS

First and foremost, I would like to thank my supervisor, George Lomonossoff, for his encouragement, enthusiasm and always open door. He gave me the freedom to explore some of my own crazy ideas, yet was always there to guide me and calm my nerves – Thank you! I would also like to thank the other members of my supervisory committee: Alison Smith for her mentoring throughout my PhD and for the encouragement to try new things, and Tony Maxwell. The drive to do a PhD and to choose a molecular farming project in particular has been shaped by several inspiring teachers and researchers whom I have had the pleasure of working with in the past. Of these, I would especially like to thank Ralf Zensen, Sebastian Springer, Hugh Mason and Attila Molnár.

I have been very fortunate to work in such a supportive, diverse and extremely fun lab group, and would like to thank the present and past members of George's lab. My particular thanks go to Keith, Stephan, Pooja, Sandra and Frank who have all helped me immensely through their willingness to share the odd "crisis coffee" and to lend an ear.

Having the opportunity to work with and visit several collaborating labs has certainly enriched my project and made day-to-day lab work very interesting. For their hospitality, I would especially like to thank my collaborators in Oxford, Robert Gilbert and Alistair Siebert; in Leeds, Dave Rowlands; and in Pirbright, Terry Jackson and Sarah Gold. I am also very grateful to Ann Meyers and Ed Rybicki, as well as Polly Roy for enabling me to start my work on Bluetongue Virus when everyone was busy dealing with the UK Bluetongue disease outbreak.

Last, but certainly not least, my special thanks go to my family and Jakob, for their support and unwavering belief in me.

TABLE OF CONTENTS

DECLARATION	3
ABSTRACT	4
ACKNOWLEDGMENTS	5
TABLE OF CONTENTS	6
LIST OF FIGURES	11
LIST OF TABLES	14
ABBREVIATIONS	15
1 GENERAL INTRODUCTION	18
1.1 VIRUS-LIKE PARTICLES	18
1.1.1 Viral Vaccines: Comparison of Existing Technologies	18
1.1.2 VLP Expression: The Story So Far	22
1.1.3 Epitope Display	24
1.1.4 Bionanotechnology	26
1.2 MOLECULAR FARMING: PLANT-BASED EXPRESSION SYSTEMS	26
1.2.1 Stable Integration	27
1.2.2 Transient Expression	28
1.2.3 Gene Silencing Suppression	29
1.2.4 Multiple Protein Expression	30
1.3 PLANT VIRAL VECTORS AND THE CPMV-BASED EXPRESSION SYSTEMS	32
1.3.1 Full Viral Vectors	32
1.3.2 Deconstructed Viral Vectors	33
1.3.3 Cowpea Mosaic Virus-based Expression Systems	36
1.3.3.1 Full CPMV viral vector	36
1.3.3.2 Deconstructed and deleted CPMV viral vectors	37
1.3.3.3 HyperTrans: CPMV-HT	39
1.4 AIMS OF THIS PROJECT	40
2 GENERAL MATERIALS AND METHODS	41
2.1 MEDIA, BUFFERS AND SOLUTIONS	41
2.2 MOLECULAR CLONING TECHNIQUES	42
2.2.1 Isolation / Purification of Plasmid DNA and DNA Fragments	42
2.2.2 Polymerase Chain Reaction (PCR)	42

2.2.3	Restriction Endonuclease Digestion.....	43
2.2.4	DNA Modification.....	43
2.2.5	DNA Ligation.....	44
2.2.6	Site-Directed Mutagenesis.....	44
2.2.7	GATEWAY® Cloning.....	44
2.2.8	DNA Sequencing.....	46
2.2.9	Agarose Gel Electrophoresis.....	46
2.2.10	Transformation of Competent Cells	46
2.3	CLONING VECTORS.....	47
2.3.1	pM81-FSC2.....	47
2.3.2	pBINPLUS.....	48
2.3.3	pENTR-ET2 and pDEST-BINPLUS	48
2.3.4	pEAQ vector series	48
2.4	TRANSIENT EXPRESSION OF PROTEINS IN <i>NICOTIANA BENTHAMIANA</i>	49
2.4.1	Transformation of <i>Agrobacterium tumefaciens</i>	49
2.4.2	Plant Growth Conditions	49
2.4.3	Agroinfiltration.....	49
2.4.4	Harvesting.....	50
2.4.5	Confocal Microscopy.....	50
2.4.6	Photography	51
2.5	PROTEIN ANALYSIS.....	52
2.5.1	Protein Extraction.....	52
2.5.2	Polyacrylamide Gel Electrophoresis (PAGE).....	52
2.5.3	Coomassie Blue Staining.....	52
2.5.4	Mass Spectrometry	53
2.5.5	Western blotting and Immunodetection.....	53
2.5.6	Quantification	54
2.5.6.1	UV irradiation of leaves.....	54
2.5.6.2	Bradford assay.....	54
2.5.6.3	Enzyme-linked Immunosorbent Assay (ELISA).....	55
2.5.6.4	GFP Fluorescence Assay.....	55
2.5.6.5	A280.....	55
2.6	VLP PURIFICATION.....	56
2.6.1	Density gradient centrifugation.....	56
2.6.2	Size-Exclusion Chromatography (SEC).....	56
2.6.3	Ultrafiltration.....	57
2.6.4	Dialysis.....	57

2.7	VLP ANALYSIS.....	57
2.7.1	Absorbance at 280nm.....	57
2.7.2	Dynamic Light Scattering (DLS)	57
2.7.3	Transmission Electron Microscopy (TEM)	58
2.7.4	Native Agarose Gel Electrophoresis.....	58
2.8	SOFTWARE.....	59
3	EXPRESSION VECTOR DEVELOPMENT	60
3.1	INTRODUCTION	60
3.1.1	The Existing CPMV Cloning Vectors.....	60
3.1.2	Recent Plant Binary Vector Developments	62
3.1.3	Aims of this Chapter	63
3.2	SPECIFIC MATERIALS AND METHODS	64
3.2.1	Construction of pENTR-ET2 and pDEST-BINPLUS.....	64
3.2.2	Construction of the pEAQ Series.....	65
3.2.3	GFP Extraction	68
3.2.4	GFP assay	68
3.2.5	YFP + CFP Expression and Confocal Microscopy	68
3.3	RESULTS.....	69
3.3.1	Gateway® Compatible Vectors for Subcloning.....	69
3.3.2	Streamlining of the pBINPLUS Binary Vector Backbone.....	73
3.3.3	The pEAQ Vector Series	75
3.3.4	The pEAQ Vectors Retain their High Expression Capability	78
3.3.5	Gateway Compatible pEAQ Vectors for High-Throughput Screening.....	79
3.3.6	Consistent Co-expression with pEAQexpress	82
3.4	DISCUSSION	86
4	EXPRESSION OF HEPATITIS B TANDEM CORE-LIKE PARTICLES	91
4.1	INTRODUCTION	91
4.1.1	Hepatitis B Virus	91
4.1.2	Hepatitis B Antigen and Particle structure	93
4.1.3	HBcAg Immunogenicity and Display of Foreign Antigens.....	96
4.1.4	HBcAg Expression in Plants.....	96
4.1.5	Tandem Core Technology.....	97
4.1.6	Aims of this Chapter	99
4.2	SPECIFIC MATERIALS AND METHODS	100
4.2.1	Cloning	100

4.2.2	Extraction of HB Tandem Core Particles.....	101
4.2.3	Sucrose Gradients.....	102
4.2.4	Cryo-EM.....	102
4.3	RESULTS.....	103
4.3.1	HBcAg and Tandem Core Gene Expression	103
4.3.2	HBcAg and Tandem Core Accumulation Over Time.....	107
4.3.3	Influence of Displayed Epitopes on Protein Solubility.....	109
4.3.4	Plant-produced HB Tandem Core Antigens Assemble into Core-like Particles ...	112
4.3.5	Whole Protein Insertions Allow Tandem Core Assembly.....	116
4.3.6	Cryo-Electron Microscopy of GFP-Tandem Cores.....	119
4.3.7	Presence of the Arginine-rich C-Terminus Impacts Nucleic Acid Encapsidation	120
4.3.8	Summary.....	122
4.4	DISCUSSION	124
5	EXPRESSION AND ASSEMBLY OF BTV-10 STRUCTURAL PROTEINS	130
5.1	INTRODUCTION	130
5.1.1	Current BTV Vaccines	131
5.1.2	Life Cycle.....	132
5.1.3	BTB Capsid Structure and Assembly.....	134
5.1.3.1	<i>Subcore-like particles (SCLP)</i>	134
5.1.3.2	<i>Core-like particles (CLP)</i>	136
5.1.3.3	<i>Virus-like particles (VLP)</i>	137
5.1.4	Aims of This Chapter	138
5.2	SPECIFIC MATERIALS AND METHODS	139
5.2.1	Cloning	139
5.2.2	Extraction Buffers.....	140
5.3	RESULTS.....	140
5.3.1	Expression and Interaction of VP3 and VP7	140
5.3.2	CLP Assembly is not Inhibited by Affinity Tagging of VP3	142
5.3.3	The Timecourse of Accumulation of VP5, VP2 and NS1 Varies	144
5.3.4	Co-expression of the Four Structural Proteins of BTB-10.....	146
5.4	DISCUSSION	149
6	EXPRESSION OF BTB-8 VIRUS-LIKE PARTICLES	151
6.1	INTRODUCTION	151
6.1.1	Aims of This Chapter	151
6.2	SPECIFIC MATERIALS AND METHODS	152
6.2.1	Cloning	152

6.2.2	BTV Extraction and Purification	154
6.2.2.1	<i>Extraction buffers</i>	154
6.2.2.2	<i>Core-like particles</i>	154
6.2.2.3	<i>Virus-like particles</i>	155
6.3	RESULTS.....	155
6.3.1	Structural Protein Expression from Wild-type and Codon-optimised Genes.....	155
6.3.2	Self-assembly of SCLPs by Expression of VP3.....	160
6.3.3	Assembly of CLPs by Co-Expression of VP3 and VP7	162
6.3.4	Assembly of VLP by Co-expression of VP3, VP7, VP5 and VP2	163
6.3.5	Stoichiometry: Optimization of Relative VLP Yield.....	165
6.3.5.1	<i>Modulation of relative expression levels by targeted use of wild-type genes</i>	166
6.3.5.2	<i>Expression of four structural proteins and P19 from a single T-DNA</i>	168
6.3.5.3	<i>Restriction of VP3 expression by targeted use of wild-type 5'UTR</i>	172
6.3.6	Particle Purification.....	174
6.4	DISCUSSION	182
7	EXPRESSION AND USE OF FLUORESCENT BTV-LIKE PARTICLES	187
7.1	INTRODUCTION	187
7.1.1	Aims of this chapter.....	189
7.2	SPECIFIC MATERIALS AND METHODS	189
7.2.1	Cloning.....	189
7.2.2	Particle Purification.....	190
7.2.3	Uptake studies.....	191
7.3	RESULTS.....	192
7.3.1	Construction of pEAQ-HT-GFP:BTv8.3co	192
7.3.2	Expression of GFP:VP3 and Association with BTV Structural Proteins.....	192
7.3.3	Optimization of fVLP yield and Integrity.....	197
7.3.4	Internalization of Fluorescent BTV-like Particles by Mammalian Cells.....	200
7.3.5	Ruby + Sapphire.....	204
7.3.6	Intracellular localization of GFP:VP3 in Plant Cells	207
7.4	DISCUSSION	208
8	DISCUSSION AND OUTLOOK	214
	REFERENCES	221
	APPENDIX A: TABLE OF CONSTRUCTS.....	238
	APPENDIX B: SEQUENCES OF CODON-OPTIMIZED BTV8 GENES	241
	APPENDIX C: PUBLICATION OF PEAQ VECTORS.....	245

LIST OF FIGURES

CHAPTER 1

Figure 1.1: Examples of full virus and deconstructed virus vector systems.34

Figure 1.2: Evolution of the CPMV polypeptide expression system.38

CHAPTER 2

Figure 2.1: Schematic representation of Gateway cloning and Gateway vectors for subcloning of CPMV expression cassettes.....45

CHAPTER 3

Figure 3.1: Schematic representation of pM81-FSC2 and pBINPLUS, the key cloning vectors of the CPMV expression system in 2007.61

Figure 3.2: Schematic representation of pENTR-ET2 and pDEST-BINPLUS, Gateway compatible versions of the key cloning vectors of the CPMV expression system.....70

Figure 3.3: Workflow comparison of restriction cloning and Gateway cloning.71

Figure 3.4: The presence of Gateway attB sites flanking the CPMV expression cassette does not negatively affect expression levels of GFP.72

Figure 3.5: Schematic representation of the production of the first pEAQ vector.74

Figure 3.6: Schematic representation of T-DNA regions of the core pEAQ-series vectors.77

Figure 3.7: GFP expression levels of pEAQ vectors are comparable to those of the parent plasmid.....79

Figure 3.8: The pEAQ-HT-DEST Gateway vectors allow high-level expression of His-tagged or untagged proteins.81

Figure 3.9: Schematic representation of T-DNA regions of the ECFP and EYFP constructs.83

Figure 3.10: Co-expression of two proteins from a single T-DNA is more homogeneous than co-infiltration.84

CHAPTER 4

Figure 4.1: Schematic representation of the genome structure of HBV.....92

Figure 4.2: Hepatitis B core antigen primary, tertiary and quaternary structure.94

Figure 4.3: Hepatitis B tandem core protein and gene constructs.....98

Figure 4.4: Schematic representation of the Hepatitis B tandem core constructs.104

Figure 4.5: Hepatitis B tandem cores can be transiently expressed in *Nicotiana benthamiana*.106

Figure 4.6: Quantification of extractable Hepatitis B core antigen over time.....	108
Figure 4.7: Epitope presentation at the c/e1-loop significantly increases aggregation of tandem core proteins.	110
Figure 4.8: Density gradient analysis of HB tandem cores.	113
Figure 4.9: Plant-produced Hepatitis B tandem cores assemble into particles.....	115
Figure 4.10: Size distribution of plant- and <i>E. coli</i> -produced monomeric and tandem HB particles.....	116
Figure 4.11: GFP tandem core fusions are expressed in plants and assemble into fluorescent core-like particles.	118
Figure 4.12: CryoEM reconstructions of HB tandem cores displaying GFP.	119
Figure 4.13: Heterotandem cores encapsidate plant nucleic acid, while homotandem cores are empty.	121
CHAPTER 5	
Figure 5.1: Bluetongue virus replication cycle.....	133
Figure 5.2: Bluetongue virus particle structures.	135
Figure 5.3: Expression and co-expression of core proteins VP3 and VP7.	141
Figure 5.4: Assembly potential of C-terminally His-tagged core proteins.....	143
Figure 5.5: Accumulation of BTV-10 structural and non-structural proteins is time-dependent.	145
Figure 5.6: BTV-10 structural proteins assemble into particles.....	147
CHAPTER 6	
Figure 6.1: Codon optimization increases the expression level of BTV-8 structural proteins by varying amounts.....	157
Figure 6.2: BTV-8 proteins are toxic to <i>N. benthamiana</i> in some combinations.....	158
Figure 6.3: BTV-8 VP3 is able to self-assemble when expressed alone.	161
Figure 6.4: Co-expression of BTV-8 VP3 and VP7 enables assembly of core-like particles.	163
Figure 6.5: Co-expression of four BTV-8 structural proteins enables assembly of virus-like particles.....	164
Figure 6.6: Co-expression of codon-optimized VP5 and VP2 with wild-type VP7 and VP3 reduces the over-representation of VP3 in particle preparations.	167
Figure 6.7: Schematic representation of the construction of an expression clone encoding four BTV structural proteins within one T-DNA.....	169

Figure 6.8: Expression of all BTV-8 structural proteins from a single T-DNA reduces over-representation of VP3.....	171
Figure 6.9: Expression of a VP3 construct with a wild-type CPMV RNA-2 leader increases the yield of stoichiometrically correct VLP fractions.....	173
Figure 6.10: Iodixanol gradients are more suited to the separation of BTV particle species than sucrose gradients.....	176
Figure 6.11: VLP integrity preservation is better in TEM grids prepared from sucrose fractions than iodixanol fractions.....	177
Figure 6.12: Purification of BTV-8 VLP intended for immunogenicity studies.....	178
Figure 6.13: Preparations of purified BTV-8 VLPs contain some particles with associated halos.....	180

CHAPTER 7

Figure 7.1: Design of a GFP:VP3 fusion construct.....	193
Figure 7.2: GFP:VP3 fusion protein is expressed in <i>N. benthamiana</i> leaf tissue and sediments in sucrose gradients.....	194
Figure 7.3: C-terminal fusion of GFP to VP3 does not significantly affect the gradient sedimentation pattern of co-expressed BTV-8 structural proteins.....	196
Figure 7.4: Lower expression levels of GFP:VP3 with a wild-type leader result in a reduced over-representation of fCLP in fVLP preparations.....	198
Figure 7.5: Purified fluorescent VLP are morphologically indistinguishable from normal VLP.....	199
Figure 7.6: Plant-produced BTV-8 fVLP bind BHK cells and are internalized.....	202
Figure 7.7: Plant-produced BTV-8 fVLP bind BHK cells and are internalized (Part 2).....	203
Figure 7.8: Production of fluorescent BTV-8 CLP and VLP with three different fluorophores.....	205
Figure 7.9: Core-like and virus-like particle size is not significantly influenced by fusion to fluorescent proteins.....	206
Figure 7.10: Intracellular localization of GFP:VP3 is influenced by co-expression of other structural proteins.....	207

LIST OF TABLES

CHAPTER 1

Table 1.1: Comparison of virus vaccine technologies.....	20
Table 1.2: Comparison of the most commonly used (VLP) expression systems.....	23
Table 1.3: Examples of plant-produced virus-like particles.....	24

CHAPTER 2

Table 2.1: Media, buffers and solutions used for molecular biology experiments.....	41
Table 2.2: E.coli strains used in this work.....	46
Table 2.3: Working concentrations of antibiotics used.....	47
Table 2.4: Protein extraction buffers used.....	51
Table 2.5: Antibodies used in this study.....	54

CHAPTER 3

Table 3.1: Oligonucleotides used in cloning of pENTR-ET2.....	65
Table 3.2: Oligonucleotides used in cloning of pEAQ vectors.....	67

CHAPTER 4

Table 4.1: Oligonucleotides used in cloning of HB tandem core constructs.....	101
Table 4.2: Summary of results obtained from expression of HBcAg and tHBcAg constructs in plants.....	123

CHAPTER 5

Table 5.1: Oligonucleotides used in cloning of BTV-10 constructs.....	139
Table 5.2: Buffers used for extraction of BTV-10 proteins and particles.....	140

CHAPTER 6

Table 6.1: Oligonucleotides used in cloning of BTV-8 constructs.....	153
Table 6.2: Buffers used purification of BTV-8 particles.....	154
Table 6.3: Sequence similarity of expressed BTV genes and proteins.....	156

CHAPTER 7

Table 7.1: Oligonucleotides used in cloning of fluorescent BTV constructs.....	190
--	-----

ABBREVIATIONS

attB	Bacteriophage Lambda attachment B site
BeYDV	Bean Yellow Dwarf Virus
BHK cells	Baby hamster kidney cells
βME	Beta mercaptoethanol
BTV	Bluetongue Virus
CEM	Cryo electron microscopy
CFP	Cyan fluorescent protein
CHO	Chinese Hamster Ovary cells
CLP	Core-like particle
co	Codon optimized
CPMV	Cowpea Mosaic Virus
C-terminus	Carboxy terminus
delRNA-2	Deleted RNA-2 expression system (CPMV)
DLS	Dynamic light scattering
DNA	Deoxyribonucleic acid
dNTP	Deoxynucleotide triphosphate
dpi	Days post infiltration
dsRNA	Double stranded ribonucleic acid
ECFP	Enhanced cyan fluorescent protein
EGFP	Enhanced green fluorescent protein
ELISA	Enzyme-linked immunosorbent assay
ER	Endoplasmic reticulum
ExB	Extraction buffer
EYFP	Enhanced yellow fluorescent protein
fCLP	Fluorescent core-like particle
FMDV	Foot and Mouth Disease Virus
fSCLP	Fluorescent subcore-like particle
fVLP	Fluorescent virus-like particle
FWT	Fresh weight tissue
GFP	Green fluorescent protein
GGG	Glycine-glycine-serine linker

GM	Genetically manipulated
GOI	Gene of interest
GUS	B-D-Glucoronidase
HA	Hepatitis A
HB	Hepatitis B
HBV	Hepatitis B Virus
HBcAg	Hepatitis B core antigen
HBsAg	Hepatitis B surface antigen
hFWT	Healthy fresh weight tissue
HIV	Human Immunodeficiency Virus
HT	<i>HyperTrans</i>
Ig	Immunoglobulin
IRES	Internal ribosome entry site
MCS	Multiple cloning site
mRNA	Messenger RNA
MW	Molecular weight
NLS	Sodium lauroyl sarcosine
NS	Non-structural protein
nt	nucleotide
N-terminus	Amino terminus
OD₆₀₀	Optical density measured at 600 nm wavelength
PBS	Phosphate buffered saline
PCR	Polymerase chain reaction
PTGS	Post-transcriptional gene silencing
PVDF	Polyvinylidene fluoride membrane
PVX	Potato Virus X
RdRp	RNA-dependent RNA polymerase
RNA	Ribonucleic acid
sAg	Surface antigen (as in HBsAg)
SCLP	Subcore-like particle
SDS-PAGE	Sodium dodecyl sulphate polyacrylamide gel electrophoresis
SGG linker	Serine-Glycine-Glycine linker
TBE	Tris/Borate/EDTA buffer
T-DNA	Transfer DNA

TEM	Transmission electron microscopy
tHBcAg	Tandem Hepatitis B core antigen
TMV	Tobacco Mosaic Virus
UA	Uranyl acetate
UV	Ultraviolet
UTR	Untranslated region
VLP	Virus-like particle
vmRNA	Viral mRNA
VP	Viral protein
WHO	World Health Organization
YFP	Yellow fluorescent protein

1 GENERAL INTRODUCTION

A virus-like particle (VLP) is a scaffold which resembles its parent virus in structure and antigenicity, while lacking the viral genome. VLPs are often able to invade host cells and are recognized by the immune system, however the lack of a functional genome renders them unable to replicate and cause infection. Such particles have recently found commercial application as inherently safe and efficacious vaccines, and are being developed for a wide range of applications ranging from basic research of viral life cycle and structure, to their use as bionanoparticles in targeted drug delivery. However, the high cost of producing VLPs in cell culture systems presents a major hurdle in the economical use of VLP technology.

The topic of this thesis is the production of VLPs using the plant-based Cowpea Mosaic Virus (CPMV) expression system. In particular, tandem Hepatitis B and Bluetongue Virus particles have been produced using a tailor-made vector system for easy and quick transient expression of multiple proteins in *Nicotiana benthamiana* leaves.

In this section, a general introduction to VLPs, plant-based expression systems, and the CPMV system in particular will be provided. For ease of reference, the background information specifically associated with vector development, Hepatitis B and Bluetongue Virus will be provided at the beginning of Chapters 3, 4 and 5, respectively.

1.1 VIRUS-LIKE PARTICLES

1.1.1 VIRAL VACCINES: COMPARISON OF EXISTING TECHNOLOGIES

In 1797, Edward Jenner used material from a fresh cowpox lesion to inoculate a small boy, who then proved to be fully protected from later infection by the more severe disease, smallpox (Riedel, 2005). This was the first example of the use of a mild virus to induce protective immunity against a deadly virus, a process which Jenner termed “vaccination.” Until its worldwide eradication in 1988, smallpox vaccines were still based

on Jenner's principle and used another *Orthopoxvirus* (*Vaccinia Virus*) to induce protective immunity against the disease agent *Variola Virus* (Fenner, 1988).

Live vaccines, modelled on this early smallpox vaccine, are still used widely. As the name suggests, such vaccines are based on live virus strains which are known to cause only a mild form of the disease, such as closely related but less virulent viruses (live, heterologous vaccines) or attenuated strains of the disease causing virus. These attenuated viruses are prepared by serial passage of the virus in cell culture, and the molecular basis for attenuation is often poorly understood (WHO, 2010a). When inoculated into the host during vaccination, the attenuated virus is limited in its pathogenicity but still able to replicate. The immune system is stimulated as though this was a natural infection, but the reduced virulence of the vaccine strain allows the body to easily overcome the disease. Live attenuated vaccines can be extremely effective, often requiring only a single dose to achieve protective immunity, and stimulating both cell-mediated and humoral immune responses. However, there is a high risk of adverse effects owing to underattenuation, reversion to a more severe form (Martin et al., 2004; Minor et al., 1986), as well as unexpectedly severe responses in some immunocompromised individuals.

Non-replicating virus vaccines, such as inactivated (killed) virus and subunit vaccines, are potentially safer, albeit less effective than live-attenuated vaccines. The safety of these vaccines lies in their inability to replicate, due to a lack or disruption of the viral genome. However, the full complement of viral antigens is often not in the correct conformation, damaged, or not present, thus affecting the immunogenicity of these vaccines. Inactivated virus vaccines are prepared by growing live virus in cell culture or egg systems, followed by inactivation to render the virus unable to replicate. This inactivation can be achieved by the use of UV irradiation, heat, or more commonly through the use of chemicals such as binary ethylenimine (Bahnmann, 1976; Dr. Mercedes Mourino, Fort Dodge Animal Health, personal communication). Each batch must be thoroughly tested for complete inactivation to ensure safety, but treatments must be mild enough to retain the immunogenicity of the vaccine. Effective immunity is achieved through a series of booster immunizations. A comparison of the discussed vaccine types is provided in Table 1.1.

Table 1.1: Comparison of virus vaccine technologies.

Characteristics	Live-attenuated	Inactivated	Subunit	Virus-like particle
Able to replicate	yes	no	no	no
Native virus structure	yes	yes	no	yes
Contains viral genome	yes	yes	no	no
Efficacy	high	medium	low	medium
Doses required	one	multiple	multiple	multiple
Amount required	low	medium	high	medium
Batch safety testing required	yes	yes	no	no
Risks	Underattenuation, reversion, opportunistic pathogens	Incomplete inactivation; batch variability, opportunistic pathogens	Protease degradation, stability	stability
Commercial examples	Oral Polio Vaccine – attenuated by serial passage in non-human cell lines ¹	Inactivated Polio Vaccine (IPV) – formaldehyde inactivated ²	Recombivax (Merck) – Hepatitis B surface antigen from yeast	Gardasil ³ (Merck), Cervarix ⁴ (GlaxoSmithKline) – Human Papillomavirus L1 VLPs from yeast / insect cells

¹(WHO, 2010b); ²(Venters et al., 2004); ³(Monie et al., 2007); ⁴(Monie et al., 2008)

Subunit vaccines can provide an inherently safe alternative to the traditional vaccines discussed above. As the name suggests, these vaccines consist of only a small portion of the virus, often the main immunogenicity determinant. As such, these vaccines are non-replicative and cannot cause disease. Recombinant subunit vaccines are viral proteins, glycoproteins, or portions thereof, which are expressed to high level in heterologous protein expression systems, such as yeast, insect cells or bacteria. The safety of these vaccines comes at the cost of efficacy as well as the speed and price of production.

Virus-like particles can have the efficacy of an inactivated vaccine with the safety of a subunit vaccine (Roy and Noad, 2008). As explained above, VLPs consist of the main structural components of a virus, but lack the viral genome. These particles resemble the parent virus in size and structure, and present the viral epitopes in the correct conformation, allowing them to be recognized by the immune system which raises an effective response. However, the empty particles are not able to replicate and therefore cannot cause disease. VLPs of a diverse range of viruses have been produced in a range of expression systems for use as vaccines. Chimaeric VLP vaccines have been developed which allow the display of many copies of a foreign epitope on their surface. These will be discussed in greater detail in the next section.

In addition to the proven vaccine technologies discussed above, some other experimental vaccine strategies have recently emerged. It is possible to induce an immune response against a viral pathogen by injecting cells with plasmid DNA containing the gene of a viral protein, which is expressed by the cellular machinery (Raz et al., 1994; Wolff et al., 1990). Portions of the expressed protein are then presented by the major histocompatibility complex on the surface of the host cell, a process which also occurs upon phagocytosis or internalization of traditional vaccines (reviewed by Gurnathan et al., 2000). Research efforts have focussed on the development of novel vectors for the targeted delivery of DNA vaccines to cells. It has been shown that particles in the range of 40 nm in diameter provide the optimal size for uptake and delivery of DNA vaccines (Minigo et al., 2007). In addition to delivery by way of biodegradable nanoparticles, heterologous viruses have also been used as carriers of DNA vaccines (Sutter and Moss, 1992; Sutter et al., 1994; Xiang et al., 2010).

1.1.2 VLP EXPRESSION: THE STORY SO FAR

A wide variety of different viruses have been used as templates for the production of VLPs: animal and plant viruses, rod-shaped and icosahedral viruses, enveloped and non-enveloped viruses. Viruses have small genomes which are encapsidated by tightly packed, symmetric protein shells of defined three-dimensional shape and size. These viral capsids often consist of only one (as in the case of Hepatitis B cores) or few structural proteins which assemble in a regular array, thereby forming a stable particle. In the case of enveloped viruses, the capsids become encased in host cell membrane by budding, and display other viral and host proteins on the outside. The assembly of structural proteins into VLPs is often not dependent on the presence of the viral genome or other elements of the virus. In fact, some VLPs even assemble *in vitro* (Morikawa et al., 1999; Rose et al., 1993). While VLPs of animal viruses can be used as vaccines in their own right (discussed here), plant virus-like particles can function as vaccines when foreign epitopes are displayed on their surface, and have found wide use in bionanotechnology (discussed in the next two sections).

Virus-like particles have been expressed in all commonly used heterologous protein expression systems. Early recombinant VLPs were expressed in prokaryotic systems (E.coli; Cohen and Richmond, 1982) and cell-free systems have also been successfully used (Bundy et al., 2008). However, eukaryotic systems have been most commonly utilized in the production of VLPs. Yeast (*S.cerevisiae*) has been employed to produce enveloped VLPs of Hepatitis B surface antigen (Valenzuela et al., 1982). Insect cells, particularly with the use of baculovirus expression vectors, have been adopted as the most widely used VLP production platform, with examples ranging from complex triple-shelled Rotavirus-like particles to enveloped Simian Immunodeficiency Virus particles (Crawford et al., 1994; Delchambre et al., 1989; Roy and Noad, 2008). Yeast and insect cells are currently used in the production of the first commercially available VLP vaccines (Merck's Gardasil and GlaxoSmithKline's Cervarix), which consists of the major structural component of Human Papillomavirus (HPV). Virus-like particles have also been successfully expressed in mammalian cell lines, such as Chinese Hamster Ovary (CHO) cells (Hobman et al., 1994), and in plants (reviewed by Santi et al., 2006). The benefits and drawbacks of the most important current VLP production platforms are summarized in Table 1.2. Examples of VLPs expressed in plants are provided in Table 1.3.

Table 1.2: Comparison of the most commonly used (VLP) expression systems.

	Prokaryotic	Eukaryotic		
	Bacteria	Yeast	Insect cell	Plants (transient)
Representative species	<i>Escherichia coli</i>	<i>Pichia pastoris</i>	<i>Spodoptera frugiperda</i>	<i>Nicotiana benthamiana</i>
Growth	Fermentation	Fermentation	Cell culture	Glasshouse
Speed of development	Fast	Slow	Slow	Fast
Yield^a	High	High	Medium	Medium
Protein folding	+	++	+++	+++
Mammalian Glycosylation^b	-	+	++	++
Disulfide bonds	no	yes	yes	Yes
Advantages	Low cost, fast and easy development, continuous batch fermentation	Eukaryotic processing, Relatively low cost, continuous batch fermentation	Near mammalian processing, easy development of baculoviruses	Post-translational processing, speed of development, low cost scalability
Disadvantages	Lack of processing, poor folding, insolubility	Selection of high expressing strains	Continuous fermentation not possible; high cost	Continuous production not possible, downstream processing

Information presented here was largely gathered from a review by Yin et al (2007).

a) Yield is highly protein dependent, and some proteins may be more compatible with specific expression systems

b) Mammalian glycosylation is more important in antibody production than VLP production. Efforts to alter expression systems to allow for mammalian glycosylation are ongoing for all mentioned eukaryotic systems

Many of the VLPs produced to date have been shown to be effective immunogens (reviewed by Roy and Noad, 2008). Not only have VLPs been shown to protect against the viral pathogen from which they are derived, some have been shown to offer cross-protection against other related strains and serotypes, as in the case of influenza VLPs (Quan et al., 2007). In some cases it is possible to produce chimaeric VLPs, which are comprised of the structural proteins of different serotypes. For example, it has been shown that the core proteins of many *Reoviridae* are sufficiently structurally conserved to allow assembly of the outer shell structural proteins of other serotypes to produce chimaeric VLPs (Kim et al., 2002; Loudon et al., 1991). Additionally, the stable structure of

VLPs makes some of them amenable to insertion of foreign antigens for display on the particle's surface. Epitope display is further discussed in the following section.

Table 1.3: Examples of plant-produced virus-like particles

Virus	Proteins	Shape	Envelope	Reference
Influenza	1	Vesicular	Yes	(D'Aoust et al., 2010; D'Aoust et al., 2008)
Hepatitis B (HBcAg)	1	Icosahedral	No	(Mechtcheriakova et al., 2006)
Norwalk Virus	1	Icosahedral	No	(Mason et al., 1996)
Hepatitis B (HBsAg)	1	Vesicular	Yes	(Mason et al., 1992)
Rotavirus	2	Icosahedral	No	(Saldaña et al., 2006)
Human Papillomavirus	1	Icosahedral	No	(Warzecha et al., 2003)

1.1.3 EPITOPE DISPLAY

In 1987, it was reported that the immunogenicity of a 19 amino acid (aa) peptide of Foot and Mouth Disease Virus (FMDV) was enhanced 500-fold by fusion of the peptide to Hepatitis core antigen (HBcAg; Clarke et al.). Today, it is generally accepted that the display of an epitope on a large carrier moiety such as a VLP increases its immunogenicity. This is due to the high density of foreign epitopes displayed on a compact structure, and may also be due to a more native conformation of the epitope (Brown et al., 1991). Though HBcAg remains one of the most commonly used carriers for epitope display (see section 4.1.3), many other VLPs have been developed for this purpose (see Table 1.3).

Attempts have been made to create chimaeric virus particles which display foreign epitopes while retaining their ability to infect and replicate in their native host. An early example of this strategy was the replacement of an antigenic site of Poliovirus type 1 with a similar site from type 3, thereby producing a chimaeric particle (Burke et al., 1988). It was soon recognized that this strategy could be used to insert sequences of entirely unrelated

pathogens, such as Human Immunodeficiency Virus (HIV), to raise neutralizing antibodies against the foreign pathogen (Evans et al., 1989).

Another notable example of replicating chimaeric virus particles is the use of the plant virus CPMV to display epitopes of FMDV and other antigens in the βB - βC loop of its small coat protein (Porta et al., 1994; Usha et al., 1993). These immunogenic particles were shown to be able to infect cowpea plants and accumulate to a high titre, thereby theoretically allowing easy scale up of production. However, it was found that some insertions were lost after several rounds of passage (Taylor et al., 1999). Also, the size of the insert was limited to 30 amino acids with larger inserts limiting virus spread and increasing the likelihood of deletions (Porta et al., 2003). Today, with the advent of more efficient expression systems (e.g. CPMV-*HT*, as discussed in section 1.3.) there is no longer a need to produce viable virus, thus allowing the development of empty CPMV-like particles (Sainsbury and Lomonosoff, 2008; Saunders et al., 2009). Such VLPs tolerate the display of much larger epitopes and even whole functional proteins (Drs. Keith Saunders and Paolo Lenzi, personal communication).

In addition to the display of foreign epitopes on the outside of VLPs, immune responses have been raised to heterologous antigens displayed on the inside of VLPs or on other non-structural viral proteins. The large size of the internal cavity of *Reoviridae* particles is amenable to the encapsidation of foreign peptides and proteins as large as GFP, some of which have been shown to elicit an immune response (Charpilienne et al., 2001; Kar et al., 2005; Tanaka et al., 1995). The non-structural protein NS1 of Bluetongue Virus (BTV) forms stable tubular structures in infected cells. NS1 fusion proteins have been shown to assemble into long tubules displaying the epitope, and these particles are efficient immunogens (Ghosh et al., 2002b; Mikhailov et al., 1996).

The fusion of foreign peptides to VLPs is not restricted to applications in vaccine development. For example, the display of half of a heteromeric coiled-coil protein on the inside of Cowpea Chlorotic Mottle Virus allows for the controlled assembly of VLPs with non-covalently linked cargo molecules on the inside of the particles (Minten et al., 2009). Also, cell attachment motifs displayed on the surface of VLPs allows the particles to be targeted to specific cells or tissues. Both of these examples of peptide display can be particularly useful in bionanotechnological and medical applications, as discussed below.

1.1.4 BIONANOTECHNOLOGY

In the past decade, viruses and in particular VLPs have found increasing use in the rapidly expanding field of bionanotechnology. Recent developments in this field have been reviewed by Soto and Ratna (2010). As previously mentioned, VLPs are being developed as carriers for the targeted delivery of drugs to specific organ types. VLPs can be loaded with molecules either by *in vitro* particle assembly in the presence of the substance, or by diffusion of the material through the pores of the particle (Comellas-Aragonès et al., 2007; Douglas and Young, 1998). The outside of the particle can then be decorated genetically through fusion of targeting motifs, or by chemical modification to display antibody fragments (Frolova et al., 2010; Soto et al., 2008).

Some other bionanotechnological applications of VLPs include: (1) their use as scaffolds for the production of metallic particles and nanowires for use as nano-scale conductors in electronics (Lee et al., 2006; Radloff et al., 2005); (2) their use as cages for the production of metallic nanoparticles of defined size, giving them special spectral properties (Aljabali et al., 2010; Mr. Alaa Aljabali, personal communication); (3) their coupling to solid surfaces for use as sensors (Steinmetz et al., 2006); (4) their coupling to fluorescent proteins, dyes and quantum dots for amplification of assay signals or live cell imaging (Brunel et al., 2010; Steinmetz, 2010). However, these applications are beyond the scope of the work described in this thesis.

1.2 MOLECULAR FARMING: PLANT-BASED EXPRESSION SYSTEMS

“Molecular farming” is a collective term for the production of commercially relevant protein products in plants and animals. In stark contrast to cell culture systems, the use of farm animals and crop plants potentially allows some common farming practices and infrastructure to be employed, thereby giving these systems a feasible advantage in terms of production costs. Being eukaryotic, both animal and plant cells are capable of folding and post-translational modification of complex protein products, providing an advantage over prokaryotic expression systems.

Research efforts in animal molecular farming have focussed mainly on the expression of foreign proteins in mammary glands for secretion within milk (Houdebine, 2000; Simons et al., 1987). Some of the many proteins produced in this way include virus-neutralizing antibodies (Castilla et al., 1998), spider silk protein (Xu et al., 2007), and human fibrinogen, which is a complex of three different proteins (Prunkard et al., 1996). The major technical drawbacks of animal molecular farming as a production system include the time and effort involved in the generation of the transgenic animals, as well as the risk of contamination with opportunistic pathogens and prions (reviewed by Houdebine, 2000). A lack of public acceptance due to ethical objections also presents a major hurdle.

Plant molecular farming became a reality in 1989 with the first production of recombinant antibody in transgenic tobacco (Hiatt et al., 1989). In the past 20 years, the field has developed rapidly, with ever more researchers and companies adopting the technology. To date, antibodies have been the pharmaceutical most commonly produced using plant-based systems (Ma et al., 1995), but a host of other products have been expressed, including human serum albumin (Sijmons et al., 1990), biodegradable plastics (Nawrath et al., 1994) and subunit vaccines, many of which are based on VLPs (see Table 1.3).

In this section, I will introduce the technological developments in the field of plant-based pharmaceutical production, with a special emphasis on the technologies used in this body of work. Additional plant-based pharmaceutical production platforms including those based on moss (Decker and Reski, 2007), algae (Griesbeck et al., 2006), plant cell culture (Doran, 2000), root secretion systems (Sivakumar, 2006) and transplastomic plants (Daniell, 2006) will not be discussed further in this thesis.

1.2.1 STABLE INTEGRATION

The first plant-made pharmaceuticals were produced by stable integration of a constitutively expressed transgene into the genomes of tobacco and potato (Hiatt et al., 1989; Sijmons et al., 1990). Individual plant cells can be transformed with a construct consisting of an expression cassette for a heterologous gene of interest (GOI) as well as a selectable marker gene (Bevan et al., 1983). By sequential growth on hormone-containing

selection media, calli can be grown from the transformed cells, followed by rooting and regeneration of whole transgenic plants.

Though many other techniques exist, transgene integration is today most commonly achieved through *Agrobacterium tumefaciens*-mediated transformation (Rao et al., 2009). The crown-gall disease-causing elements of the bacterial tumour-inducing (Ti) plasmids have been removed, and key virulence genes transferred to another plasmid (Hoekema et al., 1983). This has enabled the development of relatively small binary vectors which are compatible with *Agrobacterium*-mediated T-DNA transfer (Bevan, 1984). These binary vectors can be propagated in *E. coli* and *A. tumefaciens*, and allow for easy integration of a GOI into a multiple-cloning site within the T-DNA left and right borders (A more detailed introduction to binary vectors is found in section 3.1). By cloning the GOI within the context of a subcellular localization signal or a tissue-specific promoter or an inducible promoter, the expression of foreign proteins can be targeted both spatially and temporally in transformed plants (Cramer et al., 1999; El Amrani et al., 2004; Moore et al., 2006).

Stable integration is still used for the production of pharmaceutical proteins today and offers key advantages such as easy scale-up through sowing of seed, and may well present fewer regulatory approval hurdles due to the existing regulatory framework for GM crops (Gilbert, 2009; Spök et al., 2008). However, the slow and cumbersome regeneration of homozygous, high-expressing lines, as well as the generally low yield of recombinant protein, and problems with silencing or loss of the transgene have been the main reasons for the fast adoption of transient expression technology (Rybicki, 2010).

1.2.2 TRANSIENT EXPRESSION

In 1989, the expression of a β -D-Glucuronidase (GUS) reporter using *Agrobacterium*-mediated transformation was investigated with the finding that transient expression of the gene occurred with 1000-fold higher frequency than stable integration (Janssen and Gardner, 1989). This led to the first use of agro-infiltration technology for the transient expression of foreign genes in leaf tissue (Kapila et al., 1997; Vaquero et al., 1999).

Manual syringe agro-infiltration is a simple and low-tech method to achieve transient expression in leaf tissue, which was previously achieved by particle bombardment (Klein

et al., 1987) and microinjection methods (Neuhaus and Spangenberg, 1990). After growing an *A. tumefaciens* culture to a high density in liquid culture, the cells are pelleted and resuspended in a buffered infiltration solution. This bacterial suspension is then injected into the intercellular spaces of the leaf tissue by way of a blunt-ended syringe sealed around a small wound in the leaf surface. The suspension efficiently floods around all leaf cells, allowing the bacteria to attach and transfer the transgene-containing T-DNA into the plant cells. The morphology of *Nicotiana benthamiana* leaves makes them particularly easy to infiltrate in this way. By inducing the *Agrobacteria* within the infiltration solution with acetosyringone, a natural plant hormone released during wound response, T-DNA transfer efficiency can be further boosted to attain expression in nearly 100% of the leaf tissue (Sheikholeslam and Weeks, 1987).

Transient expression by way of agro-infiltration is an easy method to test the efficiency of a construct of interest in a laboratory setting. As with stable integration, subcellular targeting signals can be used to localize heterologous protein to the ER, chloroplast, vacuole, periplasmic space, etc. Good expression levels can usually be achieved in seven days or less thereby allowing for fast evaluation of a new construct (Marillonnet et al., 2004; Sainsbury et al., 2009). The superior yields achieved with transient expression, and the speed with which expression can be obtained, have made it a commercially viable alternative to transgenic plants (Rybicki, 2010).

For scale-up of transient expression systems, it has been necessary to find an alternative to manual injection of infiltration solution into each leaf. Vacuum infiltration allows whole plants to be infiltrated in several seconds (Kapila et al., 1997). The aerial parts of the plant are submerged in the *Agrobacterium* solution and negative pressure applied. Thereby, the air which naturally fills the intercellular spaces seeps out of the leaves and is replaced by the surrounding bacterial solution. For commercial applications, vacuum systems have been fully automated to further reduce the cost of production of pharmaceutical proteins using transient expression.

1.2.3 GENE SILENCING SUPPRESSION

During the development of transgenic plants, it was often found that expression levels could suddenly drop despite the continued presence of the transgene (Flavell, 1994). In

addition to the known problems of transgene loss or movement through recombination, post-transcriptional gene silencing (PTGS) was identified as a plant defence mechanism against pathogens which can greatly reduce the expression levels of heterologous genes by way of targeted cleavage of a transcript or changes in chromatin structure (Baulcombe, 2004; Matzke et al., 2009). Plant gene silencing has been reviewed in the aforementioned publications and will not be discussed further here.

Many plant viruses encode proteins which act as suppressors of gene silencing, thereby allowing the virus to overcome the host's defence system of PTGS (Ratcliff et al., 1997; Voinnet et al., 1999). These have been harnessed in the field of plant biotechnology to suppress the silencing of heterologous genes, thereby greatly increasing the expression levels of proteins of interest. The silencing suppressor used throughout this project is P19 of Tomato Bushy Stunt Virus. Upon infection, the viral genome along with any transgenes serves as a template for RNA-dependent RNA polymerase (RdRp), producing double-stranded RNA (dsRNA). This dsRNA is cleaved into small dsRNA fragments by a dicer-like protein. P19 has been shown to suppress silencing by binding to these 21 and 25 nucleotide dsRNA fragments, thereby blocking their recruitment by the silencing machinery (Silhavy et al., 2002). Without bound small interfering RNA, the RNA-induced silencing complex cannot be directed to specifically cleave viral transcripts, allowing the virus to overcome this host defence mechanism. In the case of transient transgene expression, co-expression of P19 can boost GOI expression levels at least 50-fold (Voinnet et al., 2003). This is often achieved by co-infiltration of an *Agrobacterium* strain containing a P19 expression cassette.

1.2.4 MULTIPLE PROTEIN EXPRESSION

Like other eukaryotic expression platforms, plants are able to fold and post-translationally modify heterologous proteins, making them ideal for the production of complex protein products. Correct folding of foreign proteins *in vivo* provides the possibility of co-expression of multiple proteins to achieve assembly of heteromeric complexes such as functional enzymes, antibodies or VLPs.

Multiple protein expression in transgenic plants can be achieved by sexual crossing of transgenics, co-transformation or re-transformation, followed by back-crossing to obtain

lines homozygous for all inserted genes (Dafny-Yelin and Tzfira, 2007). By following a strategy of sequential crossing of homozygous lines expressing the four components of secretory antibodies, heavy chain, light chain, J chain and secretory component, it has been possible to produce transgenic *Nicotiana tabacum* plants expressing functional secretory antibody at levels exceeding 200 mg / kg fresh weight tissue (FWT; Ma et al., 1995). Another notable example of these strategies is Golden Rice, where the three genes of the carotenoid biosynthetic pathway were transformed into rice plants by co-transformation with two *Agrobacterium* strains (Ye et al., 2000). Problems with expression efficiency in stable transgenics are often due to copy number, site of integration, and re-arrangement, loss or silencing of the transgene, making stable integration a cumbersome and often unreliable means of co-expressing multiple proteins (Naqvi et al., 2009).

An elegant strategy to circumvent some of the problems of multigene expression in transgenic plants has been the linking of transgenes. Such linking can be achieved by cloning of adjacent promoter-containing expression cassettes, insertion of internal ribosome entry sites (IRES) between open reading frames (Toth et al., 2001), or in-frame fusion of genes to form a polyprotein (Halpin et al., 1999). The linking of multiple genes in one expression construct allows for easier regeneration of homozygous lines and ensures that copy number and chromatin position do not affect the relative expression levels of the proteins. Co-expression of proteins at near equimolar ratios can be achieved using the polyprotein approach. Cleavage of the polyprotein to release the mature polypeptides is achieved either by design of protease cleavage sites in the linker sequences (Bedoya et al., 2010) , or by linking the proteins with a self-cleaving peptide such as the 2A sequence of FMDV (Halpin et al., 1999).

Multi-gene transient expression by agro-infiltration was first used to express antibody heavy and light chains to recover recombinant IgG (Vaquero et al., 1999). This was achieved by co-infiltration with a solution containing two *Agrobacterium* strains, both of which transferred their T-DNA into leaf cells thereby allowing co-expression of the heavy and light chains and assembly of a functional antibody. Though transient co-expression by co-infiltration is a fast and simple method to express multiple proteins in plants, it is highly dependent on the efficiency of T-DNA transfer. The copy number of the different T-DNAs transferred to each cell is random, thereby causing varying ratios of heterologous proteins to be expressed in individual cells (see section 3.3.6). This problem can be avoided by employing the polyprotein expression strategies mentioned above, or by simply cloning multiple expression cassettes onto the same T-DNA – a strategy

successfully used in this project to co-express up to five proteins of interest (see Chapters 3 and 6).

Co-expression of a suppressor of gene silencing is routinely achieved by co-infiltration with a separate *Agrobacterium* strain. Therefore, to achieve high-level expression of two genes of interest (GOI), at least three *Agrobacterium* clones must be co-infiltrated. The resulting infiltration solution can be very dense, making it difficult to manually infiltrate leaf tissue and causing increased stress on the plant as well as an increase in contaminating *Agrobacterium* proteins in downstream processing. The co-expression of multiple genes and a suppressor of gene silencing from a single T-DNA construct would thus be superior to co-infiltration.

1.3 PLANT VIRAL VECTORS AND THE CPMV-BASED EXPRESSION SYSTEMS

1.3.1 FULL VIRAL VECTORS

Parallel to the use of *Agrobacterium*-mediated expression, plant viral vectors have been developed as an alternative transient heterologous protein expression technology (reviewed by Gleba et al., 2004; Lico et al., 2008). Early viral vectors were mainly based on the full genome of a virus which included an introduced heterologous gene sequence (Gopinath et al., 2000; Porta and Lomonossoff, 1996). Expression of the GOI was obtained by local inoculation of plant tissue. This resulted in the development of symptoms of viral infection and systemic spread of the recombinant virus throughout the tissue, in addition to the high-level expression of the GOI during viral replication. Infectious virus can be harvested and used to infect more tissue for easy scale-up of expression.

Despite the obvious benefits of high expression levels and ease of application, the drawbacks of full viral vectors have led many researchers and industry to back away from their use. In the case of icosahedral viruses, the size of the viral genome is limited by the internal dimensions of the capsid structure, thereby imposing strict limitations on the size of the inserted heterologous gene. Inserted genes are also susceptible to genetic drift as well as loss by recombination. Most importantly, the production of recombinant infectious viruses presents serious bio-containment issues (Gleba et al., 2004).

In the case of co-expression of multiple proteins to achieve assembly of heteromeric protein complexes such as antibodies or VLPs, the use of full viral vectors based on monopartite viruses presents the problem of viral exclusion. Using potyvirus vectors expressing different fluorescent proteins, Dietrich and Maiss found that co-infection with two differently labelled viruses resulted in leaf areas that were infected with one or the other virus, and only rarely with both (Dietrich and Maiss, 2003). This exclusion presents a problem when the expression of a functional heteromeric protein depends on efficient co-expression of all subunits within the same cell. In the same study, it was shown that the use of two synergistic plant virus vectors can overcome the problem of exclusion, a strategy later used for the expression of functional IgG (Section 1.3.2; Giritch et al., 2006).

In an effort to maintain the high expression levels achieved with viral vectors while tackling the problems associated with the generation of infectious recombinant virus, several deconstructed viral vectors have been developed.

1.3.2 DECONSTRUCTED VIRAL VECTORS

The inherent limitations of the full viral vector approach discussed above have been addressed by the development of deconstructed viral vectors (Figure 1.1). Genes essential for virus replication, assembly and movement can be supplied *in trans* to maintain the viral infection cycle. Several key proteins are encoded by many RNA viruses currently used in plant biotechnology: (1) a viral polymerase capable of amplifying the viral genome; (2) the structural protein(s) necessary for viral capsid assembly; (3) a protease capable of cleaving viral polypeptides into functional units; (4) a movement protein essential for the cell-to-cell and systemic movement of the virus; (5) a suppressor of gene silencing. For viral vectors in which some elements of the viral infection cycle are not necessary for efficient transgene expression, another approach has been the deletion of parts of the viral genome.

One of the first deconstructed viral vector approaches has been the movement of essential viral genes to the host genome (Mor et al., 2003). The viral vector itself thereby becomes smaller and more amenable to cloning of larger inserts. Crucially, the vector can only function properly when used in conjunction with the appropriate transgenic host

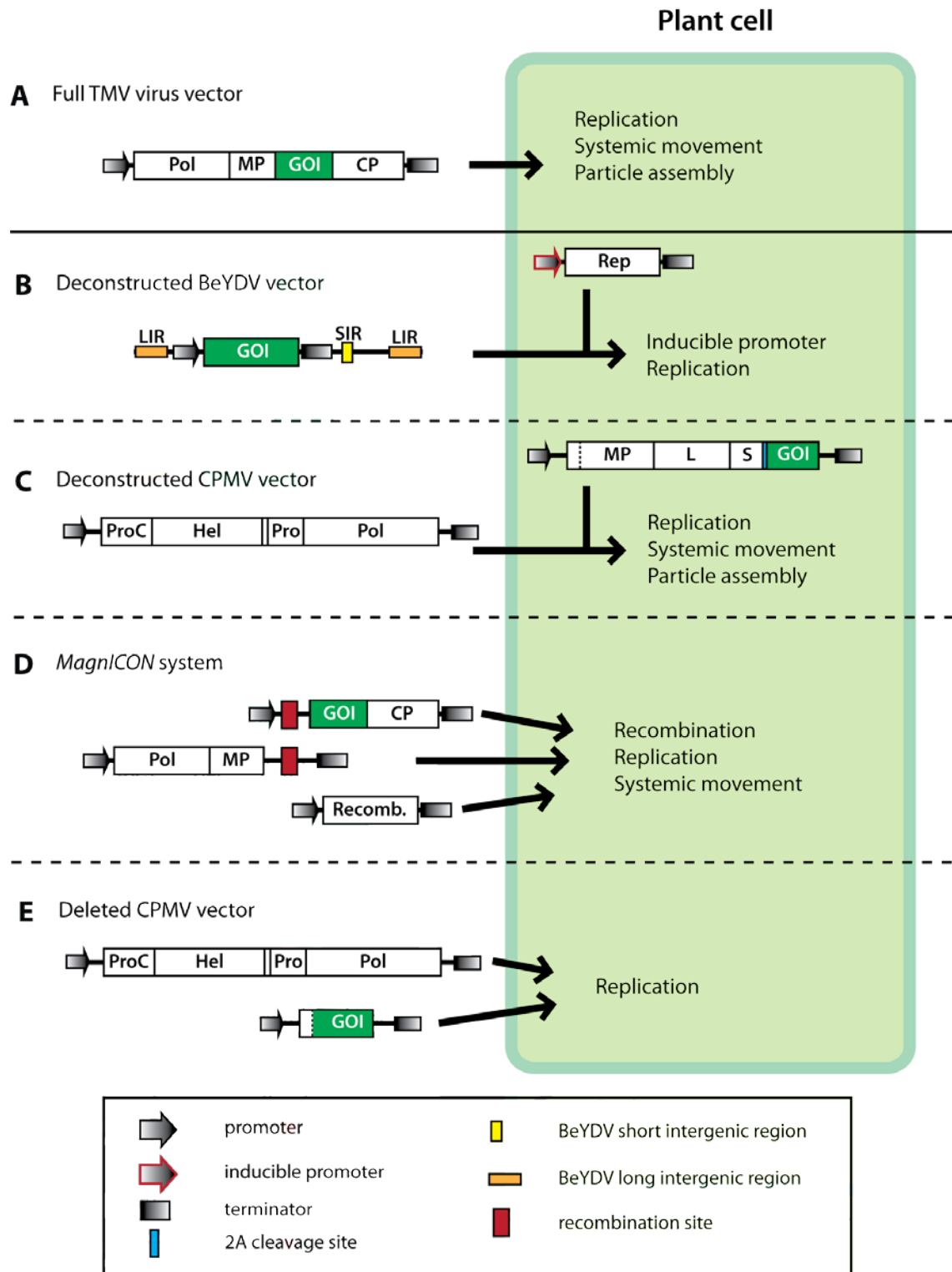


Figure 1.1: Examples of full virus and deconstructed virus vector systems.

(A) Full virus vector based on TMV cDNA with an inserted gene of interest. (B) Deconstructed BeYDV vector with an inducible replicase cassette in the host genome. (C) Deconstructed CPMV vector with a GOI-containing RNA-2 present in the transgenic host plant. (D) TMV-based *MagnICON* system relying on *in planta* recombination of two elements of a deconstructed virus genome. (E) Deleted CPMV vector system where genes for movement and coat proteins have been removed. Pol, polymerase; MP, movement protein; CP, coat protein; Rep, replicase; ProC, protease co-factor; Hel, helicase; Pro, protease; L, large coat protein; S, small coat protein; Recomb., recombinase.

plant which supplies the missing viral proteins. This provides a possible solution to the bio-containment problem of using a full viral vector.

Another notable approach is the splitting of the viral genome into two parts which must be independently supplied to a plant cell via *Agrobacterium* co-infiltration. The widely used *magnICON* system uses a deconstructed Tobacco Mosaic Virus (TMV) vector which has been split into a 5'- and a 3'-module (Gleba et al., 2005; Marillonnet et al., 2004). Each module contains viral genes and/or a heterologous gene of interest, as well as site-specific recombination sites. By co-infiltrating with three *Agrobacterium* strains to transfer the two modules as well as a construct encoding a recombinase enzyme, the TMV vector is assembled in each plant cell and allows for extremely high levels of recombinant protein production (up to 5 g / kg FWT reported). Conveniently, the modularity of the system allows for different combinations of modules to be used to allow or restrict cell-to-cell and systemic movement.

A modified *magnICON* system has been used to express functional IgG from a deconstructed viral vector. The problem of virus exclusion discussed above (Section 1.3.1) also applies to the use of deconstructed vectors based on monopartite viruses. This problem was overcome by the use of two non-competing viral vectors, TMV and Potato Virus X (PVX) to achieve efficient co-expression of heavy and light chains (Giritch et al., 2006). However, this strategy involved the co-infiltration of six separate *Agrobacterium* constructs, making it heavily reliant on dense infiltration solutions and efficient T-DNA transfer of each construct to each cell.

With the development of vacuum infiltration methods discussed above (Section 1.2.2), large-scale transient production of foreign proteins from viral vectors is no longer dependent on systemic spread. Thus, it is possible to delete the movement protein and coat proteins of the viral vector, leaving only the machinery necessary for high-level replication of the genome. An example of this is the Bean Yellow Dwarf Virus (BeYDV)-based vector system developed by researchers in the group of Dr. Hugh Mason at the Biodesign Institute, Arizona. The BeYDV vector consists of the replicase as well as the long and short intergenic regions necessary for amplification of the viral genome (Huang et al., 2009). Heterologous genes inserted in this vector are expressed at high levels of up to 0.8 g / kg within four days, without movement of the vector.

Deleted viral vectors that are not reliant on virus assembly and movement overcome the inherent limits on transgene size imposed by the vector capsid and genome. Such

deleted vectors are also not subject to the problems of transgene deletion and reversion to wild type, often encountered after serial passaging of full virus vectors (Kearney et al., 1993; Rabindran and Dawson, 2001). However, these vectors are heavily reliant on high levels of replication for efficient expression of the transgene. Replication of viral genomes, particularly those of RNA viruses, has been shown to be subject to a high mutation rate due to the low fidelity of RdRp (Drake and Holland, 1999). While essential viral genes of full viral vectors are subjected to selection pressures and deleterious mutations are selected against, in the case of a heterologous gene mutations can accumulate. This can result in the expression of truncated products or inactive forms of the protein of interest, which can be a particular problem in the heavily regulated field of biopharmaceutical production.

For the CPMV-*HT* system introduced below, it has been possible to delete all viral genes, leaving only the untranslated regions (UTR) of the viral genome which allow for hyper-translation of the gene of interest (Cañizares et al., 2006; Sainsbury and Lomonosoff, 2008).

1.3.3 COWPEA MOSAIC VIRUS-BASED EXPRESSION SYSTEMS

Cowpea Mosaic Virus is the type member of the genus *Comovirus*, family *Comoviridae*. CPMV is an icosahedral, bipartite virus with a genome consisting of self-replicating RNA-1 which encodes, amongst others, the viral polymerase and proteinase, and RNA-2 which encodes the movement protein as well as the large and small coat proteins which are expressed as a propeptide (Figure 1.2 A). As well as its natural host cowpea (*Vigna unguiculata*), the virus is also capable of infecting the *Nicotiana benthamiana*, a fast-growing, highly susceptible variety widely used in plant biotechnology and employed in this study (Goodin et al., 2008).

1.3.3.1 Full CPMV viral vector

Early CPMV-based expression systems followed the full viral vector approach discussed above (Section 1.3.1) and focussed entirely on the smaller RNA-2. The marker green fluorescent protein (GFP) was inserted between the movement protein and large coat protein, or downstream of the small coat protein (Gopinath et al., 2000). Release of the marker protein was achieved by inclusion of a protease cleavage site or FMDV 2A

sequence flanking GFP (MxGFPy; Figure 1.2 B). Though this approach was effective and produced GFP at levels of 1-2% of total soluble protein, the produced marker protein contained remnants of the flanking cleavage sites. The least modified GFP was obtained with a construct in which the N-terminus of the marker protein was fused to the C-terminus of the small coat protein via the FMDV 2A linker (CPMV/S-2A-GFP; Figure 1.2 B), which leaves only one residual proline at the N-terminus of the heterologous protein after cleavage (Gopinath et al., 2000; Ryan and Drew, 1994). This early CPMV vector was used successfully for the transient expression of Hepatitis B cores and other pharmaceutically relevant proteins (Mechtcheriakova et al., 2006; Monger et al., 2006). However, the full virus vector approach has inherent limitations of transgene loss and biocontainment issues, as discussed above. It was also found that while co-expression of two GOI from separate RNA-2 constructs results in efficient co-expression within agro-infiltrated tissue, systemic spread of the full viral vectors resulted in segregation and virus exclusion as seen for monopartite viral vectors (section 1.3.1; Sainsbury et al., 2008).

1.3.3.2 Deconstructed and deleted CPMV viral vectors

A deconstructed CPMV vector system was developed in 2006 after the observation that viral infection could be induced in otherwise healthy RNA-2 transgenic plants after agro-infiltration with an RNA-1 construct (Liu et al., 2004). By transforming plants with the aforementioned CPMV/S-2A-GFP construct, healthy plants could be recovered in which the expression of GFP could be induced by agro-infiltration with RNA-1 (Cañizares et al., 2006). However, this approach was slow due to the production of transgenic plants, and induction of expression still resulted in the production of infectious CPMV particles.

The problem of bio-containment was addressed by the development of an expression system based on deleted RNA-2 (delRNA-2), in which the movement protein and coat proteins of CPMV were removed (Figure 1.2 C; Cañizares et al., 2006). The only viral elements flanking the gene of interest in this system are the 5'- and 3'-UTRs of RNA-2, which had previously been shown to be essential for replication by RNA-1-encoded machinery. The gene silencing suppression function previously provided by the CPMV small coat protein could be replaced by supplying a suppressor of gene silencing, HcPro, *in trans*. It was further found that good expression levels could be achieved from delRNA-2 constructs in the absence of RNA-1, when co-infiltrated with a suppressor of gene silencing. Such constructs were used routinely when I started this project in 2007, and have been successfully used to express fluorescent marker proteins, IgG and hepatitis B

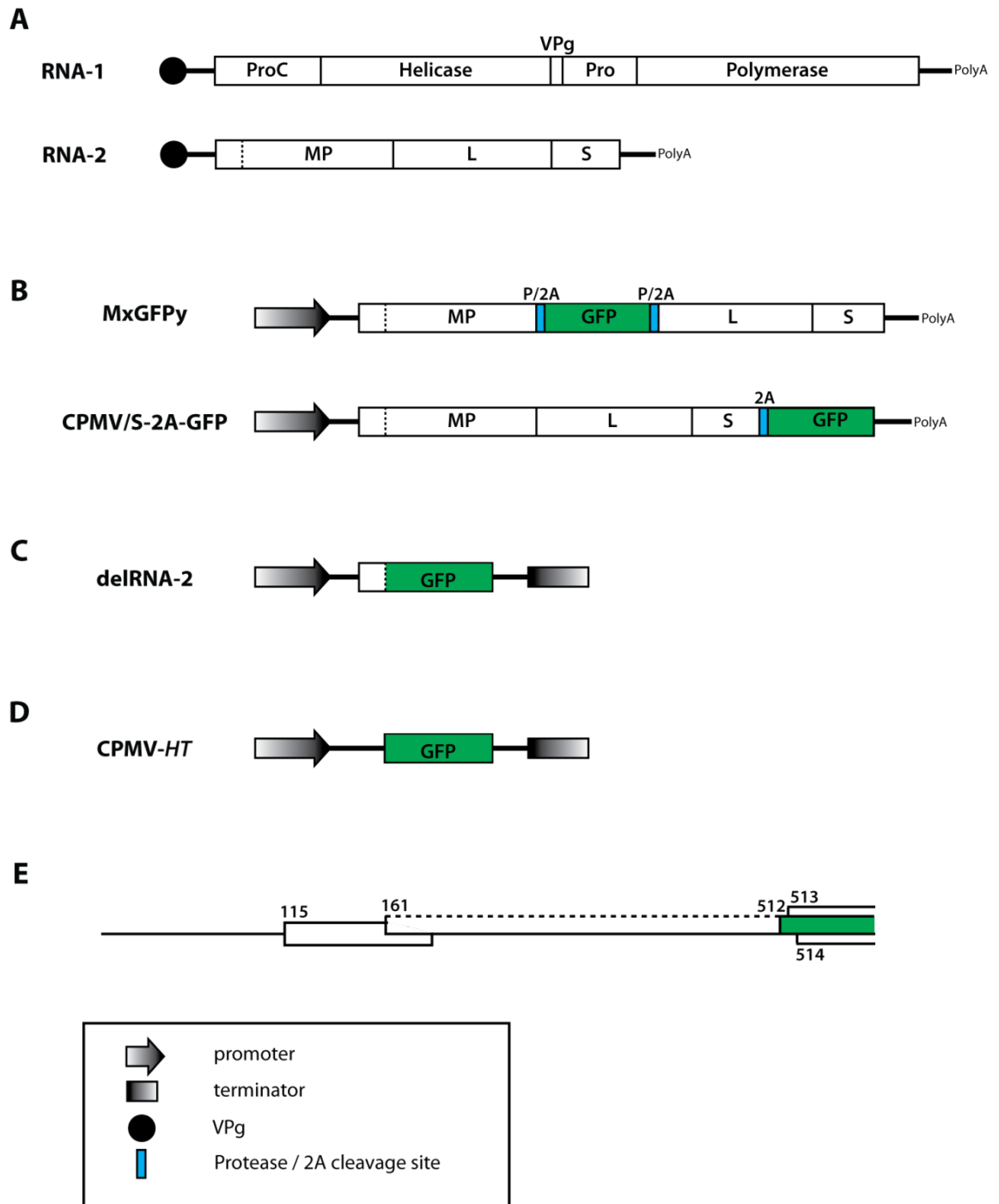


Figure 1.2: Evolution of the CPMV polypeptide expression system.

(A) Schematic representation of the CPMV genome. (B) RNA-2 constructs used in the full viral vector system of Gopinath et al, 2000. The foreign sequence (GFP) was flanked by protease or FMDV 2A cleavage sites. (C) delRNA-2 construct developed by Cañizares et al, 2006, where GFP replaces the viral genes of RNA-2. (D) CPMV-HT construct where the in-frame start codon at position 161 as well as the AUG at position 115 were removed (Sainsbury and Lomonosoff, 2008). (E) Schematic representation of the 5' UTR of CPMV RNA-2, indicating the position of open reading frames. ProC, proteinase co-factor; Pro, proteinase; MP, movement protein; L, large coat protein; S, small coat protein; P, protease cleavage site; 2A, FMDV 2A self-cleaving polypeptide. Figures modified from Sainsbury et al, 2010.

cores and empty CPMV-like particles (Sainsbury and Lomonosoff, 2008; Saunders et al., 2009).

1.3.3.3 *HyperTrans: CPMV-HT*

With the finding that replication by RNA-1 is not necessary for good expression from the delRNA-2 constructs, efforts were made to investigate whether the 5'UTR of RNA-2 could be altered to simplify cloning. The start codon of the viral movement protein, or the heterologous protein in the case of delRNA-2, is at position 512 of the RNA-2 sequence (Figure 1.2 E). Upstream of this site are two further start codons at positions 115 and 161, the latter of which is in-frame with the start codon at 512. Previous mutational studies with full virus had revealed that removal of these start codons, or frame-shifting, was detrimental to virus replication (Holness et al., 1989; van Bokhoven et al., 1993).

It was subsequently investigated whether the maintenance of this exact 5'-UTR was still needed for heterologous protein expression from delRNA-2 (Sainsbury and Lomonosoff, 2008). Rather than being detrimental, it was found that the removal of the start codons at 115 and particularly 161 increased foreign protein expression by at least 10-fold. Since mRNA levels were not affected, this increase is thought to be caused by more efficient translation, i.e. "hyper-translation."

The expression system based on the mutated 5'-UTR of RNA-2 is called CPMV-HT (or *HyperTrans*) and was used throughout most of this body of work (Figure 1.2 D). Being a deleted viral vector, agro-infiltration of a CPMV-HT construct does not result in systemic spread or production of infectious viral particles, thereby making the system safe in terms of biocontainment, and removing the limitations of transgene size imposed by encapsidation of the viral genome. The lack of contaminating CPMV particles is particularly beneficial for the production of heterologous VLP produced using the system. Efficient transgene expression is achieved by hyper-translation rather than viral vector replication, thereby reducing the risk of transgene loss, genetic drift and high mutation rates associated with replicating viral vectors. Multiple GOI can be expressed from separate RNA-2 constructs by co-infiltration, showing that the system is not subject to the viral exclusion phenomenon of other viral vectors (Sainsbury et al., 2008). These benefits make the CPMV-HT system particularly suitable for the expression of complex heteromeric VLP, as attempted in this project.

1.4 AIMS OF THIS PROJECT

The overall aim of this project was to push the boundaries of VLP expression in plants in general, through use of the CPMV expression systems. In particular, I chose to express two very different VLPs, one simple and one complex: (1) Tandem Hepatitis B cores are relatively simple particles consisting of 120 copies of a single subunit and have the potential to be used as carriers of large heterologous polypeptides; (2) Bluetongue Virus-like particles are large, highly complex structures consisting of 1440 subunits of four different structural proteins. Both of these VLPs have potential uses as vaccines as well as tools in research and nanotechnology.

To enable the expression of such complex heteromeric structures, the development of a vector series for fast cloning and efficient co-expression of multiple GOI was seen as a necessary first goal.

2 GENERAL MATERIALS AND METHODS

In general, standard molecular biological techniques were performed as described by Sambrook (1989) or according to the manufacturers instructions where specific reagents were used. General materials and methods relating to the work described in this thesis are described below. Specific materials and techniques relating to key experiments are introduced in the relevant chapters.

2.1 MEDIA, BUFFERS AND SOLUTIONS

The recipes for bacterial growth media, buffers and solutions used for molecular cloning and protein analysis experiments are listed in Table 2.1.

Table 2.1: Media, buffers and solutions used for molecular biology experiments.

Name	Recipe
Luria Bertani (LB)	10 g/l tryptone, 5 g/l yeast extract, 10 g/l NaCl adjusted to pH 7.0
LB agar	as LB, with 10 g/l Lab M No.1 agar added
ELISA Block Buffer	5% (w/v) dry milk, 0.05% (v/v) Tween-20, in PBS
βME-LDS sample buffer (3x; LDS-SB)	750 μ l 4x LDS sample buffer (Invitrogen), 250 μ l β -mercaptoethanol
MMA	10 mM MES buffer, pH 5.6; 10 mM MgCl ₂ ; 100 μ M acetosyringone
Phosphate-buffered saline (PBS)	140 mM NaCl, 15 mM KH ₂ PO ₄ , 80 mM Na ₂ HPO ₄ , 27 mM KCl
SOC	20 g/l tryptone, 5 g/l yeast extract, 0.58 g/l NaCl, 0.19 g/l KCl, 2.03 g/l MgCl ₂ , 2.46 g/l magnesium sulphate 7-hydrate, 3.6 g glucose
SNAPid Block Buffer	1% (w/v) casein, 1% (w/v) bovine serum albumin, 0.1% Tween-20, in PBS
1 x TBE	10.8 g/l Tris-HCl, 5.5 g/l boric acid, 2 mM EDTA
Western Blot Transfer buffer	3.03 g/l Tris-HCl, 14.4 g/l glycine, 20% (v/v) methanol

2.2 MOLECULAR CLONING TECHNIQUES

General techniques used for molecular cloning are described below. Details of specific cloning strategies can be found in Section 2 of each results chapter.

2.2.1 ISOLATION / PURIFICATION OF PLASMID DNA AND DNA FRAGMENTS

Plasmid DNA was prepared using the QIAGEN MiniPrep Kit, as per the manufacturer's instructions. DNA fragment purification was performed using QIAGEN PCR Purification Kit or QIAGEN Gel Extraction Kit, according to the instructions. DNA was stored at -20°C.

2.2.2 POLYMERASE CHAIN REACTION (PCR)

Amplifications of DNA fragments for subsequent cloning were carried out using the proofreading polymerase Phusion (Roche) and the supplied buffer according to the following protocol. The lowest melting temperature of the two primers was used as the annealing temperature (XX).

Recipe	50	µl	Cycles			
5x HF buffer	10	µl	98°C	2	min	
10 mM dNTPs	1	µl	98°C	30	sec	} 25 x
DNA template	1	µl	XX°C	30	sec	
10 µM forward primer	2	µl	72°C	25	sec/kb	
10 µM reverse primer	2	µl	72°C	5	min	
Phusion polymerase	0.5	µl				
dH ₂ O	33.5	µl				

Amplifications of DNA fragments for subsequent analysis by agarose gel electrophoresis (e.g. Colony PCR) were performed using GoTaq polymerase (Promega) and the supplied buffer. The annealing temperature was chosen to be 2°C lower than the lower of the two primer melting temperatures.

Recipe	20	µl	Cycles			
5x GoTaq buffer	4	µl	98°C	2	min	} 30 x
25 mM MgCl ₂	1.2	µl	98°C	30	sec	
10 mM dNTPs	0.4	µl	XX°C	30	sec	
DNA template	1	µl	72°C	1	min/kb	
10 µM forward primer	0.4	µl	72°C	5	min	
10 µM reverse primer	0.4	µl				
GoTaq polymerase	0.1	µl				
dH ₂ O	12.5	µl				

2.2.3 RESTRICTION ENDONUCLEASE DIGESTION

Restriction enzymes were obtained from New England Biolabs (NEB), Roche or Invitrogen. Restriction digests were carried out in the appropriate 1x NEBuffer (NEB), as recommended by the NEB Double Digest Finder tool:

<http://www.neb.com/nebecomm/DoubleDigestCalculator.asp>.

2.2.4 DNA MODIFICATION

As required, DNA fragments were manipulated to facilitate certain cloning strategies.

- i. Blunting of DNA ends was achieved by treatment with DNA Polymerase I Klenow fragment (NEB) supplemented with dNTPs, resulting in removal of 3' overhangs and filling in of 5' overhangs.
- ii. Blunting and 5'-phosphorylation of inserts was achieved with a Quick Blunting Kit (NEB) consisting of T4 DNA polymerase and T4 polynucleotide kinase.
- iii. Dephosphorylation of vector backbones to prevent self-ligation was performed using Calf Intestinal Alkaline Phosphatase (CIP; NEB) or Shrimp Alkaline Phosphatase (SAP; USB Affymetrix).

2.2.5 DNA LIGATION

DNA ligations were carried out using NEB T4 DNA ligase. Prior to ligation, purified DNA fragments were quantified using a NanoVue spectrophotometer (GE Healthcare), and a vector : insert molar ratio of 1 : 3 was calculated for reactions not exceeding 100 ng total DNA. Ligations were carried out at room temperature for one hour, or 16°C overnight.

2.2.6 SITE-DIRECTED MUTAGENESIS

Site-directed mutagenesis was performed to change individual nucleotides in order to introduce or remove restriction sites. Mutagenic primers were designed according to the guidelines of the Quick Change Site-directed Mutagenesis Kit Instruction Manual (Stratagene). Mutagenesis reactions were set up as follows, and included Pfu Turbo polymerase (Stratagene). Annealing temperature and extension time were chosen specifically for each primer set and DNA template employed.

Recipe	50	µl	Cycles			
10x Pfu Turbo buffer	5	µl	95°C	2	min	} 30 x
DMSO	3	ul	95°C	30	sec	
10 mM dNTPs	1	µl	XX°C	30	sec	
DNA template	1	µl	68°C	1	min/kb	
10 µM forward primer	2	µl	72°C	5	min	
10 µM reverse primer	2	µl				
Pfu Turbo polymerase	1	µl				
dH ₂ O	36	µl				

Reactions were treated with *DpnI* to cleave the parental DNA template, followed by transformation into *E. coli*.

2.2.7 GATEWAY® CLONING

Genes of interest were amplified using a set of primers allowing end-tailoring of bacteriophage λ attachment B (*attB*) sites (Figure 2.1). The BP clonase II enzyme (Invitrogen) allowed directional recombination to transfer the PCR fragment into

pDONR207, the “donor vector” backbone. Successful recombinants (called “entry clones,” pENTR...) were selected for by plating on LB agar with $\mu\text{g/ml}$ gentamycin. This newly created entry clone contained the GOI, flanked by *attL* sites. The subsequent LR reaction, facilitated by LR clonase II (Invitrogen), allowed the transfer of the GOI into a destination vector (pDEST...), thereby producing a so-called “expression clone.” Both the donor vector and the destination vector contain a cytotoxic *ccdB* gene cassette which is removed upon recombination, thereby negatively selecting transformants which did not recombine successfully.

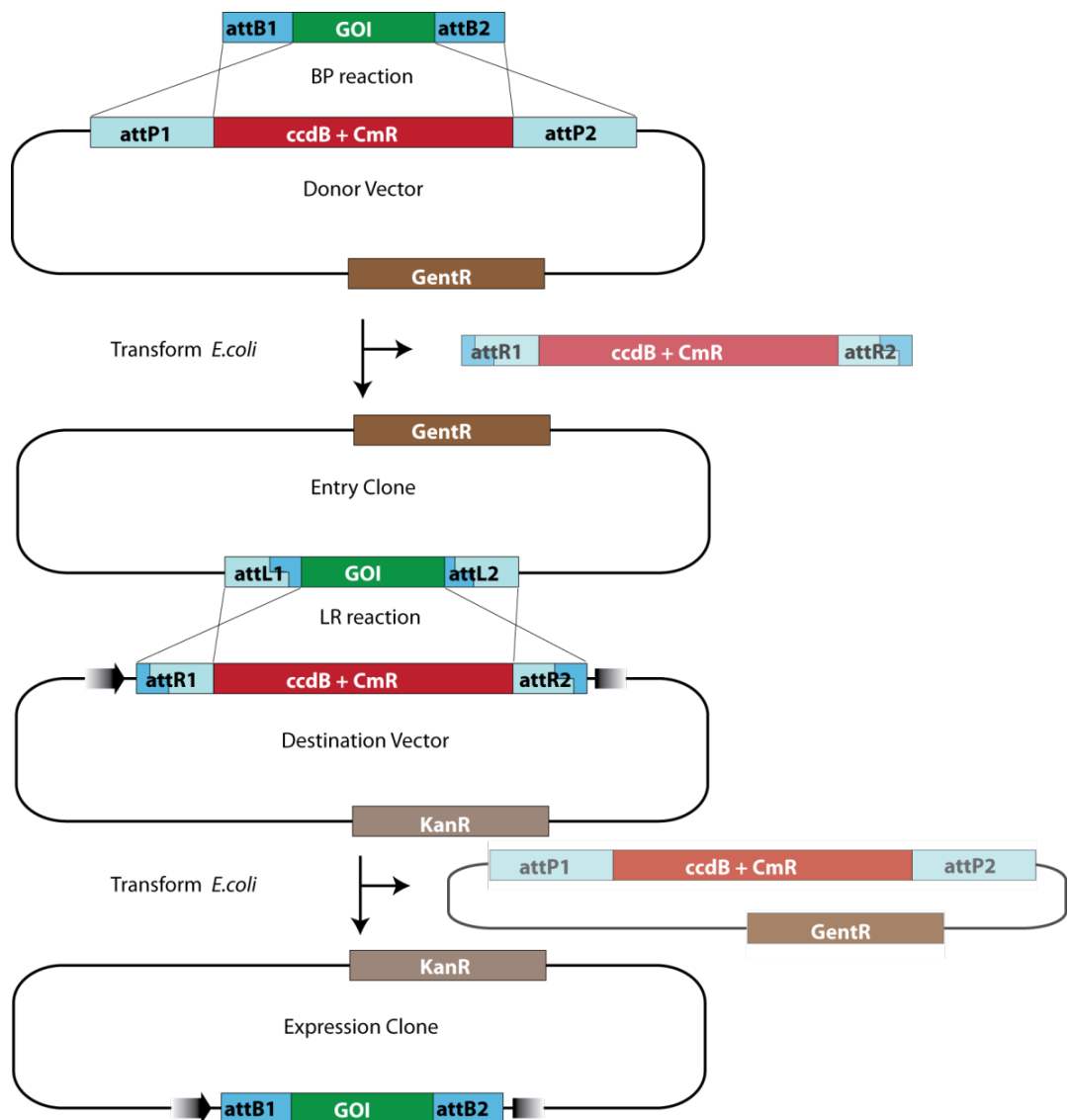


Figure 2.1: Schematic representation of Gateway cloning and Gateway vectors for subcloning of CPMV expression cassettes.

Gateway cloning involves sequential recombination reactions to transfer a gene of interest (GOI) into an expression clone. Recombination side products are indicated on right.

2.2.8 DNA SEQUENCING

All sequencing reactions were prepared using BigDye Terminator v3.1 (Applied Biosystems) according to the manufacturers instructions. Sequencing was carried out by Genome Enterprise Ltd.

2.2.9 AGAROSE GEL ELECTROPHORESIS

Agarose gel electrophoresis was used for analysis of PCR products and restriction fragments, as well as gel purification. Generally, 0.8% (w/v) agarose dissolved in 1 x Tris/Borate/EDTA (TBE) buffer was used to resolve DNA fragments larger than 500 bp. Smaller fragments were resolved in 1% or 2% (w/v) agarose gels, as required.

2.2.10 TRANSFORMATION OF COMPETENT CELLS

The strains of *E. coli* used in this work are detailed in Table 2.2.

Table 2.2: E.coli strains used in this work.

Strain	Genotype
DH5α	<i>F</i> ϕ 80 <i>dlacZ</i> Δ M15 Δ (<i>lacZYA-argF</i>) U169 <i>recA1 endA1 hsdR17</i> (<i>r_k⁻, m_k⁺</i>) <i>phoA supE44</i> λ <i>thi-1 gyrA96 relA1</i>
TOP10	<i>F mcrA</i> Δ (<i>mrr-hsdRMS-mcrBC</i>) ϕ 80 <i>lacZ</i> Δ M15 Δ <i>lacX74 deoR recA1 ara</i> Δ 139 Δ (<i>ara-leu</i>)7697 <i>galU galK rpsL</i> (<i>Str^R</i>) <i>endA1 nupG</i>
Invitrogen OneShot ccdB Survival 2 T1^R	<i>F mcrA</i> Δ (<i>mrr-hsdRMS-mcrBC</i>) ϕ 80 <i>lacZ</i> Δ M15 Δ <i>lacX74 recA1 ara</i> Δ 139 Δ (<i>ara-leu</i>)7697 <i>galU galK rpsL</i> (<i>Str^R</i>) <i>endA1 nupG fhuA::IS2</i>

Chemically competent *E. coli* were transformed by heat-shock and allowed to recover in SOC media for one hour at 37°C in a shaking incubator before plating on LB agar plates

containing the appropriate antibiotic(s). The concentrations of antibiotics used in this study are detailed in Table 2.3.

Table 2.3: Working concentrations of antibiotics used.

Antibiotic	Working concentration
Carbenicillin	100 µg / ml
Chloramphenicol	34 µg / ml
Gentamycin	7 µg / ml
Kanamycin	50 µg / ml
Rifampicin	50 µg / ml

2.3 CLONING VECTORS

In a period of continued development of cloning vectors to facilitate the use of the CPMV-*HT* expression system, standard cloning procedures were periodically changed to allow the use of new vectors. The main vectors used in this study are briefly introduced below. Details of their construction and use are found in Chapter 3.

2.3.1 pM81-FSC2

pM81-FSC2 (Sainsbury and Lomonosoff, 2008) is a 4882 bp small, high-copy plasmid containing the basic CPMV expression cassette: a gene of interest flanked by 5'- and 3'- untranslated regions of CPMV RNA-2, driven by a 35S promoter and *nos* terminator. The *in situ* GOI can be easily replaced by restriction cloning using *Nru*I and *Xho*I. However, for use with the delRNA-2 system for which it was designed, due care must be paid to the maintenance of the GOI start codon at position 512 of the RNA-2 sequence (Cañizares et al., 2006).

2.3.2 pBINPLUS

The binary vector pBINPLUS is a modified version of the classic plant expression vector pBIN19 (Bevan, 1984; van Engelen et al., 1995). The *Agrobacterium* Ti-plasmid left and right borders flank a T-DNA region containing a selection marker and a multiple-cloning site (MCS). Unique eight base-pair restriction sites *Ascl* and *Pacl* allow easy subcloning of CPMV expression cassettes from pM81-FSC2 to pBINPLUS.

2.3.3 pENTR-ET2 AND pDEST-BINPLUS

pENTR-ET2 is a Gateway-compatible alternative to pM81-FSC2 (see section 3.3.1). It contains the same CPMV expression cassette with unique restriction sites for replacement of the GOI, but includes *attL* sites. These sites allow for easier subcloning by site-specific recombination into the binary vector by LR reaction.

pDEST-BINPLUS is a Gateway destination vector in which the MCS of pBINPLUS is replaced with *attR* sites flanking a cytotoxic *ccdB* gene and resistance gene (Section 3.3.1). This can be used in LR reactions with pENTR-ET2-based plasmids to transfer CPMV expression cassettes into the binary vector T-DNA region.

2.3.4 pEAQ VECTOR SERIES

The pEAQ vector series consists of small binary vectors with T-DNA regions tailored for specific plant-expression purposes. These vectors are discussed in detail in Chapter 3.

2.4 TRANSIENT EXPRESSION OF PROTEINS IN *NICOTIANA BENTHAMIANA*

2.4.1 TRANSFORMATION OF *AGROBACTERIUM TUMEFACIENS*

In this work, binary vectors carrying expression constructs flanked by T-DNA borders were transformed into electrocompetent *Agrobacterium tumefaciens* strain LBA4404 (Hoekema et al., 1983). After electroporation at 2.5 kV, SOC media was immediately added and the cells left to recover for one hour at 28°C. Cells were then plated on LB agar containing 50 µg/ml rifampicin and 50 µg/ml kanamycin.

2.4.2 PLANT GROWTH CONDITIONS

Nicotiana benthamiana plants were grown in glasshouses maintained at 25°C and watered daily. Supplemental lighting was provided to maintain 16 hours of daylight in the winter months (October – April, inclusive). Plants were used for transient expression studies 3-4 weeks after pricking out.

2.4.3 AGROINFILTRATION

For transient expression, inoculated liquid cultures of *A. tumefaciens* strains were grown at 28°C in a shaking incubator for 24 hours in LB medium containing the appropriate antibiotics. The optical density at 600nm wavelength (OD_{600}) was measured (typically reaching OD_{600} of approximately 5) and used to calculate the volume of culture (X) needed to make an overall inoculum of $OD_{600} = 0.4$ (unless otherwise specified), according to the following equation.

The determined volume of culture was centrifuged at 4000 x g for 5 minutes to pellet the bacteria. After decanting, the pellet was resuspended in the desired volume of MMA to yield an inoculum of $OD_{600} = 0.4$.

Co-infiltration of multiple construct was achieved by mixing the required amounts of the cultures prior to pelleting. After resuspension in MMA, the resulting infiltration suspension had an OD_{600} of $n^{-0.4}$, where n is the number of different constructs to be co-infiltrated.

Small-scale experiments were designed to allow sampling from at least three separate leaves per construct. This was done to minimize the variability of expression levels observed from leaves of different age.

2.4.4 HARVESTING

Leaf tissue was harvested six days post infiltration (dpi) using the following techniques, unless otherwise specified.

Small-scale sampling was done by excising three leaf discs from three separate leaves of the same plant, using a cork borer of 11 mm diameter. Samples of this size corresponded to approximately 100 mg of healthy leaf tissue. Leaf veins were avoided where possible. Leaf discs were placed in 2 ml screw-cap tubes and either analyzed immediately or stored at -20°C .

Large-scale sampling was done by removing any large veins and non-infiltrated tissue, and recording the leaf sample weight. Leaves were then either extracted immediately in three volumes of a protein extraction buffer (Table 2.4), or stored at 20°C .

2.4.5 CONFOCAL MICROSCOPY

Unless otherwise specified, a Leica SP2 inverted confocal microscope was used to visualize fluorescent protein expression in *N. benthamiana* leaf tissue. Leaf fragments of approximately 25 mm^2 were excised from infiltrated tissue at 1 cm distance from the point of injection. Fragments were mounted on coverslips by floating the underside of the leaf portion on a water droplet, and then taking care to avoid trapped air while mounting onto a glass slide. The leaf underside was thus viewed by the microscope. Specific parameters used for the visualization of EYFP, ECFP and EGFP are detailed in Chapter 3.

Table 2.4: Protein extraction buffers used.

Name	Recipe
BTV extraction buffer (BTV ExB)	20 mM Tris-HCl , pH 8.4; 140 mM NaCl; 1 mM EDTA; 0.1% (w/v) sodium deoxycholate; Complete Protease Inhibitor Cocktail (Roche, add fresh)
BTV VLP extraction buffer	50 mM Bicine, pH 8.4; 20 mM NaCl, 0.1 % (w/v) NLS sodium salt; 1 mM DTT (add fresh); Complete Protease Inhibitor Cocktail (Roche, add fresh)
BTV CLP extraction buffer	50 mM Bicine, pH 8.4; 140 mM NaCl, 0.1 % (w/v) NLS sodium salt; 1 mM DTT (add fresh); Complete Protease Inhibitor Cocktail (Roche, add fresh)
Extraction Buffer (ExB)	50 mM Tris-HCl , pH 7.25; 150 mM NaCl; 2 mM EDTA; 0.1% (v/v) Triton X-100; 1 mM DTT (add fresh), Complete Protease Inhibitor Cocktail (Roche, add fresh)
HB Extraction Buffer 1 (HBExB1)	10 mM Tris-HCl pH 8.4, 120 mM NaCl, 1 mM EDTA, 0.75% (w/v) Sodium deoxycholate, 1 mM DTT (add fresh), Complete Protease Inhibitor Cocktail (Roche, add fresh)
Low-salt SSB	50 mM Bicine, pH 8.4; 20 mM NaCl, 0.5 % (v/v) NP-40; 10 % glycerol; 1 mM DTT (add fresh); Complete Protease Inhibitor Cocktail (Roche, add fresh)
Smith Stabilization buffer (SSB)	50 mM Bicine, pH 8.4; 140 mM NaCl, 0.5 % (v/v) NP-40; 10 % glycerol; 1 mM DTT (add fresh); Complete Protease Inhibitor Cocktail (Roche, add fresh)

2.4.6 PHOTOGRAPHY

Photography was used to document detrimental effects of certain constructs on leaf tissue, and to visualize fluorescent protein in leaf tissue and density gradients. Excitation of fluorescent proteins was achieved using Blak-Ray lamps (Ultra-Violet Product Ltd). Unless otherwise specified, all photographs were taken by Mr. Andrew Davis.

2.5 PROTEIN ANALYSIS

2.5.1 PROTEIN EXTRACTION

Small-scale samples were extracted by adding a ¼-inch ceramic bead (MP Biomedicals) and 300 µl of an appropriate extraction buffer, unless otherwise specified. Leaf tissue was homogenized using a FastPrep machine (MP Biomedicals) at speed setting 5.0 for 40 seconds. Large-scale samples were extracted by adding 3 volumes of an appropriate extraction buffer and blending in a WARING blender until homogeneous (approximately 40 seconds). Large cell debris was removed by squeezing the homogenate through one layer of Miracloth (Merck).

The composition of the protein extraction buffers used in this project are given in Table 2.4.

2.5.2 POLYACRYLAMIDE GEL ELECTROPHORESIS (PAGE)

Invitrogen's NuPAGE Bis-Tris Mini gels of 12% or 4-12% (w/v) acrylamide were used throughout this study, as indicated. Gels were run in NuPAGE MOPS buffer, supplemented with NuPAGE Antioxidant in the internal chamber, according to the manufacturer's instructions. For reducing, denaturing polyacrylamide gel electrophoresis (PAGE), two volumes of sample were mixed with one volume of 3x LD β ME sample buffer (LDS-SB) and boiled at 100°C for 5 minutes. The two protein standards used were SeeBlue Plus 2 (Invitrogen) and Broad Range Prestained Protein Marker (New England Biolabs).

2.5.3 COOMASSIE BLUE STAINING

After PAGE, protein bands in gels were visualized by addition of 20 ml InstantBlue Coomassie blue-based protein stain (Expedeon) and staining for at least one hour. Gels were destained in water for at least 30 minutes before imaging.

2.5.4 MASS SPECTROMETRY

When necessary, protein bands of interest from Coomassie blue-stained PAGE gels were identified by Mass Spectrometry, performed by the John Innes Centre Proteomics facility.

2.5.5 WESTERN BLOTTING AND IMMUNODETECTION

Western blotting was performed exclusively as a wet transfer to Polyvinylidene fluoride (PVDF) membrane. Briefly, the transfer cassette was assembled with the gel and pre-wet PVDF membrane sandwiched between layers of filter paper and sponges. Proteins were electroblotted for 1 hour at 100V, whilst maintaining a constant cooling by ice bath.

Generally, immunodetection was carried out using the SNAPid system (Millipore), which allows fast binding of antibodies and washing by applying a vacuum. Membranes were blocked with SNAPid blocking buffer, which was also used to dilute antibody solutions. The manufacturer's instructions were followed. The antibodies used in this study are listed in Table 2.5.

Immobilon Chemiluminescent HRP substrate (Millipore) was used to detect bound secondary HRP-conjugated antibody. The emitted luminescence was detected with Hyperfilm (Amersham).

Table 2.5: Antibodies used in this study.

Antibody	Antigen	Supplier
anti-rabbit-HRP conjugate	Rabbit IgG	Amersham Bioscience
anti-mouse-HRP conjugate	Mouse IgG	Promega
His-Tag Monoclonal Antibody	Penta-His tag	Novagen
Living Colors A.v. peptide antibody	GFP-based fluorescent proteins (EGFP, ECFP, EYFP, etc.)	Clontech
Monoclonal Hepatitis B Virus Core Antigen antibody (10E11)	HBcAg (aa 1-10)	Abcam
Polyclonal Hepatitis B Virus Core Antigen Antibody	HBcAg	AbD Serotec
Polyclonal anti BTV-10 core	BTV-10 VP7, BTV-10 VP3	courtesy of Polly Roy
Polyclonal anti VP5 GP638	BTV-10 VP5	courtesy of Polly Roy
Polyclonal anti-NS1	BTV-10 NS1	courtesy of Polly Roy
anti-BTV-1 VP5	BTV-1 VP5	Institute for Animal Health
anti-guinea pig Alexa Fluor	Guinea pig IgG	Molecular Probes

2.5.6 QUANTIFICATION

2.5.6.1 UV irradiation of leaves

To qualitatively show the expression of constructs containing GFP, leaves were irradiated with a hand-held Blak-Ray UV lamp (Ultra-Violet Product Ltd.).

2.5.6.2 Bradford assay

To quantify the total protein content of samples, an assay using Bradford reagent (Sigma) was performed. A bovine serum albumin standard curve was prepared using

solutions of known concentration, ranging from 3.1 to 150 µg/ml in PBS. Protein samples were diluted in PBS to fall within this range (1:50 dilution of plant extracts). Triplicate samples were mixed with Bradford reagent according to the manufacturer's instructions, and absorbance at 595 nm was read using a SpectraMAX Plus 96-well plate reader.

2.5.6.3 *Enzyme-linked Immunosorbent Assay (ELISA)*

Direct ELISA was used to quantify Hepatitis B core antigen expression in this study with a protocol modified from Huang et al. (2006). Briefly, 96-well ELISA plates were coated in duplicate with diluted samples and a dilution series of a quantified recombinant HBcAg reference (AbD Serotec). Wells were subsequently blocked with blocking buffer, and the bound HBcAg was detected with polyclonal anti-HBcAg antibody. The primary antibody was detected with anti-rabbit-HRP conjugate. TMB substrate (SIGMA) was used to elicit a colour reaction, which was stopped with 1 M sulphuric acid upon perceived saturation of the standard curve. Colour reactions were quantified by a multi-well plate reader at 450 nm. Subtraction of negative control leaf extract reactions allowed quantification of HBcAg levels in extracts by comparison to the linear regression of the standard curve and back-calculation of the dilution factors. Replicates were averaged.

2.5.6.4 *GFP Fluorescence Assay*

GFP fluorescence was used as a means of quantifying the functional GFP present in protein extracts using a method modified after Richards et al. (2003). Dilutions of plant extracts (1:100 in 0.1 M Na₂CO₃) were loaded onto black 96-well plates in triplicate. Recombinant EGFP (Clontech) was used to prepare a standard curve in diluted negative control extract. A SPECTRAmax multi-well fluorimeter was used to excite samples at 395 nm wavelength and to read the emission at 509 nm. After subtraction of negative control values, amounts of GFP present in each sample could be calculated by comparison of the emission values with the linear regression of the standard curve. Replicates were averaged.

2.5.6.5 *A280*

Purified protein samples were quantified using a NanoDrop spectrophotometer (Thermo Scientific) by measuring the absorbance at 280 nm wavelength.

2.6 VLP PURIFICATION

2.6.1 DENSITY GRADIENT CENTRIFUGATION

For the purification of VLPs, density gradients were formed by injecting solutions of increasing density into the bottom of an ultracentrifuge tube, thereby forming a step gradient with defined density boundaries. The gradient was then overlaid with plant extract. After ultracentrifugation, fractions were collected by piercing the bottom of the tube.

Density gradient materials used include sucrose, iodixanol (Optiprep) and glycerol. A concentrated solution (60% w/v of sucrose, or 50% v/v of iodixanol or glycerol) was prepared in such a way to ensure a 1x buffer concentration. This concentrated stock was then used to make further dilutions in 1x buffer, thus ensuring a constant buffer and salt concentration throughout the gradient.

Specific density gradient media compositions and ultracentrifugation parameters were dependent on the properties of the particles to be purified. These are described in more detail in Chapters 4, 5 and 6.

2.6.2 SIZE-EXCLUSION CHROMATOGRAPHY (SEC)

Size-exclusion chromatography (SEC), or gel filtration, is a means of buffer exchange and allows the removal of density gradient media. Low molecular weight components are retarded in the Sephadex G-25 matrix, while proteins and VLPs are eluted from the column.

Iodixanol gradient media has been found to be more efficiently removed by SEC than other methods such as dialysis (Thompson and Buck, 2007). In this study PD-10 desalting columns (Amersham) were used according to the manufacturer's instructions.

2.6.3 ULTRAFILTRATION

Ultrafiltration was used as a method for buffer exchange and concentration of VLP samples. Dilute VLP preparations were applied to a 100 kDa molecular-weight cutoff column (Microcon or Amicon, Millipore) and centrifuged. This allowed buffer and small solutes to pass through the membrane while retaining and concentrating the VLP above.

2.6.4 DIALYSIS

Dialysis was used as a method of buffer exchange and to remove density gradient medium from samples. Buffer and small solutes pass through a semi-permeable membrane along a concentration gradient from the small sample reservoir into a large volume of buffer, and vice-versa. In this study, Slide-A-Lyzer dialysis cassettes (Pierce) and Float-A-Lyzer dialysis tubing (Spectrum Laboratories) were used.

2.7 VLP ANALYSIS

2.7.1 ABSORBANCE AT 280NM

The absorbance of protein samples at 280 nm wavelength (A₂₈₀) was used as a means of protein quantification. Readings from 1.5µl of sample were taken using a NanoDrop machine (Thermo Scientific). This technique was only used with purified protein and VLP samples. Due to the complex composition of some VLPs (inclusion of nucleic acid, heteromeric complexes), the A₂₈₀ value was not heavily relied upon.

2.7.2 DYNAMIC LIGHT SCATTERING (DLS)

VLP and CLP samples were analyzed by Dynamic Light Scattering (DLS) to determine particle radii and the degree of aggregation. A Dynapro Titan DLS machine with dynamics

software version 6 was used in this study. Readings were taken at a count rate of 1-2 million counts for 10 seconds and repeated 10 times.

2.7.3 TRANSMISSION ELECTRON MICROSCOPY (TEM)

Transmission electron microscopy (TEM) was used to image VLPs, measure their size, and as a qualitative means of determining particle integrity. Samples were adsorbed onto hexagonal, plastic- and carbon-coated copper grids, which were then washed by floating on water droplets. Finally, grids were negatively stained with 2% (w/v) uranyl acetate (UA) for 20 seconds, and stain removed using blotting paper.

Particles were imaged using a FEI Tecnai G2 20 Twin TEM with a bottom-mounted digital camera.

2.7.4 NATIVE AGAROSE GEL ELECTROPHORESIS

Native agarose gel electrophoresis was used to determine qualitative differences in particle surface characteristics, and to show nucleic acid encapsidation. Agarose gels (1% w/v in TBE) were run in duplicate by loading 10 µg of purified protein sample per lane, then applying 60 V for 2 hours. One gel was stained in a dilute bath of ethidium bromide for 30 minutes to detect nucleic acid. To detect protein, the other gel was stained with Brilliant Blue R Concentrate (Sigma Aldrich) for 30 minutes and destained in 20% methanol, 7.5% acetic acid solution.

2.8 SOFTWARE

- Vector NTI Advance 11 (Invitrogen) was used for vector design, *in silico* cloning strategies, sequence analyses and alignments, as well as predictions of protein sequences, sizes and attributes.
- The BLAST function of the National Center for Biotechnology Information website (<http://blast.ncbi.nlm.nih.gov/Blast.cgi>) was used both for nucleotide and protein sequence alignments.
- VIPERdb (<http://viperdb.scripps.edu/>), a database for published structures of icosahedral viruses, was used for visualization of whole capsid structures.
- Crystallographic structures were viewed and imaged using the freeware PyMol programme (DeLano Scientific).
- Microsoft Excel was used for calculations, plots and linear regressions associated with ELISA and fluorescence assays.

3 EXPRESSION VECTOR DEVELOPMENT

3.1 INTRODUCTION

The deleted CPMV expression system (Cañizares et al., 2006), particularly with the advent of *HyperTrans (HT)* technology (Sainsbury and Lomonossoff, 2008), has proved to be an extremely useful tool for the expression and production of heterologous proteins in plants. The CPMV-*HT* system is mainly used in transient expression rather than stable transformation, easily producing milligram quantities of recombinant protein within six days of infiltration, with detectable levels after as little as two days post infiltration. With the speed and simplicity of transient expression, the molecular cloning step presents the major bottleneck to the speed at which new constructs can be tested.

3.1.1 THE EXISTING CPMV CLONING VECTORS

In 2007, the standard cloning procedure into the existing CPMV vectors required a labour-intensive five days and often longer. The first step relied on the restriction enzyme-based cloning of an amplified gene of interest (GOI) into a small, high-copy *E. coli* vector, pM81-FSC2 (Figure 3.1; Sainsbury and Lomonossoff, 2008). Constructs had to be carefully designed to ensure that the start codon of the GOI was at position 512 of the RNA-2 sequence, and that it remained within the same frame as the start codon at position 161 (see Figure 1.2 E). This was due to previous findings that disruption of this frame dependence and alterations to the 5'-UTRs had a detrimental effect on RNA-2 replication (Holness et al., 1989; van Bokhoven et al., 1993). These strict limitations meant that it was not possible to include a multiple cloning site (MCS) or site-specific recombination sites to facilitate cloning. After screening of pM81-FSC2 clones, an *Ascl-Pacl* fragment containing the GOI flanked by the delRNA-2 sequences was subcloned into the large binary vector pBINPLUS (Figure 3.1; Cañizares et al., 2006; van Engelen et al., 1995). This cloning strategy used existing vectors which were not created for transient expression but rather designed for stable integration.

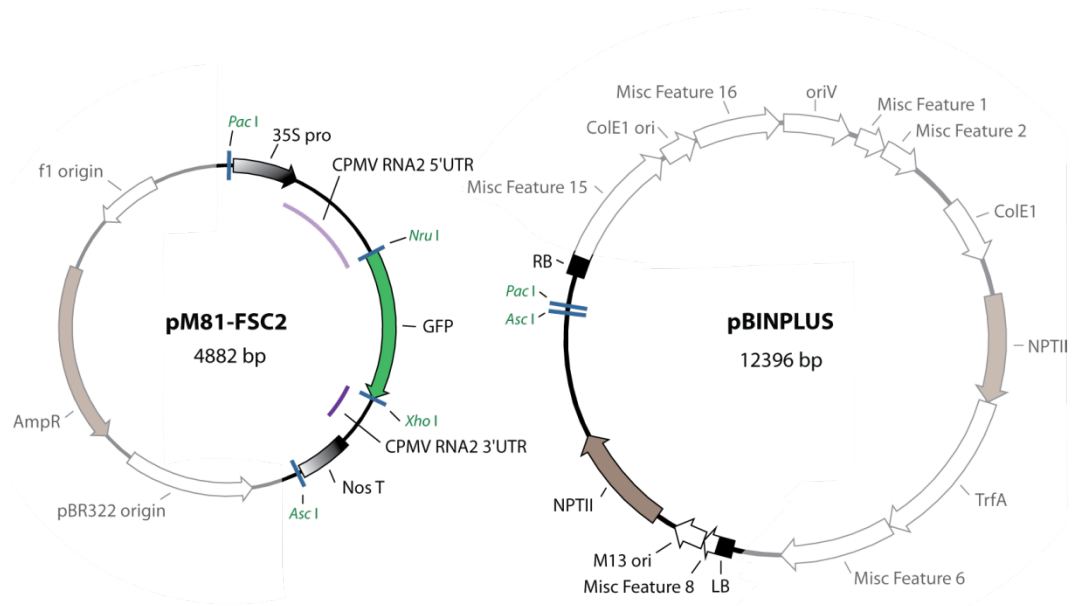


Figure 3.1: Schematic representation of pM81-FSC2 and pBINPLUS, the key cloning vectors of the CPMV expression system in 2007.

The unique restriction sites *Nru*I and *Xho*I allow replacement of the GFP gene in pM81-FSC2 with a gene of interest. Subcloning of the expression cassette into the binary vector pBINPLUS is achieved by restriction cloning into *Pac*I - *Asc*I.

Two serendipitous discoveries allowed the existing two-step cloning system to be radically changed at the start of this project. First, it was noted that expression from delRNA-2 constructs upon co-infiltration with P19, was not severely impacted by the omission of RNA-1. Without the CPMV replication machinery, the expression system was now non-replicating. Secondly, the frame dependence within the 5'-UTR was investigated to see whether removal of the upstream AUGs had any deleterious effect on this non-replicating vector. Incredibly, the removal of the in-frame start codon at position 161 actually increased expression levels of the transgene over 10-fold (Sainsbury and Lomonosoff, 2008). Without the previous strict positioning limitations, it now appeared possible to improve the existing CPMV cloning system by implementing some of the recent advances in molecular cloning and plant binary vector development.

3.1.2 RECENT PLANT BINARY VECTOR DEVELOPMENTS

For nearly three decades, Ti-based binary vectors have been used and optimized for the transfer of heterologous genes into plant cells (Lee and Gelvin, 2008). Recent optimizations of binary vectors have targeted five key areas: vector size, cloning efficiency, GOI targeting and tagging, expansion of host range, and use for multi-gene expression. Some examples of these advances are reviewed below.

A smaller vector size greatly facilitates insertion of fragments of interest into the binary vector. The pCB vector series (Xiang et al., 1999) has a minimized pBIN19-based backbone of less than half the original size, allowing the design of multiple-cloning sites with more unique restriction sites than in the parent plasmid. The pGreen series benefits from an even smaller backbone of less than 3 kb (www.pGreen.ac.uk). This is achieved by supplying essential replication genes *in trans* on a separate plasmid, pSoup (Hellens et al., 2000).

In the past decade, site-specific recombination has been increasingly used as an efficient alternative to restriction cloning. Gateway technology (see Section 2.2.7) based on bacteriophage lambda site-specific recombination (Hartley et al., 2000) has been most widely adopted. The earliest Gateway-compatible binary vector for *Agrobacterium*-mediated overexpression in plants was p*2GW7, which contains a Gateway cassette flanked by 35S promoter and terminator sequences (Karimi et al., 2002). This and a wide array of other Gateway binary vectors have been made available through the University of Gent website (<http://gateway.psb.ugent.be/>). More recently, a cloning system based on Type II secretion restriction enzymes has been developed which allows efficient subcloning of a transgene into a pX vector in a 5 minute reaction (Engler et al., 2008). This 'Golden Gate' cloning system promises to be as simple as Gateway cloning, but leaves genes of interest without flanking recombination sites.

Precise subcellular targeting or tagging of a recombinant protein can be important for folding and assembly, accumulation, and purification. A number of vector series have been developed for these purposes. pSAT vectors allow N- and C-terminal tagging with fluorescent markers and have been shown to allow targeting to specific cellular compartments (Tzfira et al., 2005). The pEarleyGate series of Gateway-compatible vectors can be used for subcellular targeting, affinity tagging as well as fluorescent tagging (Earley et al., 2006).

Some of the aforementioned developments have enabled the construction of binary vectors for the simultaneous expression of multiple genes from a single plasmid. pSAT vectors have been used to co-express three cassettes from the same vector through sequential restriction cloning (Tzfira et al., 2005). A MultiRound Gateway vector system has been used for the co-delivery of seven transgenes from a single vector (Chen et al., 2006). Remarkably, Golden Gate shuffling has been shown to enable the simultaneous subcloning of nine fragments in defined order and orientation within a single reaction (Engler et al., 2009).

Binary vectors can generally be used for transient expression through agro-infiltration (see Section 1.2.2), but they are often designed to allow the recovery of stable transformants. For that reason, binary vectors generally contain a selectable marker gene, which is superfluous for transient expression purposes. Conversely, these vectors do not contain an expression cassette for a suppressor of gene silencing, as these are often not compatible with the recovery of stable transgenics. Gene silencing plays an important role in plant development, and impairment of the pathway by constitutive expression of a suppressor of gene silencing causes developmental defects in the regenerated tissue. When used transiently, a suppressor of gene silencing is generally supplied by co-infiltration with another *Agrobacterium* strain containing a plasmid encoding the suppressor sequence (Cañizares et al., 2006; Voinnet et al., 2003).

3.1.3 AIMS OF THIS CHAPTER

The overall aim of the work described in this chapter was to make the CPMV-*HT* expression system (Sainsbury and Lomonossoff, 2008) more user-friendly. In order to facilitate the cloning steps required for the expression of numerous Hepatitis B and Bluetongue Virus proteins (see Chapters 4 – 7, Appendix A), the existing vector system was improved in several respects. Here, I firstly demonstrate the use of Gateway cloning technology as an alternative to restriction cloning. I subsequently show that the existing binary vector, pBINPLUS, can be reduced to half of its original size without impact on transient expression yields. Based on this minimalized backbone, the pEAQ vector series has been created and tailored to different expression requirements, such as transient expression through the inclusion of a suppressor of gene silencing. In particular, the benefits of co-expressing two genes from the same T-DNA construct have been shown.

3.2 SPECIFIC MATERIALS AND METHODS

Materials and methods specifically pertaining to this chapter are described in detail below. Unless otherwise specified, the general molecular biological techniques were used as detailed in Chapter 2.

3.2.1 CONSTRUCTION OF PENTR-ET2 AND PDEST-BINPLUS

pBINPLUS (van Engelen et al., 1995) was converted into a Gateway destination vector using the Gateway Destination Vector Conversion Kit (Invitrogen) according to the manufacturer's instructions. The vector was digested with *Ascl* and *Pacl*, followed by blunting with Polymerase I large (Klenow) fragment and dephosphorylation with Calf Intestinal Phosphatase (NEB).

For the construction of pENTR-ET2, pM81-FSC2 was amplified with end-tailoring primers attB1-35S-pro-F and attB2-NosT-R (Table 3.1) to engineer portions of Gateway attachment B (*attB*) sites around the CPMV-*HT* expression cassette. A second round of amplification with attB1 adapter and attB2 adapter completed the flanking *attB* sites. BP clonase II enzyme (Invitrogen) was used for site-specific recombination with pDONR207 (Invitrogen) to yield pENTR-ET2beta. Transformants were sequenced with pDONR207 F and pDONR207 R oligonucleotides.

The *NruI* site of the pDONR207-derived backbone was removed by site-directed mutagenesis (see Section 2.2.6) using primers pENTR-FSC2-*NruI*-F and pENTR-FSC2-*NruI*-R. This resulted in the entry vector pENTR-ET2 with unique *NruI* and *XhoI* sites to allow pM81-FSC2-based cloning strategies to be used.

Table 3.1: Oligonucleotides used in cloning of pENTR-ET2.

Name	Sequence ^a	Function
attB1-35S-pro F	AAAAAGCAGGCTT <u>Attaattaa</u> gaattcgagctccaccgc	Amplification of 35S-promoter upstream of <i>PacI</i> site of pM81-FSC1; end-tailoring of partial <i>attB1</i> ; sense
attB2-NosT R	agaaagctgggtagg <u>cgcgcca</u> AG CTTGAGACTC	Amplification of <i>nos</i> terminator downstream of <i>Ascl</i> site of pM81-FSC1; end-tailoring of partial <i>attB2</i> ; antisense
attB1 adapter	GGGGACAAGTTTGTACAaaa agcaggct	Universal adapter to end-tailor complete <i>attB1</i> site; sense
attB2 adapter	GGGGACCACTTTGTACAagaa agctgggt	Universal adapter to end-tailor complete <i>attB2</i> site; antisense
DONR207 F	gttaacgctagcatggatctcg	Sequencing of pENTR207 Entry clones; sense
DONR207 R	tcagagattttgagacacggg	Sequencing of pENTR207 Entry clones; antisense
ENTR-FSC2-Nru-F	gggtataaatgggctcg <u>agataatgt</u> cgggcaatc	Site-directed mutagenesis removal of <i>NruI</i> site in pENTR-FSC2 backbone; sense
ENTR-FSC2-Nru-R	gattgcccgcattatc <u>tcgagcccat</u> ttataccc	Site-directed mutagenesis removal of <i>NruI</i> site in pENTR-FSC2 backbone; antisense

^a END-TAILORING is shown in uppercase, restriction enzyme recognition sites are underlined, mutations are underlined and bold.

3.2.2 CONSTRUCTION OF THE PEAQ SERIES

pBD-FSC2-GFP-*HT* (Appendix C, Figure 1; Sainsbury et al., 2009), a derivative of pBINPLUS (van Engelen et al., 1995) containing a CPMV-*HT* cassette for GFP expression within the *Ascl-PacI* sites, was used as a parent plasmid for minimalization of the vector backbone. This GFP expression cassette contains the U162C *HyperTrans* mutation for increased translation efficiency (Sainsbury and Lomonosoff, 2008).

The parent plasmid was amplified with three pairs of primers (Table 3.2) to produce three fragments: (1) pBD-LB-F (binding upstream of a natural *AhdI* site) and pBD-RB-ApaI-R amplified the T-DNA region; (2) pBD-ColEI-ApaI-F and pBD-TrfA-SpeI-R resulted in a fragment comprising the TrfA and NPTII cassettes and ColE1 *E. coli* origin of replication; (3) pBD-oriV-SpeI-F and pBD-oriV-AhdI-R amplified oriV, the RK2 origin of replication. Purified

PCR products were restriction enzyme -digested as needed and subjected to a three-part ligation to yield pEAQbeta. Sequencing of junctions revealed that 1.2 kb near the *nos* terminator in the T-DNA fragment had been deleted unintentionally. In a second step, pBD-FSC2-GFP-*HT* was amplified with pMini>pMicroBIN-F2 and pBD-RB-ApaI-R, and pEAQ-beta was amplified with pBD-ColEI-ApaI-F and pMini>pMicroBIN-R. Following digestion with *ApaI* and *FseI* and purification, these fragments were ligated to yield pEAQ-GFP-*HT*.

pEAQexpress-GFP-*HT* was obtained by amplifying the 35S:P19 cassette of pBIN61-P19 (Voinnet et al., 2003) with 35SP19-Fse-F and -R (Table 3.2), then cloning into the unique *FseI* site of pEAQ-GFP-*HT*. Similarly, pEAQspecialK-GFP-*HT* was obtained by amplifying the *nos* promoter and terminator NPTII cassette of pBD-FSC2-GFP-*HT* with pBD-NPTII-FseI-F and -R, then cloning into the *FseI* site of pEAQ-GFP-*HT*. Insertions resulting in transcription away from the left border gave consistently lower plasmid yields (3 clones of each orientation were tested, data not shown) and were termed pEAQselectK(rev).

pEAQspecialK was obtained by amplifying the 35S:P19 cassette with 35SP19-PacI-F and 35SP19-AscI-R (Table 3.2) and cloning the fragment into the *MluI* – *AsiSI* sites of pEAQselectK. pEAQspecialK was used by Dr. Frank Sainsbury to make pEAQ-*HT* by replacing the GFP gene with a multiple cloning site (Sainsbury et al., 2009).

To obtain the pEAQ-*HT*-DEST vectors, a Gateway vector conversion kit (Invitrogen) was used to insert the appropriate reading frame (Rf) cassettes containing a chloramphenicol resistance gene and *ccdB* gene for selection, flanked by *attR* recombination sites, into pEAQ-*HT*. In this way, ligation of RfC.1 into the *StuI* / *NruI* digested vector yielded pEAQ-*HT*-DEST1; ligation of RfA into the *SmaI* / *StuI* digested vector yielded pEAQ-*HT*-DEST2; and ligation of RfB into the *SmaI* / *NruI* digested vector yielded pEAQ-*HT*-DEST3.

Table 3.2: Oligonucleotides used in cloning of pEAQ vectors.

Name	Sequence^a	Function
35SP19-Pacl-F	<u>TTAATTA</u> Agaattcgagctcggtacc cccctactcc	Amplification of 35S-P19 cassette; end-tailoring of Pacl; sense
35SP19-Ascl-R	<u>GGCGCGCC</u> atcttttatctttagagtta agaactcttctg	Amplification of 35S-P19 cassette; end-tailoring of Ascl; antisense
35SP19-Fsel-F	<u>GGCCGGCC</u> gaattcgagctcggtac cccc	Amplification of 35S-P19 cassette; end-tailoring of Fsel; sense
35SP19-Fsel-R	<u>GGCCGGCC</u> atcttttatctttagagtta ag	Amplification of 35S-P19 cassette; end-tailoring of Fsel; antisense
C1	aacgttgtcagatcggtcttcggcacc	Sequencing of CPMV cassettes; sense
C3	ctgaaggggacgacctgtaaacaggag g	Sequencing of CPMV cassettes; antisense
pBD-ColEI-Apal-F	<u>GACTTAGGGCC</u> cgccatttccgcg cagacgatgacgtcact	Amplification of region 1704 – 5155 of pBD-FSC2-GFP- <i>HT</i> ; end-tailoring of Apal; sense
pBD-TrfA-Spel-R	<u>GCATTA</u> <u>ACTAGT</u> cgctggctgctga acccccagccggaactgacc	Amplification of region 1704 – 5155 of pBD-FSC2-GFP- <i>HT</i> ; end-tailoring of Spel; antisense
pBD-LB-F	gccactcagcttctcagcggcttt	Amplification of region 6338-12085 of pBD-FSC2-GFP- <i>HT</i> ; sense
pBD-RB-Apal-R	TATTAGGGCCCccggcgccagatct ggggaaccctgtgg	Amplification of region 6338-12085 of pBD-FSC2-GFP- <i>HT</i> ; end-tailoring of Apal; antisense
pBD-oriV-Spel-F	<u>GTAGCACTAGT</u> gtacatcaccgacg agcaaggc	Amplification of region 14373-670 of pBD-FSC2-GFP- <i>HT</i> ; end-tailoring of Spel, sense
pBD-oriV-Ahdi-R	<u>CAGTAGACAGGCTGT</u> Ctcgcggc cgagggcgagccc	Amplification of region 14373-670 of pBD-FSC2-GFP- <i>HT</i> ; end-tailoring of Ahdi, antisense
pMini-->pMicroBIN-F2	<u>GGCCGGCCACGCGT</u> TATCTGC <u>AGAGCGATCGC</u> aacagctatgacc atgattacccaagctg	Amplification of region 2969-85 of pEAQbeta; end-tailoring of Fsel-Mlul-AsiSi; sense
pMini-->pMicroBIN-R	<u>GCGATCGCT</u> CTGCAGATA <u>ACG</u> <u>CGTGGCCGGCC</u> ctcactggtgaaa agaaaaaccaccagctacattaaaaac gtcc	Amplification of region 2969-85 of pEAQbeta; end-tailoring of AsiSi-Mlul-Fsel; antisense
pBD-NPTII-Fsel-F	<u>GGCCGGCCTACAGT</u> atgagcggg gaattaagggagtcacg	Amplification of the NPTII cassette from pBD-FSC2-GFP- <i>HT</i> ; end-tailoring of Fsel; sense
pBD-NPTII-Fsel-R	<u>GGCCGGCCTACAGT</u> cccgatctag taacatagatgacaccgcg	Amplification of the NPTII cassette from pBD-FSC2-GFP- <i>HT</i> ; end-tailoring of Fsel; antisense

^a END-TAILORING is shown in uppercase, restriction enzyme recognition sites are underlined, mutations are underlined and bold.

3.2.3 GFP EXTRACTION

Samples for the analysis of GFP expression consisted of three discs from different leaves of the same plant, obtained using the end of a 15 ml Corning tube. These corresponded to approximately 90 mg healthy fresh weight tissue (hFWT). Samples were extracted in 270 μ l Extraction buffer (ExB; Table 2.4).

3.2.4 GFP ASSAY

Fluorescence was used to quantify yields of active GFP in the samples using a modified version of a published protocol, as described previously (Section 2.5.6.4; Richards et al., 2003). Information about sample size and dilution was used to back-calculate the yield of fluorescently active GFP expressed in g per kg hFWT.

3.2.5 YFP + CFP EXPRESSION AND CONFOCAL MICROSCOPY

The genes for YFP and CFP were obtained from vectors pEYFP and pECFP (BD Living Colors), respectively. EYFP has an excitation maximum at 513 nm and an emission maximum at 527 nm with a brightness [(quantum yield)*(extinction coefficient)] of 151% of EGFP (http://www.clontech.com/products/detail.asp?product_id=10419&product_group_id=1437&product_family_id=1417&tabno=2). ECFP has an excitation maximum at 433 nm and an emission maximum at 475 nm with a brightness of 17% of EGFP. The stark difference in relative brightness required the signal of ECFP to be boosted relative to EYFP in order to obtain images with a detectable colour shift in the merged image, indicating co-localization.

Fluorescence was imaged using a Leica SP2 inverted confocal microscope. ECFP was excited with 85% laser intensity at 458 nm (836 V gain, 1.4 % offset). EYFP was excited with 21% laser intensity at 514 nm (488 V gain, 1.9% offset).

3.3 RESULTS

The development of a more efficient vector system was seen as a necessity to make the CPMV-*HT* system more user-friendly. Following on from efforts to make the existing cloning vectors Gateway compatible (see Section 3.3.1), a whole new vector series (pEAQ) was created. The work described in sections 3.3.2 to 3.3.5 was shared equally with Dr. Frank Sainsbury (Laval University, Quebec City, Canada; formerly JIC).

In order to monitor any possible effects of alterations to the expression vectors, a CPMV expression cassette encoding the enhanced green fluorescent protein (EGFP) was maintained in the vectors. Expression levels could thus be compared easily by UV irradiation of leaves (qualitative) or by a multi-well plate fluorescence assay (quantitative).

3.3.1 GATEWAY® COMPATIBLE VECTORS FOR SUBCLONING

Transient expression using the CPMV-*HT* system is a quick method to determine whether a protein of interest is amenable to expression in plants. Once a gene is cloned into a binary vector and transformed into *Agrobacterium*, expression can be detected as soon as two days post infiltration. Thus, at the start of this thesis, the most time-consuming steps in the screening of new constructs were the cloning and subcloning of the gene, which took at least five days, but often longer. Particularly the restriction enzyme-based subcloning of the expression cassette into the large pBINPLUS vector was inefficient and often required repeated attempts.

Gateway cloning is an alternative to traditional restriction cloning, relying on site-specific recombination to move DNA fragments from one vector to another (see Section 2.2.7). This process is faster and often more reliable than restriction enzyme-based subcloning.

In order to make the existing cloning system Gateway-compatible, both pM81-FSC2 and pBINPLUS (Figure 3.1) had to be modified to accommodate site-specific recombination (attachment) sites. To achieve this, the expression cassette (*PacI* – *Ascl* fragment) of pM81-FSC2 was amplified with end-tailoring primers to insert *attB1* and *attB2* sites up- and downstream of the cassette, respectively. A subsequent BP reaction

with pDONR207 yielded the entry clone pENTR-ET2 (Figure 3.2). This high-copy plasmid retained all of the unique restriction cloning sites utilized in customary cloning strategies for insertion of a gene of interest into pM81-FSC2. The resulting *attL* sites just outside of the *PacI*-*AscI* fragment made this vector amenable to Gateway LR reactions, while maintaining its ability to serve as a source for *AscI*-*PacI* cassettes, which will become relevant for pEAQexpress cloning (Section 3.3.3)

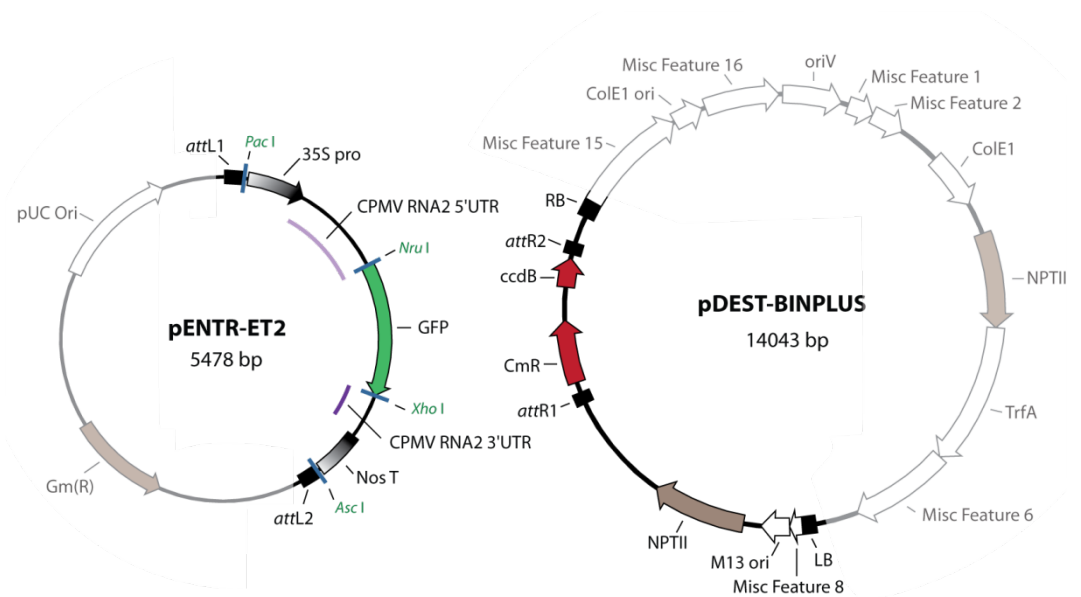


Figure 3.2: Schematic representation of pENTR-ET2 and pDEST-BINPLUS, Gateway compatible versions of the key cloning vectors of the CPMV expression system.

The unique restriction sites *NruI* and *XhoI* allow replacement of the *gfp* gene in pENTR-ET2 with a gene of interest. Subcloning of the expression cassette into the binary vector pDEST-BINPLUS is achieved by site-specific recombination between the *attL* sites of pENTR-ET2 and the *attR* sites of pDEST-BINPLUS.

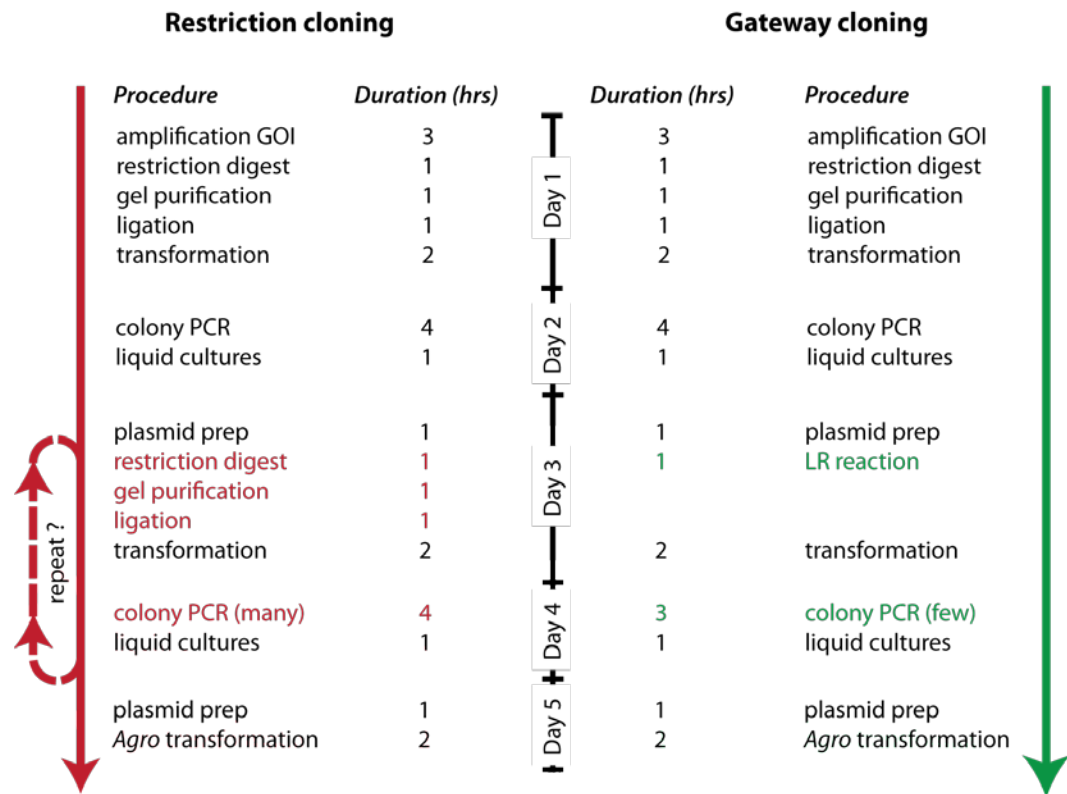


Figure 3.3: Workflow comparison of restriction cloning and Gateway cloning.

When obtaining a new clone for expression with the CPMV system, Gateway cloning is faster and more efficient. Key steps in each procedure are listed with their approximate duration in hours. Differences between the two strategies are highlighted in red and green.

Using the Gateway Destination Vector Conversion Kit (Invitrogen), the widely used binary vector pBINPLUS was converted to the destination vector pDEST-BINPLUS. In this vector, the MCS inclusive of *Ascl* and *Pacl* was replaced by a cassette containing the cytotoxic *ccdB* gene and the chloramphenicol resistance gene, flanked by *attR* sites.

Using these new Gateway vectors, subcloning could now be achieved in a one hour site-specific recombination reaction between the *attL* sites of a pENTR-ET2 clone and the *attR* sites of pDEST-BINPLUS, in the presence of the LR clonase enzyme. Potential background colonies are suppressed by the presence of the cytotoxic *ccdB* gene in unrecombined pDEST-BINPLUS, and the lack of kanamycin resistance in the pENTR-ET2 clone.

The Gateway LR reaction has never failed during my 3-year PhD project, showing that it is far more reliable than traditional restriction enzyme-based subcloning. Being able to forego the traditional *Ascl-Pacl* digest, gel purification, vector preparation and ligation

steps, Gateway subcloning is also less labour-intensive and saves approximately half of a day's work (Figure 3.3).

In order to determine whether the presence of Gateway attachment sites on the outside of the expression cassette has any effect on expression levels, GFP expression from pDEST-BINPLUS constructs were compared to those of pBINPLUS constructs. The observed GFP fluorescence intensity from constructs with the *HT* mutation was not affected by the presence of *attB* sites (Figure 3.4 A). By using equivalent constructs with wild type leader sequences (i.e. delRNA-2, not *-HT*) which give far lower expression levels, it was easier to see minute differences in fluorescence intensity between the two constructs. Comparison of pBINPLUS-GFP and pDEST-BINPLUS-GFP showed that expression from the Gateway construct may be slightly better than from the traditional pBINPLUS construct (Figure 3.4 A). Direct comparison of crude extracts derived from the infiltrated leaf tissue by SDS-PAGE (Figure 3.4 B) showed that there was minimal variation between the GFP expression achieved from the Gateway vectors, compared with restriction-cloned vectors.

These results indicate that Gateway-compatible versions of the standard CPMV cloning vectors allow for easier and more reliable subcloning, without affecting expression levels.

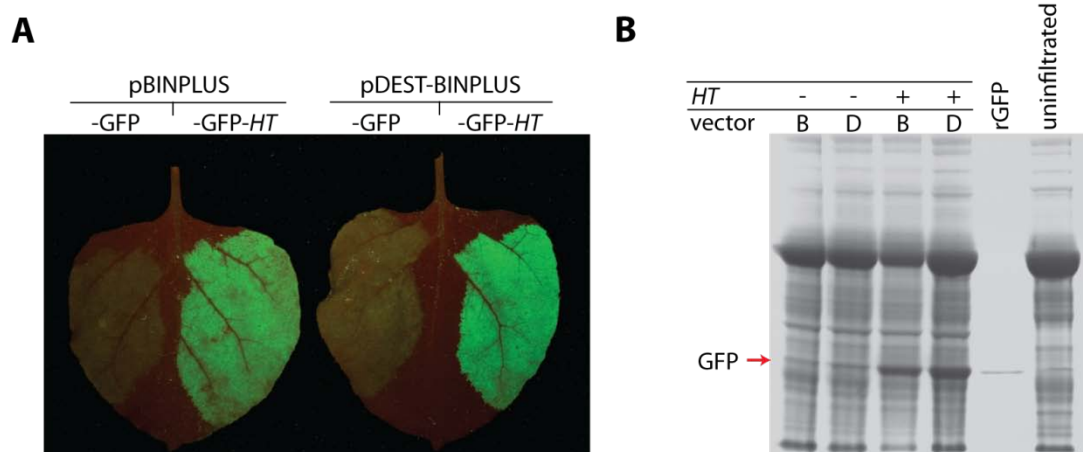


Figure 3.4: The presence of Gateway *attB* sites flanking the CPMV expression cassette does not negatively affect expression levels of GFP.

Leaves were agro-infiltrated with P19 and the GFP constructs in pBINPLUS or pDEST-BINPLUS vector backbones as indicated. (A) UV photograph of leaves harvested 6 dpi. (B) Coomassie-stained SDS-PAGE of crude extracts from constructs indicated. *HT* = *HyperTrans*; B = pBINPLUS backbone; D = pDEST-BINPLUS backbone.

3.3.2 STREAMLINING OF THE pBINPLUS BINARY VECTOR BACKBONE

First generation binary vectors such as pBIN19 (Bevan, 1984) were created to allow efficient transformation of plant tissue by stable integration of a transgene. These vectors were constructed by using pre-existing restriction sites of other plasmids to assemble fragments with desired functional elements: T-DNA region, resistance cassette, origin of replication, etc. The complete sequence of pBIN19 was published 10 years after its first use, revealing large stretches of sequence which could not be annotated and assigned a function (Frisch et al., 1995). Improvements to this early binary vector resulted in construction of pBINPLUS (van Engelen et al., 1995). However, the changes undertaken did not include the rationalization of the vector backbone. To achieve the goal of creating a vector series for easy and efficient cloning, and ultimately one-step cloning, it was essential to reduce the backbone size of the binary vector. Smaller vectors often have more unique restriction sites and are more compatible with commercial DNA purification kits which often have a cut-off of 10 kb.

In order to monitor any possible effects of alterations to the expression vector backbone, pBD-FSC2-GFP-*HT* was chosen as the parent plasmid. This is a pBINPLUS-derived plasmid containing a *HyperTrans* cassette for the expression of the marker protein GFP.

Figure 3.5 shows how selective amplification and ligation of certain regions of the 14.4 kb pBD-FSC2-GFP-*HT* resulted in the intermediate vector pEAQbeta and ultimately yielded a minimalized vector of 7.2 kb, pEAQ-GFP-*HT*. Computational analysis of the pBINPLUS vector backbone revealed the regions deemed essential for the functionality of the binary vector for transient expression purposes. The fragment between the left and right borders, shown in red, is the T-DNA which is transferred to the plant cell via type IV secretion. The fragment shown in orange contains the ColEI origin of replication, the *neomycin phosphotransferase* (NPTIII) gene for kanamycin resistance, and the *TrfA* gene encoding a replication initiation protein. Finally, the original origin of replication of pBIN19, oriV, is shown in yellow. End-tailoring PCR allowed these fragments to be fused in a 3-part ligation to yield the intermediate vector pEAQbeta (Figure 3.5 B). Since the CPMV-*HT* system is used for the transient expression of proteins, the *neomycin phosphotransferase* gene in the T-DNA region is superfluous, as there is no need to select for positive transformants. In a second cloning step, a portion of the T-DNA region

encompassing the NPTII cassette for kanamycin selection of transgenics was removed (dotted line).

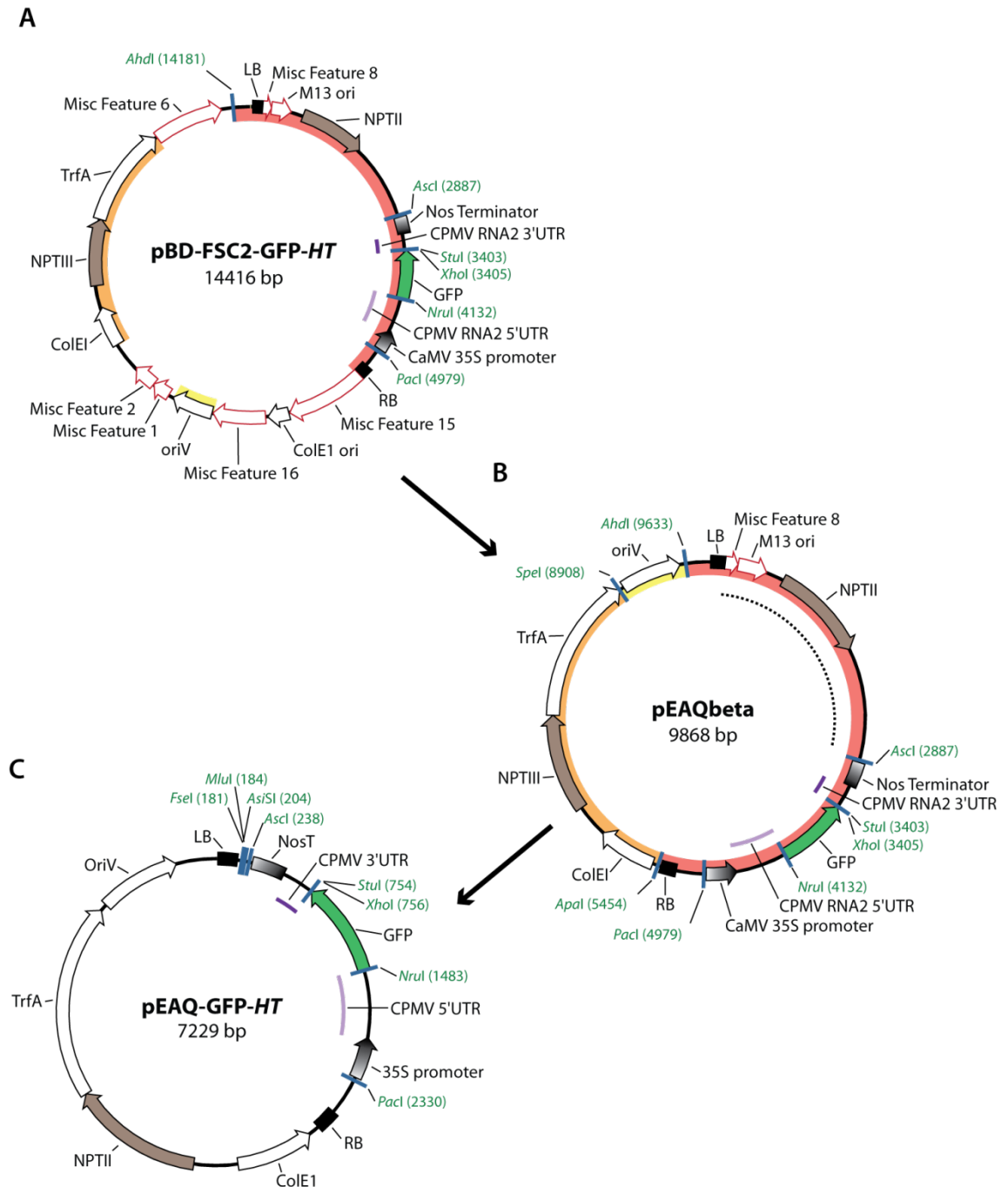


Figure 3.5: Schematic representation of the production of the first pEAQ vector.

(A) pBINPLUS-based expression vector used as a template. Amplified regions highlighted (red, orange, yellow). (B) Resulting vector from three-part ligation of amplified regions. (C) Final pEAQ vector obtained by minimalization of the T-DNA region: removal of NPTII resistance cassette -dotted line in (B).

The resulting vector pEAQ-GFP-*HT* (Figure 3.5 C) was half of the size of its parent vector. However, the removal of 7.2 kb of sequence did not affect its ability to replicate in *E. coli* and *A. tumefaciens*, giving a plasmid yield comparable to other pBINPLUS-based plasmids (data not shown). The minimalization also did not appear to affect the transient GFP expression levels achieved from this vector, qualitatively determined by examination of infiltrated leaves under UV light (see Section 3.3.4). The pEAQ backbone alone, without the CPMV expression cassette between the *Ascl* and *Pacl* sites, is 5137 bp in size, making it one of the smallest binary vectors in use.

3.3.3 THE PEAQ VECTOR SERIES

The optimal route for expression of a foreign protein using the CPMV system can be dependent on the protein product itself, as well as its intended use. For mass production of a protein, easy scale-up is essential and the development of stable transgenics may be ideal. However, for applications in research and product development, it may be more important to have an easy-to-use and fast expression system such as transient expression via agro-infiltration. For complex products such as Bluetongue Virus-like particles, it is essential to ensure efficient co-expression of two or more genes in the same cell. Since every one of these expression strategies has different vector requirements, such as the presence of a selectable marker, suppressor of gene silencing, or multiple expression cassettes on a single T-DNA, we decided to create a vector series tailored to different applications – the pEAQ vectors.

When constructing pEAQ-GFP-*HT*, an MCS was introduced between the left border and the *Ascl* site of the T-DNA region (Figure 3.6). The overhangs produced by digestion with *Mlu*I and *Asi*SI are compatible with the overhangs of *Ascl* and *Pacl*. This compatibility allows for the insertion of a second *Ascl* – *Pacl* CPMV expression cassette, resulting in the loss of the *Mlu*I and *Asi*SI restriction sites. The other expression cassette (containing *gfp* in the case of pEAQ-GFP-*HT*) can be easily replaced by any other *Ascl* – *Pacl* cassette from pM81-FSC2-, pBINPLUS- or pEAQ-based plasmids, thereby allowing co-expression of two genes of interest from one T-DNA. The benefits of this will be discussed in section 3.3.6. Subcloning of expression cassettes into the pEAQ vectors is facilitated by the small size of the vector.

The unique and rare 8-bp recognition sequence of *FseI* provides a site for the insertion of another expression cassette. This site was used to introduce a cassette for the co-expression of P19, a suppressor of gene silencing. The resulting vector, pEAQexpress, is tailored for the high-level transient co-expression of two genes of interest. By having the P19 cassette present on the same T-DNA, this effectively allows expression of three foreign genes from a single *Agrobacterium* construct. This simplifies the preparation of infiltration solution, makes syringe infiltration easier, and decreases the amount of bacteria infiltrated into each leaf, thereby reducing both the stress on the plant and the load of contaminating bacterial proteins in downstream processing.

A second vector was made by the insertion of a NPTII cassette for kanamycin resistance into the *FseI* site. By allowing for the selection of positive integration events through growth on kanamycin-containing media, the resulting vector pEAQselectK is tailored for the co-expression of one or two genes of interest in transgenic plants. By co-infiltration with another *Agrobacterium* for P19 expression, this vector can also be used to screen constructs transiently. Whilst screening clones for the direction of insertion of the NPTII cassette, it was noted that all pEAQselectK clones with the cassette in the unintended reverse orientation (i.e. stop codon closest to the left border) gave up to 2-fold higher plasmid yields. Hence, this vector should be preferentially used.

A P19 cassette was also inserted into the *MluI*-*Asi*SI sites of pEAQselectK to yield pEAQspecialK. This vector can be used for high-level transient expression and has the potential to be used for stable integration.

As stated previously, the discovery of enhanced translational efficiency through removal of the in-frame AUG at position 161 obviated the need to maintain frame integrity between the open reading frames at positions 161 and 512 (see Figure 1.2 E). This made it possible to insert additional sequences, such as a MCS or Gateway recombination sites, between the 5'-UTR and the start codon of the GOI. In order to allow for direct cloning of a gene of interest into pEAQspecialK, and to enable easy N- and/or C-terminal His tagging, Dr. Frank Sainsbury created pEAQ-HT by replacing the GFP gene of pEAQspecialK with a MCS (see Figure 3.6, bottom; Sainsbury et al., 2009)

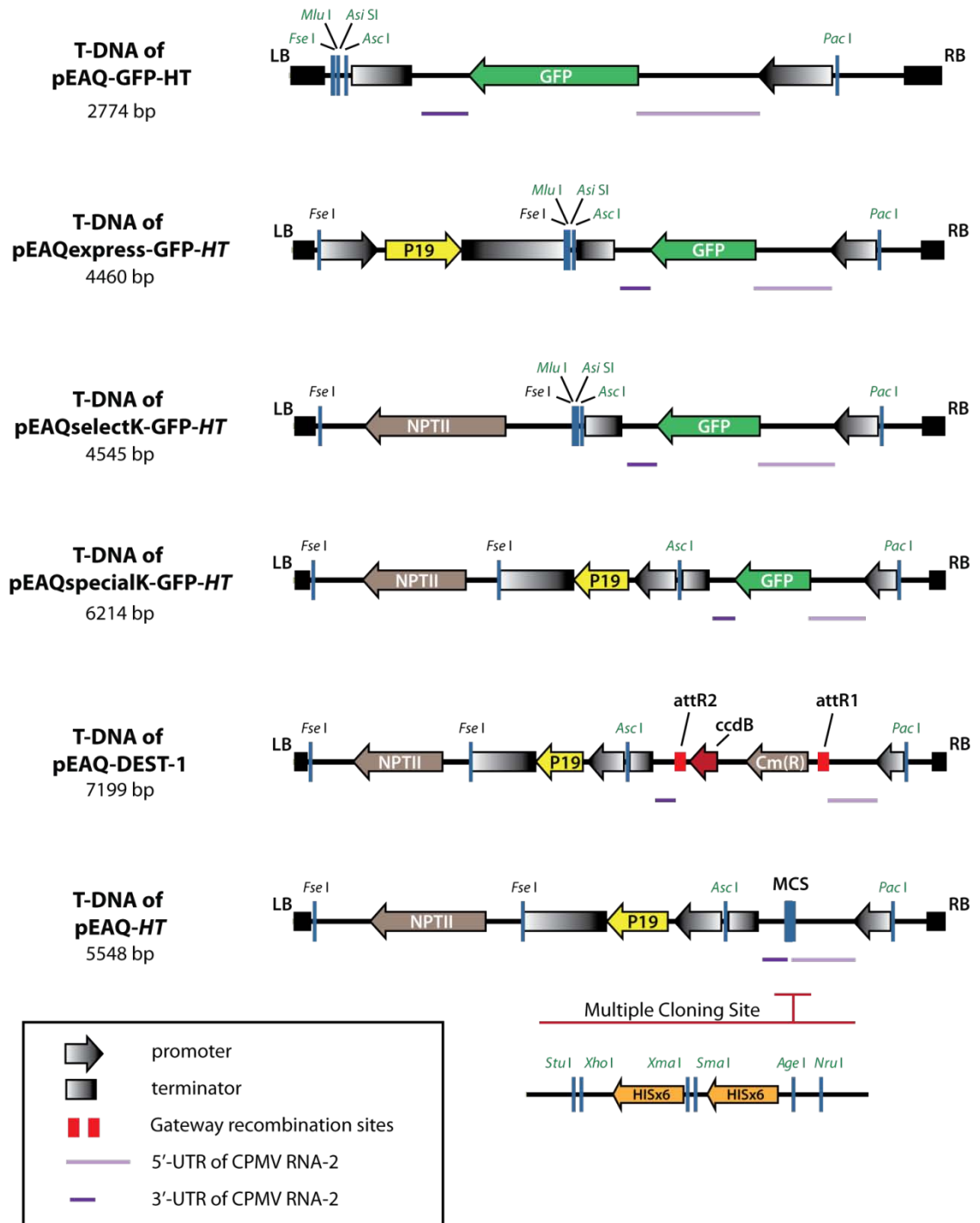


Figure 3.6: Schematic representation of T-DNA regions of the core pEAQ-series vectors.

Genes and resistance cassettes are identified within the schematic. Unique restriction sites available for cloning and sub-cloning are indicated in green. For pEAQ-HT, a close-up of the multiple cloning site (MCS) allowing His-tagging is provided below. Promoters and terminators associated with NPTII genes were omitted for clarity.

3.3.4 THE PEAQ VECTORS RETAIN THEIR HIGH EXPRESSION CAPABILITY

The transient expression efficiency of the pEAQ series of vectors was investigated by agro-infiltration of *N. benthamiana* leaves. Constructs without a P19 cassette were supplied with this suppressor of gene silencing *in trans*, by co-infiltration with pBIN61-P19 (Voinnet et al., 2003). Irradiation of infiltrated leaf tissue with UV light qualitatively showed that expression levels of GFP are comparable between all pEAQ vectors and their parent plasmid pBD-FSC2-GFP-HT (Figure 3.7 A).

Further analysis of leaf extracts by SDS-PAGE revealed a distinct protein band at 27 kDa, corresponding to the size of GFP (Figure 3.7 C). This band is visible in all samples except the negative control extract of pBINPLUS-infiltrated tissue, as expected.

A spectrofluorometric GFP assay allowed the amount of GFP in the samples to be quantified by comparison to a standard curve of known concentrations of recombinant EGFP (Figure 3.7 B). Expression levels from the parent plasmid pBD-FSC2-GFP-HT and the pEAQ and pEAQexpress constructs approached 1 g/ kg FWT. Interestingly, the two constructs harbouring the NPTII cassette in reverse orientation, namely pEAQselectK and pEAQspecialK, gave significantly higher expression levels, reaching 1.25 g / kg FWT in the case of pEAQspecialK.

To show whether plasmids containing a P19 cassette could be infiltrated at higher dilutions of inoculum, pEAQexpress and pEAQspecialK were infiltrated at 2-fold dilutions (indicated by 1:2 in Figure 3.7). Indeed, this dilution factor did not have a significant impact on expression levels. The ability to use less *Agrobacteria* further simplifies the preparation of infiltration solutions.

These results show that the pEAQ-based constructs are equal or better in their transient expression capability when compared with pBINPLUS-derived constructs, and can be used interchangeably.

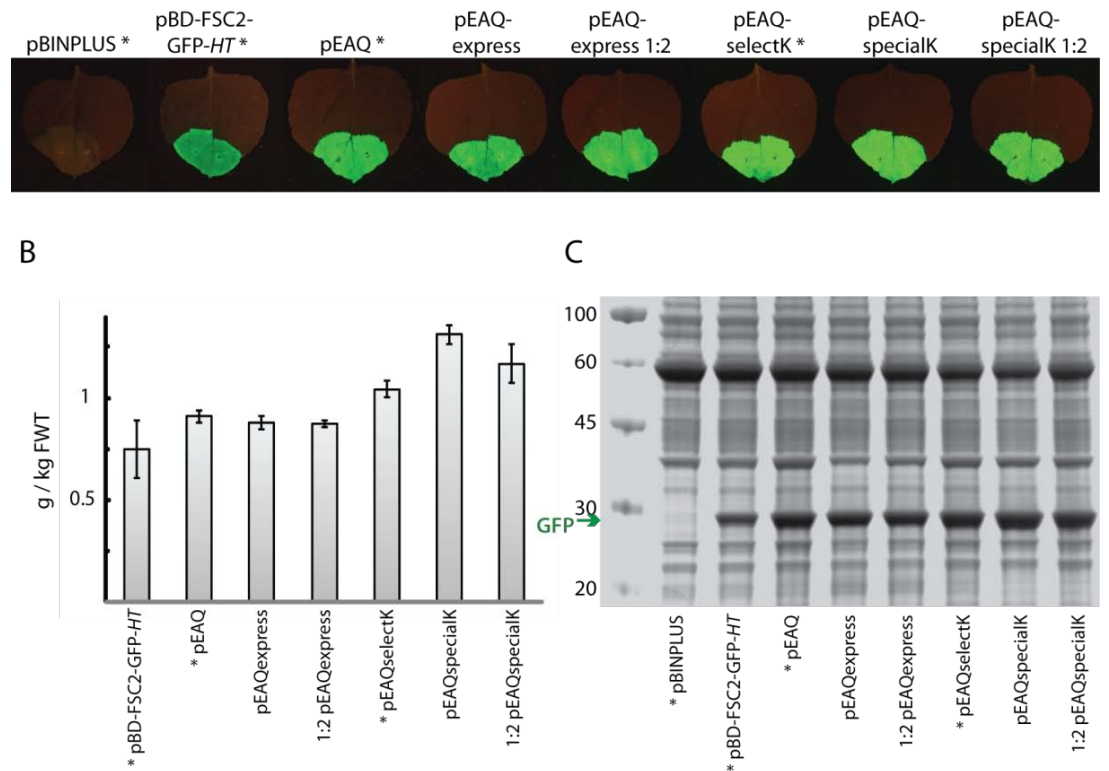


Figure 3.7: GFP expression levels of pEAQ vectors are comparable to those of the parent plasmid.

Leaves were infiltrated with *Agrobacterium* suspensions of equal density as indicated. * marks co-infiltrations with P19. Inoculums marked with '1:2' were infiltrated with a 2-fold dilution. (A) UV illumination of leaves at 7 dpi. (B) Quantitative GFP fluorescence assay. Data represent six independent repetitions with standard error indicated. (C) Coomassie-stained SDS-PAGE of extracts derived from the leaves shown in (A).

3.3.5 GATEWAY COMPATIBLE pEAQ VECTORS FOR HIGH-THROUGHPUT SCREENING

Gateway technology, as introduced previously, provides an easy, quick and reliable alternative to restriction-based cloning, thereby making it a system of choice for high-throughput screening applications. Gateway compatible vectors exist for all commonly used expression systems (bacterial, yeast, mammalian, insect and plant). In order to make it easier for researchers to test the benefits of the CPMV-*HT* system for their own purposes, we constructed three Gateway-compatible versions of the pEAQ-*HT* vector (see Section 3.3.3).

The pEAQ-*HT* MCS (Figure 3.6, bottom) was digested with three combinations of blunt-cutting enzymes, followed by ligation of an appropriate Gateway *ccdB* cassette to maintain the desired reading frame. Digestion with *Stul* and *Nrul* resulted in pEAQ-*HT*-DEST-1 which is used to express untagged proteins (Figure 3.6). Digestion with *SmaI* and *Nrul* gave rise to pEAQ-*HT*-DEST-2 which can be used to create a N-terminal His tag fusion. Digestion with *Stul* and *SmaI* resulted in pEAQ-*HT*-DEST-3 which is useful to create a C-terminal His tag fusion when used in an LR reaction with an entry clone in which the GOI lacks a stop codon.

To test the expression efficiency of these three vectors, they were used in recombination reactions with entry clones harbouring the *gfp* gene with or without a stop codon, as required (Figure 3.8 A). The resulting constructs, pEAQ-GW-GFP, pEAQ-GW-His-GFP and pEAQ-GW-GFP-His, were used in a transient expression assay. Expression levels were quantified by GFP fluorescence assay (Figure 3.8 B). Active GFP was detected at levels of 0.7 – 1.1 g per kg FWT, with untagged GFP expressed at the lower and GFP-His expressed at the higher end. This large range could be due to plant-to-plant variability. It could also be caused by differences in protein stability or fluorescence intensity caused by the N- and C-terminal extensions of attachment B sites and His tags.

Protein extracts were separated on SDS-PAGE gels (Figure 3.8 C). Coomassie blue staining revealed a size shift in the His-tagged GFP variants when compared to the untagged GFP, as expected. To prove protein identity and show the presence of affinity tags, Western blots and immunodetection were carried out. An anti-GFP antibody detected antigen in all GFP-containing samples but not the control, as expected. As in the Coomassie blue-stained gel, the bands detected for the His tagged variants were slower migrating. In the case of GFP-His, the affinity tag appeared to be lost in some cases, resulting in a second, fast migrating GFP band which was also visible in the Coomassie blue-stained gel. The anti-His antibody detected its antigen in the His-tagged GFP samples only, as expected.

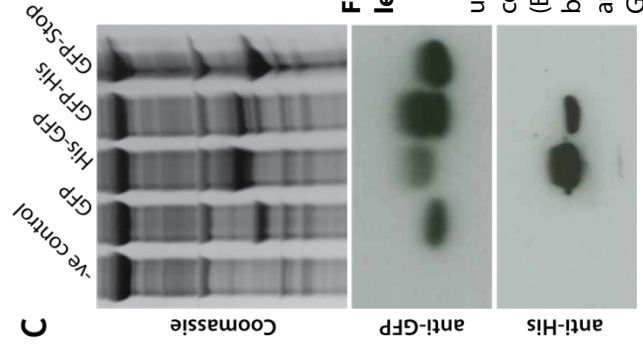
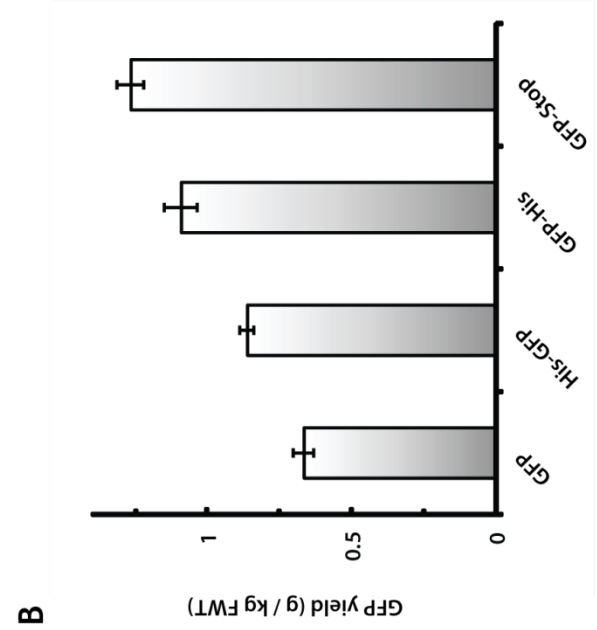
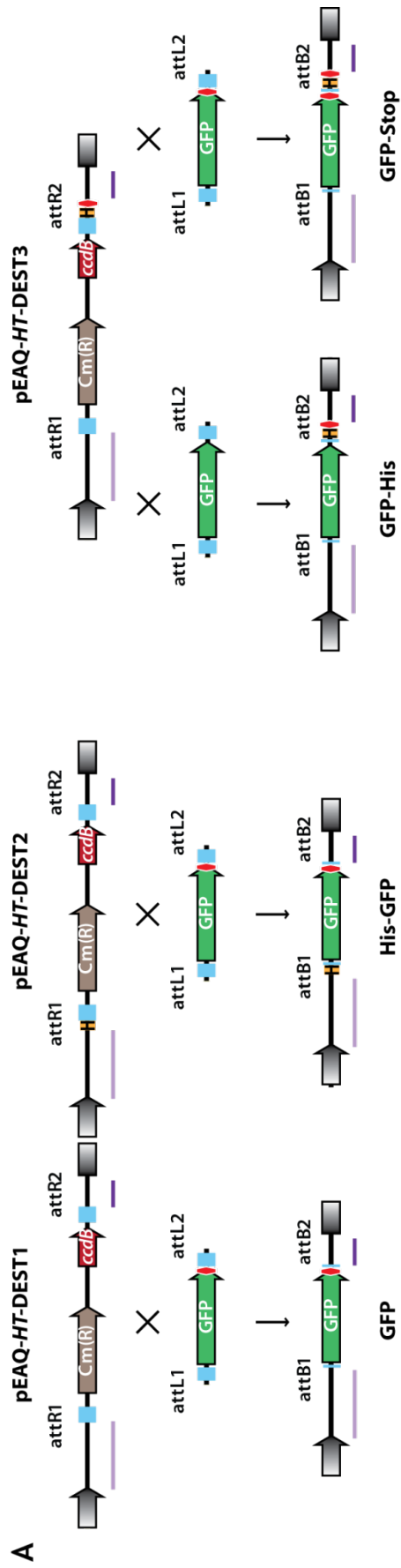


Figure 3.8: The pEAQ-HT-DEST Gateway vectors allow high-level expression of His-tagged or untagged proteins.

(A) Schematic representation of LR reaction clones used to produce four Gateway expression clones. Some stop codons are indicated to highlight differences between constructs. (B) GFP fluorescence assay quantified functional GFP yields. Error bars are based on three biological replicates. (C) SDS-PAGE analysis of plant extracts. Western blots were probed with anti-GFP and anti-His antibodies, as indicated.

Though equal amounts of sample were loaded when preparing the SDS-PAGE and Western blots, the signal intensities observed varied considerably. Most notably, N-terminally His-tagged GFP gave the most intense staining in the Coomassie blue gel, indicating a higher amount of recombinant protein in this sample compared with GFP-His. This is not, however, reflected in the GFP fluorescence assay or the anti-GFP Western blot, indicating that some of the expressed protein may be misfolded.

When mistakenly using the GFP entry clone with a stop codon to make C-terminally His-tagged GFP with pEAQ-*HT*-DEST-3, the resulting construct pEAQ-GW-GFP-Stop produced an untagged version of GFP. This was analyzed alongside the other constructs. Surprisingly, the fluorescence level achieved from this clone was higher (1.25 g / kg FWT) than that of the other constructs (Figure 3.8 B). As expected, the protein did not contain a His-tag, as shown by the lack of signal in the anti-His Western blot (Figure 3.8 C). This result showed that all three GFP variants can be produced by different LR combinations of pEAQ-*HT*-DEST-2 or pEAQ-*HT*-DEST-3 with entry clones with or without stop codon.

The results show that the pEAQ-*HT*-DEST vectors can be used for transient expression of untagged and His tagged proteins of interest, to levels comparable to the other pEAQ vectors (see Section 3.3.4).

3.3.6 CONSISTENT CO-EXPRESSION WITH pEAQEXPRESS

The vector pEAQexpress was constructed to allow efficient expression of two genes of interest with P19. Previously, co-expression of two proteins was achieved by co-infiltration of three *Agrobacterium* clones, each harbouring either of the two genes of interest or P19, as was exemplified by the expression of IgG heavy and light chains (Sainsbury and Lomonosoff, 2008). This approach relies on the efficiency of the *Agrobacterium*-mediated T-DNA transfer to ensure that every cell expresses all three genes. By including all genes of interest on the same T-DNA, pEAQexpress constructs should offer more reliable co-expression.

In order to demonstrate the benefits of pEAQexpress constructs for co-expression, confocal microscopy was utilized to show the co-localized expression of cyan fluorescent protein (CFP) and yellow fluorescent protein (YFP). For this purpose, three new constructs were made (Figure 3.9). pEAQ-*HT*-CFP and pEAQ-*HT*-YFP were based on pEAQ-*HT* and

allow expression of CFP or YFP, respectively. pEAQexpress-CFP-YFP contained both expression cassettes for YFP and CFP. These constructs, as well as pEAQ-*HT* as a negative control, were agroinfiltrated into separate leaves of *N. benthamiana*, each at an optical density of 0.2. Additionally, some leaves were infiltrated with a mixture of the pEAQ-*HT*-YFP and pEAQ-*HT*-CFP inocula, with an overall total $OD_{600} = 0.4$. An optical density of 0.2 was previously determined to be sufficient to give even coverage of expression in all cells (data not shown).

On the sixth day post inoculation, leaves were observed using a Leica SP2 inverted confocal microscope (Figure 3.10 A). YFP was excited at 514 nm and the emission at 590 nm was recorded in green. CFP was excited at 458 nm and the emission at 510 nm was recorded in red. Merged images of the two channels showed co-localization as a yellow or orange signal.

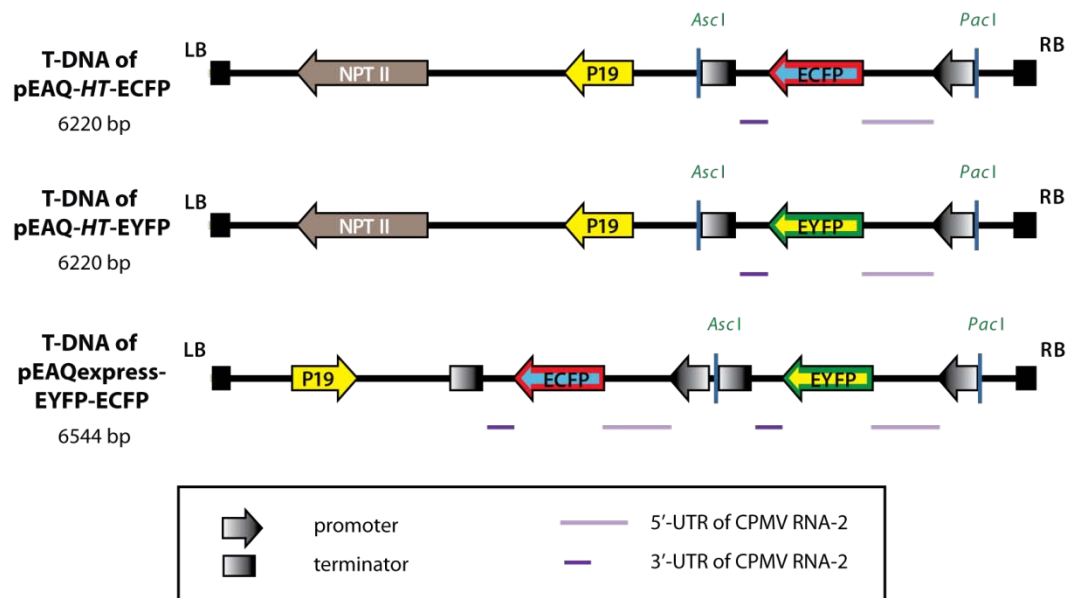


Figure 3.9: Schematic representation of T-DNA regions of the ECFP and EYFP constructs.

The arrangement of genes and resistance cassettes is identified within the schematic. ECFP and EYFP cassettes are presented with a red or green border, respectively, to indicate the colours chosen to represent fluorescent signals from these proteins in later experiments. Promoters and terminators associated with NPTII genes were omitted to preserve figure clarity.

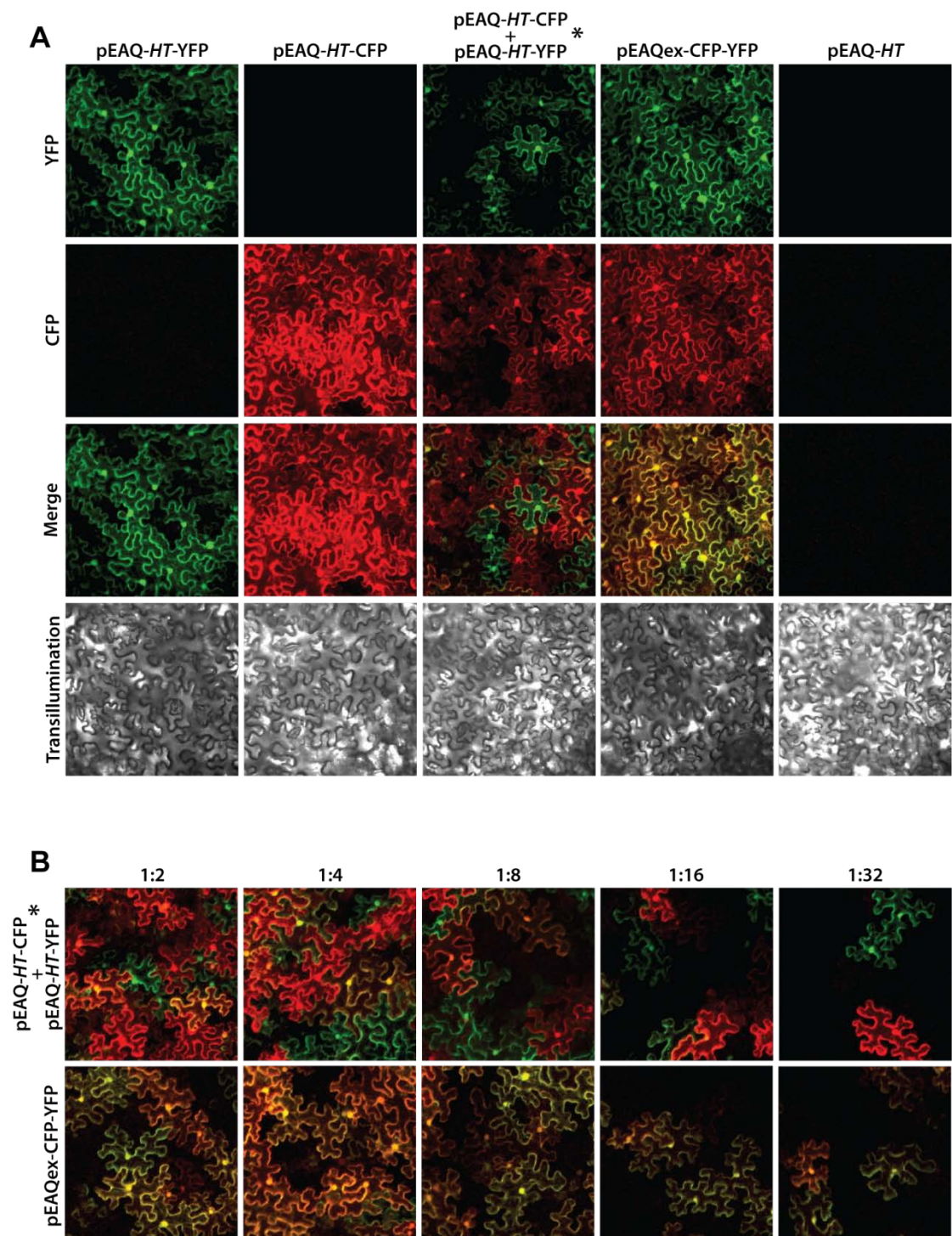


Figure 3.10: Co-expression of two proteins from a single T-DNA is more homogeneous than co-infiltration.

Plants were agro-infiltrated with constructs as indicated. At 6 dpi, leaves were viewed using a Leica SP2 Confocal microscope to image YFP (green) and CFP (red) fluorescence. (A) Expression of YFP and CFP from *Agrobacterium* solutions at $OD_{600} = 0.2$. (B) Co-expression of YFP and CFP from *Agrobacterium* dilution series. YFP and CFP channels are merged. * For co-infiltrated tissue, original *Agrobacterium* solutions contain an $OD_{600} = 0.2$ for each construct, overall $OD_{600} = 0.4$.

As expected, pEAQ-*HT*-YFP gave a signal only in the YFP channel, resulting in only green cells in the merged image. Equally, pEAQ-*HT*-CFP gave a signal only in the CFP channel, resulting in red cells in the merged image. The cells of the leaf co-infiltrated with both the YFP and the CFP construct responded to excitation in both channels. Though the merged image showed an even coverage of expression throughout the tissue, i.e. most cells were fluorescent, only a few cells were noticeably yellow /orange. In most cells expression of either one or the other fluorescent protein appeared to dominate (Figure 3.10 A, pEAQ-*HT*-CFP + pEAQ-*HT*-YFP).

As expected, leaf tissue infiltrated with the pEAQexpress-CFP-YFP construct produced signals in both the CFP and the YFP channels (Figure 3.10 A). The merged image showed all cells in a shade of yellow or orange, indicating that these cells were efficiently co-expressing both proteins. Though there were slight variations in the shading, with some cells redder or greener than others, this was far less pronounced than in the co-infiltrated leaf tissue.

Interestingly, in the cases where both fluorescent proteins were co-expressed, the intensity of the fluorescent signal in each channel was lower than when the respective protein was produced on its own. This may indicate that cells have a specific capacity for the expression of a certain protein. In other words, when two versions of that protein (YFP and CFP differ only in nine amino acids) are co-expressed in the same cell, their respective expression levels do not appear to be additive.

In order to determine whether efficient co-expression from pEAQexpress constructs persists even at high *Agrobacterium* dilutions, a two-fold dilution series of the previously used inocula was prepared. Confocal microscopy showed that at dilutions exceeding 1:4 (i.e. total $OD_{600} < 0.5$), expression became far more patchy, with some cells not expressing any foreign protein. At a dilution factor of 1:32 ($OD_{600} \approx 0.006$), only individual cells were expressing fluorescent protein, while most cells did not appear to be subjected to T-DNA transfer. At all dilutions, tissue infiltrated with pEAQexpress-CFP-YFP gave efficient co-expression of both genes of interest in every expressing cell. Instances of co-expression in the case of tissue co-infiltrated with two *Agrobacterium* strains became rarer with increasing dilution factors, as expected.

Upon protein extraction of these tissues, overall CFP and YFP yields would probably be similar irrespective of whether or not both genes were transferred on the same T-DNA, thereby giving the impression of efficient co-expression. However, this experiment shows

that the efficient cellular co-expression required by pairs of interacting proteins would be best achieved by cloning of two genes onto a single T-DNA in a vector such as pEAQexpress.

3.4 DISCUSSION

A series of cloning vectors has been constructed to facilitate the use of the CPMV-*HT* expression system for the easy and quick production of heterologous proteins in plants. The new vectors address the main drawbacks of the pBINPLUS-based (van Engelen et al., 1995) cloning system previously used in the group. These drawbacks included the large size of the binary vector backbone, inefficiency of subcloning, the need for *in trans* delivery of a suppressor of gene silencing, and the heavy reliance on the efficiency of *Agrobacterium*-mediated T-DNA transfer for co-expression of multiple proteins. The pEAQ vector series has been published in Plant Biotechnology Journal (Sainsbury et al., 2009) and, together with the *HyperTrans* technology, is already a widely used tool in the research community and industry.

A crucial step in the design of the new vector series was the minimalization of the pBINPLUS binary vector backbone. In 1999, Xiang *et al.* had shown that it is possible to remove half of the backbone of pBIN19, an early binary vector (Bevan, 1984), without impacting its functionality. We decided to use an existing pBINPLUS-based GFP expression vector as the parent plasmid, with the advantage of having a ColE1 origin of replication which produces higher plasmid yields when compared with the pBIN19 vector. The CPMV-*HT* expression cassette for GFP allowed the easy monitoring of any impact of the vector manipulations on recombinant protein yield. A two-step cloning procedure yielded pEAQ-GFP-*HT*, an expression vector half the size of its parent plasmid, with no impact on functionality in transient expression. At a size of 5.1 kb, the vector (without the GFP cassette) is one of the smallest binary vectors currently available.

A multiple cloning site was designed to allow for the insertion of three expression cassettes: two sites are compatible with *Ascl*-*Pacl* digested CPMV-*HT* expression cassettes, and another site can be used to insert an expression cassette for a suppressor of gene silencing or a selectable marker. Of the five restriction sites chosen for this MCS, four have

8 bp recognition sequences making them rare cutters. This design reduces the likelihood of these recognition sequences being present in the gene of interest. The adjacent *MluI* and *AsiSI* sites produce sticky ends which are compatible with the ends of any standard *Ascl* – *Pacl* digested CPMV expression cassette. This allows previously prepared fragments to be easily inserted into this second location, without the need for PCR to end-tailor new restriction sites. Upstream of these two expression cassette insertion sites, the *FseI* site allows for cloning of another fragment of interest, and was used to insert P19 in the case of pEAQexpress, or NPTII in the case of pEAQselectK.

The pEAQexpress vector is particularly tailored for the transient expression of two genes of interest. This vector contains an expression cassette for the suppressor of silencing P19 (Silhavy et al., 2002; Voinnet et al., 2003), which is commonly used to boost expression levels of recombinant protein in plants. Gene silencing suppressors are commonly supplied *in trans* by co-infiltration with another *Agrobacterium* clone. Supplying P19 on the same T-DNA as the gene(s) of interest has four key advantages: Firstly, the preparation of inoculum is dependent on the growth of only one *Agrobacterium* culture, making the preparation of infiltration solutions easier. Secondly, using one *Agrobacterium* culture instead of two allows the use of an infiltration solution of lower optical density, making the infiltration process easier. Thirdly, the lower overall optical density means that the negative impact of *Agrobacterium* on the plant is reduced, which may, in turn, have a positive effect on expression levels. Finally, infiltrating less *Agrobacteria* yields less contaminating bacterial proteins upon extraction.

This thesis reports the first successful attempt to include P19 on the same T-DNA as the gene of interest. Previously, P19 had been included on a separate T-DNA of the helper plasmid pSoup associated with pGreenII (Hellens et al., 2005). The effect of the suppressor of gene silencing from this second T-DNA was only evident six days post infiltration, indicating that the transfer of two T-DNAs from a single *Agrobacterium* is inefficient. The modular nature of the pEAQ vectors also enables the replacement of the P19 cassette with that encoding another gene silencing suppressor, if this is required.

The pEAQselectK vector contains a kanamycin resistance cassette in the *FseI* cloning site and is especially suited for the production of transgenic plants expressing up to two genes of interest. Interestingly, the presence of the NPTII cassette in the opposite orientation, compared with pBINPLUS, yielded approximately twice as much plasmid in a standard miniprep, indicating an effect on copy number. A higher level of GFP

fluorescence was detected in both vectors containing this NPTII cassette (pEAQspecialK, see Figure 3.7), compared to the other pEAQ vectors and the parent plasmid. If the higher copy number observed in *E. coli* also occurs in *Agrobacterium*, this may result in the delivery of more transcriptionally active T-DNA in each host cell, thereby explaining the higher expression levels achieved with these vectors.

By examining co-expression of ECFP and EYFP on a cellular level, I have shown that traditional co-infiltration is not able to produce consistent co-expression in every cell (Figure 3.10). In fact, most cells appear to express one fluorescent protein more than the other. This effect is not likely due to inherent properties of the proteins themselves, as ECFP and EYFP differ only in nine amino acids. Two theories could explain the effect: (1) The presence of T-DNA in a plant cell may have an inhibitory effect on future transfer events. This would allow the first T-DNA to dominate and cause the observed higher expression of one fluorescent protein. (2) The number of *Agrobacteria* infecting the same cell may be low. On average, the ratio of ECFP transfer events and EYFP transfer events should approach 1:1. Hypothetically, if a cell receives T-DNA at the same rate from each of only four bacteria, the chance of equal ECFP and EYFP transfer events is only 37.5%. At such a low inoculum concentration, it is more likely that a cell will receive more of one type of T-DNA than the other, thereby producing different relative amounts of the two proteins.

As previously explained, pEAQexpress has the capacity to harbour two *Ascl* – *Pacl* CPMV expression cassettes for the consistent co-expression of two genes of interest, in addition to P19, from the same T-DNA. By examining the expression of ECFP and EYFP from this vector, I was able to show that co-expression from pEAQexpress is achieved in every infected cell (Figure 3.10). In fact, the relative expression levels of the two proteins appear to be consistent throughout the tissue, as indicated by the consistently yellow-orange merge image. This consistency is likely due to the equal rate of transfer of the two encoding genes, by inclusion on the same T-DNA. The ability to achieve co-expression of two (or more) proteins in every single cell is especially important for proteins which need to interact, such as the different structural proteins comprising bluetongue virus-like particles. The expression of multiple components of an enzymatic pathway also requires all components to be present for efficient turnover of the substrate. For the expression and assembly of heteromeric complexes such as Bluetongue virus-like particles (see Chapters 5 - 7), it is not only important to ensure co-expression in every cell but to ensure a certain stoichiometric ratio. Other benefits of co-expression from a single T-DNA and

thus a single *Agrobacterium* strain mirror the four benefits of including P19 on the same construct, as discussed above.

pEAQselectK can couple a kanamycin resistance cassette with two CPMV expression cassettes for co-expression in stable transformants. Though this has not been tested so far, the use of this vector to produce transgenic lines should also allow for consistent co-expression of the two genes. Additionally, integration of the two genes of interest into the plant genome should be coupled to the same location. This strategy should reduce the influence of genetic locus and copy number on relative expression levels of the two proteins, though it does not ensure equimolar expression of the two proteins as in the case of self-cleaving 2A-polyproteins (Halpin et al., 1999). Most strategies for co-expression of multiple transgenes involve the sequential transformation and recovery of homozygous lines until all wanted transgenes are inserted. By including two transgenes on the same T-DNA, a single transformation event should be sufficient to recover co-expressing lines. For the obtaining of homozygous lines through selfing, the close proximity of the two genes should allow them to be selected as one.

In pEAQspecialK, both the NPTII and P19 cassettes are present on the T-DNA. The NPTII cassette was found to enhance plasmid yield and expression levels compared with vectors lacking this cassette, or having it in the opposite orientation (Figure 3.7), pEAQspecialK thus combines the benefits of this cassette with the presence of a suppressor of gene silencing. It was also thought that this vector may be useful for checking constructs through transient expression followed by stable integration without the need for additional subcloning. However, the wild-type P19 included in this and the pEAQ-HT vector makes the recovery of transgenic plants impossible (Dr. Frank Sainsbury, personal communication). Recent work has shown that the replacement of wild-type P19 with a mutant P19 to produce pEAQspecialKm allows recovery of apparently healthy transgenic plants while maintaining a boost of expression levels associated with co-expression of a gene silencing inhibitor (Saxena et al., 2010).

Gateway-compatible versions of pEAQ-HT provide a fast and efficient alternative to this standard restriction cloning vector. The pEAQ-HT-DEST vectors enable existing entry clones to be used to transfer a gene of interest into the CPMV-HT expression cassette whilst fusing a N- or C-terminal His affinity tag if needed. This is a convenient way to allow groups that have never worked with the system before to determine its usefulness for their purposes. Many researchers world-wide use Gateway compatible cloning vectors for

other expression systems (bacterial, fungal, mammalian, etc.) and may be more willing to try the CPMV-*HT* system in a compatible form. The production of new constructs is also greatly simplified by use of Gateway cloning. The few steps involved in this cloning method make it ideally suited to high-throughput applications. Recombination reactions can be performed in 96-well PCR plates incubated in a PCR machine without the need for labour intensive gel extractions. Subsequent screening of colonies can be restricted to one or two colonies per clone, due to the effective negative selection of bacteria transformed with the unrecombined, cytotoxic *ccdB* gene-containing destination vector.

In conclusion, this chapter describes the construction of a series of pEAQ binary cloning vectors tailored for the use of the CPMV-*HT* system for different applications. All of the vectors, including Gateway-compatible versions, have been used to obtain expression levels equal to or exceeding those obtained with the pBINPLUS derived parent vector. This allows these vectors to be used interchangeably for the expression of heterologous proteins in plants. For the purposes of this project, the efficiency of cloning with these vectors is a particular asset, allowing many constructs to be developed and tested. The pEAQ's small binary vector size, the ability to accommodate multiple expression cassettes, and the non-replicative nature of the CPMV-*HT* expression system make this combination uniquely suitable for the expression of heteromeric complexes such as Bluetongue VLPs, as well as the more simple Hepatitis B particles discussed next.

4 EXPRESSION OF HEPATITIS B TANDEM CORE-LIKE PARTICLES

4.1 INTRODUCTION

This chapter describes the use of the CPMV-*HT* transient expression system to produce Hepatitis B (HB) core particles at high levels in plants. These particles are homomultimeric, icosahedral structures assembled from the small Hepatitis B core antigen (HBcAg). As such, these particles were chosen as an example of a relatively simple VLP, to be contrasted with the highly complex, heteromeric Bluetongue particles discussed in the next chapters. HB particles have been used by many researchers for the display of foreign epitopes for vaccine development purposes. Steric hindrance associated with large epitope and protein insertions was the driving force in the development of Hepatitis B tandem cores by the groups of David Rowlands (University of Leeds) and David Stuart (University of Oxford), as well as the company Iqur Ltd. The tandem core construct allows the main immunogenic loop of every second HBcAg monomer to be modified, thus reducing steric hindrance associated with the folding insert. Hepatitis B tandem cores displaying a number of epitopes have been successfully expressed and shown to assemble in plants.

Following a brief introduction of Hepatitis B virus, this chapter will focus on the structure of the HBcAg and the tandem Hepatitis B core antigen (tHBcAg), before moving onto the results obtained.

4.1.1 HEPATITIS B VIRUS

Hepatitis B Virus (HBV) is the type member of the *Hepadnaviridae* family of liver-infecting DNA viruses. HBV infections are endemic in all areas of the globe, with an estimated 2 billion people infected and accounting for 600 000 deaths annually (WHO, 2008).

HBV can cause acute and chronic liver infections, depending on its route of transfer. Horizontal transfer via body fluids causes acute viral hepatitis in 90% of cases (reviewed

by Rehmann and Nascimbeni, 2005). The virus is usually cleared within several weeks, providing life-long immunity to re-infection. Vertical transmission to the neonate is the major cause of chronic liver infections leading to death by liver cirrhosis or cancer in 25% of infected individuals later in life.

The infectious agent of viral hepatitis, a 42 nm particle comprising a nucleocapsid of 28 nm diameter enveloped by a lipid bi-layer, was first identified by electron microscopy of serum from infected individuals (Dane et al in 1970). These "Dane particles" are a minor fraction of the total HB antiserum-recognized particles, most of which are 22 nm subviral Hepatitis B surface antigen (HBsAg) particles.

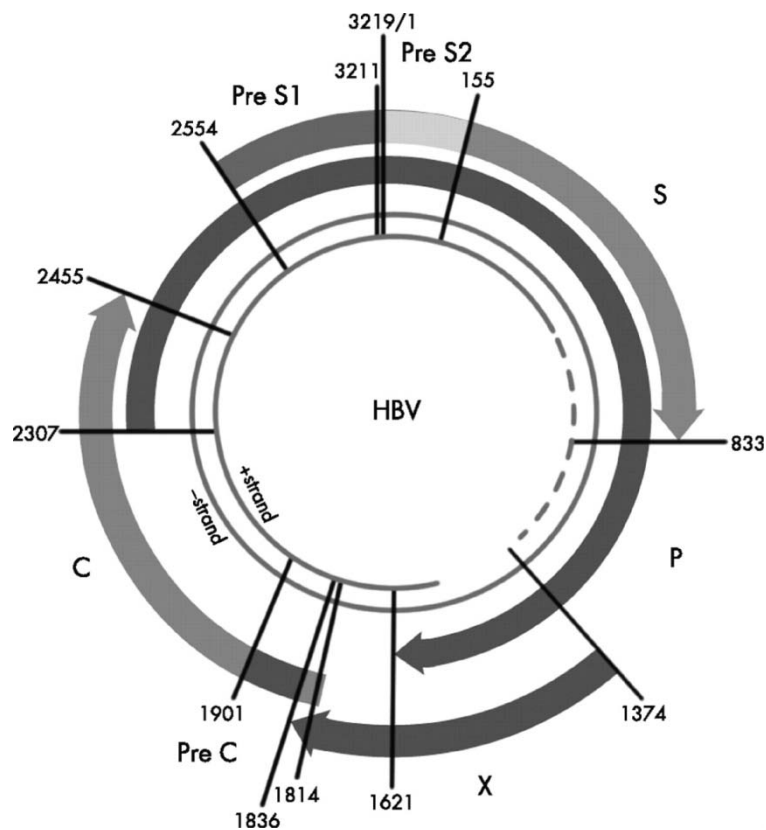


Figure 4.1: Schematic representation of the genome structure of HBV.

The open reading frames of the four subgenomic mRNAs are indicated by arrows. HBcAg is the product of translation of the C region (1901 - 2455). HBeAg is the product of translation of the Pre C and C regions (1814 - 2307). C = core; S = surface; P = polymerase; X = X antigen. (Figure copyright: Park et al., 2006)

Within the first decade after identification of the Dane particle, DNA polymerase activity was shown to be associated with the DNA-containing core particle. The HBV genome was first cloned and heterologously expressed in *E. coli* in 1979 (Burrell et al., 1979). In the same year, sequencing of the HBV genome (Figure 4.1) enabled the identification of the viral genes and allowed first analyses of the gene structure and amino acid composition (Pasek et al., 1979).

The Hepatitis B virus structure is that of an enveloped icosahedral capsid containing a 3.2 kb, partially double-stranded DNA genome. Upon receptor-mediated interaction with a hepatocyte membrane, the virus is internalized via endocytosis, thereby shedding its envelope through membrane fusion. The released nucleocapsid is transported to the nucleus where it disassembles, releasing the viral genome. The nicked circular genome acts as a template for transcription of four co-terminal messenger RNAs, which, upon export into the cytoplasm, allow production of viral proteins by the host translational machinery (reviewed by McLachlan, 1991).

Assembly of the virus begins in the cytoplasm, where HBcAg assembles around the longest mRNA and the viral DNA polymerase to form the nucleocapsid. Six different lengths and glycoforms of surface antigen are co-translationally translocated to the endoplasmic reticulum (ER) membrane and allow budding of the formed capsid into the ER lumen. Fully formed particles are then exported via the Golgi apparatus.

In addition to the mature HBV particle, infection results in an accumulation of other viral products in the blood stream. Subviral particles of 22 nm diameter are the result of spontaneous budding of HBsAg particles without nucleocapsid (Dane et al., 1970). Some stages of infection also give rise to a large amount of freely circulating E antigen (HBeAg), a nonstructural protein encoded by the same gene as HBcAg. The E antigen is thought to cause T-helper cell tolerance in infants of HBeAg-positive mothers, resulting in the high 90% rate of chronic infections through vertical transmission (Milich et al., 1997).

4.1.2 HEPATITIS B ANTIGEN AND PARTICLE STRUCTURE

The first insight into the structure of HBcAg came with the sequencing of the HBV genome and identification of the HBcAg gene in 1979 (Pasek et al., 1979). The core antigen used in this study is based on a 21 kDa protein consisting of 183 aa (Figure 4.2 A).

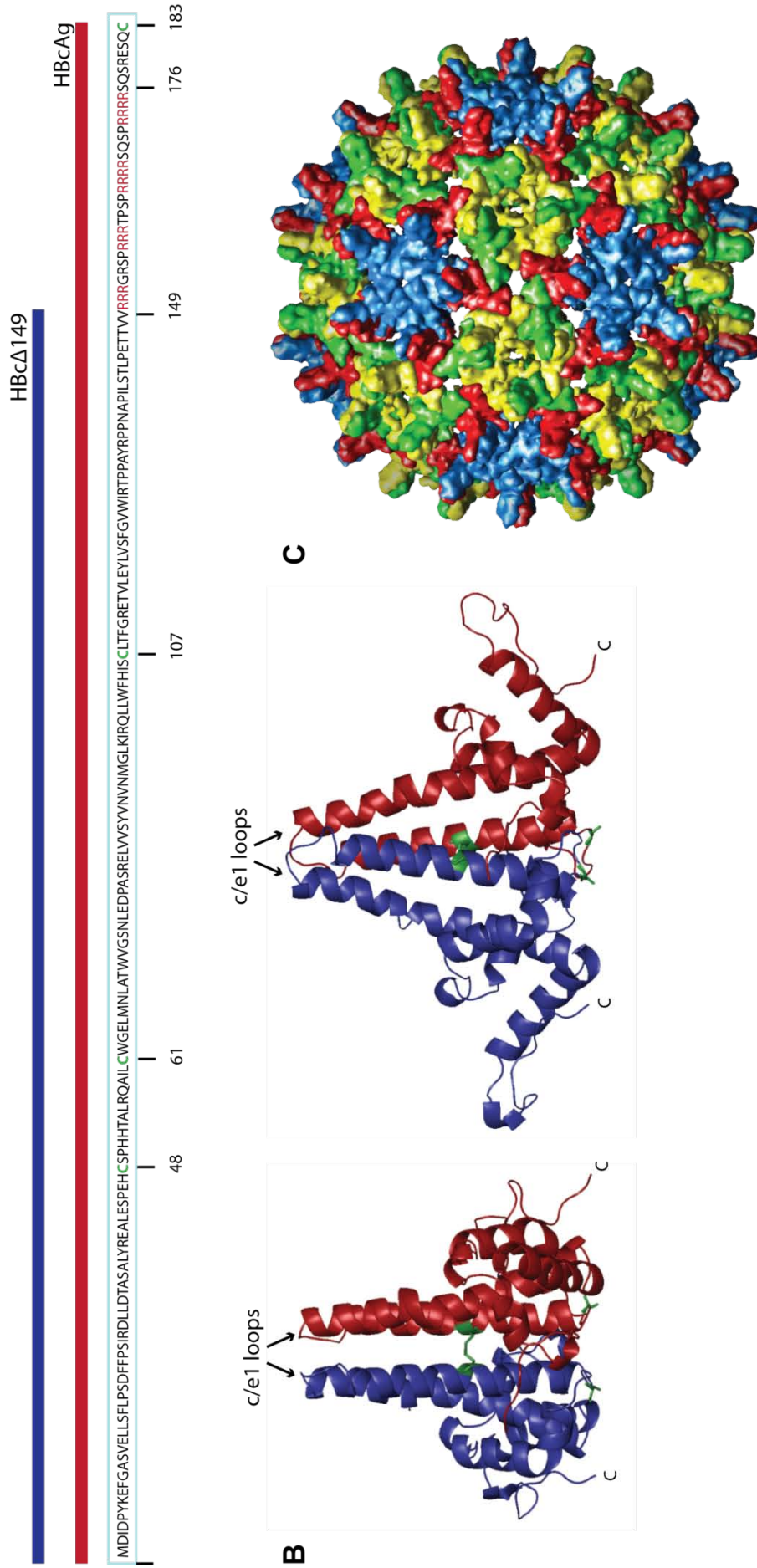


Figure 4.2: Hepatitis B core antigen primary, tertiary and quaternary structure.

(A) HBcAg amino acid sequence. Cysteine residues are shown in green; C-terminal arginine residues are shown in red; key residues are numbered below; length of commonly used variants indicated above. (B) HBcAg dimer ribbon structure from two orientations. Cys48 (free thio) and Cys61 (disulfide bridge) are shown in green. (C) Surface rendered T=4 structure. The four chains of the asymmetric unit are shown in different colours. Ribbon diagrams were made using Pymol software and published structural data (Wynne et al., 1999). C = C terminus.

The 36 amino acid carboxy terminus features four arginine-rich repeats, giving it an overall positive charge. This protamine-like domain is required for nucleic acid binding and encapsidation, but is not essential for particle assembly (Gallina et al., 1989).

HBcAg is expressed in the cytosol and adopts a largely alpha-helical structure (Figure 4.2 B). A homodimer is formed by the interaction of a hairpin consisting of the two longest amphipathic helices of one monomer with that of another (Böttcher et al., 1997). As determined by cryo-electron microscopy (CEM), this gives the dimer a hammer-like appearance, with the four-helix bundle forming the 'handle' (Crowther et al., 1994).

The stability of the HBcAg particle is, in part, due to the presence intra- and interprotein disulfide bridges. The full-length protein contains four cysteine residues: Cys48, Cys61, Cys107, Cys183. The dimer binding surface at the two hairpins is always stabilized by a Cys61-Cys61 disulfide bridge (Figure 4.2 B; Wynne et al., 1999; Zheng et al., 1992). Zheng et al found that a Cys48-Cys48 bridge could also form in some cases to further stabilize the dimer. However, the crystallographic data of a truncated ~~HBcAg~~ particle showed no evidence of this covalent bond (Wynne et al., 1999). The cysteine residue at position 107 is buried within the monomer and is not involved in S-S bond formation. Although the amino-terminal 144 amino acids of HBcAg are sufficient for particle assembly (Birnbaum and Nassal, 1990), the truncation of the carboxy terminus has implications for the stability of the particles. In fact, Cys183 can form disulfide bridges with the same residue of an adjacent dimer, thereby stabilizing the core particle (Wynne et al., 1999).

Despite the importance of the C-terminal domain of HBcAg for particle stability, a truncated version consisting of the first 149 amino acids (HBc Δ 149, Figure 4.2 A) is often used, especially for biotechnological applications. This has the advantage of allowing high-level expression and efficient capsid assembly, while disabling the encapsidation of host mRNA (Zheng et al., 1992).

The first electron micrographs of recombinant *E. coli*-derived HBcAg particles published in 1982 show two distinct size classes (Cohen and Richmond, 1982). These were later identified by CEM to be two icosahedral structures with different triangulation numbers. A minority of the particles measures 32 nm in diameter and consists of 180 subunits, with a triangulation number of T=3. The majority of particles (~85%) are larger, measuring 36nm in diameter and consisting of 240 subunits arranged as 120 dimers (Böttcher et al., 1997; Crowther et al., 1994). Both particle structures have a 'spiky'

appearance, owing to the two alpha-helical hairpins protruding from each dimer (Figure 4.2 C).

4.1.3 HBcAg IMMUNOGENICITY AND DISPLAY OF FOREIGN ANTIGENS

During natural HBV infection and clearance, antibodies are raised against surface antigen, E antigen as well as core antigen. The shared main antigenicity determinant of HBcAg and HBeAg, which are derived from the same open reading frame, was found to be located between amino acids 74-89 (Salfeld et al., 1989) of HBcAg. This corresponds to the hairpin loop exposed on the tip of the spike in the assembled HBcAg particle and is called the c/e1 loop (Figure 4.2 B).

Hepatitis B core particles were first used as carriers for epitopes by N- terminal fusion of 20 amino acids of FMDV (Clarke et al., 1987), and C-terminal fusion of epitopes of HBsAg and HIV (Stahl and Murray, 1989). Although such particles elicit an immune response against the inserted epitope, a stronger immune response, especially a T-cell response, is still raised against HBcAg itself by way of the immunodominant c/e1 loop. Schödel et al have shown that the strongest response against a foreign epitope is achieved when this is displayed internally at the c/e1 loop (Schödel et al., 1992).

In 1991, researchers inserted foreign epitopes of up to 40 amino acids into the c/e1 loop and found a 10-fold higher immune response against the foreign epitope from these particles when compared with an N-terminal fusion (Brown et al., 1991). The c/e1 loop has since been used by many groups for the display of foreign antigens (Schödel et al., 1996; Walker et al., 2008; Whitacre et al., 2009)

4.1.4 HBcAg EXPRESSION IN PLANTS

Having been successfully expressed in many heterologous systems, such as bacteria, yeast, and insect and mammalian cell culture, it is no surprise that HBcAg was one of the first VLPs to be expressed in plants. In 1998, the purification of HBcAg VLPs from transgenic tobacco plants was reported (Tsuda et al., 1998). Yields were estimated at 12-

24 mg HBcAg per kg fresh weight tissue and plant-derived HBcAg was shown to be equivalent to bacterial HBcAg in terms of its use in haemagglutination inhibition assays.

Transient expression of HBcAg was first achieved in the Lomonossoff group using PVX and CPMV full-length viral vectors (Mechtcheriakova et al., 2006). Using the CPMV viral vector, yields after purification were low (ca. 10 mg / kg FWT) and comparable to those achieved in transgenic tobacco, while yields from the PVX-based vector were at least five-fold higher. Soon after, Huang et al (2006) expressed HBcAg using the ICON Magniffection system (Marillonnet et al., 2004) to high estimated levels of 2.4 g / kg FWT within seven days of infiltration. These particles were shown to be immunogenically equivalent to *E. coli*-derived HBcAg upon intraperitoneal injection. Interestingly, the plant-derived particles also induced an immune response upon mucosal delivery (intranasal and oral), indicating their potential as oral vaccines.

More recently, HBcAg has been transiently expressed using the CPMV-*HT* system, to levels exceeding 1 g / kg FWT (Sainsbury and Lomonossoff, 2008). High yields (0.8 g / kg) were also achieved transiently using a DNA replicon vector based on Bean Yellow Dwarf Virus (Huang et al., 2009).

To date, plants have been used to express two epitope-displaying HBcAg variants: A 21 amino acid immunogenic epitope of FMDV and a 16 kDa anthrax protective antigen (PA-D4) were both inserted into the c/e1 loop of HBcAg and expressed in transgenic tobacco plants (Bandurska et al., 2008; Huang et al., 2005).

4.1.5 TANDEM CORE TECHNOLOGY

Despite these successes in heterologous expression and epitope display, HBcAg is still not used as a universal peptide vaccine display platform. This has two main reasons: Firstly, the insertion of a foreign sequence into an internal protein loop places structural constraints on the insert. In order to allow proper folding, large inserts must either have their natural N- and C-terminus in close proximity, or they must be attached via long flexible peptide linkers. Secondly, the close proximity of the two c/e1 loops in the dimer structure limits the size of insert that can be successfully displayed. Large insertions prevent particle assembly through steric hindrance (Nassal et al., 2008). The tandem Hepatitis B core (tHBcAg) was developed to alleviate these steric constraints on the insert.

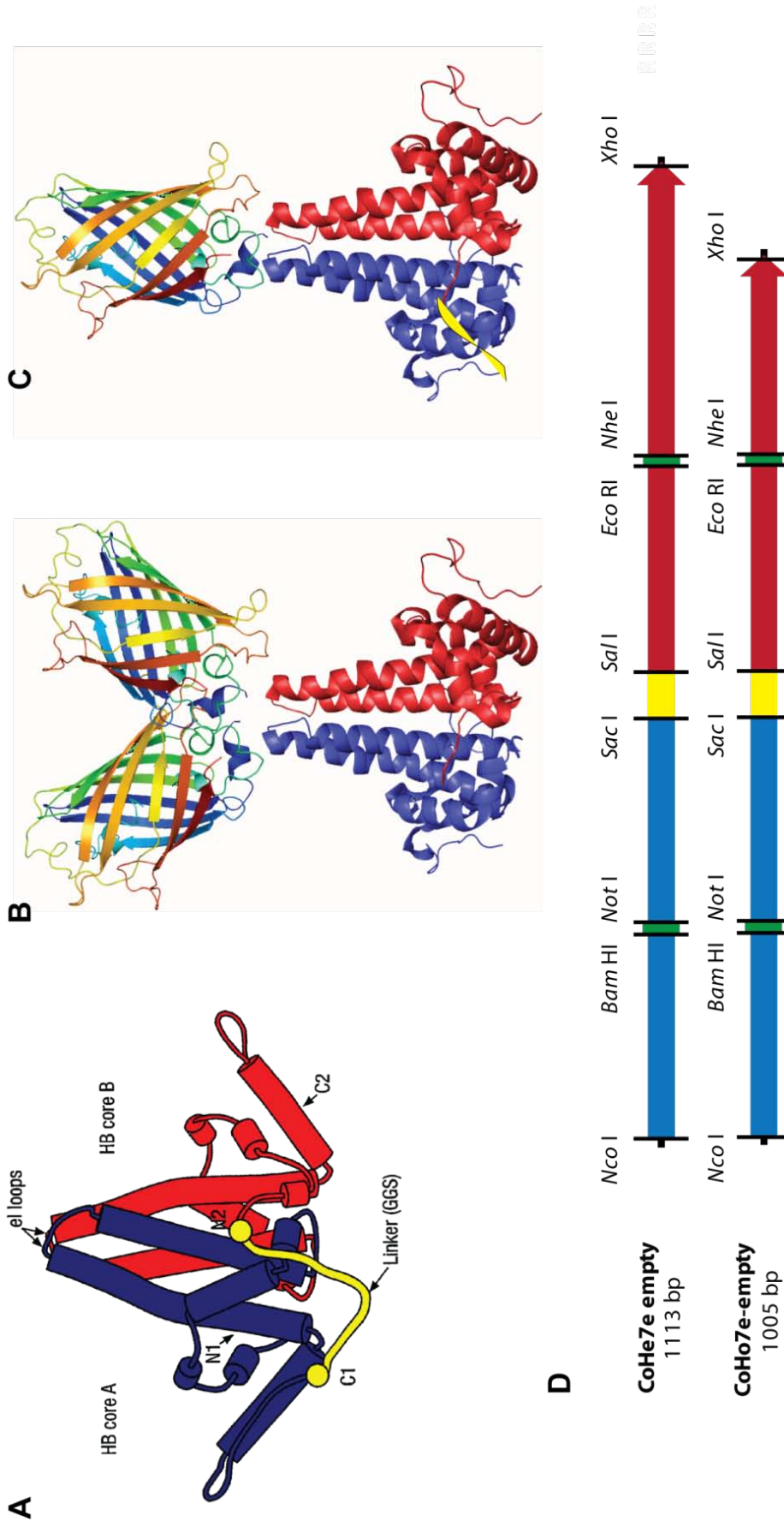


Figure 4.3: Hepatitis B tandem core protein and gene constructs.

(A) Schematic of HB tandem core structure indicating c/e1 loops, N- and C-termini of the two HB core monomers (blue and red) and the flexible linker (yellow; adapted from Gehin et al., 2004, Fig. 1). (B-C) Ribbon diagram overlay of GFP (rainbow) and HBcAg dimer (blue/red) structures, illustrating the steric hindrance associated with insertion of a foreign gene into every c/e1 loop of HBcAg (B) versus insertion in one c/e1 loop per dimer in the case of HB tandem core constructs (C). (D) Schematic representation of heterotandem and homotandem core genes indicating core A (blue), core B (red), GGS linker (yellow), c/1 loops (green). Key restriction sites for insertion of foreign sequences are indicated (black).

Through computational analyses of the HBcAg particle structure, the tandem core gene constructs were designed to allow fusion of two HBcAg monomers through a flexible peptide linker (Figure 4.3 A; Gehin et al., 2004) This genetic fusion increases the versatility of the HB core antigen as an epitope carrier in two ways. Firstly, expression of the complete dimer structure as a single peptide allows the display of a foreign epitope from one of the two c/e1 loops, while leaving the other loop unchanged. Thus, the resulting particles can be decorated with half of the number of foreign epitopes, providing more space for proper folding of large inserts, such as whole proteins (Figure 4.3 B-C). Secondly, the two c/e1 loops of the dimer can now be addressed separately. This gives the tandem core potential to be used as a multivalent vaccine platform through the insertion of two different foreign epitopes in the two c/e1 loops of the tHBcAg

When work on this project commenced in 2007, the developers of the tandem core technology had already demonstrated the ability of tHBcAg to form particles in *E. coli*. Insertion of a small HBsAg epitope as well as insertion of the *gfp* gene into the c/e1 loop of core B had also been successful. However, epitope-displaying particles prepared from *E. coli* were heterogeneous in their appearance under the TEM. In addition to the expected T=3 and T=4 particles, other particulate forms exceeding 100 nm in diameter were also abundant. This heterogeneity makes the characterization of these tandem core particles difficult, and it would also prove problematic in the bid for regulatory approval as a drug.

In a bid to determine whether a plant-based expression system could alleviate these problems, I used the CPMV-*HT* system to express tandem core particles. Two versions of the tandem core were used in this work. Homotandem core (CoHo7e) constructs consist of two truncated HBc Δ 149 genes fused by a glycine-serine-rich linker. Heterotandem cores (CoHe7e) consist of a truncated HBc Δ 149 (core A) fused to a full length HBcAg (core B) through a glycine-serine-rich linker (Figure 4.3 D).

4.1.6 AIMS OF THIS CHAPTER

The work presented in this chapter demonstrates the use of the CPMV-*HT* expression system in the production of monomeric and tandem Hepatitis B particles in leaf tissue. Tandem core constructs with and without inserts can be expressed transiently and are

shown to assemble into virus-like particles of regular shape and size. Development of the pEAQ vector series (Chapter 3) allowed many different constructs to be cloned and tested with relative ease. The expression levels of HBcAg achieved using the *HyperTrans* technology (Sainsbury and Lomonosoff, 2008) are 100-fold higher than those previously reported from the full-length CPMV viral vector (Mechtcheriakova et al., 2006), bringing them in line with the yields achieved using the *Magn/CON* system (Huang et al., 2006), but without the need for viral replication. The use of the *CPMV-HT* system also avoids the problem of contaminating CPMV virions. These characteristics make the *CPMV-HT* system, in conjunction with the pEAQ vector series, an ideal system for the transient expression of tandem HB particles for medical applications.

4.2 SPECIFIC MATERIALS AND METHODS

4.2.1 CLONING

Tandem HB constructs CoHe7e-empty, CoHe7e-eGFPs, CoHo7e-sAg, CoHo7e-sAg,eGFP contained within the pET28b backbone were obtained from Dr. Lucy Beales (Iqur Ltd). From these, new pET28b clones for CoHo7e-empty, CoHe7e-sAg, CoHe7e-sAg,eGFP were prepared by restriction cloning using unique restriction sites contained within the hetero- and homotandem core constructs (see Figure 4.3). Constructs were transferred to the *CPMV-HT* expression system in one of two ways: (1) Constructs were amplified with T7_20mer_for and HBcAg_dual_StuI_rev (see Table 4.1), digested with *NcoI* - *StuI* and ligated into pM81-FSC1 (as pM81-FSC2, but with other unique restriction sites), followed by *AscI* - *PacI* subcloning into pBINPLUS or pEAQ-*HT*, as previously described. (2) Constructs were amplified with attB1-CoHx7e-fwd and attB2-CoHe7e-rev or attB2-CoHo7e-rev, followed by amplification with attB1 adapter and attB2 adapter to end-tailor Gateway attachment B sites. These PCR products were then transferred to pEAQ-DEST-1 (Chapter 3) by sequential Gateway BP and LR recombination reactions.

Table 4.1: Oligonucleotides used in cloning of HB tandem core constructs.

Name	Sequence ^a	Function
T7_20mer_for	taatacgactcactataggg	Universal primer for amplification from the T7 promoter; sense
HBcAg_dual_Stul_rev	GGAGGCCTATCTCActcgagac attgctttcag	Primer for end-tailoring of <i>Stul</i> site to CoHe7e constructs; antisense
attB1-CoHx73-fwd	AAAAAGCAGGCTTAatggacat cgatccgtac	Primer for end-tailoring of partial <i>attB1</i> site to 5'-end of tandem core constructs; sense
attB2-CoHe7e-R	AGAAAGCTGGTATCActcgag acattggcttc	Primer for end-tailoring of partial <i>attB2</i> site to 3'-end of CoHe7e constructs; antisense
attB2-CoHo7e-R	AGAAAGCTGGGTATCActcga gaacaaccgtcgt	Primer for end-tailoring of partial <i>attB2</i> site to 3'-end of CoHo7e constructs; antisense
attB1 adapter	GGGACAAGTTTGTACAaaa agcaggct	Universal adapter to end-tailor complete <i>attB1</i> site; sense
attB2 adapter	GGGACCACTTTGTACAagaa agctgggt	Universal adapter to end-tailor complete <i>attB2</i> site; antisense

^a END-TAILORING is shown in uppercase, restriction enzyme recognition sites are underlined.

4.2.2 EXTRACTION OF HB TANDEM CORE PARTICLES

Protein extractions of small and large-scale samples were performed as previously described (Section 2.5.1). The aggregation experienced with some epitope-containing constructs necessitated the use of two different extraction protocols.

1. Monomeric HBcAg, CoHe7e-empty, CoHo7e-empty: Tissue was homogenized in 3 volumes of **Extraction Buffer (ExB)**: 50 mM Tris-HCl pH 7.25, 150 mM NaCl, 2 mM EDTA, 0.1% (v/v) Triton X-100, supplemented with 1 mM DTT and Complete Protease Inhibitor Cocktail (Roche). Whole extracts were clarified by centrifugation at 13 000 rpm (16 000 x g in microcentrifuge), 2 minutes, 4°C.
2. Epitope-containing tandem core constructs: Tissue was homogenized in 3 volumes of **HB Extraction Buffer 1 (HBexB1)**: 10 mM Tris-HCl pH 8.4, 120 mM NaCl, 1 mM EDTA, 0.75% (w/v) Sodium deoxycholate, supplemented with 1 mM DTT and Complete Protease Inhibitor Cocktail (Roche). Whole extracts were clarified by initial centrifugation at 9 000 x g, 10 minutes, 4°C, followed by decanting and a second spin at 3 500 x g, 5 minutes, 4°C.

Due to the reduced contamination with chlorophyll upon extraction with HBexB1, this buffer was also sometimes used to purify monomeric and empty tandem core particles, albeit at lower yield.

4.2.3 SUCROSE GRADIENTS

Sucrose solutions of 50%, 40% and 30% (w/v) sucrose were prepared by dilution of a 60% (w/v) solution of sucrose in 10 mM Tris-HCl pH 8.4, 120 mM NaCl stock solution with the appropriate amount of 10 mM Tris-HCl pH 8.4, 120 mM NaCl. Gradients were prepared by underlaying sucrose solutions of increasing density (500 μ l each) in a suitable ultracentrifuge tube and carefully overlaying the clarified extract to fill the tube. Gradients were centrifuged in a swing-out rotor (SW41Ti) at 40 000 rpm, 2.5 hours, 4°C. Depending on the scale of the experiment, larger or smaller swing-out rotors were used and the volume of sucrose solutions and centrifugation speed were adjusted accordingly.

4.2.4 CRYO-EM

Cryo-electron microscopy (CEM) and reconstructions were performed in collaboration with Dr. Robert Gilbert and Dr. Alistair Siebert (Division of Structural Biology, University of Oxford).

Sucrose fractions were buffer exchanged for 10 mM Tris-HCl pH 8.0, 50 mM NaCl. Holey carbon grids were glow discharged for 30 seconds, then loaded into a Cryoplunge 3 machine (Gatan UK). Samples (5 μ l) were adsorbed onto grids at ~60% humidity, blotted for 2 seconds, then plunged into liquid ethane to flash-freeze. CEM was performed on a Tecnai F30 microscope at 300 kV accelerating voltage under low-dose conditions. Images on Kodak S0-163 film were scanned at 7 μ m step size. Selected particles were corrected for contrast transfer function and processed using EMAN and Spider software.

3D reconstructions were prepared using computational tools for icosahedral particle reconstructions based on the method described by Fuller (1987; http://www.embl.de/ExternalInfo/fuller/EMBL_Virus_Structure.html).

4.3 RESULTS

4.3.1 HBcAg AND TANDEM CORE GENE EXPRESSION

The expression of HBcAg particles using CPMV-based expression systems had previously been demonstrated (Mechtcheriakova et al., 2006; Sainsbury and Lomonosoff, 2008). To examine whether high-level expression of tHBcAg could also be achieved, constructs obtained from Dr. Lucy Beales (iQur Ltd.) were cloned into pEAQ vectors containing the *HT* mutations. The constructs tested included homo- and heterotandem cores with insertions two different foreign polypeptides within the c/e1 loop of core B (Figure 4.4): (1) A 40 aa immunogenic epitope of HBsAg epitope (sAg) as an example of a medically relevant antigen insertion; (2) The 27 kDa EGFP protein as a model large protein insert whose expression and proper folding could be tracked easily. Tandem HBcAg containing both of these inserts, one in each c/e1 loop of cores A and B, were also expressed to demonstrate the versatility of the tHBcAg technology for the display of two different antigens on the same particle.

The constructs were agroinfiltrated into *N. benthamiana* leaf tissue and samples were harvested after seven days. All HB constructs induced chlorosis in the infiltrated leaf tissue, when compared to an empty vector control (Figure 4.5 A). Necrotic spots were visible in some leaves infiltrated with monomeric HBcAg, CoHe7e-empty and CoHo7e-empty. Generally, this effect was more visible in older leaves (not shown). Tandem core constructs containing an insert did not appear to induce necrosis at 7 dpi.

For reducing, denaturing SDS-PAGE analysis, whole crude extract (without clarification) was used for each sample to avoid any loss of tHBcAg within the clarification pellet (Figure 4.5 B-C). An anti-HBcAg Western blot detected distinct bands of different mobility in all samples infiltrated with HB constructs, corresponding to the expected molecular weights (MW) of the constructs (compare Figure 4.4 and Figure 4.5 C). This was very good news, because it showed that good expression could be achieved from a wide range of different tHBcAg constructs using the CPMV-*HT* system. Tandem cores, consisting of two HBcAg monomers linked by a peptide linker, were of approximately twice the molecular weight of monomeric HBcAg (21 kDa). Where both hetero- and homotandem versions were examined, the heterotandem band was of higher MW than the homotandem band, as expected. With the exception of CoHo7e-empty, all tandem

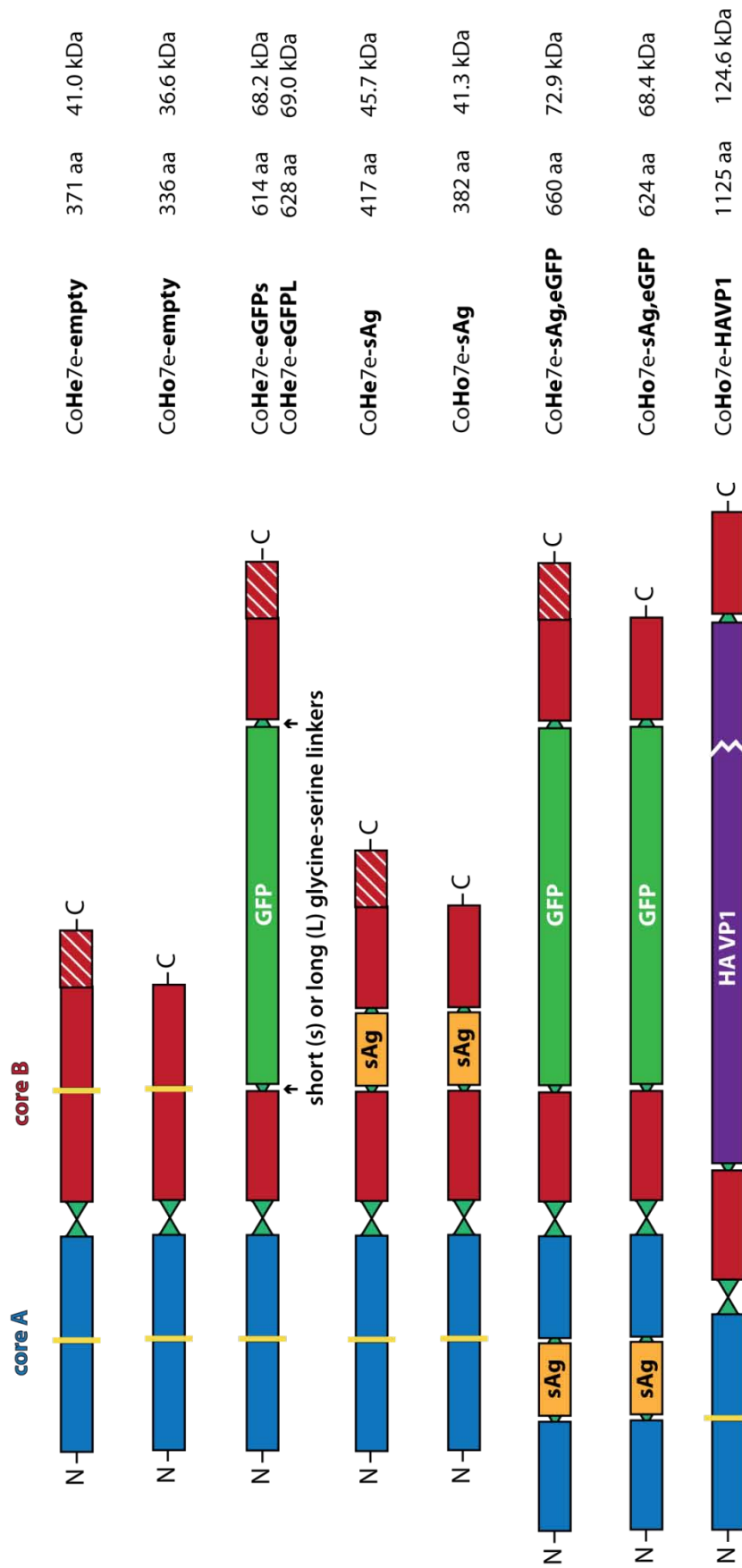


Figure 4.4: Schematic representation of the Hepatitis B tandem core constructs.

Two HBcAg coding regions are genetically fused resulting in a peptide linker. The c/e1-loop of each half of the tandem core can be addressed separately to allow display of different polypeptides. Core A is truncated at amino acid 149; Core B is either truncated at amino acid 149 (homotandem core - CoHo7e) or full length (heterotandem core - CoHe7e).

core samples gave some additional bands of higher MW than the monomer detected in the blot. These likely corresponded to dimers and multimers which were insufficiently disrupted during boiling, indicating that the expressed proteins assemble into higher order structures or aggregates. Homotandem core antigens containing inserts (CoHo7e-sAg and -sAg,eGFP) also produced some fast migrating bands recognized by the primary antibody. These were most likely breakdown products, indicating that the homotandem core construct is inherently less stable than the corresponding heterotandem core construct. Our collaborators were impressed by the generally low level of tHBcAg breakdown products in the plant samples, because protein stability had been a problem in the *E. coli* and yeast expression systems.

Coomassie blue staining of a duplicate SDS-PAGE gel run in parallel with that used for Western blotting showed that the tHBcAg versions differed markedly in their expression levels (Figure 4.5 B). The most intense band by far was obtained from the homotandem CoHo7e-sAg,eGFP, while the protein band corresponding to the heterotandem version, CoHe7e-sAg,eGFP, was barely detectable. These differences in band intensity were not due to variations in loading: Since the band obtained from the Rubisco large subunit at 51 kDa was similar in intensity in all samples loaded, it can be inferred that any differences in other band intensities were due to variability in expression levels of those proteins. Generally, the homotandem core constructs appeared to be expressed to higher levels than their heterotandem equivalents. This is consistent with the observation that homotandem constructs are also expressed to higher levels in *E. coli* (iQur, personal communication). The clear visibility of tHBcAg bands in crude extract samples provides a clear indication that these proteins were expressed at high levels in plants, which was a very important prerequisite for the success of future work on their characterization.

These results show that tHBcAg displaying different polypeptides, ranging from small epitopes to whole proteins, can be expressed in plants, both as homotandem cores as well as heterotandem cores. One construct, however, failed to express. This was a homotandem core with a very large, 789 aa insertion of Hepatitis A VP1 in the c/e1 loop of core B (CoHo7e-HAVP1; Figure 4.4). On numerous attempts, I failed to detect any HBcAg in these samples, indicating that there may be a limit to the size and/or complexity of the inserts tolerated in the tandem core (data not shown).

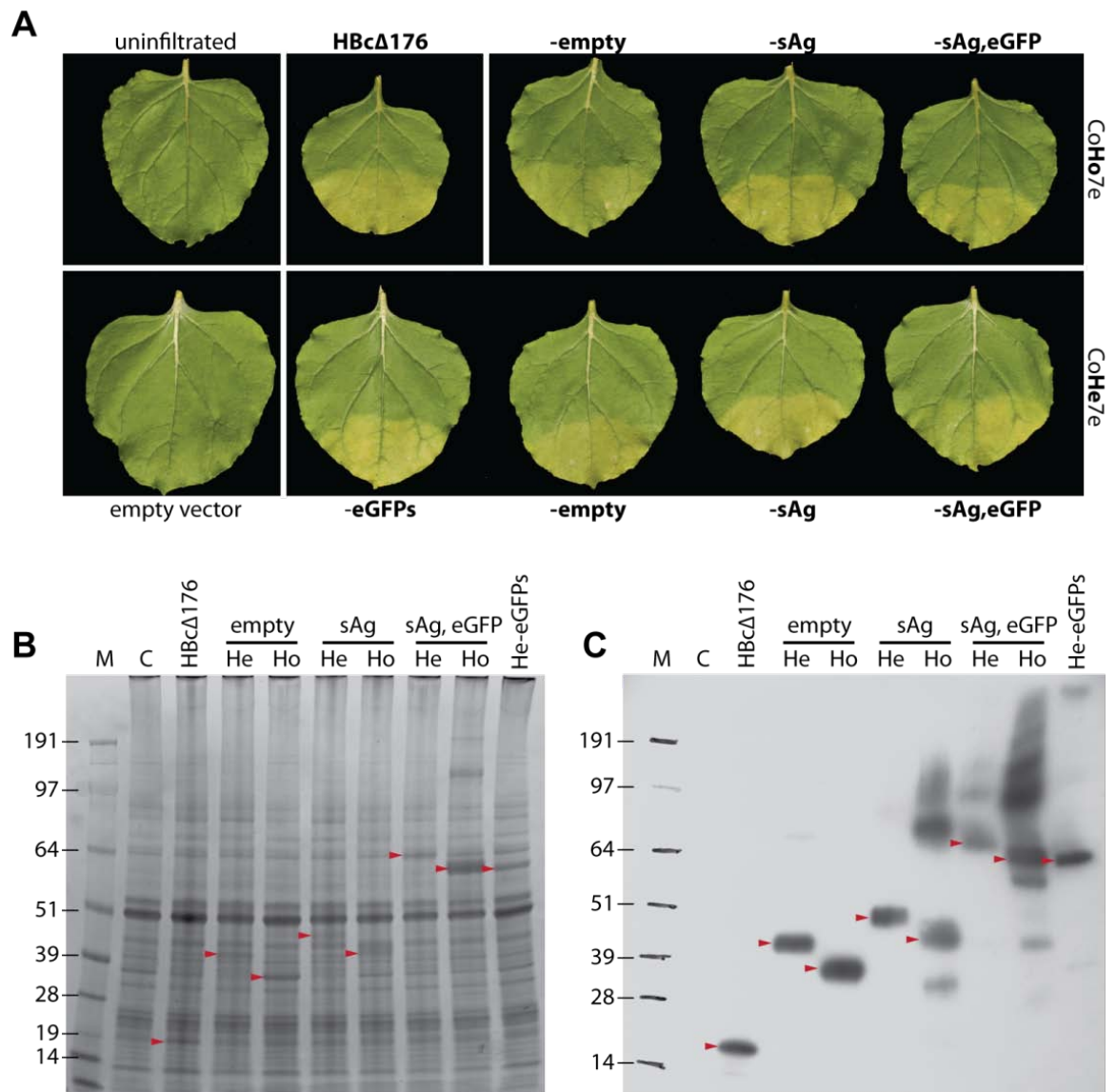


Figure 4.5: Hepatitis B tandem cores can be transiently expressed in *Nicotiana benthamiana*.

(A) Day light photograph of leaves harvested 7 dpi, after infiltration with indicated pEAQ-based Hepatitis B constructs. (B) Coomassie-stained SDS-PAGE of crude extracts from constructs indicated. (C) Duplicate SDS-PAGE, subjected to Western blotting and monoclonal anti-HBcAg Ab immunodetection of HBcAg and tHBcAg. Red arrows indicate the location of bands corresponding to HBcAg or tandem core monomers. M = SeeBlue Plus 2 marker; C = empty vector control.

4.3.2 HBcAg AND TANDEM CORE ACCUMULATION OVER TIME

To determine the optimal time point for harvesting of monomeric and tandem core-expressing leaf tissue, a time course experiment was performed. Twelve plants were infiltrated in such a way that each of three leaves had three infiltrated patches expressing different constructs: pEAQ-*HT* as a negative control, pEAQ-*HT*-HBcAg (monomeric) or pEAQ-*HT*-CoHe7e-empty (tandem). The leaves of one plant were harvested every 24 hours (later time points at 48 hour intervals), and samples consisting of three leaf discs from three separate leaves were frozen for later analysis.

Clarified extracts were used in an enzyme-linked immunosorbent assay (ELISA) to quantify the extractable immunogenic material (Figure 4.6 A). A commercially available recombinant *E. coli*-produced HBcAg (AbD Serotec) standard was used to prepare a standard curve. Monomeric HBcAg was expressed to high levels of 300 mg /kg FWT within the first 48 hours post infiltration. The yield continued to rise until the fifth day, when a plateau was reached. After seven days, necrosis was evident in some of the infiltrated tissue, and more pronounced in the older leaves. The extent of the necrosis was highly variable between plants and after 10 days some leaf tissue was dry and brittle while other leaves still contained moisture. Yields measured from dry samples were lower than those achieved from tissue with some remaining moisture.

Due to the variability in sample weight depending on the extent of necrosis, yields were calculated per kilogramme of healthy fresh weight tissue (hFWT). The samples contained the same area of leaf tissue (2.85 cm²), which weighs approximately 100 mg if obtained from a healthy plant.

In this particular experiment, the highest yield of soluble HBcAg was 0.5 g / kg hFWT. In other experiments, yields were up to 2-fold higher than this, which could be due to variability in plant age and health, or seasonal variability.

As seen for monomeric HBcAg, the CoHe7e-empty construct also showed a maximum expression at 5 dpi, followed by a plateau and a decline in extractable immunogenic material around day 10. However, appreciable levels of tandem core were only detected after 3-4 dpi, which was later than in the case of monomeric HBcAg. The maximum yield of soluble CoHe7e-empty appeared to be five-fold lower than that obtained for monomeric HBcAg. This is inconsistent with the results of other experiments, where Coomassie blue staining and anti-HBcAg Western blot analysis indicated similar

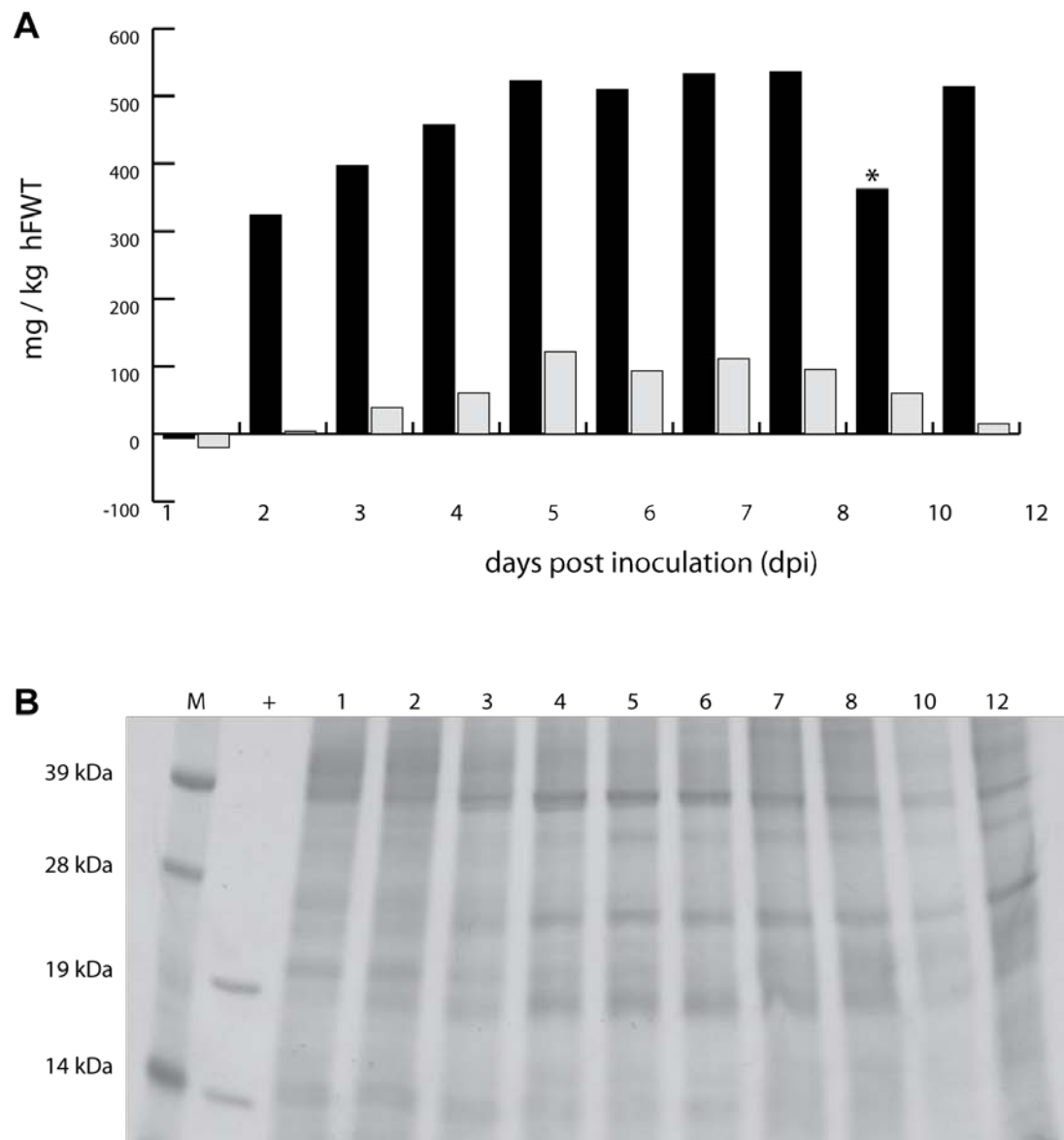


Figure 4.6: Quantification of extractable Hepatitis B core antigen over time.

Plants were agro-infiltrated with constructs as indicated. Leaf samples (3 discs from separate leaves of the same plant) were harvested and stored at -20°C every 24 hrs. Samples were homogenized in HBexB1 and clarified at $3000 \times g$, 5 min. (A) Direct ELISA quantification of HB core antigen expression from monomeric HBcAg (black) and heterotandem core (grey) constructs. Measurements represent single extracts. * sample consisting of entirely necrotic tissue - not representative. (B) Coomassie-stained 12% SDS-PAGE of monomeric HBcAg extracts. M = SeeBlue Plus 2 marker; + = *E. coli* recombinant HBcAg control

expression levels of monomeric and empty tandem HB core (see Figure 4.5 B-C). This low signal may, in part, be due to altered accessibility of the epitopes recognized by the anti-HBcAg polyclonal antibody used in ELISA, which could have a negative impact on signal intensity. The ELISA result would be more reliable if a tHBcAg control of known concentration was used to generate the standard curve for the tandem core samples.

The results of the time course experiment indicate that the ideal time point to harvest tandem and monomeric HB core antigen expressing tissue is at least 5 dpi.

4.3.3 INFLUENCE OF DISPLAYED EPITOPES ON PROTEIN SOLUBILITY

The display of foreign epitopes on the surface of a virus particle can significantly alter the surface characteristics (charge, hydrophobicity, structure) of the particle. These changes also have a profound effect on physical properties such as molecular weight and isoelectric point (pI), making the chimaeric particle behave differently during extraction and purification.

At the start of this project, a standard procedure used successfully for HBcAg was used in particle preparation, involving extraction in Extraction Buffer (ExB), followed by a clarification spin at 13 000 rpm (16 000 x *g* avg) to remove cell debris. Subsequent Western blotting and immunodetection revealed the presence of HB antigen in the clarified extracts of empty tandem core samples, but not in the clarified extracts of cores displaying GFP (data not shown). Illumination of the clarified extract and cell debris pellet using UV light revealed the presence of fluorescence in the pellet, but not the soluble fraction of this sample, indicating that the GFP-tagged tHBcAg is expressed, but forms insoluble aggregates.

To verify the location of HB antigen after the low-speed clarification spin, both the soluble fraction (clarified extract) and the insoluble fraction (pellet) were boiled in reducing LDS-SB and separated by SDS-PAGE (Figure 4.7 A). In the case of monomeric HBcΔ176 and empty heterotandem core, the HB antigen was found almost entirely in the clarified extract (E) with main bands of 20 kDa and 41 kDa, respectively. These particles were expected to have similar surface properties as they both do not contain a foreign epitope.

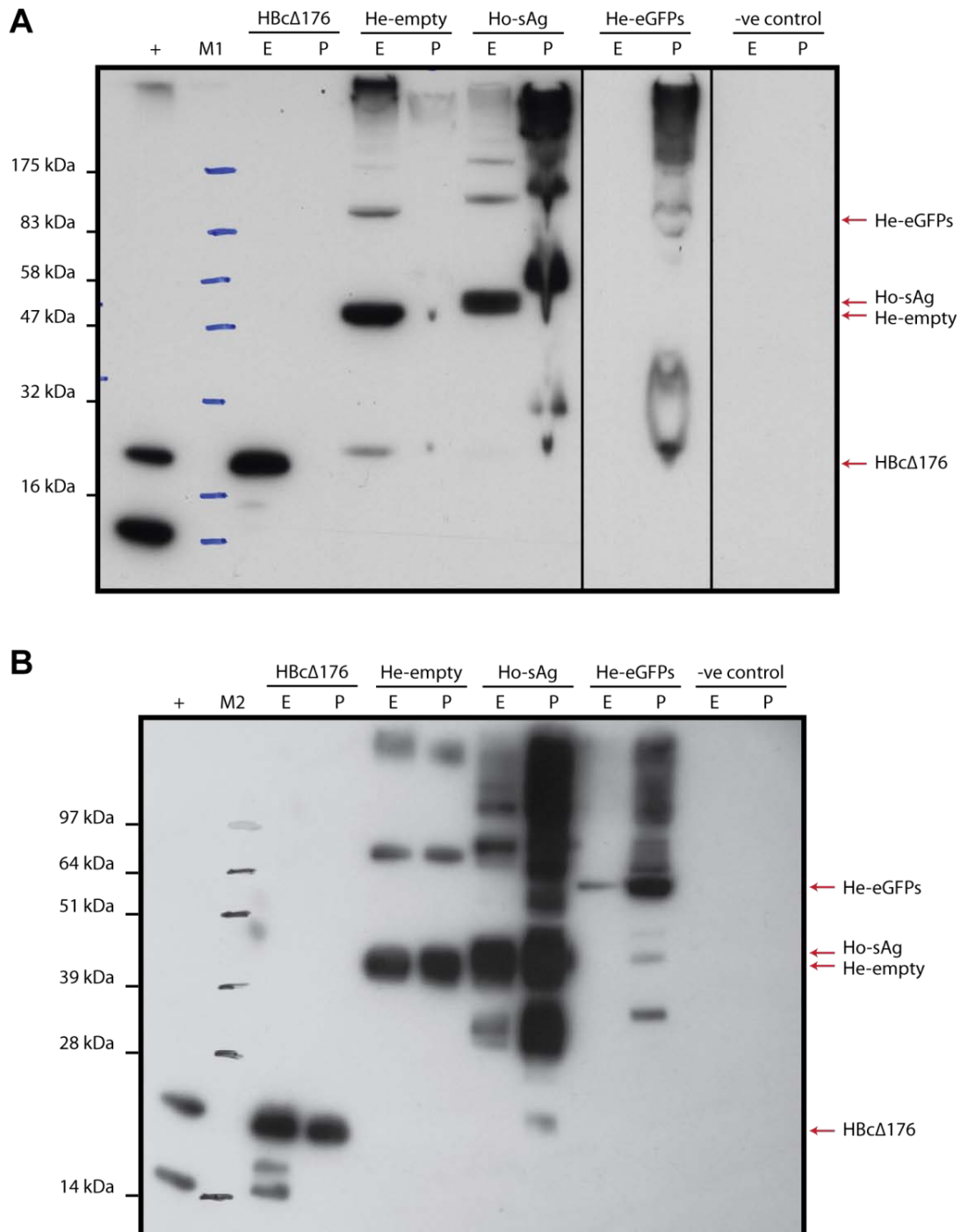


Figure 4.7: Epitope presentation at the c/e1-loop significantly increases aggregation of tandem core proteins.

Plants were agroinfiltrated with constructs as indicated. Leaf samples (3 discs) were homogenized in 3 volumes of extraction buffer and clarified. Pellets were extracted by boiling in LDS-SB (same volume as extraction buffer), followed by clarification. (A) Standard extraction buffer (ExB) was used, resulting in aggregation of cores carrying epitopes. (B) Hepatitis B extraction buffer 1 (HBExB1) was used, resulting in reduced aggregation of epitope carrying cores, and increased aggregation of 'empty' cores. M1 = NEB Broad Range marker; M2 = SeeBlue +2 Marker; + = recombinant HBcAg; E = extract; P = pellet; -ve control = empty vector.

Insertion of a 50 amino acid epitope of HBsAg into the e1-loop of homotandem core B (CoHo7e-sAg) reduced the solubility of this protein in comparison with the empty tHBcAg. While there was still a good signal in the clarified extract, a more intense signal was obtained from the insoluble pellet. This indicates that much of the expressed HB protein had aggregated, thereby causing it to be removed during the clarification spin.

Insertion of the whole *gfp* gene (encoding 245 amino acids) into the heterotandem core B (CoHe7e-eGFPs) caused all of the expressed tHBcAg to pellet as a result of the initial clarification step. While there was a strong HB antigen signal in the pellet fraction of this sample, no HB antigen was detected in the clarified extract. This validated the previous observation that the GFP fluorescence is detected exclusively in the pellet.

Though the display of a foreign sequence was shown to cause aggregation of the tHBcAg, the presence of dimers in the pellet fractions indicated that some ordered interactions between the proteins was still taking place. The strong signal near the wells of all tandem core samples was a further indication that the protein may be assembling into stable structures which are not easily dissociated by boiling in reducing LDS-SB. If the epitope-displaying tHBcAg are able to assemble into ordered particles, the apparent aggregation may be caused by the extraction conditions used in the experiment.

In an effort to recover soluble GFP tandem cores, the extraction buffer composition was altered several times to change buffer and salt concentrations, or to change the pH. The recovery of a protein in soluble form depends on interactions of the surface residues with the surrounding solution, the composition of which can have profound effects on protein solubility. Ultimately, changes to the standard protein extraction buffer (ExB), mainly by raising the pH and lowering the salt content, resulted in HB extraction buffer (HBexB1) which is better suited to the extraction of soluble epitope-displaying tHBcAg particles. The Western blot in Figure 4.7 B was prepared following the same procedure as used previously (Figure 4.7 A), but using HBexB1 instead of ExB as the extraction buffer. In the case of GFP-displaying tandem core (CoHe7e-eGFPs), this extraction buffer allowed a small portion of the expressed antigen to be recovered in the soluble fraction. However, HBexB1 was less well suited to the extraction of empty monomeric and tandem HB core antigen, as shown by the presence of strong signals in the pellets of these samples which had previously been soluble.

The results show that the display of foreign epitopes in the c/e1-loop of tandem HB core antigen alters its solubility. Furthermore, aggregation may be avoided by changing

the buffer composition. A new buffer, HBexB1, which allows for better extraction of GFP-displaying cores and also produces extracts with lower chlorophyll contamination levels, was used subsequently for work on tHBcAg chimaeras.

4.3.4 PLANT-PRODUCED HB TANDEM CORE ANTIGENS ASSEMBLE INTO CORE-LIKE PARTICLES

The superior immunogenicity of VLPs, compared with subunit vaccines, is widely accepted (see section 1.1; Tissot et al., 2010). To realize their true potential, tandem Hepatitis B core constructs must be shown to assemble into particles resembling monomeric HBcAg particles.

Homo- and heterotandem core constructs (empty, -sAg and -sAg,eGFP) were transiently expressed as previously described. Leaf tissue was harvested 6 dpi, extracted using HBexB1, clarified and loaded onto discontinuous sucrose gradients (Figure 4.8 A). After centrifugation, fractions were collected, separated on denaturing SDS-PAGE gels and tested for anti-HBcAg reactivity on a Western blot (Figure 4.8 B-C). CoHe7e-empty was detected in fractions 3 and 4, corresponding to the 30-40% sucrose fractions where monomeric HBcAg particles are generally found. The sedimentation of the material to the middle of the gradient and the lack of signal from lower density fractions indicated efficient assembly into large structures such as VLPs. In contrast, CoHo7e-empty gave strong signals in all fractions of the gradient, with a peak in fraction 3. The presence of tandem core protein in fractions 1 and 2 indicates that a proportion of homotandem core did not assemble into particles and therefore did not band with the particulate material at 30-40% sucrose.

Tandem core constructs with an HBsAg epitope, with and without eGFP, have been shown to express well in plants (Figure 4.5). However, extracts derived from heterotandem core constructs did not give the expected signal in sucrose gradient fractions (Figure 4.8 B). CoHe7e-sAg was not detected in the gradient, indicating that it was not present in the clarified extract but pelleted during the clarification spin, a sign of aggregation. A weak signal was detected for CoHe7e-sAg,eGFP in fractions 1 and 2, indicating that the small amount of antigen present in the clarified extract did not form particles resembling empty heterotandem cores, which banded in fraction 3. The low signal intensity may be due to aggregation and removal of a majority of CoHe7e-

sAg,eGFP during clarification. In contrast to these heterotandem versions, CoHo7e-sAg and CoHo7e-sAg,eGFP did produce a good anti-HBcAg signal (Figure 4.8 C). However, most of the immuno-reactive material was found in fractions 1 and 2 of the gradient, indicating that it had not formed particles.

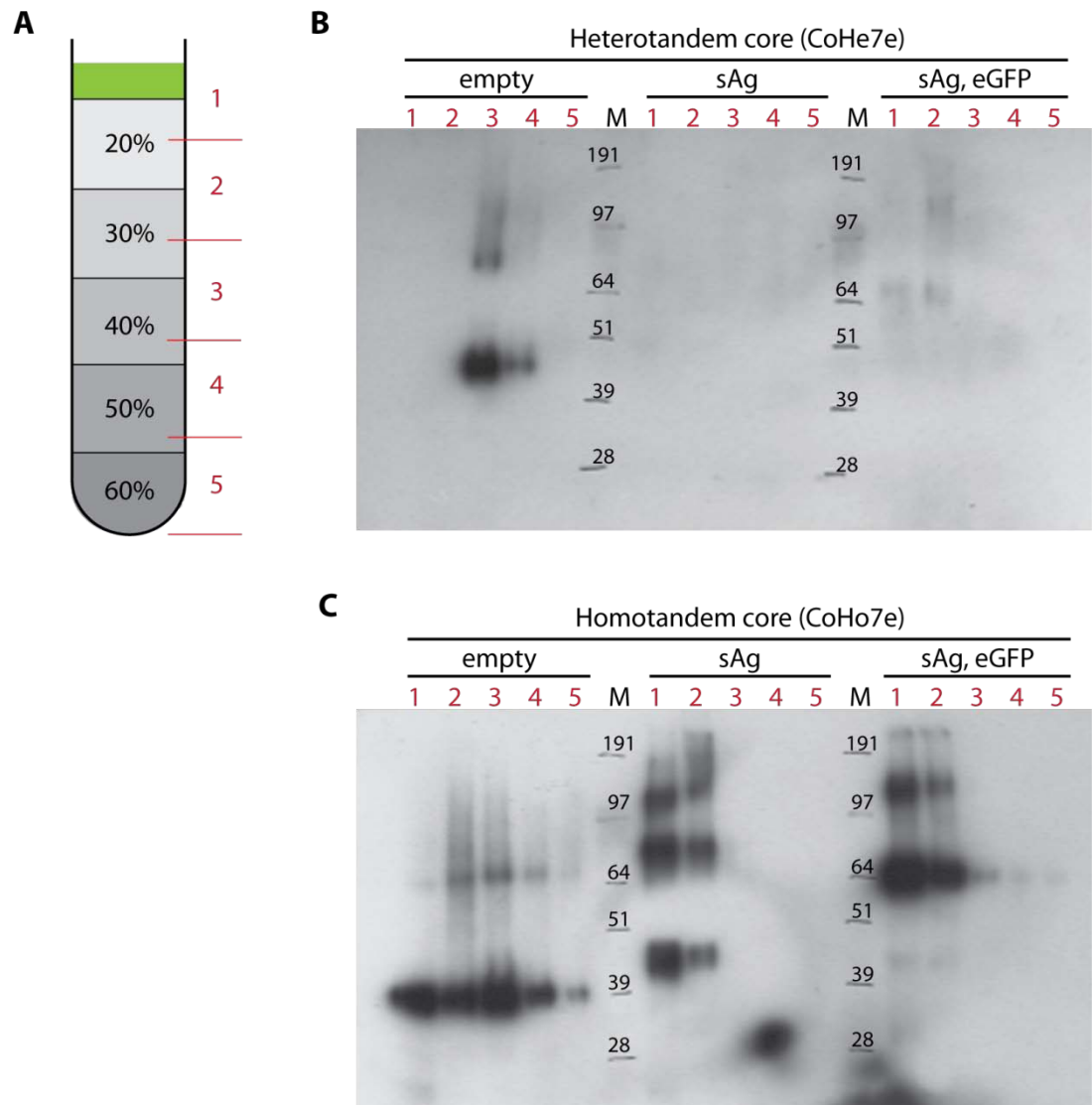


Figure 4.8: Density gradient analysis of HB tandem cores.

Leaf tissue was extracted with HBexB1, clarified at 9000 x g prior to loading on sucrose step gradients as shown in (A). After ultracentrifugation (217 000 x g avg, 4°C, 2.5 hrs), gradients were fractionated from top as shown in red. (B-C) Anti-HBcAg Western blot analysis of gradient fractions (numbered in red) separated on 12% SDS-PAGE gels. M = SeeBlue Plus2.

In order to conclusively show that plant-produced empty hetero- and homotandem cores assembled into VLPs, transmission electron microscopy (TEM) was used to observe the major immuno-reactive fractions of discontinuous sucrose gradients (Figure 4.9). For comparison, purified *E. coli*-derived tandem and monomeric HB cores (a kind gift from Mr. Kris Holmes, University of Leeds), as well as purified plant-derived monomeric HB Δ 176 expressed with the CPMV-*HT* system, were also imaged at the same magnification.

TEM showed that empty tHBcAg produced using the CPMV-*HT* system did assemble into VLPs of regular shape and size (Figure 4.9 A, C). Furthermore, the particles resembled monomeric HBc Δ 176 (Figure 4.9 E). In all three cases, a majority of the particles appeared to be of the larger T=4 type. However, smaller T=3 particles were also visible (arrows). Closer scrutiny revealed that the surface of the particles was not smooth but covered in small spikes, as is expected of Hepatitis B core particles.

E. coli-derived empty hetero- and homotandem cores (Figure 4.9 B and D, respectively) also assemble into VLP. Homotandem cores, however, appear less stable and more heterogeneous than the heterotandem core version. This may, however, be an artefact of sample preparation, storage and age: The supplied *E. coli* monomeric HBc Δ 149 sample was at least 5x more concentrated than the tHBcAg samples, as revealed by Coomassie blue-stained SDS-PAGE (data not shown). However, I was only able to find one cluster of particles (Figure 4.9 F) in grids prepared from this sample. These particles resemble plant-derived HBc Δ 176 particles, but are not abundant enough to allow analysis of their size.

The mean particle size of homo- and heterotandem cores, regardless of their origin, was approximately 34 nm diameter, as determined by TEM (Figure 4.10). Plant-produced monomeric HBc Δ 176 have a mean diameter of 37 nm and appear to be more regular in size.

These results show that empty tandem core proteins can assemble into structures resembling monomeric HBcAg particles in plants as well as in *E. coli*. However, inclusion of an epitope in the c/e1 loop significantly impacts solubility and assembly of these constructs.

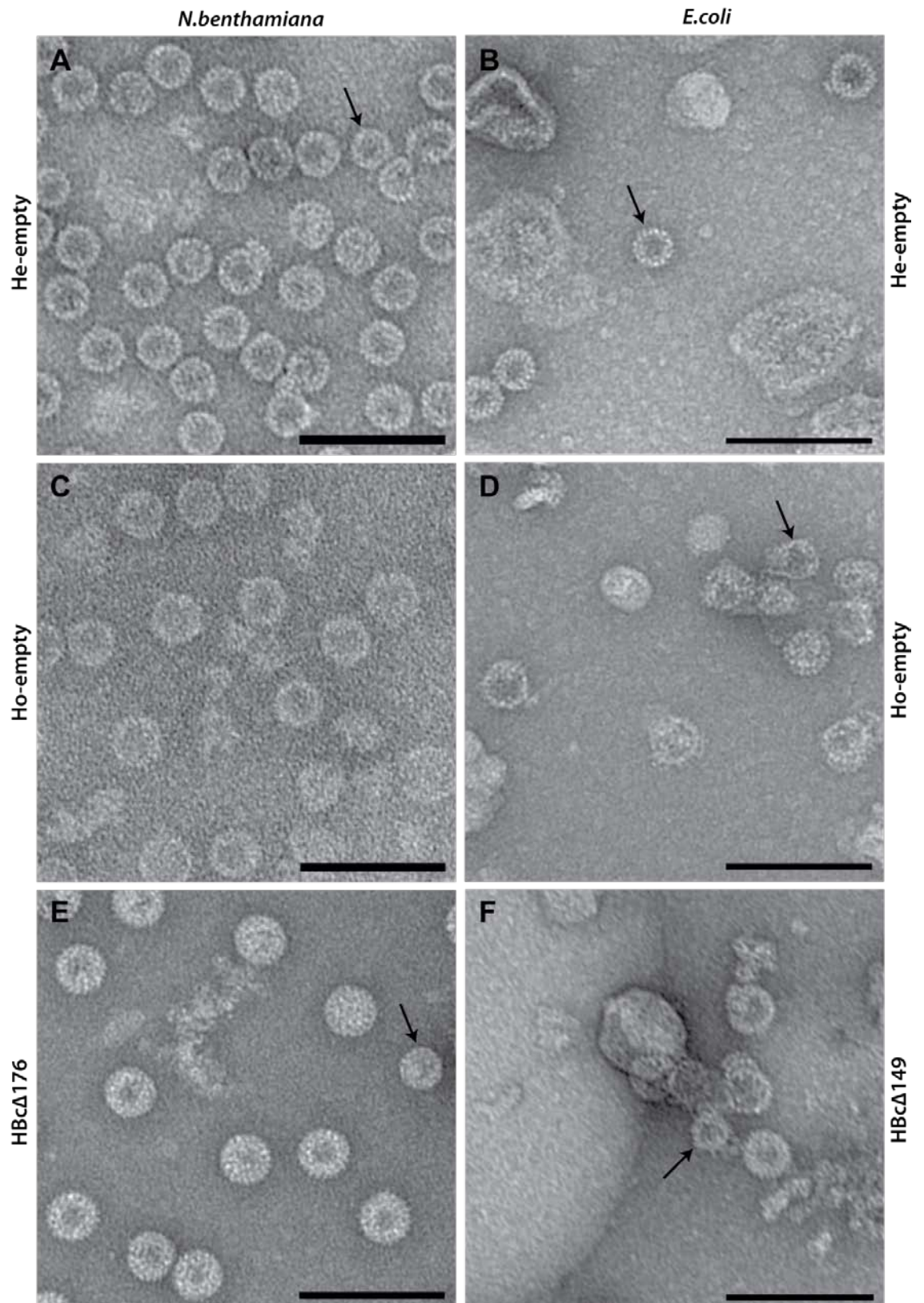


Figure 4.9: Plant-produced Hepatitis B tandem cores assemble into particles.

Samples are negatively stained with 2% UA and imaged at 50 000 x magnification. Scale bar = 100 nm. Arrows indicate smaller, T=3 particles. (A-B) CoHe7e-empty; (C-D) CoHo7e-empty; (E-F) monomeric HBcAg as indicated. (A-C-E) plant-produced particles. (B-D-F) *E. coli* - produced particles, a kind gift of Mr. Kris Holmes, University of Leeds.

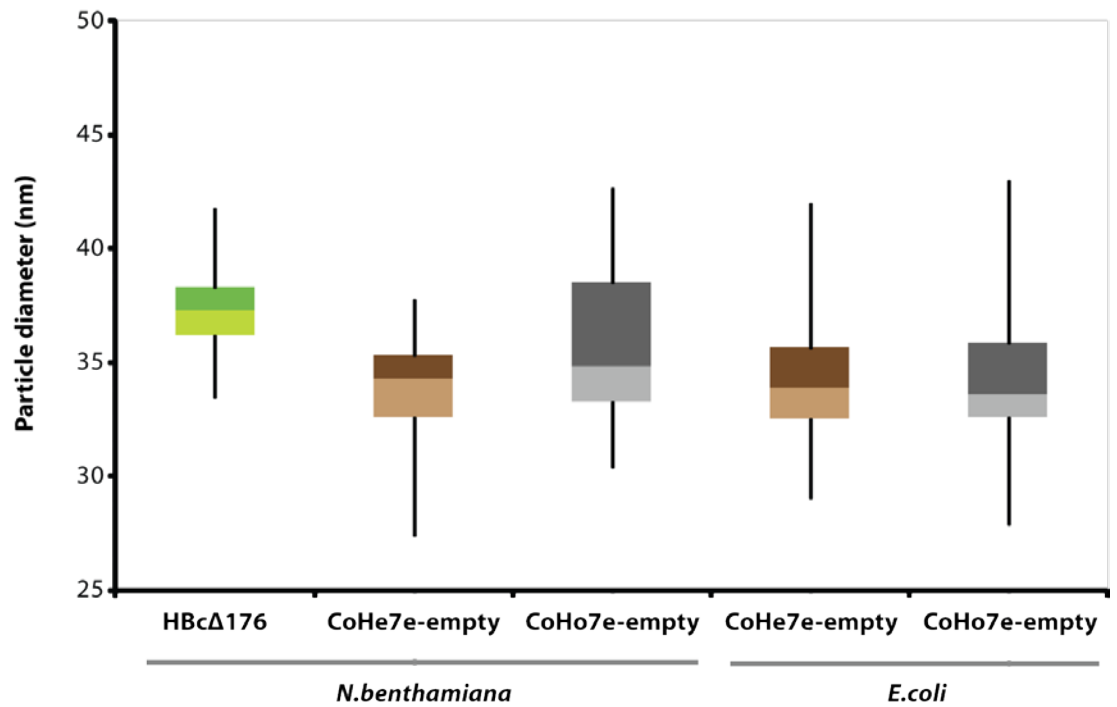


Figure 4.10: Size distribution of plant- and *E. coli*-produced monomeric and tandem HB particles.

Box plot analysis of the size distribution of particles in TEM images of different constructs. 100 or 50 particles were measured for *N. benthamiana* or *E. coli* samples, respectively, using Adobe Photoshop. Data was analyzed with Microsoft Excel.

4.3.5 WHOLE PROTEIN INSERTIONS ALLOW TANDEM CORE ASSEMBLY

Previous experiments have shown that it is possible to express tHBcAg with an insert of a whole protein, namely GFP, in one of the c/e1 loops (Sections 4.3.1 and 4.3.3). It was found, however, that these fusion proteins tended to aggregate leading to their loss during the initial clarification step. This problem was partially overcome by adapting the extraction buffer to allow some of the CoHe7e-eGFPs to be recovered in the soluble fraction (Section 4.3.3). In this section, I report the results of an investigation into whether the recovered soluble CoHe7e-eGFP protein assembles into VLP displaying functional GFP.

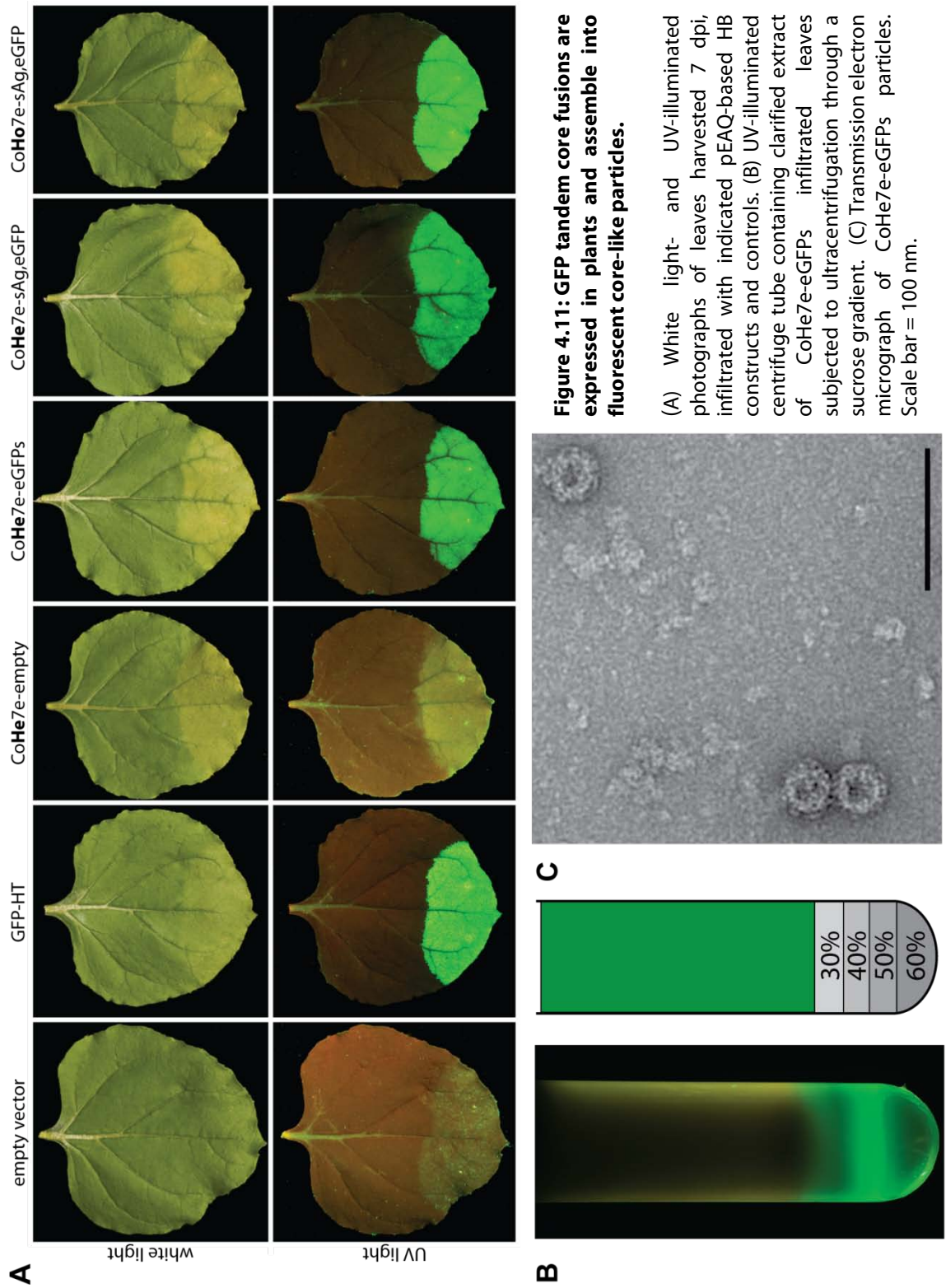
Hepatitis B tandem core constructs containing GFP (i.e. –eGFPs and –sAg,eGFP) were transiently expressed in *N. benthamiana* leaves as previously described. Upon irradiation with a hand-held UV lamp, GFP fluorescence was detected in all leaves infiltrated with the

GFP-containing constructs, but not in control tissue (Figure 4.11 A). Visually, the fluorescence intensity obtained from CoHo7e-sAg,eGFP was as high as that of the control construct expressing soluble GFP (pEAQ-GFP-*HT*). The heterotandem core constructs showed slightly lower fluorescence intensity, indicating lower GFP yields or reduced fluorescence intensity due to misfolding.

To further investigate the ability of GFP tandem cores to form particles, leaf tissue expressing CoHe7e-eGFPs was harvested 7 dpi and extracted with HBexB1 as described previously. This particular construct was chosen because it enabled recovery of some soluble antigen, while the –sAg,eGFP constructs were entirely insoluble. Clarified extract was loaded onto a short discontinuous sucrose gradient. Following ultracentrifugation, the ultracentrifugation tube was illuminated with a hand-held UV lamp, revealing an intensely fluorescent band in the 40% sucrose step (Figure 4.11 B). No visible fluorescence was detected in the top part of the gradient, indicating that the majority of the fluorescent material had assembled into large structures that sediment to the 40% sucrose layer. Similar results were obtained with CoHe7e-eGFPL, a construct in which the GFP insert is flanked by longer (10 aa) glycine-serine-rich linkers (data not shown).

To conclusively show the presence of VLP, and to determine their morphology and purity, the GFP-containing fraction was observed using TEM (Figure 4.11 C). Particles in this fraction had a regular shape and size, proving that a 27 kDa protein insertion in the c/e1 loop of the heterotandem core does not abolish its ability to fold and assemble into CLPs. The mean particle size was 41 nm in diameter ($n = 10$), which constituted a 3.5 nm increase in radius when compared with CoHe7e-empty particles (Section 4.3.4). This increase in size correlates well with the dimensions of GFP, a beta barrel of 4.2 nm length and 2.4 nm diameter (Pawley, 2006). Morphologically, the GFP tandem core particles were distinctly different from their empty counterparts, with a less rigid appearance (compare Figure 4.11 C and Figure 4.9 A).

The yield of purified GFP tandem cores was estimated at 10 ug / g FWT, or approximately 5-10% of the yield of purified CoHe7e-empty particles.



4.3.6 CRYO-ELECTRON MICROSCOPY OF GFP-TANDEM CORES

The ability to prepare soluble GFP tandem core particles to high purity and at yields of 10 ug/ g FWT made it possible to use these particles for structural analysis by cryo-electron microscopy (CEM). This technique enables the determination of a particle's 3D structure through computational averaging of multiple particle images. Three types of tandem core particles were transiently expressed and purified as described in Section 4.2: CoHe7e-empty, CoHe7e-eGFPs and CoHe7e-eGFPL. Grids were prepared for these samples by flash freezing in liquid ethane to embed the particles in vitreous ice. CEM and subsequent reconstructions were performed in collaboration with Dr. Robert Gilbert and Dr. Alistair Siebert, University of Oxford.

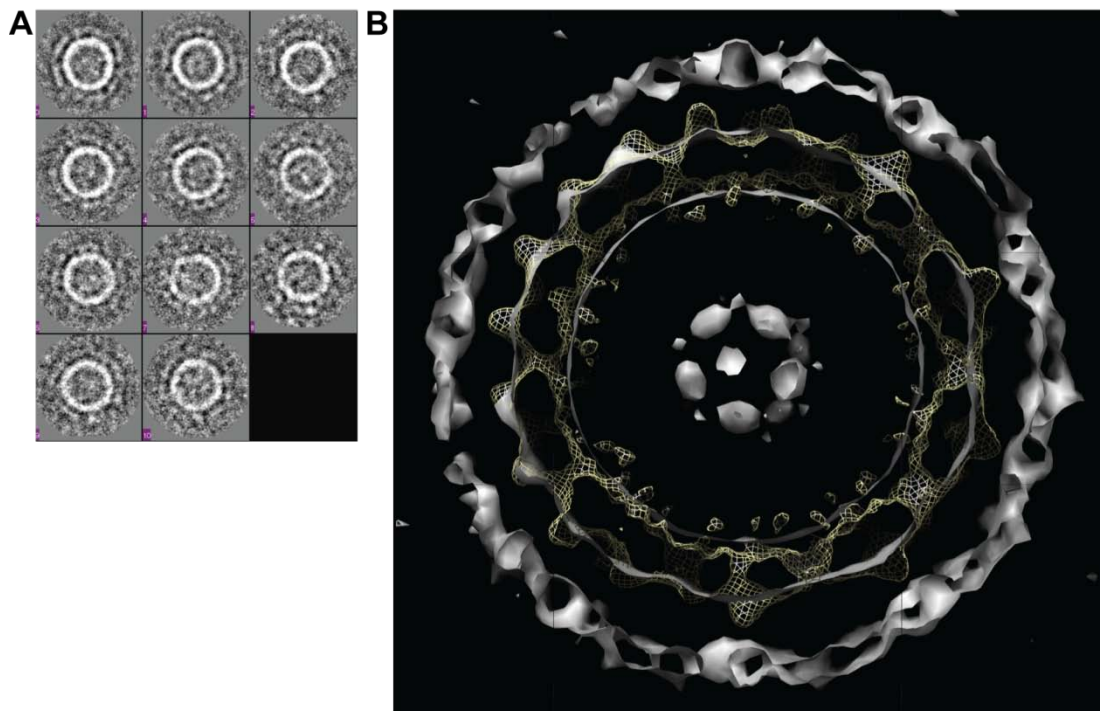


Figure 4.12: CryoEM reconstructions of HB tandem cores displaying GFP.

Purified CoHe7e-eGFPL particles were flash-frozen in vitreous ice, then subjected to cryo electron microscopy. (A) Class averages obtained from 339 individual particles using EMAN software. (B) Cross-section of a surface rendered reconstruction of particles. HB tandem core-associated density shown as a grid. Density associated with GFP (outside) and internal density (nucleic acid) is shown in silver. Cryo-EM and computational analyses were performed in collaboration with Dr. Alistair Siebert and Dr. Robert Gilbert (Univ. of Oxford).

Images obtained from the CoHe7e-eGFPL (approx. 40 µg/ ml) were used for subsequent computational analysis. 339 independent particles were picked from the CEM image and class averages produced with EMAN software (Figure 4.12 A). These were used to obtain a digital reconstruction image using computational tools for icosahedral particle reconstructions based on the method described by Fuller (1987).

The cross-section of the digital reconstruction shows the location of areas of density associated with protein or nucleic acid in the particle (Figure 4.12 B). The density associated with the Hepatitis B core is shown as a grid. The outside surface of this density layer is covered with protrusions corresponding to the two amphipathic α -helical hairpins which form the handle of the wild-type HBcAg dimer's hammer shape (see Section 4.1.2). This hammer-like appearance of the tandem core is best visible in the frontal sections of the three spikes at the 3 o'clock position. These data indicate that the GFP tandem core is able to assemble into particles with a core structure resembling that of wild-type HBcAg.

Surrounding the tandem core particle is a layer of density shown in grey. This represents the protruding GFP barrels attached to one c/e1 loop of every tandem core spike. The lack of visible barrel structures is most likely due to the flexibility of the linker between GFP and the rigid core structure. Nevertheless, the presence of this density layer proves that the insertion in the c/e1 loop is presented on the outside of the particle. Some density is also visible at the core of the particle (grey). This may be due to encapsidation of nucleic acid through the interaction of the arginine-rich C-terminus of the heterotandem core.

Further refinement of the obtained CEM reconstruction of CoHe7e-eGFPL is currently underway. The other two particle types, CoHe7e-empty and CoHe7e-eGFs, have not been reconstructed to date.

4.3.7 PRESENCE OF THE ARGININE-RICH C-TERMINUS IMPACTS NUCLEIC ACID ENCAPSIDATION

The C-terminal Arginine-rich 34 amino acids of HBcAg play a role in stabilizing the assembled core particle, but they are not essential for particle assembly (Birnbaum and Nassal, 1990; Wynne et al., 1999). The truncated HB Δ 149 retains its ability to assemble while losing its ability to non-specifically bind host RNA (Gallina et al., 1989). For medical

applications such as the use as vaccines, it may be easier to gain regulatory approval for such nucleic-acid free particles.

The ability of plant-produced homo- and heterotandem cores to bind plant nucleic acid was investigated by native agarose gel electrophoresis. 10 μ g of partially purified tandem cores and two monomeric HB cores were separated at 60 V for 2 hours. One gel was stained with Coomassie blue protein stain (Figure 4.13 A), while a duplicate gel was stained with ethidium bromide to visualize nucleic acid (Figure 4.13 B).

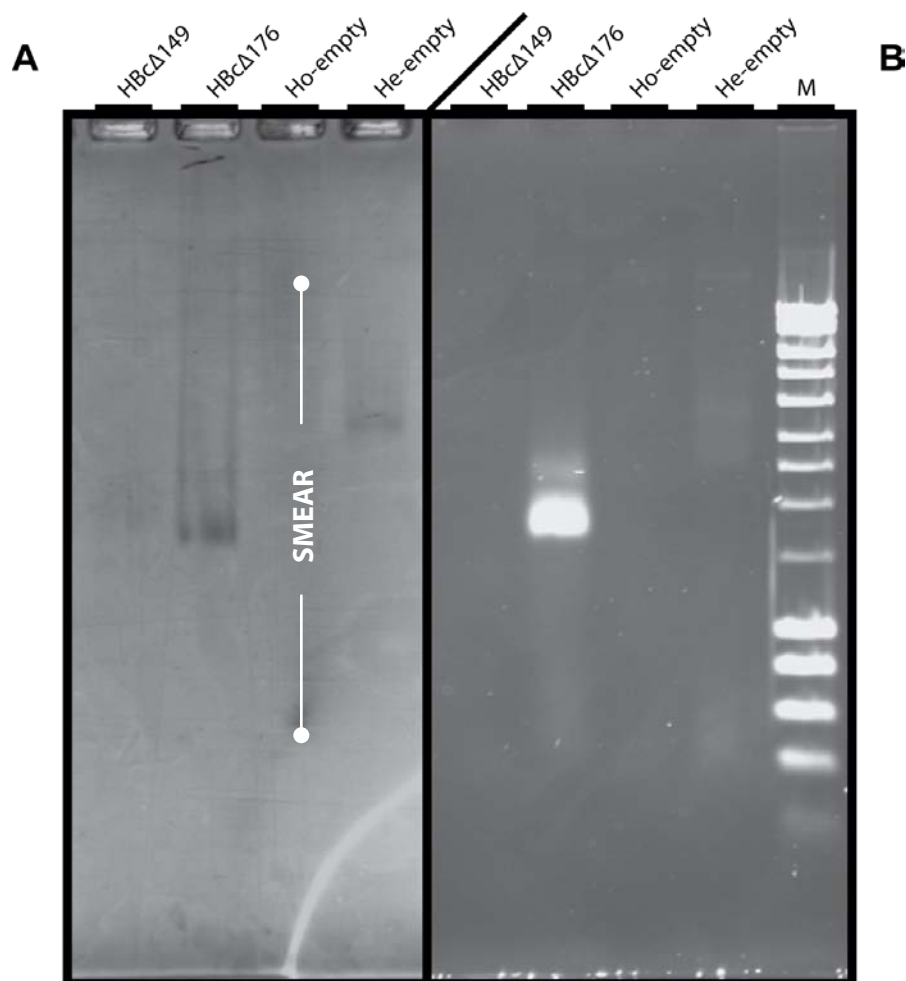


Figure 4.13: Heterotandem cores encapsidate plant nucleic acid, while homotandem cores are empty.

Partially purified particles from sucrose gradients were subjected to duplicate native agarose gel electrophoresis. Approximately 10 μ g of particles were loaded per lane. HBC Δ 149 was produced in *E. coli* (a gift from Mr. Kris Holmes, University of Leeds), all other samples were produced in *N. benthamiana*. (A) Coomassie blue staining to detect total protein. (B) Ethidium bromide staining to detect nucleic acid. M = DNA marker Hyperladder I.

Distinct bands were visible in the Coomassie blue-stained gel only for particles which retained the protamine-like domain at their C-terminus (HB Δ 176 and CoHe7e-empty). The electrophoretic mobility of the truncated versions (HB Δ 149 and CoHo7e -empty) is not distinct, resulting in a broad smear. This may be due to the lower stability of particles lacking the C-terminal domain.

The duplicate ethidium bromide-stained gel revealed the presence of nucleic acid in monomeric HB Δ 176 particles, indicated by a strong signal at equal electrophoretic mobility as the Coomassie-visualized band. By comparison, the truncated HB Δ 149 (E.coli-produced; a kind gift from Mr. Kris Holmes, University of Leeds) did not appear to bind nucleic acid, which would otherwise have resulted in a broad smear in the EtBr-stained gel.

Equally, the heterotandem cores were able to bind some nucleic acid, indicated by a faint signal in the EtBr-stained gel. However, binding was much reduced when compared with the monomeric HB Δ 176. This finding can be explained by the presence of only one arginine-rich domain per tandem core, resulting in half as many of these nucleic acid binding domains per particle when compared with monomeric HBcAg. In the case of homotandem cores, the lack of any arginine-rich domain resulted in empty particles, shown by the lack of EtBr staining in this lane.

Overall, the results indicate that plant-produced heterotandem cores, but not homotandem cores, are able to bind some host nucleic acid. However, this binding is much reduced compared with monomeric HB Δ 176.

4.3.8 SUMMARY

The results obtained using the different HBcAg and tHBcAg constructs expressed in this project are summarized in Table 4.2.

Table 4.2: Summary of results obtained from expression of HBcAg and tHBcAg constructs in plants.

Construct Name		Insert A	Insert B	Expression	Solubility	Gradient^a	Assembly^b
monomeric	HBcΔ176	n/a	n/a	yes	yes ^{c,d}	middle	TEM
tandem	He empty	none	none	yes	yes ^{c,d}	middle	TEM
	Ho	none	none	yes	yes ^{c,d}	top - middle	TEM
	He sAg	none	sAg (40 aa)	yes	no ^d	n/a	n/i
	Ho	none	sAg (40 aa)	yes	partial ^d	top	no (TEM)
	He eGFPs	none	EGFP (245 aa)	yes	partial ^d	middle	TEM
	He eGFPL	none	EGFP (245 aa)	yes	partial ^d	middle	CEM
	He sAg,eGFP	sAg (40 aa)	EGFP (245 aa)	yes	marginal ^d	top	TEM
	Ho	sAg (40 aa)	EGFP (245 aa)	yes	partial ^d	top	n/i
	Ho HAVP1	none	HA VP1(789 aa)	no	n/a	n/a	n/a

He = heterotandem; Ho = homotandem; n/a = not applicable; n/i = not investigated

a) position within sucrose gradient after ultracentrifugation. "Top" indicates unassembled particles, "Middle" indicates assembled particles.

b) particles visualized by TEM or CEM

c) solubility in ExB

d) solubility in HBexB1

4.4 DISCUSSION

In this project, several tHBcAg fusions have been successfully expressed in plants using the CPMV-*HT* system. Furthermore, the ability of some of these constructs to form stable core-like particles has been demonstrated. Particularly in the case of GFP tandem cores, plant-produced particles appear to be far more regular in size and shape than particles expressed in *E. coli* and yeast (personal communication, Prof. David Rowlands, University of Leeds)

As previously introduced, HBcAg lends itself to the display of foreign epitopes for vaccine development. HBcAg can be expressed to high levels in *E. coli* and other expression systems and is able to self-assemble. HB core particles are heat- and pH-stable structures which are highly immunogenic. When epitopes are displayed in the immunodominant c/e1 loop on the tip of the dimer, the resulting particles induce a stronger immune response than the epitope would on its own (Brown et al., 1991).

Insertions into the c/e1 loop are limited in size and shape, due to the close proximity of the two loops in the dimer structure. In *E. coli*, it is possible to produce particles displaying GFP in every c/e1 loop (Kratz et al., 1999). However, only 40% of the GFP is functional, indicating that folding of the fluorophore may be sterically hindered. Other proteins may be less suitable for internal fusions due to instability or the distance between their N- and C-terminus. One recent strategy to tackle these problems has been the insertion of a protease cleavage site immediately upstream of the foreign protein sequence, allowing the insert more freedom to move and fold while also having a positive impact on assembly (Walker et al., 2008). The tandem HB core (Gehin et al., 2004) presented in this work represents another strategy to improve assembly and folding of HBc displaying large protein inserts.

As previously introduced, the tHBcAg is a genetic fusion of a truncated HBcAg (HBc Δ 149) with another full-length or truncated core antigen, thereby yielding heterotandem and homotandem cores, respectively. The two halves of the tandem core are connected by a flexible glycine and serine-rich peptide linker, enabling them to fold into an HBcAg dimer-like structure and assemble into VLP in *E. coli* and yeast. This genetic fusion has two main advantages: Firstly, the two c/e1 loops of each particle spike can be addressed separately, allowing the display of only one large insert per spike and 120 per

particle, thereby providing more space for correct folding (e.g. CoHe7e-eGFPs). Secondly, the two c/e1 loops of the tandem core can contain two different smaller inserts, thus ensuring co-localisation on each spike (e.g. CoHe7e-sAg,eGFP). This may be particularly useful if the pair of inserts interact.

Plant expression of tandem HB core constructs with and without inserts has been possible using the CPMV-*HT* system (Figure 4.5). The mobility of tandem core proteins in SDS-PAGE varies with the length of insert and the presence of the arginine-rich C-terminus of the heterotandem core, as expected. Some bands of lower mobility, likely corresponding to dimers and multimers, are visible particularly in the constructs containing an insert. Notably, breakdown products are only visible in homotandem core constructs containing an insert, providing a first indication that these are less stable than their heterotandem core counterparts. The apparent stability of plant-produced tandem core proteins was particularly notable, as the *E. coli*-produced material suffers from proteolysis and breakdown.

Transient expression of HBcAg is very fast, being detectable within two days and reaching yields of over 0.5 g / kg within five dpi (Figure 4.6). Empty heterotandem core accumulation is detectable from 3 dpi, but apparently only reaches 1/5 of the level of monomeric HBcAg, as detected by ELISA. However, the quantification of tHBcAg using ELISA optimized for HBcAg may be unreliable: During the ELISA test, extracted core antigen is not denatured and remains in its particulate state. The polyclonal antibody used in the test may have a lower affinity for tHBcAg, which may be in a different conformational state than HBcAg. ELISA quantification relies on the comparison to a standard of known concentration, in this case commercially available monomeric HBcAg, thereby possibly underestimating the concentration of tandem HB present in each sample. The qualitative results of other experiments (Figures 4.5, 4.7) did not reflect the stark difference in yields between monomeric and tandem HB core antigen observed using ELISA.

Insertions into the c/e1 loops of the tandem core play a large role in determining the particle's characteristics due to their exposure on the outside of the particle. Surface morphology is visibly different when GFP is inserted in this position (Figure 4.11). More importantly, the charge, isoelectric point and hydrophobicity of an insert can alter the particles' solubility in certain buffers, causing them to aggregate (Figure 4.7). Whether the observed aggregation occurs upon synthesis in the plant cytosol, or happens after

extraction is not clear. However, I would expect aggregated protein within the cell to be targeted and degraded by the cellular machinery. The high yield of epitope-displaying tHBcAg suggests that this does not occur and may be an indication that aggregation takes place upon extraction, or that tandem HBcAg evades the plant's proteolytic machinery.

Recovery of even small amounts of CoHe7e-eGFPs was only possible when extraction conditions and the extraction buffer were changed drastically. The resulting HB extraction buffer 1 (HBexB1) contains lower concentrations of buffer, salt and EDTA, a different detergent, and has a higher pH than the extraction buffer used as standard (ExB). Though HBexB1 has a negative effect on solubility of empty tHBcAg, it was used preferentially for all HB samples due to the dramatically reduced levels of contaminating chlorophyll found in the soluble fraction (data not shown).

Neither HBexB1, nor standard extraction buffer were amenable to the extraction and detection of soluble particles containing a portion of the HB surface antigen (-sAg). Computational analysis found that this epitope has an isoelectric point of 7.7, very close to the pH of plant extracts and possibly playing a role in the aggregation of these proteins. However, substitution of the Tris buffer component of HBexB1 with two other Good buffers to raise and lower the pH, respectively, did not solve this problem (data not shown).

Due to the stringency of the regulatory approval process, only constructs which assemble into particles of regular shape and size will have potential merit as a vaccine. Hence, it was important to show that tandem HB core antigens can assemble into HB core-like particles when expressed in plants.

Sucrose density gradients were used to determine whether HB tandem core material sediments in the expected density fractions of 30-40% sucrose, as is the case for particulate monomeric HBcAg (Birnbaum and Nassal, 1990; Figure 4.8). As expected, empty homo- and heterotandem core proteins sediment to this area of the gradient, indicating that they are able to form VLP. This was confirmed by TEM analysis of the relevant fractions (Figure 4.9). In contrast to the heterotandem version, CoHo7e-empty is found in all fractions of the gradient, indicating that the sample consists of a heterogeneous population of assembled, disassembled and possibly aggregated particles. This reflects the finding of Birnbaum and Nassal (1990) that the truncated HBc Δ 149 does not sediment in a clear band but rather produces a smear throughout the

gradient. This result provides further evidence of the inherently lower stability and integrity of HBc Δ 149-based homotandem core particles.

At first glance, sucrose gradient analyses of sAg and sAg,eGFP homo- and heterotandem cores seemed to show that these did not assemble into VLP, because they did not sediment to the same area of the gradient as assembled empty tandem core particles. However, I hypothesize that a proportion of these constructs do form particles and that the presence of the sAg epitope on their surface causes them to aggregate. This would explain why the total amount of HBcAg detected by Western blotting of these sucrose fractions seemed far lower than the amount detected in crude extract, indicating that a large proportion of the tHBcAg was removed during the initial clarification step prior to gradient loading. If assembled sAg-displaying particles aggregate, then the only soluble form of these antigens will be unassembled, explaining their position in the low density layers of the gradients. Furthermore, the finding that homotandem core constructs are generally less stable than their heterotandem counterparts explains why the homotandem versions of sAg-containing constructs gave more intense anti-HBcAg signals in the gradient analysis.

A further indication of the particulate nature of aggregated tandem core material is the finding that CoHe7e-eGFPs particles can be recovered after optimization of extraction conditions. Only upon changing of the extraction buffer and clarification spin was it possible to recover soluble GFP tandem core antigen, which was pelleted during clarification on previous attempts (Figure 4.7). The recovered GFP tandem core is in the form of regular core-like particles of 41 nm diameter (Figure 4.11). These particles, though regular in shape and size, are morphologically distinct from empty tandem core particles, as expected (compare Figure 4.9 A). I expect that similar results can be achieved by stringent optimization of extraction conditions for sAg and sAg,eGFP tHBcAg particles, however time did not permit this to be undertaken.

The production of homogeneous GFP tHBcAg particles constituted a breakthrough in the establishment of tandem core technology. To date, it has not been possible to produce particles of comparable quality using *E. coli* and yeast expression systems. A key aim of this project, namely obtaining cryo-EM data for GFP tandem core particles, was now possible. The resulting cross-section image (Figure 4.12) provides new insight into the structure of epitope-presenting tHBcAg particles. The structure of the HB core is easily distinguishable by the presence of spikes on its outer surface. Where the cross-section

dissects a spike, the hammer-like appearance of the folded tandem core is visible and resembles the shape of natural HBcAg dimers (Crowther et al., 1994).

In the GFP tandem core particle, each spike should be decorated with one GFP barrel structure as shown in Figure 4.3 C. Though the GFP barrels are not uniquely distinguishable in the cryo-EM reconstruction, the presence of a density layer surrounding the tHBcAg particle, and the fluorescence of the particle are indicative of the presence of GFP. In the CoHe7e-eGFPL fusion protein, the GFP barrel is separated from the HB core protein by a flexible 10 aa glycine-serine-rich linker to allow it more space and flexibility to fold properly. It is not surprising, therefore, that cryo-EM reconstructions, through averaging of many separate particles, would show a diffuse density layer, because the fluorophores are not rigidly attached to the structural core. Further refinement may allow more detailed structures to be identified. It would also be interesting to see whether CEM reconstructions derived from the CoHe7e-eGFPs construct, which has shorter 3 aa G/S-linkers would allow individual GFP molecules to be resolved.

Cryo-EM detects all protein and nucleic acid density associated with a particle. The density on the inside of the GFP heterotandem core is likely due to nucleic acid encapsidation. This is not surprising, as the heterotandem core protein has an arginine-rich C-terminus which has been shown to bind host RNA non-specifically (Birnbaum and Nassal, 1990; Cohen and Richmond, 1982; Gallina et al., 1989). To further investigate nucleic acid binding of hetero- and homotandem cores, purified empty tandem core particles were subjected to native agarose gel electrophoresis, followed by ethidium bromide staining (Figure 4.13). This revealed that heterotandem cores do encapsidate nucleic acid, though at a much lower level than monomeric HBc Δ 176.

Native agarose gel electrophoresis is a useful tool to detect slight changes in surface charge and composition of particle variants. It is thus not surprising that heterotandem cores have a shifted mobility compared with monomeric HBc Δ 176, as the latter contains more nucleic acid, has more arginine-rich regions and lacks the glycine-serine-rich linker of tHBcAg. It was surprising to find, however, that empty homotandem core particles did not produce a distinct band in the Coomassie blue-stained gel (Figure 4.13 A), but rather a diffuse smear. As these particles are not expected to contain any nucleic acid, this is an indication that even purified homotandem core particles consist of a heterogeneous, less stable population than heterotandem cores.

TEM analysis of plant- and *E. coli*-produced monomeric and tandem core particles shows that all particles are similar in size and morphology. A spiky surface is visible even at 50 000 x magnification. Measurement of particle diameter reveals that tandem core particles are on average 2 nm smaller than monomeric HBt76 particles (Figure 4.11). This may be due to differences in amino acid composition and folding, making the tandem core particles more compact. It is also evident that plant-produced empty homotandem core particles are more variable in size than heterotandem cores.

Overall, the data suggest that plant-produced homotandem core constructs are less stable than their heterotandem core counterparts. From a regulatory perspective, homotandem cores may be preferred due to their lack of nucleic acid. However, the high proportion of unassembled antigen, low stability, and structural heterogeneity of homotandem core particles are drawbacks.

The work reported in this chapter has shown that tHBcAg can be produced efficiently in plants using the CPMV-*HT* system, that it assembles into regular CLP structures, and that it is possible to display whole protein chains on their surface. Through optimization of extraction conditions and density gradients, it was possible to produce particle preparations of superior purity and homogeneity to those prepared from *E. coli*. The plant-produced GFP tandem core particles were of regular size and shape, and did not exhibit the size variation (up to 100 nm diameter) seen with *E. coli*-produced GFP tandem cores (Aadil El-Turabi, personal communication). This enabled us to obtain cryo-EM reconstructions of the GFP-displaying tandem core, a major breakthrough for the tandem core technology. The GFP tandem core presented here is the largest “epitope” to have been displayed on plant-produced HBcAg. Plant-based expression may be the most efficient and economical method of producing HB tandem core particles for commercial applications.

The success achieved in expressing many versions of the relatively simple tHBcAg was very encouraging and led us to attempt the expression of more complex VLPs, namely Bluetongue virus-like particles (Chapter 5).

5 EXPRESSION AND ASSEMBLY OF BTV-10 STRUCTURAL PROTEINS

5.1 INTRODUCTION

Given the success achieved with the production of hepatitis B particles using the CPMV-*HT* system (Chapter 4), I decided to investigate whether the expression system could be used to produce more complex VLPs. To this end, I focussed on the expression of Bluetongue virus-like particles, whose size, composition and stoichiometry would make them the most complex VLPs to have been expressed in plants. Expression of a heteromultimeric VLP takes full advantage of the pEAQ vectors (Chapter 3), which allowed me to easily clone and test many constructs, and provided the ideal tool for the simultaneous co-expression of multiple proteins within the same cells.

Bluetongue Virus (BTV) is the type member of the *Orbivirus* genus within the Reoviridae family of double-stranded RNA (dsRNA) viruses. BTV causes the most severe symptoms in sheep and cattle, but is able to infect other domesticated and wild ruminants. First identified in South Africa, the virus has rapidly spread throughout the world and is now found wherever its vector, the biting midge, thrives (Carpenter et al., 2009). There are currently 24 known serotypes of BTV and recovery does not result in significant cross-protective immunity.

Bluetongue disease is characterised by an inflammation of the face, mouth and tongue of the animal, sometimes resulting in a cyanotic (blue) tongue. Other symptoms of acute infection include lameness, fever and abortion of the foetus. Recovery is generally slow and mortality rates vary widely depending on serotype. The economic impact of BTV arises not only from the loss of livestock, but also the emaciation of recovering animals and the movement and trade restrictions imposed by governments in a bid to stop the spread of the disease.

The spread of BTV is influenced by several factors. Gradual climate change is contributing to the widening of potential habitats for the vector *Culicoides* species (Wittmann and Baylis, 2000). The small size of the insect vector enables it to be transported over great distances by strong winds, thereby enabling it to spread BTV across large bodies of water. Additionally, the use of airplanes in cargo transport provides

an additional accelerant of spread. Finally, the use of multivalent inactivated and live-attenuated vaccines has been shown to be the cause of emergence of previously unreported serotypes in areas of vaccine use.

In contrast to FMDV, BTV cannot be eradicated by the culling of an infected animal population. Once an area has been exposed, reservoirs of virus will be found in the host animal, the vector, as well as wild ruminants in the area. The only feasible means of combating BTV is a comprehensive vaccination programme.

5.1.1 CURRENT BTV VACCINES

Two types of vaccine are currently used. Live-attenuated vaccines have been used successfully for many years, are inexpensive and require only a single dose. However, the risks of reversion, recombination in the host or vector, and spread to newly impregnated ewes must be carefully considered. Since the 1980s, chemically inactivated vaccines have been available and are currently used to control the European outbreak. These are more expensive to produce than live-attenuated vaccines, require the administration of two doses and each batch must be thoroughly tested. However, these inactivated vaccines are safer, due to the inability of the virus to replicate.

Multivalent vaccines are available to afford simultaneous protection against several BTV serotypes. However, cross-protection is limited due to the high variability in the outer shell of the different serotypes (Section 5.1.3). Multivalent vaccines thus consist of a cocktail of different serotypes. The danger of using such a multivalent vaccine has recently been highlighted by the finding that a genome segment of a BTV-16 isolate from Italy shared 100 % sequence identity with the same segment of a BTV-2 live-attenuated vaccine strain used in Italy in 2002 (Batten et al., 2008). This indicates that gene segment reassortment had occurred, resulting in a novel field strain. Such reassortants of orbiviruses can often have novel characteristics and heightened virulence compared to their parent strains (Nuttall et al., 1992).

Virus-like particle and subunit vaccines could provide an inherently safe alternative to traditional vaccines. At doses exceeding 50 µg, a recombinant VP2, the main immunogenicity determinant of BTV, induces neutralizing antibody production when tested in sheep (Roy et al., 1990). Efficacy is increased up to 100-fold when VP2 is

assembled within a VLP, and doses of 10^6 VLP are sufficient to confer protective immunity when administered with an adjuvant (Roy et al., 1992). Despite its potential, after nearly 20 years, no commercial VLP vaccine has been produced for BTV. This is likely due to the high cost associated with the only proven BTV VLP production system, insect cells. Though commercial production of VLP vaccines is possible for human application, the low cost needed for a viable veterinary vaccine cannot be achieved in this way. A more cost-effective production platform for BTV VLP is therefore needed to enable this superior vaccine technology to be deployed in practice.

5.1.2 LIFE CYCLE

Bluetongue virus is able to replicate in its ruminant host as well as the insect vector. Cell entry and replication are schematically illustrated in Figure 5.1. Upon feeding, the midge transfers the virus into the host, where the outer shell protein VP2 mediates cell attachment. The virus enters the cell by way of endocytosis, with conflicting reports suggesting clathrin-dependent and clathrin-independent pathways (Forzan et al., 2007; Gold et al., 2010). The acidification of the early endosome is necessary for infection and allows the outer shell of the virus to dissociate from the core particle. The other outer shell protein, VP5, plays a role in membrane permeabilisation, allowing the core particle to enter the cytoplasm (Hassan et al., 2001).

The BTV core particle contains the 10 dsRNA genome segments as well as three minor structural proteins: VP6 has helicase activity allowing it to unwind dsRNA (Stäuber et al., 1997), VP1 is an RNA-dependent RNA polymerase (Boyce et al., 2004), and VP4 synthesizes 'cap' structures at the 5'-end of viral messenger RNA (vmRNA; Martinez-Costas et al., 1998). The minor structural proteins and the viral genome are enclosed within a stable core of VP3 and VP7, which remains intact throughout viral replication. Within the cytoplasm, the core becomes transcriptionally active and extrudes capped viral mRNA (vmRNA) which is translated by the host machinery to synthesize the seven structural (VP) and three non-structural (NS) proteins. The positive-strand vmRNA also serves as a template for minus-strand synthesis to form dsRNA.

The assembly mechanism of BTV particles is not well understood. BTV structural proteins have been shown to co-localize to virus inclusion bodies with non-structural

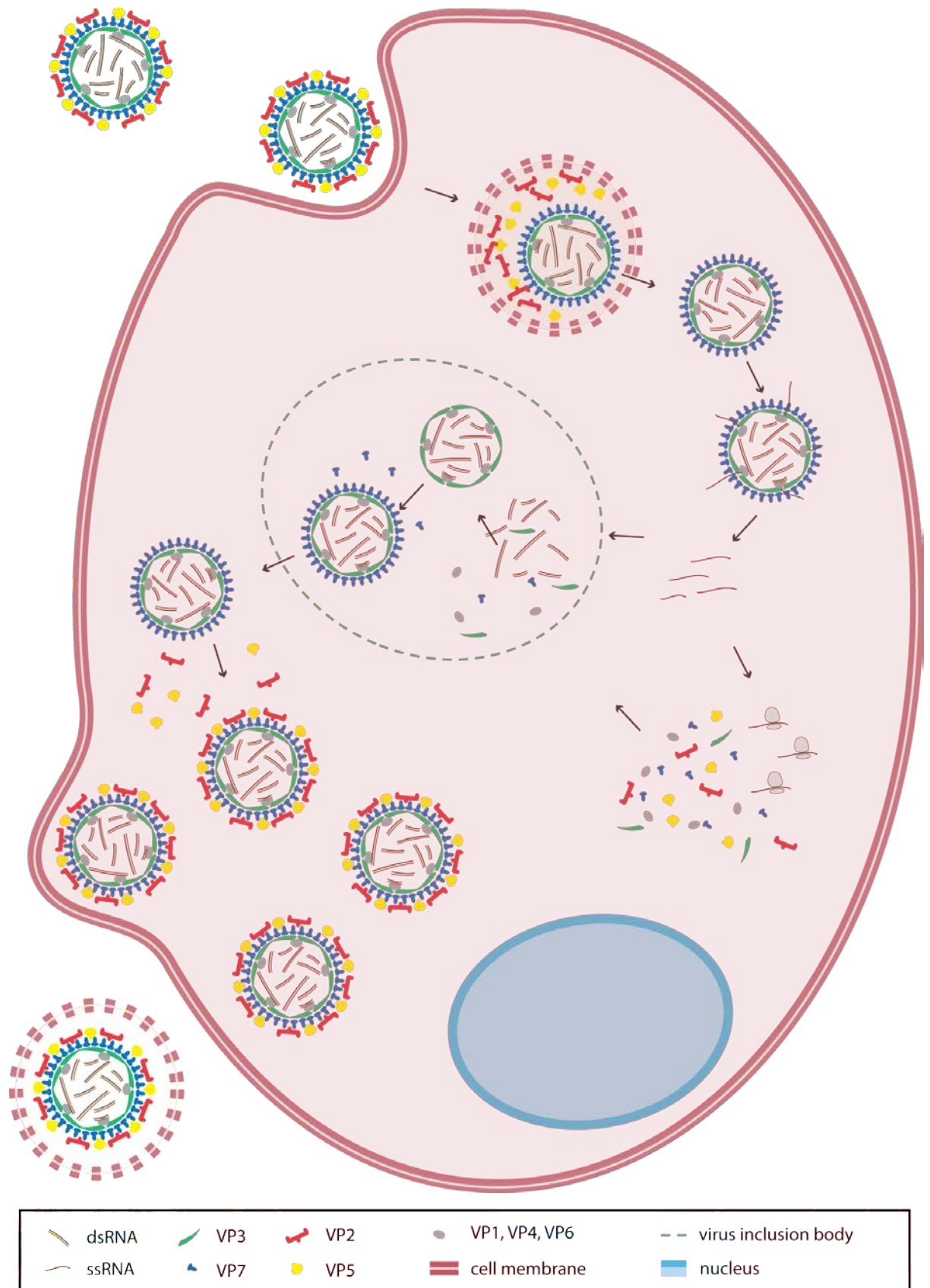


Figure 5.1: Bluetongue virus replication cycle.

Schematic illustration of the stages of cell entry, replication and cell egress of Bluetongue virus in infected cells. Non-structural proteins were omitted from the illustration.

protein NS2, indicating that this is the site of viral assembly. Here, the dsRNA genome is associated with BTV structural proteins (Grimes et al., 1998; Loudon and Roy, 1992; Nason et al., 2004), however it is not known how the selective encapsidation of ten different dsRNA segments occurs. Non-structural protein NS3 is located in the cellular membrane of infected invertebrate cells and has been shown to allow fully assembled virus particles to egress from insect cells without lysis (Celma and Roy, 2009).

In insects, viral uptake occurs during feeding. While virus particles can infect both mammalian and insect cells, it has been shown that only insect cells can also be infected by core particles. These attach to the cells via an RGD motif of VP7 (Basak et al., 1997; Tan et al., 2001), providing another mode of virus entry into cells.

5.1.3 BTV CAPSID STRUCTURE AND ASSEMBLY

Bluetongue virus is a non-enveloped, icosahedral virus of approximately 80 nm diameter. Here, I will focus on the four major structural proteins VP2, VP3, VP5 and VP7, which are sufficient for the assembly of virus-like particles (French et al., 1990). These proteins assemble to form a capsid consisting of three concentric protein shells (Figure 5.2). The outer two shells of the virus can be removed to produce core and subcore particles.

5.1.3.1 *Subcore-like particles (SCLP)*

The innermost subcore layer of BTV is formed of 120 subunits of VP3. This 103 kDa protein has the shape of a thin (up to 35 Å) triangular wedge, and interacts with dsRNA and the minor structural proteins on the inside of the particle, and VP7 on the outside. VP3 is highly conserved between the 24 serotypes of BTV, indicating its crucial role in particle formation.

The protein forms decamers as the first detectable structure in BTV assembly (Kar et al., 2004). These decamers consist of five dimer structures in which each of the two VP3 molecules takes on a slightly different conformation. The decamers assemble into a thin subcore structure of pseudo T=2 symmetry, with a diameter of approximately 55 nm (Grimes et al., 1998). VP3 is amenable to N- and C-terminal extensions without abolishing

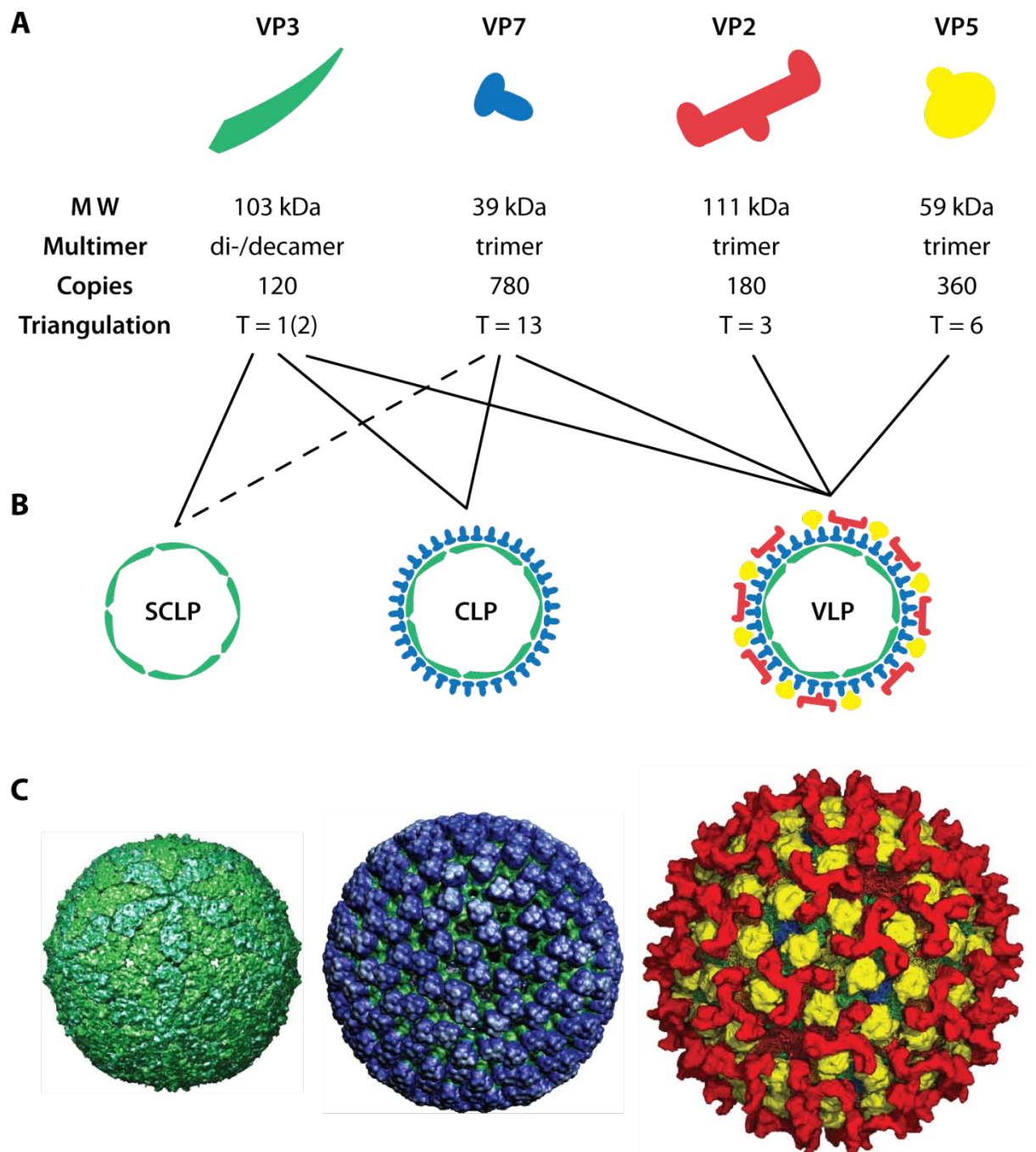


Figure 5.2: Bluetongue virus particle structures.

Schematic illustration of the subunits and forms of BTV-like particles and subparticles. (A) The four main structural proteins and information about their molecular weight (MW), multimer assembly, copies per particle and triangulation number. (B) Schematic representation of subcore-like particle (SCLP), core-like particle (CLP) and virus-like particle (VLP) and their components. (C) Surface-rendered representations of subcore, core and virus particles. Modified from published structural images (<http://viperdb.scripps.edu>; www.iah.bbsrc.ac.uk).

its ability to assemble, allowing peptides, epitopes and even GFP to be fused to the particles (Kar et al., 2005; Tanaka et al., 1995).

BTV subcore-like particles can be obtained from full VLP by removal of the outer shell and stripping of the VP7 layer by low pH and low salt treatments, respectively (Loudon and Roy, 1991). It is possible to produce SCLPs directly by co-expression of VP3 with a mutant VP7 incapable of assembly; however, it is reportedly not possible to produce subcore-like particles by expression of VP3 alone using the baculovirus system (Hewat et al., 1992; Loudon and Roy, 1992). BTV subcore particles have a strikingly angular appearance when visualized using negative staining and TEM, and a spherical appearance when observed by cryo-EM (Hewat et al., 1992).

5.1.3.2 Core-like particles (CLP)

Core-like particles are formed by the assembly of a VP7 layer onto SCLPs. VP7 is the smallest (39 kDa) and most abundant of the structural proteins of BTV, with 780 copies making up a full complement in each particle. VP7 molecules have two domains: an upper β -sandwich domain comprising the internal section of the polypeptide, and a lower α -helix bundle composed of the N- and C-terminal sections (Grimes et al., 1995). Large hydrophobic surfaces allow the protein to form stable trimers which interact tightly with the VP3 surface below. Like VP3, the sequence of VP7 is highly conserved between serotypes, and N- and C-terminal extensions to VP7 weaken its interaction with VP3.

In authentic core particles, VP7 trimers assemble on to the VP3 scaffold to form 260 protrusions, with a triangulation of $T=13$. This gives the particles a distinct “spiky” appearance when viewed using TEM. BTV core particles were first termed “BTV D” (D for dense), referring to the higher buoyant density of the core in relation to the full virus particle, termed “BTV L” (L for light; Martin and Zweerink, 1972). It is interesting to note that both virus and core particles were obtained in these early purification attempts, due to the higher relative stability of the core. It was later found that pure core particle preparations can be easily obtained from virus preparations by low pH treatment (Mertens et al., 1987).

BTV CLPs have been produced in insect cells using a dual recombinant baculovirus for the co-expression of VP3 and VP7 (French and Roy, 1990). These particles are devoid of nucleic acid and have a sedimentation coefficient of 225 S, much lower than the 470 S of the authentic core particle, which can be produced by removal of the outer shell of the

authentic virus (French and Roy, 1990; Martin and Zweerink, 1972). Though they resemble authentic core particles when imaged using TEM, structural analyses by CEM revealed that baculovirus-produced CLPs lack 60 trimers of VP7 around the five-fold axes. When produced from full VLP, these 60 trimers are present as expected, indicating that an interaction with the outer shell proteins VP5 and/or VP2 may be necessary for full CLP assembly (Hewat et al., 1994). It is also interesting to note that baculovirus-produced CLPs have a larger diameter than authentic core particles (Hewat et al., 1992).

Co-expression of VP7 causes a stark change in intracellular localization of VP3: When expressed on its own VP3 is co-localized with proteasomes, but in the presence of VP7 its cellular localization is close to the nucleus (Kar et al., 2005). This is evidence of the importance of the close interaction of VP3 and VP7 in the assembly of BTV particles.

5.1.3.3 *Virus-like particles (VLP)*

Bluetongue virus-like particles consist of all four major structural proteins, with an outer layer of VP5 and VP2 surrounding the CLPs. In the full virion, this outer shell consists of 360 copies of the 59 kDa VP5, and 180 copies of the 111 kDa VP2.

VP2 is the major immunogenicity determinant of BTV and its sequence varies greatly among the different serotypes. The protein has haemagglutination activity and is involved in cell attachment and entry of BTV into vertebrate host cells (Hassan and Roy, 1999). VP2 (T=3) forms triskelion-shaped trimers with two distinct domains: A central hub domain has sialic acid-binding activity while the tip domains protrude from the virion surface and are likely receptor-binding domains (Zhang et al., 2010). No receptor has been found to date, however.

The spaces between the three “legs” of the VP2 trimers are filled with 120 globular VP5 trimers which form weak interactions with the underlying VP7 layer (Zhang et al., 2010). VP5 (T=6) lies slightly recessed from the outer edge of the particles. Structural studies have shown VP5 to have features resembling membrane fusion proteins of enveloped viruses and it has been confirmed that VP5 acts to permeabilize the membrane of the host cell (Forzan et al., 2004). It is thought that VP5 undergoes a conformational change upon receptor binding and endocytosis, which activates it to allow permeabilization of the endosome and movement of the core particle into the cytoplasm. VP5 also contains a SNARE-like domain which is essential in its interaction with lipid rafts and cellular

membranes. It may also play a role in virus assembly and egress, through interaction with the membrane and viral NS3 (Bhattacharya and Roy, 2008).

Full VLPs of BTV were first expressed in the baculovirus system in 1990 (French et al.). Assembly of VP5 and VP2 was found to be co-dependent, with neither protein assembling into stable particles in the absence of the other. It has been possible to produce chimeric VLP by expressing the core proteins VP3 and VP7 of one serotype with the outer shell proteins VP5 and VP2 of another serotype (Loudon et al., 1991). This is likely due to the homology of core proteins between serotypes.

With a diameter of up to 85 nm, VLPs are significantly larger than CLPs. However, most TEM images of virus-like and authentic virus particles published in the available literature contain some core-like or core particles as well, indicating that purified virus and VLP preparations are always a mixture of different viral particles (French et al., 1990; Hewat et al., 1994; Martin and Zweerink, 1972; Roy et al., 1992).

5.1.4 AIMS OF THIS CHAPTER

Bluetongue VLPs have been shown to be a safe and effective alternative to traditional BTV vaccines, but have not been exploited as such. To date, VLPs have only been successfully produced in insect cell systems, which are too expensive to yield affordable veterinary vaccines. Transient expression in plants is a potentially cheaper alternative eukaryotic expression platform.

In this chapter I will show that it is possible to express the major structural proteins of Bluetongue virus serotype 10 in plants by using the *CPMV-HT* expression system. BTV-10 is an isolate from the USA, which had previously been shown to assemble into VLPs in the insect cell system (French et al., 1990). Furthermore, plant-produced BTV-10 VP3 and VP7 can assemble into core-like particles upon co-expression. An association with VP5 is also indicated.

5.2 SPECIFIC MATERIALS AND METHODS

5.2.1 CLONING

The genes for BTV-10 VP2, VP3, VP5, VP7 and NS1 contained within pUC19 vectors were kindly provided by Prof. Polly Roy (London School of Hygiene and Tropical Medicine). Genes for VP3 and VP7 were amplified from their source using the primers listed in Table 5.1 and inserted between the RNA-2 5'- and 3'-UTR sequences of pENTR-ET2 using *Nco*I and *Stu*I. C-terminally His-tagged versions were made by end-tailoring. Expression cassettes were then transferred to pDEST-BINPLUS by recombination. Cloning into pEAQ-*HT* using *Age*I and *Xho*I was used for the production of C-terminally His-tagged constructs of VP5, VP2 and NS1. A table of constructs is provided in Appendix A.

Table 5.1: Oligonucleotides used in cloning of BTV-10 constructs.

Name	Sequence ^a	Function
BTV-10 VP3 NcoI F	GACATG <u>CC</u> atggctgctcagaatg agcaac	Primer for end-tailoring of <i>Nco</i> I site to BTV-10 VP3; sense
BTV-10 VP3 StuI R	GAAGG <u>C</u> ctacacagttggcgcagcc ag	Primer for end-tailoring of <i>Stu</i> I site to BTV-10 VP3; antisense
BTV-10 VP7 NcoI F	GACATG <u>CC</u> atggacactatcgccgc aagag	Primer for end-tailoring of <i>Nco</i> I site to BTV-10 VP7; sense
BTV-10 VP7 StuI R	GAAGG <u>C</u> ctacacatagggcgcgcg	Primer for end-tailoring of <i>Stu</i> I site to BTV-10 VP3; antisense
BTV10.2-AgeI-F	TTAC <u>CGG</u> Tatggaggaattcgatc accagtg	Primer for end-tailoring of <i>Age</i> I site to BTV-10 VP2; sense
BTV10.2-XhoI-R	TT <u>CTCGAG</u> ctaacatttagtagctt cg	Primer for end-tailoring of <i>Xho</i> I site to BTV-10 VP2; antisense
BTV10.3-HIS-StuI-R	GAAGG <u>CCT</u> AGTGGTGGTGGTG GTGGTGcacagttggcgcagccag	Primer for end-tailoring of 6 x His tag and <i>Stu</i> I site to BTV-10 VP3; antisense
BTV10.5-AgeI-F	TTAC <u>CGG</u> Tatggggaagataatca aatcg	Primer for end-tailoring of <i>Age</i> I site to BTV-10 VP5; sense
BTV10.5-XhoI-R	TT <u>CTCGAG</u> tcaagcatttcgtaaga agagg	Primer for end-tailoring of <i>Xho</i> I site to BTV-10 VP5; antisense
BTV10.7-HIS-StuI-R	GAAGG <u>CCT</u> AGTGGTGGTGGTG GTGGTGcacatagggcgcgcg	Primer for end-tailoring of 6 x His tag and <i>Stu</i> I site to BTV-10 VP7; antisense
BTV10.NS1-AgeI-F	TTAC <u>CGG</u> Tatggagcgcttttgag aaaatacaatatcagtg	Primer for end-tailoring of <i>Age</i> I site to BTV-10 NS1; sense
BTV10.NS1-XhoI-R	TT <u>CTCGAG</u> ctaatactccatccacat ctgag	Primer for end-tailoring of <i>Xho</i> I site to BTV-10 NS1; antisense

^a END-TAILORING is shown in uppercase, restriction enzyme recognition sites are underlined, **mutations** are underlined and bold.

5.2.2 EXTRACTION BUFFERS

The extraction buffers used for the work presented in this chapter are detailed in Table 5.2.

Table 5.2: Buffers used for extraction of BTV-10 proteins and particles.

Name	Recipe
Extraction buffer (ExB)	50 mM Tris-HCl, pH 7.25; 150 mM NaCl; 2 mM EDTA; 0.1% (w/v) Triton X-100; 1 mM DTT; Complete Protease Inhibitor Cocktail (Roche, add fresh)
BTV extraction buffer (BTV ExB)	20 mM Tris-HCl, pH 8.4; 140 mM NaCl; 1 mM EDTA; 0.1% (w/v) sodium deoxycholate; Complete Protease Inhibitor Cocktail (Roche, add fresh)
Smith Stabilization buffer (SSB)	50 mM Bicine, pH 8.4; 140 mM NaCl, 0.5 % (v/v) NP-40; 10 % glycerol; 1 mM DTT (add fresh); Complete Protease Inhibitor Cocktail (Roche, add fresh)

5.3 RESULTS

5.3.1 EXPRESSION AND INTERACTION OF VP3 AND VP7

To date, Bluetongue virus proteins have not been expressed in plants. However, it has been shown that structural proteins VP2 and VP6 of the closely related rotavirus assemble into core-like particles when co-expressed in tomato (Saldaña et al., 2006). In order to determine whether BTV structural proteins could be expressed in *N. benthamiana* using the CPMV-*HT* system, genes for the structural proteins of BTV serotype 10 were obtained from Prof. Polly Roy and cloned into pENTR-ET2 for easy subcloning by Gateway recombination into pDEST-BINPLUS (Chapter 3).

Agrobacterium suspensions containing the constructs pDEST-BD-BTV10.3 and pDEST-BD-BTV10.7, encoding VP3 and VP7 (Figure 5.3 A), were infiltrated (individually or in combination) into leaf tissue which was harvested 5 dpi (Figure 5.3 A). Samples were extracted using regular extraction buffer (ExB; as used previously for HBcAg) and clarified extracts separated by SDS-PAGE and subjected to Western blotting using a polyclonal

antibody raised against baculovirus-produced BTV 10 cores which should detect both VP3 and VP7 (a kind gift from Prof. Polly Roy). A signal was observed on film only after 20 minutes of exposure (Figure 5.3 B). Tissue expressing VP3, with and without VP7, produced a signal deemed to correspond to VP3 (103 kDa). Tissue expressing VP7 alone produced a signal at approximately 38 kDa, which is likely VP7. This VP7 band was not as pronounced in the co-infiltrated tissue. Negative control extract did not produce co-migrating bands, giving further indication that the observed signal was specific.

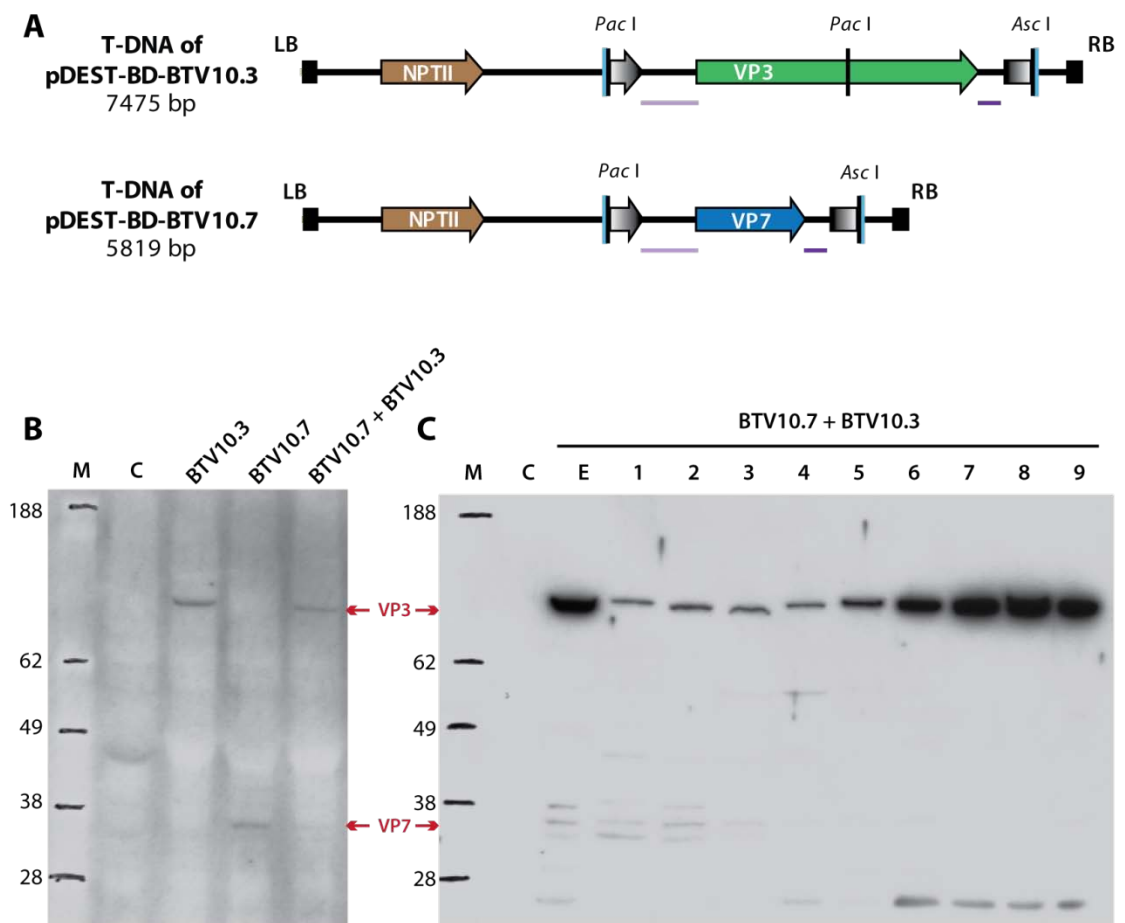


Figure 5.3: Expression and co-expression of core proteins VP3 and VP7.

(A) Schematic representation of the T-DNA regions of plasmids for expression of BTV-10 VP3 and VP7. (B-C) Leaves were (co-)infiltrated with constructs as indicated, harvested 5 dpi and frozen for storage. Samples were extracted using 3 volumes of ExB. (B) Western blot detection of VP3 and VP7 in clarified extracts using anti-BTV-10 core polyclonal antibody (received from Prof. Polly Roy). (C) Anti-BTV-10 core Western blot analysis of sucrose cushion fractions. Clarified extract was spun through a two-step 70%-35% sucrose cushion and fractions collected from top (1) to bottom (9). M = SeeBlue protein marker; C = empty vector control; E = clarified extract; bars under constructs indicate 5'- and 3'-UTRs.

To determine whether VP3 and VP7 could assemble into larger structures, leaf tissue was co-infiltrated with VP3 and VP7 constructs. Co-infiltration is a method often used for the co-expression of multiple proteins in leaf tissue, and is reasonably effective at high *Agrobacterium* titres (Chapter 3). Leaf tissue was first extracted and clarified, then loaded onto a sucrose cushion. After ultracentrifugation, fractions were obtained from the top of the gradient and analysed by SDS-PAGE and Western blotting (Figure 5.3 C). A strong signal for VP3 was detected in the clarified extract as well as all sucrose fractions. The signal was most intense, however, in fractions 6-9, indicating that most of the VP3 had assembled into particles or aggregated and thus sedimented further down the gradient. A clear signal for VP7 was not present in any fractions. However, three faint bands at 30 – 38 kDa were present in the extract and fractions 1-2, and may correspond to unassembled VP7 and breakdown products thereof. Another prominent band at 25 kDa was present in fractions 6-9 showing co-migration with VP3. This band is not seen in the negative control extract, indicating that it is BTV-specific. However, it cannot be said whether this is a breakdown product of VP7 or VP3. It is important to note that the antibody, which had been subjected to ambient temperature during shipping, was showing signs of fungal growth at the time that this blot was produced.

5.3.2 CLP ASSEMBLY IS NOT INHIBITED BY AFFINITY TAGGING OF VP3

To aid detection of VP3 and VP7 expression, and to determine the effect of C-terminal extensions on the assembly potential of the two proteins, a histidine affinity tag was genetically fused to the C-terminus of these proteins, by amplification of the genes with BTV10.3-HIS-StuI-R (for VP3) and BTV10.7-HIS-StuI-R (for VP7) end-tailoring primers (Table 5.1). Combinations of untagged and His-tagged VP3 and VP7 were co-expressed and extracts separated on discontinuous 10 - 60 % sucrose gradients (Figure 5.4). Gradient fractions were run on duplicate SDS-PAGE and Western blots probed with anti-BTV-10 core and anti-His antibody, respectively.

After co-expression, untagged VP3 and VP7 were detected in fractions 6 and 7 at the bottom of the gradient, using anti-BTV-10 core antibody. The intensity of the VP3 signal was higher than the VP7 signal, indicating that either there was less VP7 than VP3 in these fractions, or that the polyclonal anti-BTV-10 core antibody had a higher affinity for VP3 than for VP7. While VP3 was found exclusively in the high density fractions, VP7 was also

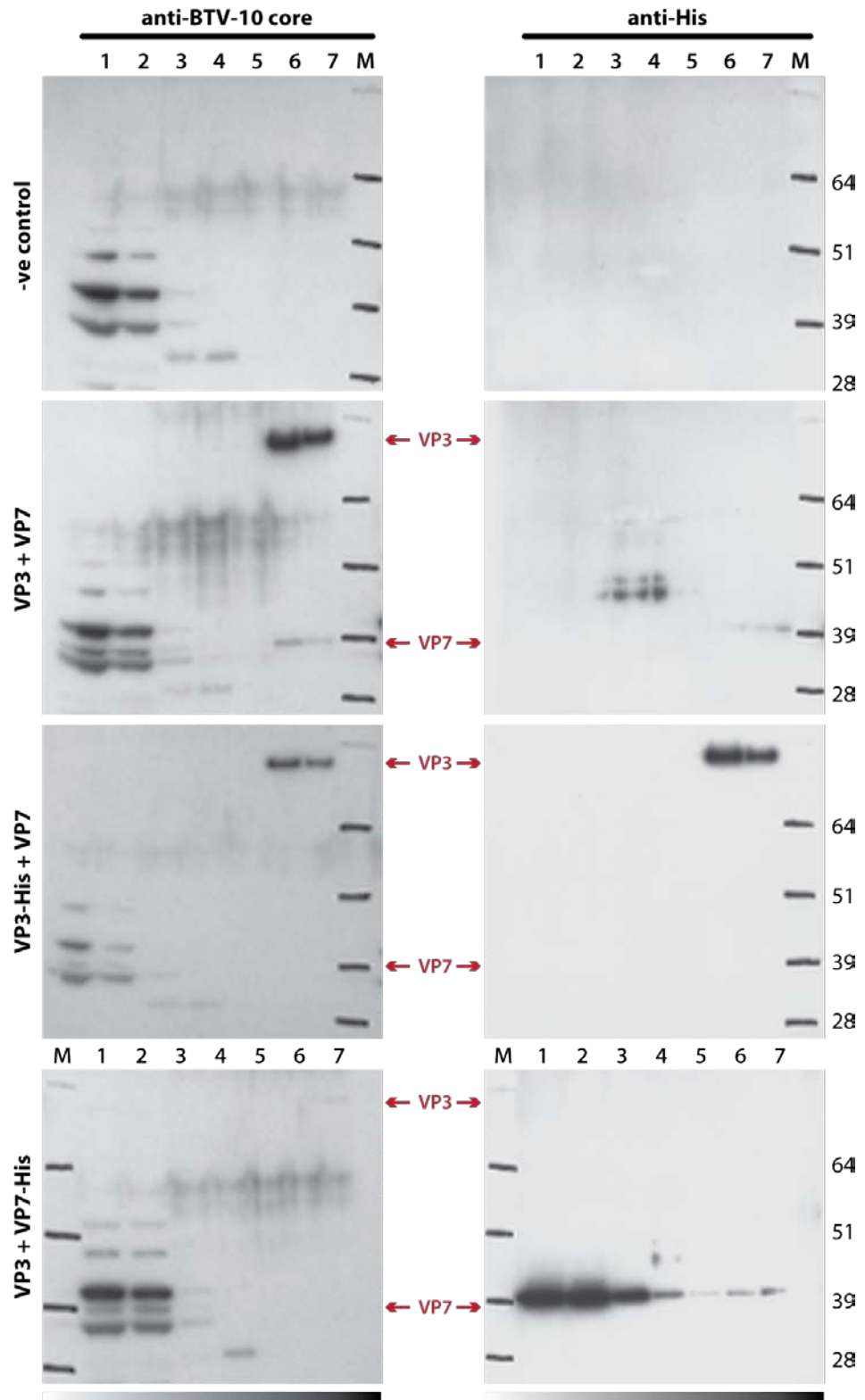


Figure 5.4: Assembly potential of C-terminally His-tagged core proteins.

Leaves were infiltrated with combinations of untagged and His-tagged VP3 and VP7 constructs as indicated. Clarified extracts were separated on 10% - 60% discontinuous sucrose gradients and fractionated from the top. Fractions were run on SDS-PAGE in duplicate and Western blots probed with anti-BTV-10 core polyclonal antibody (left) or anti-His monoclonal antibody (right). M = SeeBlue +2 protein marker with molecular weights indicated.

detected in fractions 1 – 3, indicated by a band which was not present in the negative control. This suggests that all of VP3 was bound in a larger structure, while some VP7 was unbound. The anti-His antibody did not pick up the untagged proteins, as expected.

Co-expression of C-terminally His-tagged VP3 with untagged VP7 also resulted in VP3-His sedimenting in fractions 6 and 7. This indicates that its ability to form particles/aggregates was not inhibited by the His tag. VP3-His was also detected by the anti-His antibody, as expected. A faint signal for free VP7 was detected in fractions 1 and 2. However, the absence of a signal in fractions 6 and 7 may be due to the lower affinity of the antibody for VP7.

Co-expression of C-terminally His-tagged VP7 with untagged VP3 appears to inhibit the formation of larger structures. VP7-His is detected by both antibodies in fractions 1 – 3. The sensitivity of the anti-His antibody is far higher, producing a strong signal in fractions 1 – 3 and some signal in the rest of the gradient. This may be due to a small proportion of VP7-His aggregation/assembly, or it may be due to inaccuracies in fractionation. Interestingly, VP3 is not detected by anti-BTV-10 core antibody. Co-expression of both His-tagged proteins produced only a small signal for VP7-His in fractions 1 and 2 in the anti-His Western blot (data not shown).

5.3.3 THE TIMECOURSE OF ACCUMULATION OF VP5, VP2 AND NS1 VARIES

Full BTV virus-like particles contain an outer layer consisting of VP5 (59 kDa) and VP2 (111 kDa), which must be co-expressed with VP3 and VP7 to achieve assembly. In order to test whether VP5 and VP2 are expressed using the CPMV-*HT* system, it was necessary to produce His-tagged versions due to a lack of a specific antibody. This was done by amplification of constructs (obtained from Prof. Polly Roy) with end-tailoring primers (Table 5.1) to allow cloning into pEAQ-*HT* using *AgeI-XhoI* restriction fragments (Figure 5.5 A). The initial expression test, in which leaves were infiltrated with individual constructs followed by harvesting 6 dpi, resulted in detectable levels of VP5-His, but not VP2-His (data not shown). To determine whether this finding was specific to harvesting after six days, a time course experiment was performed. Infiltrated leaves were harvested 2, 4, 6 and 9 dpi, and frozen for later analysis. Crude extracts were separated on SDS-PAGE and an anti-His Western blot was performed (Figure 5.5 C). A strong signal was observed

for VP5-His at the expected size of 59 kDa. Surprisingly, VP5-His was already detectable two days post infiltration, and levels increased until at least 9 dpi. Multimers of >100 kDa were observed, resulting in a smear near the top of the blot. In contrast, VP2-His was only detectable at 9 dpi, confirming previous findings that it is not found in significant quantities in leaf tissue harvested 6 dpi. This could be due to slower transcription and/or translation, lower stability, faster degradation, or a combination of these factors. This result shows that optimal expression of BTV proteins and particles requires later harvesting than expression of HBcAg (Chapter 4).

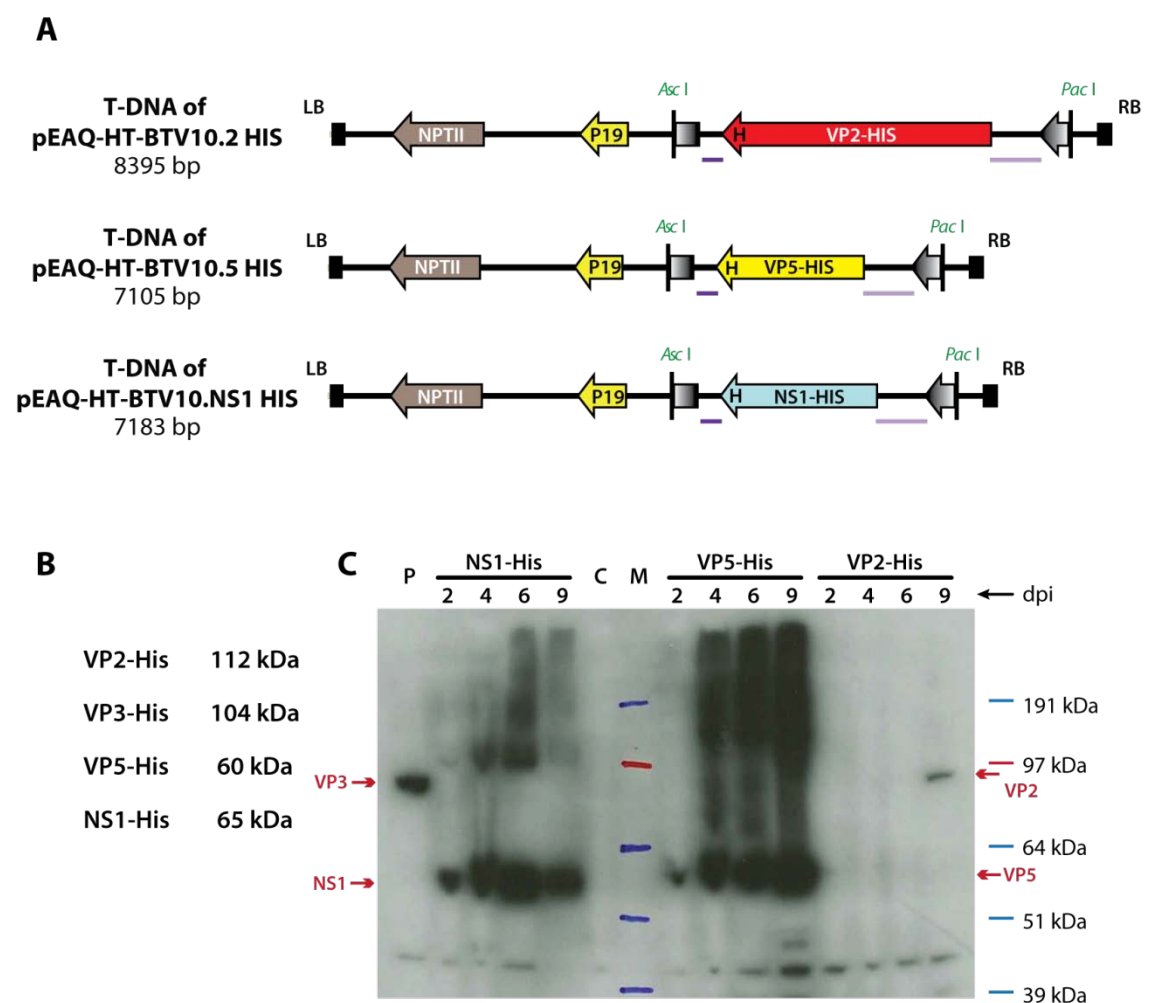


Figure 5.5: Accumulation of BTV-10 structural and non-structural proteins is time-dependent.

(A) Schematic representation of the T-DNA regions of plasmids for expression of BTV-10 VP2-His, VP5-His and NS1-His. (B) Expected sizes of His-tagged BTV-10 proteins. (C) Anti-His Western blot of crude extracts separated on SDS-PAGE. Leaves were infiltrated with the above constructs separately and harvested 2, 4, 6 and 9 days post infiltration. C = empty vector control; M = SeeBlue +2 protein marker; P = positive control BTV-10 VP3-His.

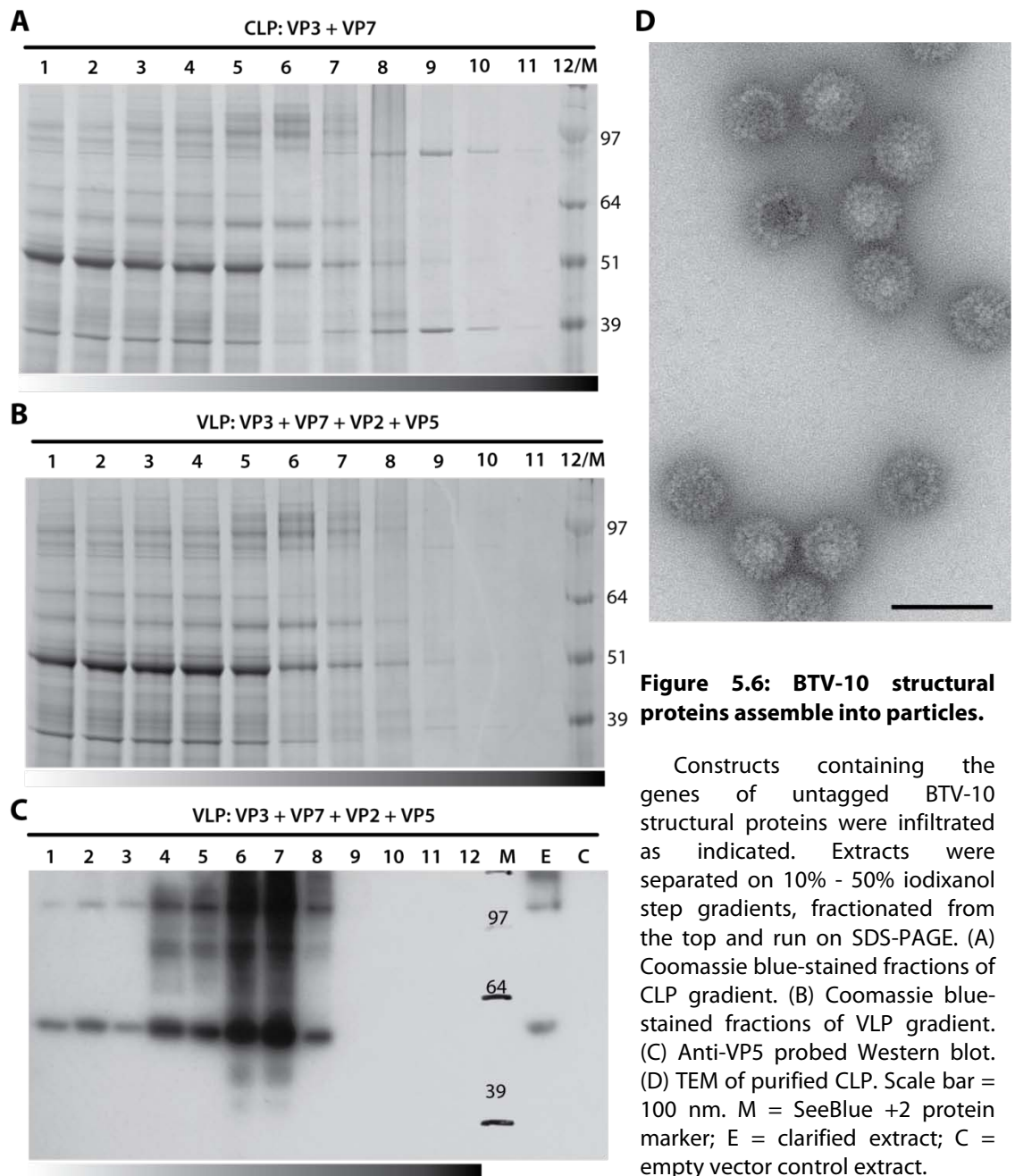
The BTV non-structural protein NS1 forms tubules in infected cells and has been shown to be amenable to epitope presentation and use in medical applications (Mikhailov et al., 1996). To test whether NS1 can be expressed in plants, a C-terminally His-tagged version was expressed in the previously described time course experiment (Figure 5.5). It is noteworthy that leaf tissue became necrotic after six days, and was dry and brittle by day nine. However, NS1-His was detectable as early as 2 dpi and throughout the time course (Figure 5.5 C). In earlier expression trials, immunodetection was performed on clarified extracts (in BTV extraction buffer) and yielded no detectable NS1-His (data not shown), suggesting that all of the antigen was lost during clarification. This may be due to assembly of NS1-His into long tubules which remain entangled in the cell debris, or it could be due to aggregation, or a combination of the two. Alteration of the extraction conditions and especially the extraction buffer may make it possible to extract soluble NS1, however this work was not undertaken due to time constraints.

5.3.4 CO-EXPRESSION OF THE FOUR STRUCTURAL PROTEINS OF BTV-10

Assembly of BTV structural proteins into regular core-like and virus-like particles is crucial for their potential use as a vaccine. Co-sedimentation of VP3 and VP7 in sucrose gradients, as shown previously (Figure 5.3), provided an indication that core-like particles can assemble in plants. However, to provide conclusive evidence of particle formation, visualisation using TEM was required. In order to produce enough material for TEM analysis, and to allow all four (untagged) BTV proteins to be expressed, plants were subsequently harvested at a later time point, 9 dpi. Production was also scaled up by loading more extract (in SSB buffer, an extraction buffer developed to stabilize BTV particles; see Table 5.2) onto larger gradients. This provided enough material for visualisation using Coomassie blue-staining (Figure 5.6 A-B).

Co-expression of VP3 and VP7 resulted in bands of the expected mobility in fractions 7-11 of the gradient, with most accumulating in fraction 9, corresponding to the 30 – 40% iodixanol interface (Figure 5.6 A). Iodixanol (Optiprep™, Axis-Shield) is a density gradient medium which was recommended to me by collaborators, who had found it to be superior to sucrose for use in VLP preparation. In this experiment, most of the plant protein was restricted to the upper eight fractions of the gradient, away from the BTV proteins, showing that the BTV core proteins can be readily purified by density gradient

centrifugation. TEM analysis of such fractions revealed particles of regular shape and size (Figure 5.6 D). These plant-produced BTV-10 core-like particles had a diameter of approximately 70 nm and a spiky appearance, characteristic of authentic BTV core particles and baculovirus-produced CLPs (French and Roy, 1990).



Co-expression of all four structural proteins and P19 by co-infiltration of five different *Agrobacterium* constructs did not give evidence of full VLP formation (Figure 5.6 B). Although VP3 and VP7 were detectable in fraction 9 as before, bands corresponding to the expected sizes of VP2 and VP5 were not visible. Without access to anti-VP2 antibody, it was impossible to determine whether VP2 was present in the sample. VP5 expression could be detected by Western blotting. As before, a strong signal for monomeric VP5 was detected at 59 kDa, and multimers were detected at higher molecular weight. The presence of multimers is a good indication that VP5 is able to form homotrimers, the functional units which assemble around the BTV core. Surprisingly, VP5 did not co-sediment with the majority of VP3 and VP7, and was entirely absent in fractions 9-12. Most VP5 was detected in fractions 5 – 6, corresponding to 20 – 30 % iodixanol. This suggests that VP5 was associated with particles or aggregates, allowing it to sediment in the gradient. A slower sedimentation rate does not preclude its association with CLPs, as it has been shown that authentic BTV particles have a lower buoyant density (1.36 g/cm³) in caesium chloride than core particles (1.38 g/cm³; Martin and Zweerink, 1972).

Interestingly, the expression levels of VP3 and VP7 were far lower when co-expressed with VP5 and VP2 than when expressed independently of the outer shell proteins. Since the optical density of each *Agrobacterium* was the same in both infiltrations, this should not be due to dilution factor, but could be an effect of multiple competing *Agrobacteria*. Another explanation for this may be that the SSB extraction buffer is unsuitable for the extraction of soluble VLPs, but amenable to CLP extraction. It is likely that an extract will contain VLPs, CLPs, SCLPs and intermediates. In that case, fully assembled VLPs would be lost during the clarification spin, along with most of the VP5 and VP2 protein, leaving only CLPs and some intermediate structures to be separated on the density gradient. However, all subsequent attempts with different extraction buffers failed to yield detectable levels of fully assembled BTV-10 VLPs (data not shown), indicating that the production of these particles may not be possible with the production system. In order to investigate these possibilities further, it would be crucial to obtain anti-BTV-10 VP2 antibody, and to increase expression levels by codon-optimisation, for example (Chapter 6).

The results show that it is possible to express BTV-10 structural proteins VP2, VP3, VP5 and VP7, as well as non-structural protein NS1 in plants. Furthermore, VP3 and VP7 co-expressed in plants assemble into core-like particle structures resembling CLPs and core particles produced in other systems. However, the evidence of VP5 association with CLP structures is not conclusive.

5.4 DISCUSSION

Virus-like particles of BTV-10 have been shown to assemble through co-expression of the four main BTV structural proteins in insect cells, and their efficacy as a vaccine has been validated by several groups (French and Roy, 1990; Roy et al., 1994; Roy et al., 1992; Stewart et al., 2010). Nevertheless, a VLP-based commercial vaccine has not been developed, owing to the high cost associated with the baculovirus expression system. In this chapter I have shown that it is possible to express BTV-10 structural proteins in plants, and that some of these assemble into particles. This opens the door to the exploitation of plants as a potentially cheaper production system for the production of an inherently safe Bluetongue vaccine.

Expression was attempted using structural proteins of BTV serotype 10, isolated in the USA (Sugiyama et al., 1982). The core proteins VP3 and VP7 of BTV-10 were successfully expressed using the CPMV-*HT* system. They assembled into core-like particles resembling authentic, virus-derived cores as well as CLPs produced in insect cells (French et al., 1990).

For the production of an effective vaccine, it is essential to produce VLPs which present a full complement of VP5 and VP2 on the outside. Expression of these two proteins individually revealed that their expression and accumulation vary widely, with VP5 detectable after two days, and VP2 detectable after nine days. This presents a problem for the production of full VLP, and was the reason to delay harvesting until 9 dpi in all subsequent experiments.

Though it was not possible to conclusively show the assembly of VP5 and VP2 on these CLPs, the use of an anti-VP5 antibody showed that VP5 forms multimers and sediments within a sucrose gradient, indicating that it may be associated with CLPs. Assuming that the recovery of particles decorated with VP5 is dependent on the simultaneous assembly of VP2, as previously reported (French et al., 1990), the presence of VP5 in high density gradient fractions implies that BTV-10 VP2 also assembles on CLPs when co-expressed in plants. Proof of this could be provided by immunogold labelling of expressed particles with antibodies raised against VP2, but these were not available.

In addition to being efficient vaccines in their own right, some virus-like particles, such as Hepatitis B cores (Chapter 4), can also be used as carriers for the display of foreign epitopes. BTV proteins also have the potential to be used in this manner. Epitope fusions

to BTV VP3 are also possible and C-terminal extensions have been shown to allow core-like particles to assemble when co-expressed with VP7 in insect cells (Tanaka et al., 1995). Efforts to express C-terminal His-tag fusions of VP3 in plants have also resulted in assembled particles which co-migrate with VP7 in density gradients. In contrast, His-tagging of VP7 inhibited particle formation. Interestingly, it has been found that the insertion of a 13 amino acid epitope of Bovine Leukemia Virus (BLV) at the C-terminus of VP3 has resulted in insect cell-produced CLPs which were shown to raise antibodies against BLV (Tanaka et al., 1995). This shows that presentation of an epitope on the inside layer of BTV, likely within the empty cavity of the particle, provides a means of using BTV as an epitope carrier. In fact, the large lumen of the BTV-like particle is able to accommodate 120 copies of GFP, N-terminal VP3 fusions of which have allowed core-like particles to assemble within VP7-expressing insect cells (Kar et al., 2005). Attempts to produce such fluorescent particles in plants are discussed in Chapter 7.

Another BTV protein which has been used for epitope display is non-structural protein NS1, which forms long tubules in infected cells and is thought to function in assembly of the virus (Owens et al., 2004). It has been possible to express NS1 fusion proteins displaying large foreign epitopes and even whole proteins, using the baculovirus system (Ghosh et al., 2002b; Mikhailov et al., 1996). Furthermore, it was shown that these fusion proteins form tubule structures and can be used as immunogens (Ghosh et al., 2002a). Preliminary expression trials with BTV-10 NS1 show that this protein can be efficiently expressed in *N. benthamiana* using CPMV-*HT* constructs, with detectable levels accumulating within two days post infiltration (Figure 5.5). NS1 was found to be entirely insoluble; however this might be alleviated through optimisation of the extraction conditions and buffer. In the future, further experiments could be performed to test whether expression of NS1 fusion proteins is possible in plant tissue.

The results presented in this chapter provide evidence that BTV-10 proteins can be expressed in plants using the CPMV-*HT* system, and that they can assemble into particle structures. However, proof of the assembly of full VLPs consisting of all four structural proteins eluded me. This motivated me to attempt the expression of another, more pertinent BTV serotype, BTV-8 (Chapter 6).

6 EXPRESSION OF BTV-8 VIRUS-LIKE PARTICLES

6.1 INTRODUCTION

The successful expression and assembly of the structural proteins of BTV serotype 10 provided a good indication that the CPMV-*HT* transient plant-based expression system could be used to produce BTV particles. However, attempts to produce full BTV-10 VLPs failed to give conclusive evidence of the assembly of the outer shell proteins VP5 and VP2 onto the core-like particle. This led me to investigate the expression and assembly of another serotype, BTV-8, to determine whether this inability to produce full BTV VLP was general. Being the first BTV serotype to break out in the United Kingdom in 2007, BTV-8 was also highly pertinent at the time.

BTV serotype 8 was first detected in the Netherlands in August 2006 and quickly spread to surrounding Central Europe with 2000 farms being affected by January of the following year. The vector *Culicoides obsoletus* was shown to survive the winter, and BTV-8 spread widely within continental Europe in 2007, affecting tens of thousands of farms (Mehlhorn et al., 2007; Szmaragd et al., 2010). The first case of BTV in the UK was detected in Suffolk at the end of September, 2007. Due to the cold autumn temperatures, spread was minimal and restricted to 125 farms by early 2008. During the winter, a swift response by government and scientists, as well as the recent availability of a vaccine made it possible to commence a vaccination programme in May 2008 (Szmaragd et al., 2010). While BTV-8 continued to spread in continental Europe in 2008, no cases were reported in the United Kingdom. The 2006-2008 outbreak in Europe demonstrated the effectiveness and importance of fast and comprehensive vaccination against BTV.

6.1.1 AIMS OF THIS CHAPTER

The aim of this chapter is to demonstrate the expression of BTV-8 structural proteins in plants, and their assembly into subcore-like, core-like and virus-like particles. In an effort to maximize the yield of these proteins, codon-optimized versions of the wild-type genes

were also expressed. The pEAQ vectors (Chapter 3) were used as an essential tool in the expression of BTV-8 proteins, ensuring that multiple proteins could be consistently co-expressed in the same plant cells. Furthermore, selective use of wild-type and *HyperTrans* CPMV RNA-2 leaders was used to modulate relative expression levels of the four BTV proteins to maximize recovery of fully assembled VLPs. A purification protocol for recovery of high quality VLP preparations was developed to enable sufficient material to be produced for immunological analysis.

6.2 SPECIFIC MATERIALS AND METHODS

6.2.1 CLONING

Wild-type genes for BTV-8 VP2, VP3, VP5, VP7 and NS3 were amplified from BTV-8 cDNA (BTV-8 strain NET2008, sequences published in GenBank) provided by Dr. Ann Meyers (University of Cape Town). Genes were amplified from their source using the primers listed in Table 6.1 and inserted between the RNA-2 5'- and 3'-UTR sequences of pEAQ-*HT* using restriction cloning. The gene for NS3 was amplified to end-tailor Gateway *attB* sites for cloning into pDONR207 and subcloning into pEAQ-*HT*-DEST-1 (Gateway cloning is described in Chapters 2 and 3).

Codon-optimized versions of the BTV-8 genes for expression in *N. benthamiana* were synthesized by GeneArt AG (see Appendix B). These genes were excised and cloned into pEAQ-*HT* using restriction cloning. Expression cassettes were excised from the pEAQ-*HT* clones and subcloned into the vector pEAQexpress (Chapter 3) to yield pEAQex-BTV8.5co-BTV8.2co, pEAQex-BTV8.7co-BTV8.3co and pEAQex-BTV8.7-BTV8.3. These were combined to form pEAQex-BTV8-52co73 for expression of four structural proteins and P19 from a single T-DNA, as described in section 6.3.5.2.

A further clone was prepared by replacing the 5'UTR of the BTV8.3 cassette of pEAQex-BTV8.7co-BTV8.3co with the wild-type CPMV RNA-2 5'UTR, thereby producing pEAQex-BTV8co-7HT-3, as described in section 6.3.5.3. A table of constructs is provided in Appendix A.

Table 6.1: Oligonucleotides used in cloning of BTV-8 constructs.

Name	Sequence ^a	Function
BTV8-NS3-attB1	AAAAAGCAGGCTatgctatccgg gctgac	Primer for end-tailoring of partial <i>attB1</i> site to 5'-end of BTV-8 NS3; sense
BTV8-NS3-attB2	AGAAAGCTGGGTcaggttaatg gcatttcg	Primer for end-tailoring of partial <i>attB2</i> site to 3'-end of BTV-8 NS3; antisense
BTV8-VP7-F	CGatggacactatcgctgcaagag	Primer for amplification of BTV-8 VP7; sense
BTV8-VP7-R	Cctacacatagggcgcg	Primer for amplification of BTV-8 VP7; antisense
BTV8.2-Sall-R	TATCGT <u>CGA</u> ctatacattgagcagc ttagttaacac	Primer for end-tailoring of <i>Sall</i> site to BTV-8 VP2; antisense
BTV8.2-XmaI-F	TAT <u>CCCGG</u> Gatggaggagctagc gattc	Primer for end-tailoring of <i>XmaI</i> site to BTV-8 VP2; sense
BTV8.3-StuI-R	TAC <u>AGG</u> Cctacacagtggcgagc	Primer for end-tailoring of <i>StuI</i> site to BTV-8 VP3; antisense
BTV8.3-XmaI-F	TAT <u>CCCGG</u> Gatggctgctcagaat gagc	Primer for end-tailoring of <i>XmaI</i> site to BTV-8 VP3; sense
BTV8.5-Sall-R	TATCGT <u>CGA</u> Ctcaggcatttcttaa gaagagtgggatac	Primer for end-tailoring of <i>Sall</i> site to BTV-8 VP5; antisense
BTV8.5-XmaI-F	TAT <u>CCCGG</u> Gatggggaaaatcata aagtcctaag	Primer for end-tailoring of <i>XmaI</i> site to BTV-8 VP5; sense

^a END-TAILORING is shown in uppercase, restriction enzyme recognition sites are underlined, mutations are underlined and bold.

6.2.2 BTV EXTRACTION AND PURIFICATION

6.2.2.1 Extraction buffers

The extraction buffers used for the work presented in this chapter are detailed in Table 6.2.

Table 6.2: Buffers used purification of BTV-8 particles.

Name	Recipe
BTV extraction buffer (BTV ExB)	20 mM Tris-HCl , pH 8.4; 140 mM NaCl; 1 mM EDTA; 0.1% (w/v) sodium deoxycholate; Complete Protease Inhibitor Cocktail (Roche, add fresh)
Smith Stabilization buffer (SSB)	50 mM Bicine, pH 8.4; 140 mM NaCl, 0.5 % (v/v) NP-40; 10 % glycerol; 1 mM DTT (add fresh); Complete Protease Inhibitor Cocktail (Roche, add fresh)
Low-salt SSB	50 mM Bicine, pH 8.4; 20 mM NaCl, 0.5 % (v/v) NP-40; 10 % glycerol; 1 mM DTT (add fresh); Complete Protease Inhibitor Cocktail (Roche, add fresh)
BTV VLP extraction buffer	50 mM Bicine, pH 8.4; 20 mM NaCl, 0.1 % (w/v) NLS sodium salt; 1 mM DTT (add fresh); Complete Protease Inhibitor Cocktail (Roche, add fresh)
BTV CLP extraction buffer	50 mM Bicine, pH 8.4; 140 mM NaCl, 0.1 % (w/v) NLS sodium salt; 1 mM DTT (add fresh); Complete Protease Inhibitor Cocktail (Roche, add fresh)

6.2.2.2 Core-like particles

The purification protocols for core-like particles were optimised throughout the project. Optimal results deemed to produce sufficient material for animal trials were obtained from leaves infiltrated with pEAQex-BTV8co-7HT-3 using the following protocol.

Leaf tissue expressing BTV-8 VP3 and BTV-8 VP7 was harvested 9 dpi and fresh tissue homogenized in three volumes of BTV CLP extraction buffer using a Waring blender at 4°C. Note that tissue was never frozen. Homogenate was filtered through two layers of Miracloth and clarified by centrifugation at 4 200 x g, 10 °C, for 5 minutes. Clarified extract was layered onto sucrose four-step gradients of 30 – 60 % sucrose in 20 mM Tris-HCl, 140 mM NaCl, pH 8.4. Gradients consisted of 3 ml of each sucrose solution, overlaid with 24 ml of clarified extract. Gradients were spun in an ultracentrifuge at 21.5 K rpm, 10 °C, for 3

hours using a Surespin 630 rotor. Nine fractions of 1 ml were collected by piercing the bottom of the tube. Fractions were analysed by separating 1/100th of each sample on 4-12 % NuPage SDS-PAGE gels followed by Coomassie blue staining. The best fractions (in terms of BTV protein content, stoichiometry and lack of contamination; usually fractions 2-3) were incrementally diluted to a final factor of 1:2 with 140 mM Tris-HCl, 140 mM NaCl, pH 8.4 and separated on a second sucrose gradient as before, this time using 1 ml sucrose steps in an SW41-Ti rotor. Gradients were fractionated from the bottom and fractions analysed for purity by SDS-PAGE, as before. Particles were stored at 4 °C.

6.2.2.3 *Virus-like particles*

The procedure described for CLP preparation was also followed for the purification of virus-like particles, after co-infiltration with pEAQex-BTV8co-7HT-3 and pEAQex-BTV8.5co-BTV8.2co. BTV VLP extraction buffer was used, and all sucrose solutions and dilution buffers contained a lower salt concentration of 20 mM NaCl.

6.3 RESULTS

6.3.1 STRUCTURAL PROTEIN EXPRESSION FROM WILD-TYPE AND CODON-OPTIMISED GENES

Following the demonstration that it is possible to produce BTV-10 CLPs (though not VLPs) in plants using the CPMV-*HT* system, attention turned to the expression of a more relevant serotype, BTV-8, which was rapidly spreading throughout Europe from 2006.

BTV serotypes share a high degree of sequence similarity in their core proteins, but differ markedly in the primary structure of their outer shell. Table 6.3 compares the four structural proteins and genes of BTV-8 and BTV-10 at the nucleotide and amino acid level. Sequence conservation is highest for the innermost protein VP3 (90.3 %) and lowest for the outer shell protein VP2 (53%). The differences in the genes of VP3 and VP7, however, are not reflected in the amino acid composition. The core proteins of BTV serotypes 8 and 10 are (nearly) identical. In stark contrast, the outer shell protein VP2, the major immunogenicity determinant of BTV, shares only 40.7 % sequence identity between these two serotypes. This supports the finding that BTV VLP vaccines afford limited protection

across heterologous serotypes (Roy et al., 1994). VP5 is also not well conserved at an amino acid sequence identity of 78.8 % between these serotypes. However, the quaternary structures of these two proteins, globular trimers of VP5 and triskelion trimers of VP2, have not been reported to differ considerably between serotypes. However, only limited structural information is available for the outer shell of BTV.

Table 6.3: Sequence similarity of expressed BTV genes and proteins.

BTV-8	BTV-10		BTV-8 codon optimized	
	Nucleotide	Amino acid	Nucleotide	Amino acid
VP3	90.3 %	99.7 %	76.9 %	100 %
VP7	87.8 %	100 %	77.1 %	100 %
VP5	69.4 %	78.7 %	75.8 %	100 %
VP2	53.0 %	40.7 %	75.6 %	100 %

Sequence identity expressed in % of BTV8 wild-type genes / proteins.

Codon-optimisation is widely used as a means of increasing heterologous protein yield, though it is not always successful (Laguía-Becher et al., 2010; Maclean et al., 2007). In order to test whether codon-optimisation for *N. benthamiana* would have a beneficial effect on expression levels of BTV-8 proteins, optimised version of all four genes were synthesized by GeneArt AG (Appendix B). Though identical to the wild-type proteins at the amino acid level, these genes were only approximately 75 % identical at the nucleotide level (Table 6.3). The wild-type genes were amplified from cDNA of BTV-8 (a kind gift from Dr. Ann Meyers University of Cape Town). Both versions of each gene were cloned into pEAQ-HT using restriction cloning (Section 6.2). Codon-optimised versions are labeled “co.”

To test for efficiency of expression of the BTV-8 genes, all constructs were expressed individually in *N. benthamiana*. Agro-infiltrated tissue was harvested 8 dpi and clarified extract analysed by SDS-PAGE (Figure 6.1). The expression levels achieved for all four structural proteins, regardless of codon usage, were high enough to enable distinct bands to be identified by comparison to a negative control extract. In all cases, codon-optimization for *N. benthamiana* had a positive effect on recombinant protein yield,

though the degree of improvement varied between the four genes. Remarkably high yields of VP2 were achieved using the codon-optimized construct. The difference in expression level between codon-optimized and wild-type versions of VP5 and VP7 was not as marked, but estimated at 3-fold. The codon-optimized VP5 construct also produced to bands of lower electrophoretic mobility, which were identified as BTV-8 VP5 and likely correspond to VP5 multimers (Figure 6.1, asterisks). In the case of VP3, the codon-optimized construct caused necrosis in the leaf tissue which rendered it dry and brittle. Though the state of the tissue made a yield comparison between the two constructs impossible, it is worth noting that the most abundant extractable protein in the necrotic VP3co tissue was VP3, indicating that it is indeed expressed at very high levels. The presence of VP3 in the necrotic tissue also indicated that the protein is very stable.

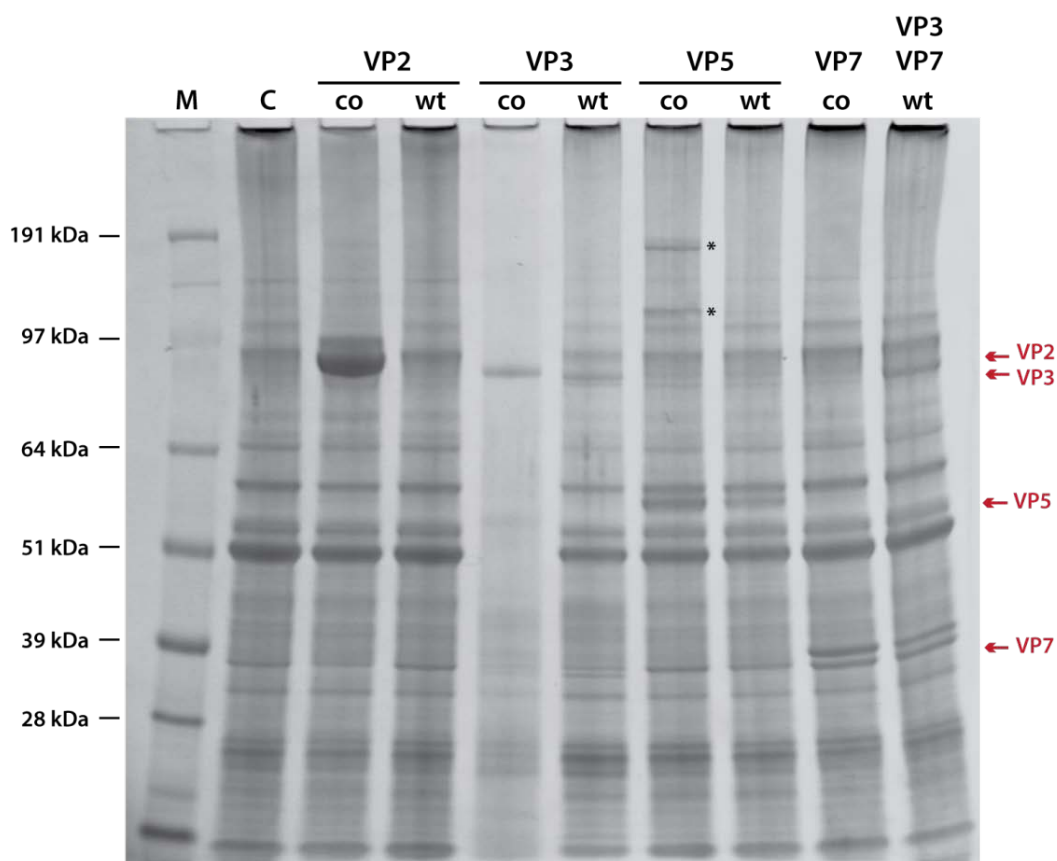


Figure 6.1: Codon optimization increases the expression level of BTV-8 structural proteins by varying amounts.

Leaves were agro-infiltrated with codon-optimized (co) and wild-type (wt) BTV-8 constructs as indicated and harvested 8 dpi. Clarified extracts from three leaf discs were separated 4-12% SDS-PAGE and stained with Coomassie blue. Note that the tissue infiltrated with the VP3co construct was necrotic and dry. Note also that the wild-type VP7 construct used contained wt VP3 on the same T-DNA. * = bands of this mobility later confirmed as VP5. M = SeeBlue +2 marker; C = empty vector control.

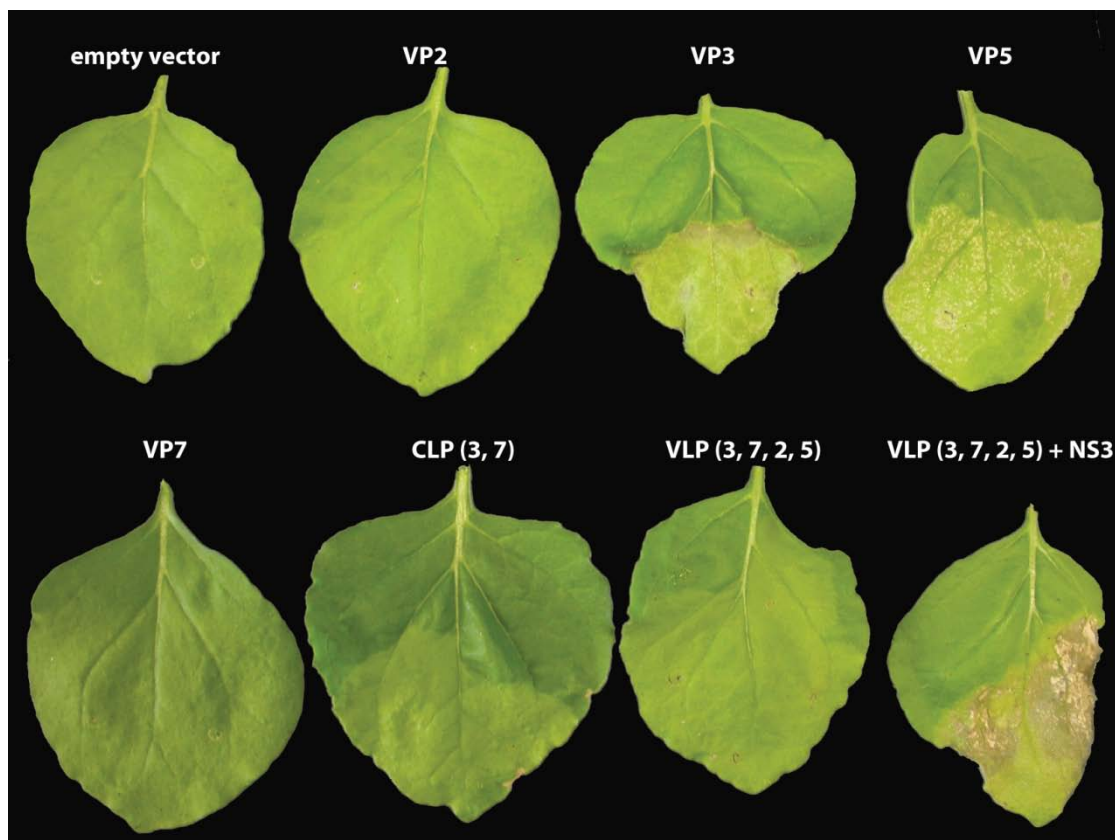


Figure 6.2: BTV-8 proteins are toxic to *N. benthamiana* in some combinations.

Leaves were agro-infiltrated with codon-optimized BTV-8 constructs individually and in combinations as indicated. Leaves were harvested 9 dpi and imaged in bright light. Note: The black background was created digitally using Photoshop to enhance clarity - leaf images were not altered.

Some of the expressed BTV-8 protein constructs, namely VP3, VP5 and NS3, appeared to induce chlorosis and/or necrosis in the expressing tissue. To test this further, codon-optimised constructs were agro-infiltrated individually or co-infiltrated in the combinations needed to produce CLPs and VLPs and observed 9 dpi (Figure 6.2). Expression of VP2 and VP7 alone appeared to have little effect on leaf tissue, similar to the empty vector control. Young tissue expressing VP3 alone appeared to grow more slowly than surrounding healthy tissue, was chlorotic and had large necrotic patches. Necrosis appeared to be worse in older leaves, an effect also seen with other toxic constructs. Expression of VP5 alone made the leaf tissue chlorotic and induced small necrotic lesions.

Leaf tissue expressing VP3 and VP7 was chlorotic, but did not exhibit the necrosis and growth inhibition seen from VP3 alone. Similarly, tissue expressing all four structural proteins was chlorotic but not necrotic. These results suggest that structural proteins which are toxic to the plant on their own (VP3 and VP5) lose their toxicity when expressed in combination with the structural proteins with which they interact. For example, if most VP3 assembles into core-like particles when co-expressed with VP7, it would be surrounded by a VP7 layer and 'hidden' from host machinery which would otherwise mount a response. The effect of co-expression on leaf response suggested that the BTV structural proteins may be interacting in a favourable way.

The non-structural protein NS3 has been shown to localize to the plasma membrane of infected cells and is key to virus-particle egress (Celma and Roy, 2009; Hyatt et al., 1991). Assuming that the interaction of NS3 and the outer shell of assembled particles is sufficient for egress, it is possible that co-expression of NS3 with the four BTV structural proteins may allow BTV VLPs to accumulate in the intercellular space. Heterologous proteins which are secreted can be harvested from the intercellular spaces by re-infiltration with buffer and low-speed centrifugation, thereby circumventing the contamination of preparations with plant cell proteins (Dr. Ann Meyers, personal communication). Such a strategy would facilitate downstream processing. To test whether this is possible, leaves were co-infiltrated with five constructs for NS3 and the four structural proteins. Though NS3 was never detected after extraction, the co-infiltration of this construct had a toxic effect on the leaf tissue, indicating that the gene was expressed (Figure 6.2). Necrosis was observed five days post infiltration, making re-infiltration of the tissue with buffer impossible. Later attempts to infiltrate the NS3 construct 5 days after the other constructs failed to provide proof of the presence of VLP in the intercellular space.

These data show that it is possible to express BTV-8 structural proteins in *N. benthamiana* using the CPMV-*HT* system. Furthermore, the milder effects of co-expression on leaf health indicate that the expressed proteins interact *in vivo*, indicating that the production of BTV-8 CLP and even VLP would be possible.

6.3.2 SELF-ASSEMBLY OF SCLPs BY EXPRESSION OF VP3

Hewat *et al.* (1992) reported that BTV subcore-like particles (Section 5.1.3.1) consisting of only VP3 cannot be obtained by sole expression of VP3 using the baculovirus system, but that they can be made from CLPs by stripping off the VP7 layer in low salt buffer. In the same year, it was reported that SCLPs can be purified from insect cells directly only by co-expression with an N-terminally tagged VP7 which is unable to form a stable shell around the VP3 (Loudon and Roy, 1992).

To determine whether plant-produced VP3 is able to self-assemble without the presence of VP7, tissue was infiltrated with pEAQ-*HT*-BTV8.3co and harvested 9 dpi. As previously found, expressing tissue was largely necrotic, though a band of chlorosis appeared immediately adjacent to the infiltrated area (Figure 6.3 A), suggesting that a mobile plant response was raised. Upon extraction in BTV VLP extraction buffer, clarified extract was separated on sucrose step gradients. Fractions corresponding to 40 - 50% (i.e. where assembled BTV particles are usually found) were separated on SDS-PAGE and stained with Coomassie-blue (Figure 6.3 B). A clear band was visible near the 97 kDa marker at the expected mobility of VP3, suggesting that VP3 had self-assembled or aggregated.

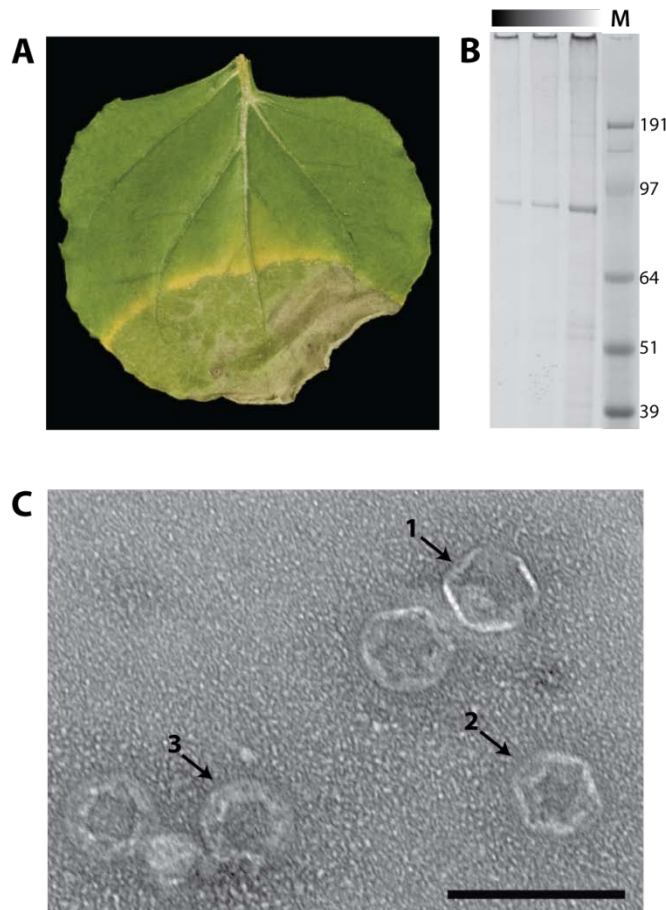


Figure 6.3: BTV-8 VP3 is able to self-assemble when expressed alone.

Leaves were agro-infiltrated with pEAQ-*HT*-BTV8-VP3co and harvested 9 dpi. Clarified extract was run on a discontinuous sucrose gradient and fractionated. (A) Photograph of infiltrated leaf. (B) Coomassie blue-stained SDS-PAGE gel with three sucrose gradient fractions containing VP3. (C) TEM image of purified BTV-8 subcore-like particles. Arrows indicate 3 different orientations of the same particle species. Scale bar = 100 nm.

Transmission electron microscopy of gradient fraction provided proof that BTV-8 VP3 was able to self-assemble when expressed in plants (Figure 6.3 C). Subcore-like particles are clearly visible after negative staining. Depending on their orientation on the TEM grid and the viewing angle, particles have three different appearances: (1) angular particles with 6 very thin sides; (2) less angular particles, with less distinct sides; (3) rounded particles. These observations are in accordance with the published structure of baculovirus-produced SCLPs and correspond to views along the two-, three- and fivefold axis, respectively (Hewat et al., 1992).

These results show that BTV-8 VP3 can self-assemble independent of other BTV proteins when expressed in *N. benthamiana*, in contrast to the situation in insect cells.

6.3.3 ASSEMBLY OF CLPs BY CO-EXPRESSION OF VP3 AND VP7

Previous work had shown that it is possible to express BTV-10 VP3 and VP7 in plants, and that they assemble into CLP structures resembling baculovirus-produced CLPs (Section 5.3.4). In order to determine whether BTV-8 CLPs can also be produced, codon-optimised constructs for VP3 and VP7 were co-infiltrated and harvested 9 dpi. Tissue was extracted in SSB and clarified extracts loaded onto 10 – 45 % iodixanol gradients (Figure 6.4 A). Fractions were collected from the bottom, then separated on SDS-PAGE gels which were stained with Coomassie blue (Figure 6.4 B). As found previously with BTV-10 (Figure 5.6 A), VP3 and VP7 co-sedimented in the gradient. Bands corresponding to the two proteins were found in the range of 15 – 40 % iodixanol, with a peak at 35 %. The majority of contaminating plant protein did not sediment below 25 % iodixanol, thereby leaving the BTV-containing fractions relatively pure. From the staining observed on the gel, yield was estimated to be at least 200 µg / g FWT.

Purified BTV-8 CLPs were visualised by TEM using negative staining (Figure 6.4 C) The particles had the spiky appearance characteristic of BTV cores and resembled the previously produced BTV-10 CLPs (Figure 5.6 D), with a mean diameter of 70 nm. Dynamic light scattering (DLS) analysis of BTV-8 CLPs shows that 95% of the sample has an average diameter of 73.2 nm (data not shown), a figure that is in good accordance with the size estimated by TEM.

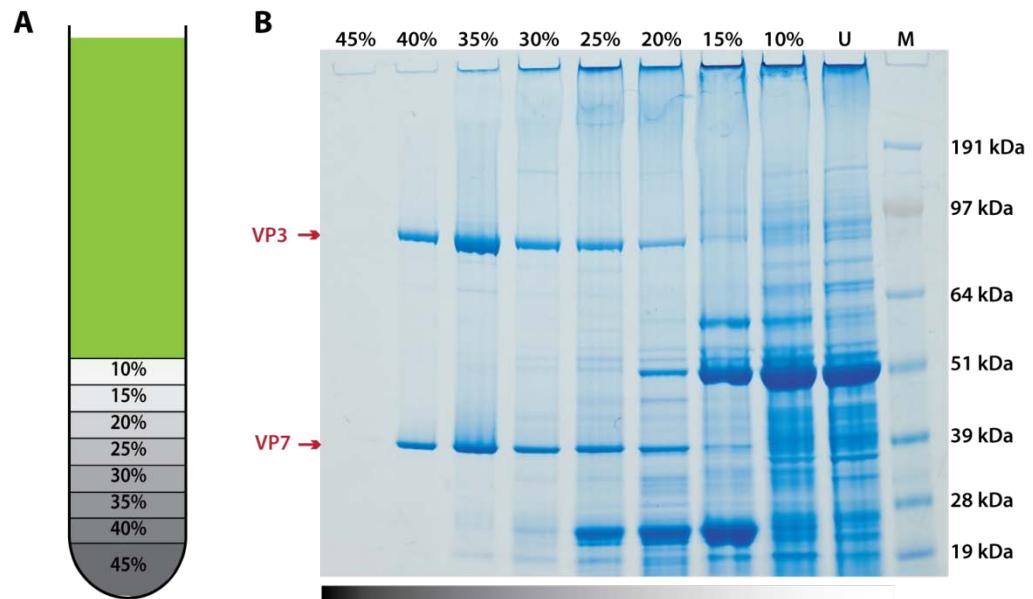


Figure 6.4: Co-expression of BTV-8 VP3 and VP7 enables assembly of core-like particles.

Constructs containing the genes of BTV-8 structural proteins VP3 and VP7 were co-infiltrated and leaves harvested 9 dpi. (A) Extracts were separated on 10% - 45% iodixanol step gradients and fractions collected from the bottom. (B) Coomassie blue-stained 4-12% SDS-PAGE gel of gradient fractions. M = SeeBlue +2 protein marker; U = upper phase (0% iodixanol). (C) TEM of purified BTV-8 CLP. Scale bar = 100 nm.

6.3.4 ASSEMBLY OF VLP BY CO-EXPRESSION OF VP3, VP7, VP5 AND VP2

Previous work on BTV-10 had failed to conclusively show production of full virus-like particles (Section 5.1.3.3) by co-expression of the four main structural proteins (Section 5.3.4). However, co-expression of the four main BTV-8 structural proteins showed a decrease in toxicity associated with VP5 expressed on its own, thereby indicating that VP5 may be able to interact with the other BTV structural proteins *in planta* (Section 6.3.1). To determine whether this interaction occurs and whether full VLPs are produced, the four BTV-8 structural proteins were co-expressed by co-infiltration of four constructs, and subjected to analysis as described in the previous section.

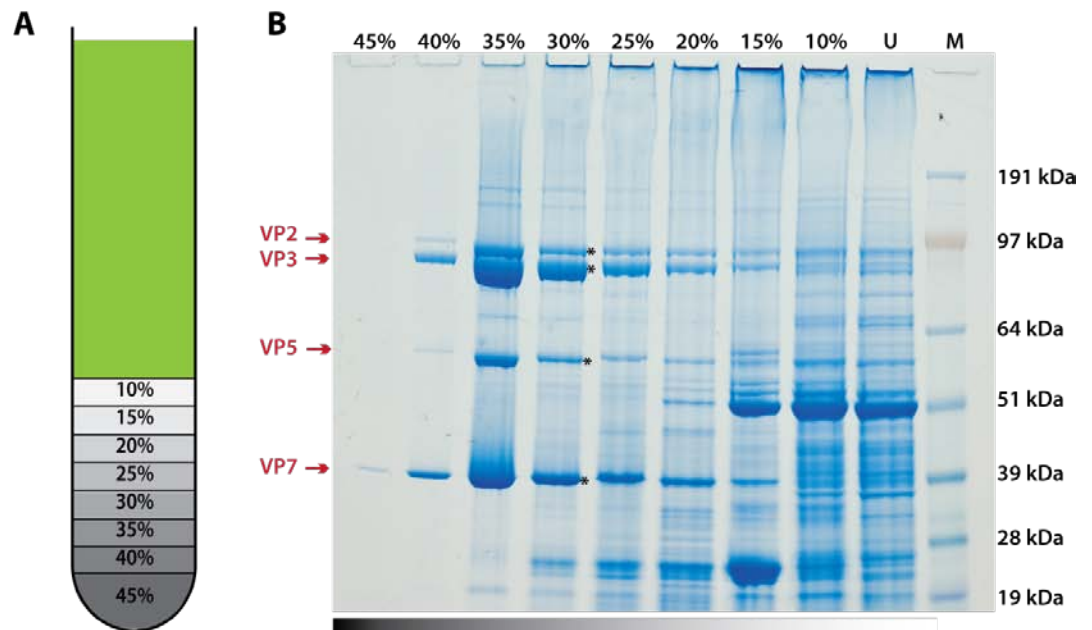


Figure 6.5: Co-expression of four BTV-8 structural proteins enables assembly of virus-like particles.

Constructs containing the genes of BTV-8 structural proteins VP2, VP3, VP5 and VP7 were co-infiltrated and leaves harvested 9 dpi. (A) Extracts were separated on 10% - 45% iodixanol step gradients and fractions collected from the bottom. (B) Coomassie blue-stained 4-12% SDS-PAGE gel of gradient fractions. Protein bands excised for mass spectrometric analysis indicated by asterisk. M = SeeBlue +2 protein marker; U = upper phase (0% iodixanol). (C) TEM of purified BTV-8 VLP. Contaminating CLP indicated by arrow. Scale bar = 100 nm.

Coomassie blue staining of density gradient fractions revealed a high yield and co-sedimentation of the expressed BTV-8 structural proteins (Figure 6.5 B). Bands corresponding in mass to VP2, VP3, VP5 and VP7 were found in the range of 15 – 40 % iodixanol, with a majority found in the 35 % fraction. As with CLPs, this provided a good degree of purity due to lower sedimentation rate of contaminating plant proteins. The clean and well separated bands of the 30% fraction were excised and submitted for mass spectrometric analysis which confirmed the identity of the proteins (see asterisks in Figure 6.5 B). Total BTV protein yield in the gradient fractions was estimated to be approximately 300 ug / g FWT.

Purified particles were observed using TEM. The micrograph in Figure 6.5 C illustrates well the morphology of BTV VLPs. With a mean diameter of 87 nm, virus-like particles have a less distinct surface than CLPs. They are characterised by a thicker shell, with the empty inside of the particle appearing smaller than in CLPs. For comparison, a CLP in the same micrograph is marked with an arrow. DLS analysis of purified BTV VLPs shows that 67% of the mass of the sample forms a species of particle with an average diameter of 96 nm, the rest of the sample forms aggregates (data not shown). Though this value is not a reliable measure of size due to the heterogeneity of the sample, it does illustrate a size shift and tendency to aggregate which is not seen for CLPs (Section 6.3.3).

The recovery of high yields of all four structural proteins in gradient fractions was the most exciting day of my PhD. The confirmation of the presence of VLP by TEM represented a major leap forward in my project, opening up many possibilities for optimization of expression and purification. It was also key to the later production of particles for immunogenicity studies, as well as fluorescent BTV VLPs (Chapter 7).

The appearance of VLP preparations under TEM was highly variable throughout this project, often showing an abundance of partially (dis-)assembled VLPs, CLPs or SCLPs, with only few VLP structures. Optimisation of extraction and purification conditions as well as practice in grid preparation and TEM technique improved the consistency in the quality of VLPs imaged. This indicates that much of the variability in particle preparation may be due to damage during down-stream processing and TEM grid preparation. However, the stoichiometric ratio of the expressed proteins also plays a crucial role and is discussed in more detail in the next section.

6.3.5 STOICHIOMETRY: OPTIMIZATION OF RELATIVE VLP YIELD

In contrast to other viruses, such as CPMV and FMDV, the structural proteins forming the capsid of BTV are not present in equimolar ratios. Full BTV-like particles contain 180 copies of VP2, 120 copies of VP3, 360 copies of VP5 and 780 copies of VP7. This complex stoichiometry is further complicated by differing affinities of the structural proteins for one another, resulting in highly stable core-like particles and less stable VLP and SCLP structures.

Aiming to achieve the highest possible expression levels of each of the four proteins may lead to high yields of BTV proteins, but does not guarantee the recovery of particle preparations containing a high proportion of fully assembled VLPs. This section reports three attempts to modulate expression of the four structural proteins in order to optimise virus-like particle yield by (1) the targeted use of wild-type and codon-optimised genes, (2) the co-expression of all structural proteins from a single T-DNA, and (3) the use of CPMV RNA-2 5'-untranslated regions with and without the *HT* mutations.

The stoichiometry of the proteins in a given VLP preparation can be easily judged by observation of the relative intensity of Coomassie blue-stained bands on an SDS-PAGE gel. In Bluetongue virus capsids, structural protein size is, to some extent, inversely proportional to the copy number per assembled particle: The lower the mass of a structural protein, the higher its copy number in each particle. Hence, separation of purified virus on reducing SDS-PAGE followed by Coomassie blue staining produces bands of similar intensity for the four main structural proteins (Martin and Zweerink, 1972). Analyses in this section take advantage of this characteristic. In a density gradient fraction, a relative excess of VP3 and VP7 is indicative of a high proportion of CLP, while an excess of just VP3 indicates contaminating subcore-like particles. Inspection of the Coomassie gel of Figure 6.5 B shows that BTV-8 VLP preparations produced by co-infiltration of four codon-optimized *HyperTrans* constructs contained an excess of VP3 and VP7, resulting in a high proportion of CLP. This made such preparations unsuitable for immunogenicity studies.

6.3.5.1 Modulation of relative expression levels by targeted use of wild-type genes

In order to achieve a lower amount of contaminating CLP structures in VLP preparations, an attempt was made to modulate expression levels of VP3 and VP7 through the use of wild-type genes. Initial expression trials had made use of the high expression levels achieved from codon-optimised genes for all structural proteins.

New pEAQexpress constructs were made by sequential subcloning of *Ascl-Pacl* digested expression cassettes from the BTV-8 pEAQ-*HT* plasmids. These new pEAQex constructs incorporate two BTV-8 genes as well as P19 on the same T-DNA, thereby ensuring consistent co-expression of these genes in every plant cell. Two constructs were made for expression of VP7 and VP3 from codon-optimised and wild-type genes: pEAQex-BTV8.7co-BTV8.3co and pEAQex-BTV8.7-BTV8.3, respectively. It was previously found that

codon-optimized genes give at least 3-fold higher expression levels than the wild-type genes (Figure 6.1). One construct was made for co-expression of codon-optimised VP5 and VP2 (pEAQex-BTV8.5co-BTV8.2co).

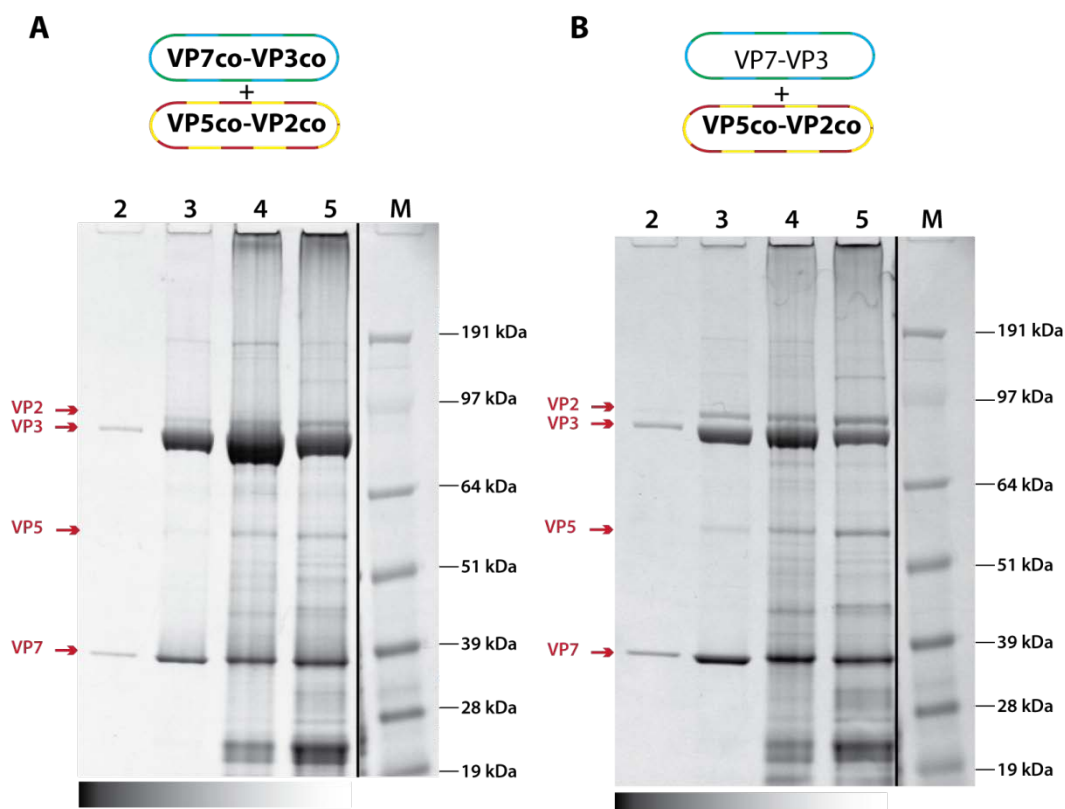


Figure 6.6: Co-expression of codon-optimized VP5 and VP2 with wild-type VP7 and VP3 reduces the over-representation of VP3 in particle preparations.

Leaves were agro-infiltrated with constructs as indicated and harvested 8 dpi. Clarified extracts were separated on iodixanol step gradients. Fractions were collected from the bottom, separated on 4-12% SDS-PAGE gels and Coomassie blue stained. (A) Co-infiltration of pEAQexpress constructs carrying codon-optimized genes for all four structural proteins. (B) Co-infiltration of pEAQexpress constructs carrying codon-optimized genes for VP5 and VP2, and wild-type genes for VP3 and VP7. M = SeeBlue +2 marker; 2-5 = gradient fraction numbers.

To analyse the effect of combining wild-type genes for core proteins with codon-optimised genes for outer shell proteins, combinations of these constructs were agroinfiltrated and iodixanol gradients performed on harvested material 8 dpi, as previously described. Relevant gradient fractions were analysed by reducing SDS-PAGE and Coomassie staining (Figure 6.6). In both combinations, all four BTV structural proteins

were clearly visible in the stained gel. In this particular experiment, by far the most abundant structural protein isolated from tissue expressing entirely codon-optimized genes was VP3, indicating a high proportion of SCLP in the preparation. This may be due to the location of the VP3 gene near the right border of the T-DNA, thus favouring its expression relative to VP7. This does not explain the low abundance of VP5 and VP2, however. It is necessary to note that the plants were grown under aberrant growth conditions at the time, due to technical problems, and were stunted in growth and generally unhealthy. This may also have played a significant role in these experiments. However, the two combinations presented in this experiment were prepared in parallel and were subject to the same conditions, and can nevertheless be directly compared.

The amount of VP3 in the preparation from the wild-type construct (Figure 6.6 B) is much lower than that obtained from the codon-optimised construct (Figure 6.6 A), as was hoped. Although it can be assumed that overall levels of VP7 expression are lower from the wild-type construct, the amount of VP7 obtained from this combination was higher than that obtained from the codon-optimised construct. The relative intensities of the VP3 and VP7 bands in Figure 6.6 B more closely approach the expected ratio than those of the codon-optimised versions in Figure 6.6 A, indicating a higher proportion of CLPs than SCLPs. Expression levels of VP5 and VP2 were expected to be equal in the two experiments. However, the combination of codon-optimised VP5 and VP2 with wild-type VP7 and VP3 appears to yield slightly more outer shell proteins in the gradient fractions. This is particularly evident when comparing fractions 5.

Though this experiment was not ideal due to prolonged problems with plant health, it can nevertheless be concluded that the combination of lower-expressing wild-type genes of VP3 and VP7 with codon-optimized genes for VP5 and VP2 favours the accumulation of more fully assembled particles when compared with the expression of exclusively codon-optimized genes. Thus down-regulation of the expression of VP3 and VP7 relative to VP2 and VP5 appears to be a potentially useful strategy for optimising the proportion of fully assembled VLP.

6.3.5.2 *Expression of four structural proteins and P19 from a single T-DNA*

It has been previously shown that co-infiltration of multiple *Agrobacterium* strains is not an efficient means of co-expressing multiple proteins in a cell (Section 3.3.6). The

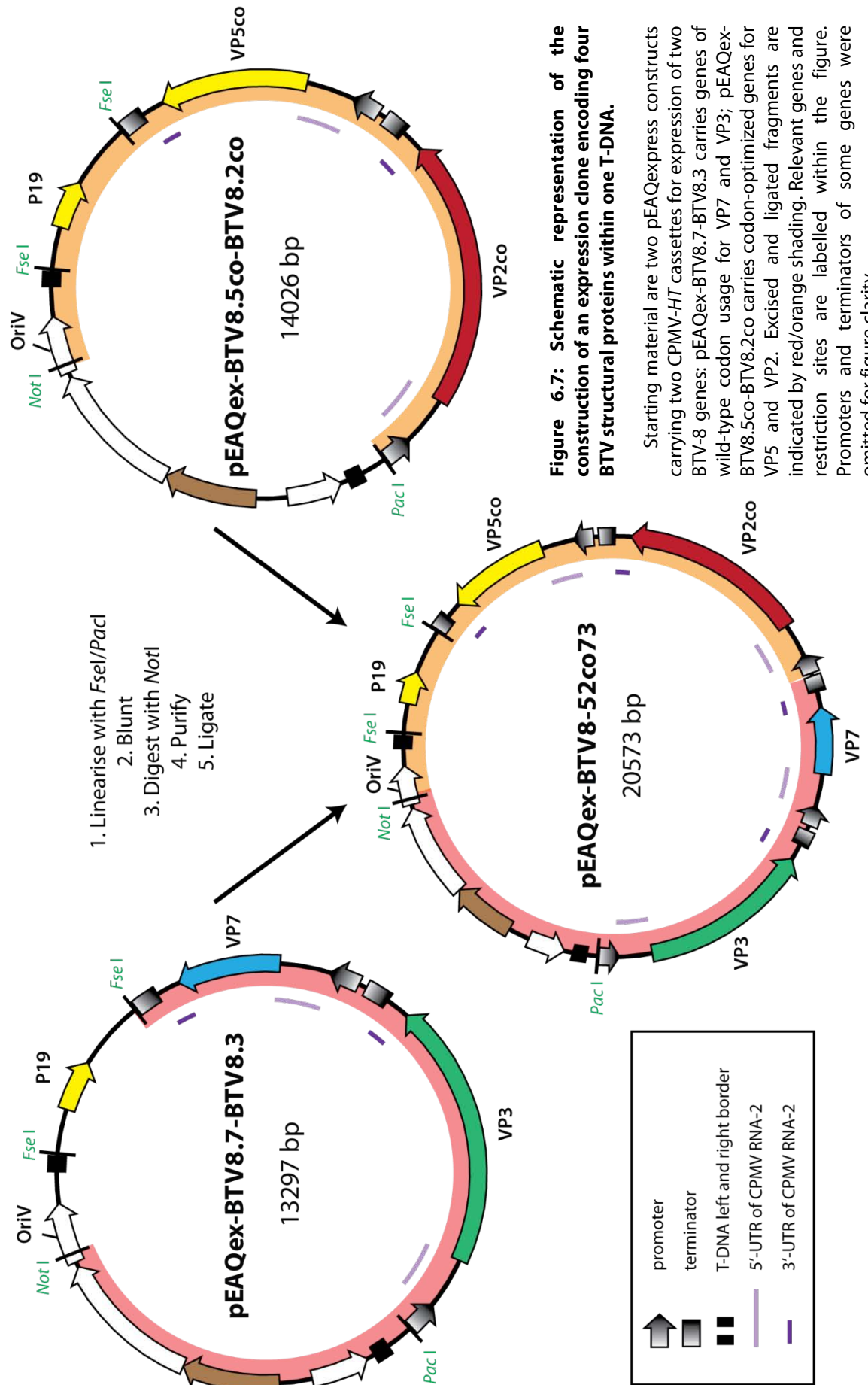


Figure 6.7: Schematic representation of the construction of an expression clone encoding four BTV structural proteins within one T-DNA.

Starting material are two pEAQexpress constructs carrying two CPMV-*HT* cassettes for expression of two BTV-8 genes: pEAQex-BTV8.7-BTV8.3 carries genes of wild-type codon usage for VP7 and VP3; pEAQex-BTV8.5co-BTV8.2co carries codon-optimized genes for VP5 and VP2. Excised and ligated fragments are indicated by red/orange shading. Relevant genes and restriction sites are labelled within the figure. Promoters and terminators of some genes were omitted for figure clarity.

pEAQexpress vector is a useful tool to ensure efficient co-expression of two proteins as well as P19 in each cell by transfer of a single T-DNA construct. Such pEAQexpress constructs have already been shown to successfully express BTV structural proteins by combining genes for the core proteins (VP3 and VP7) on one pEAQexpress construct, and those for the outer shell proteins (VP2 and VP5) on another (Section 6.3.5.1). However, successful assembly of BTV virus-like particles requires all four structural proteins to be expressed in every cell.

In order to ensure efficient co-expression, and to determine whether this has an effect on levels of VLPs obtained, genes for all four BTV structural proteins were cloned onto a single T-DNA construct. Drawing from the results presented in the previous section, it was decided that a combination of wild-type VP3 and VP7 genes and codon-optimized VP5 and VP2 genes would be optimal. Due to the size and similarity of the two starting plasmids, pEAQex-BTV8.7-BTV8.3 and pEAQex-BTV8.5co-BTV8.2co, it was necessary to employ a more complicated cloning strategy involving the vector backbone and incompatible ends (Figure 6.7). The vectors were digested with *FseI* or *PacI*, respectively, and incompatible ends removed / filled in. Both linearised vectors were then digested with *NotI*, cutting within the OriV origin of replication and producing sticky ends. This strategy ensured ligation of the two fragments in the correct orientation. The correct assembly of the resulting pEAQex-BTV8-52co73 (short for VP5co-VP2co-VP7-VP3) was confirmed by multiple restriction digests. This vector contains a T-DNA region spanning over 16 kb.

In order to determine whether expression from a single T-DNA construct increases the relative amounts of fully assembled VLPs, leaves were infiltrated with pEAQex-BTV8-52co73 alone, or co-infiltrated with pEAQex-BTV8.7-BTV8.3 and pEAQex-BTV8.5co-BTV8.2co. Harvested tissue was subjected to extraction in low-salt SSB and iodixanol gradient centrifugation as previously described. Relevant fractions were separated on SDS-PAGE and the gel stained with Coomassie blue (Figure 6.8). As before (Section 6.3.5.1), co-infiltration of the two constructs resulted in an overrepresentation of VP3, i.e. subcore-like particles. However, the experiment presented here yielded relatively more VP5 and VP2 in the particle fractions, indicating a higher proportion of assembled VLPs, irrespective of whether one or two constructs were infiltrated. This may be due to better extraction of soluble VLPs by lowering of the salt concentration of the buffer (low-salt SSB versus SSB).

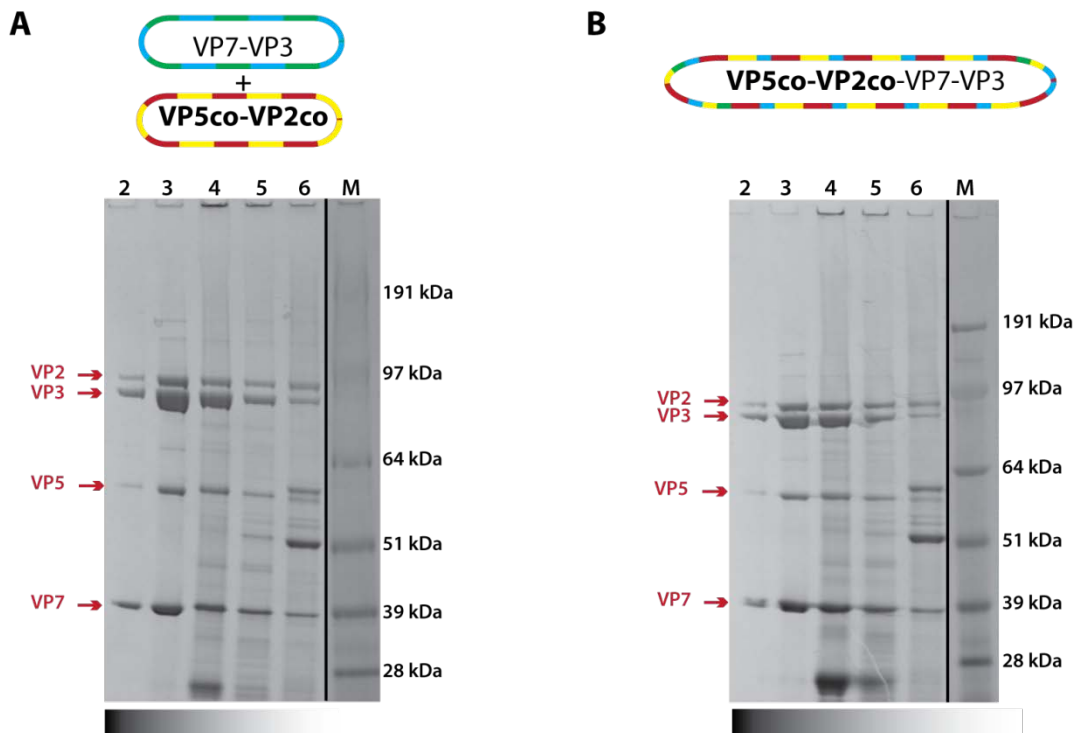


Figure 6.8: Expression of all BTV-8 structural proteins from a single T-DNA reduces over-representation of VP3.

Leaves were agro-infiltrated with constructs to introduce codon-optimized VP5 and VP2, and wild-type VP7 and VP3 genes as indicated, and harvested 10 dpi. Clarified extracts were separated on iodixanol step gradients. Fractions were collected from the bottom, separated on 4-12% SDS-PAGE gels and Coomassie blue- stained. Co-infiltration of pEAQexpress constructs carrying codon-optimized genes for all four structural proteins. (A) Co-infiltration of two *Agrobacterium* strains carrying constructs for VP7-VP3 and VP5-VP2, respectively. (B) Infiltration with a single *Agrobacterium* for expression of all four structural proteins from a single T-DNA. M = SeeBlue +2 marker; 2-6 = gradient fraction numbers.

Levels of VP5 and VP2 recovery do not appear to be greatly improved by expression from the pEAQex-BTV8-52co73 construct, relative to co-infiltration (Figure 6.8 B and A, respectively). This indicates that the relative proportion of VLP compared with CLP and SCLP is not significantly improved by expression of all structural proteins from a single construct in this configuration. However, it may be possible that changes in the relative positions of the gene expression cassettes on the T-DNA may produce a better effect. Due to the difficulties of cloning such large constructs, this possibility was not investigated further.

6.3.5.3 Restriction of VP3 expression by targeted use of wild-type 5'UTR

Previous attempts to limit the expression of the BTV core proteins VP3 and VP7 have provided an indication that this strategy might help to maximise the yield of fully assembled VLPs by restricting the production of CLPs (Section 6.3.5.1-2). However, these experiments still resulted in an over-accumulation of VP3 in the form of SCLPs. Assuming that outer shell proteins VP5 and VP2 are expressed to a high level, the restriction of both VP3 and VP7 expression may result in VP7 becoming the limiting factor in VLP assembly. Without an intact VP7 layer, the outer shell could not interact with the forming particles and would be lost in the low density fractions of a gradient upon purification. A better strategy may therefore be the selective and drastic limitation of VP3 expression while maintaining very high levels of VP2, VP5 and VP7 expression. If VP3 becomes the limiting factor in particle assembly, any VP3 that does form SCLPs should encounter an abundance of VP7, VP5 and VP2, ensuring that any particles formed will be full VLPs.

The high expression levels achieved using the mutated leader of the CPMV-*HT* system represent a vast, ca. 10 - 25-fold improvement over those levels attained using the wild-type 5'UTR of CPMV RNA-2 (Sainsbury and Lomonosoff, 2008). The selective use of 5'-UTRs with and without the *HyperTrans* (*HT*) mutations may therefore provide a useful means of modulating relative expression levels when multiple proteins are produced.

In order to test whether the use of a wild-type 5'UTR for the expression of VP3 would yield a higher ratio of fully assembled VLPs, the 5'UTR of the codon-optimized VP3 expression cassette was replaced by a wild-type version. The new pEAQexpress vector was called pEAQex-BTV8co-7HT-3, to indicate that both genes are codon-optimised but only the VP7 gene is flanked by a *HyperTrans* leader. This construct was agro-infiltrated with pEAQex-BTV8.5co-BTV8.2co, and compared to co-infiltration with constructs containing entirely codon-optimized genes expressed from *HyperTrans* cassettes. As previously seen, this latter combination produced fractions whose stoichiometry was indicative of VLPs, but also yielded fractions with a large over-representation of VP3, indicating SCLPs (Figure 6.9 A, lane 5). In contrast, expression of VP3 from a wild-type leader construct greatly reduced the level of VP3 purified in the same fraction (lane 5), while boosting the yield of stoichiometrically correct BTV proteins in the other fractions (Figure 6.9 B). This slight increase in VLP yield may be due to the lower level of VP3 expression allowing plant cell resources to be spent on elevated production of the other viral proteins.

Overall, the use of a wild-type CPMV 5'UTR for the expression of VP3 provides the best strategy (of those discussed here) for ensuring high yields of stoichiometrically sound VLP preparations. Thus, pEAQex-BTV8co-7HT-3 was used in conjunction with pEAQex-BTV8.5co-BTV8.2co during the preparation of virus-like particles for immunogenicity studies.

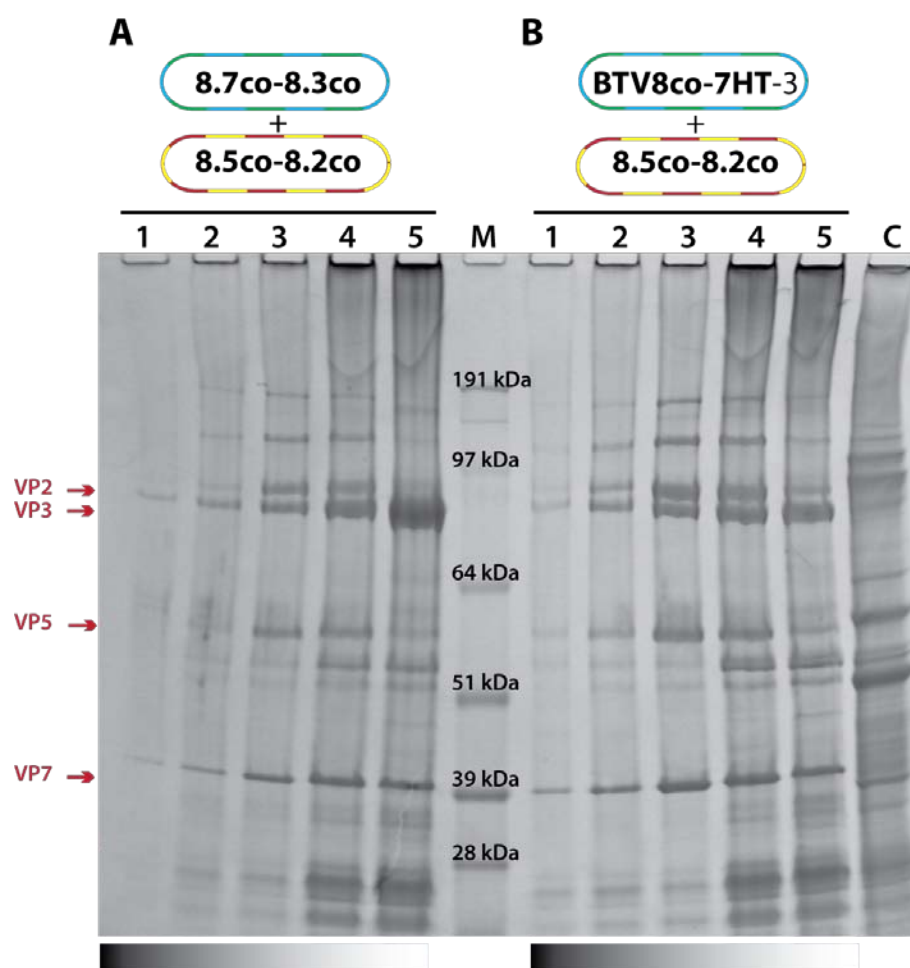


Figure 6.9: Expression of a VP3 construct with a wild-type CPMV RNA-2 leader increases the yield of stoichiometrically correct VLP fractions.

Leaves were agro-infiltrated with codon-optimized constructs as indicated and harvested 8 dpi. Clarified extracts were separated on sucrose step gradients. Fractions were collected from the bottom, separated on 4-12% SDS-PAGE gels and Coomassie blue stained. (A) Co-infiltration of pEAQexpress constructs carrying *HyperTrans* cassettes for all four structural proteins. (B) Co-infiltration of pEAQexpress constructs carrying *HyperTrans* cassettes for VP5, VP2, and VP7 a wild-type leader cassette for VP3. M = SeeBlue +2 marker; 1-5 = gradient fraction numbers; C = empty vector control.

6.3.6 PARTICLE PURIFICATION

Bluetongue virus-like particles, CLPs and SCLPs are large icosahedral structures with a higher sedimentation coefficient than most plant proteins. Hence, it is possible to achieve partial purification by a simple density gradient centrifugation, as shown previously. For analysis of protein ratios and TEM, this level of purity is sufficient. However, for the purpose of immunogenicity and efficacy studies in sheep, it is important to produce particle preparation of high purity and homogeneity. It was also important that preparations be devoid of detergents and other reagents commonly used in plant protein extraction.

In order to optimise purification protocols for BTV-8 CLPs and VLPs, buffer protocols and density gradient conditions were continuously modified, taking into consideration past experience and information gathered from published literature and personal communications. Some key findings and the final optimised purification protocol are presented here.

Extraction buffer compositions and purification protocols used for the isolation of BTV particles vary widely in the literature. The buffer recipes used during this project are detailed in Section 6.2.2. As a starting point, a protocol provided by Dr. Rob Noad (London School of Hygiene and Tropical Medicine, personal communication) was used for the extraction of BTV-10 and BTV-8 particles (BTV extraction buffer). This buffer works well for core-like particles of both serotypes. However, the apparent failure to produce BTV-10 virus-like particles was reason to change the buffer composition. In Smith Stabilisation Buffer (SSB) the Good buffer Bicine was substituted for Tris-HCl as the buffering agent, due to its acid dissociation constant (pK_a) being closer to the required pH and its concentration was increased from 20 mM to 50 mM to increase buffering capability. The detergent NP-40 was used (French et al., 1990), and 10% glycerol added for stabilisation. The first successful preparations of BTV-8 VLPs from plant tissue were prepared using this SSB extraction buffer (Section 6.3.4). However, in hindsight, this positive result was probably influenced more by the change in serotype and codon-optimization than by the extraction buffer used.

The extraction buffer SSB was further altered to accommodate a lower salt concentration of 20 mM after personal discussions with Dr. Meredith Stewart (London School of Hygiene and Tropical Medicine, UK), thereby yielding low-salt SSB (Section

6.3.5.2). The final modification of the extraction buffer took into account information obtained from Dr. Peter Mertens (personal communication), who suggested that the use of 0.1 % sodium lauroyl sarcosine (NLS) detergent is optimal for storage of VLPs to avoid aggregation. This gave the extraction buffer used most successfully for extraction and purification of VLPs, which was called “BTV VLP extraction buffer”.

Sucrose density gradients are commonly used to analyse and purify BTV preparations (French et al., 1990; Martin and Zweerink, 1972). However, the iodixanol density gradient medium Optiprep, may have some key advantages over other gradient media. It is claimed that virus preparations in Optiprep retain a higher rate of infectivity, suggesting that they are more intact (Møller-Larsen and Christensen, 1998). Additionally, concentrated iodixanol fractions can be injected directly into small animals for antibody production, without adverse effects.

In order to determine which of the two gradient media is optimal for plant-produced BTV particles, pooled clarified extract of BTV-8 CLP-expressing tissue (infiltrated with pEAQex-BTV8.7-BTV8.3) was applied to Optiprep and sucrose step-gradients, as shown in Figure 6.10 A. Gradient tubes were imaged after ultracentrifugation. Two distinct bands were visible in the Optiprep gradient, while the sucrose gradient did not appear to contain a distinct band. Both gradients were carefully fractionated by collecting drops from the bottom of the tube.

Analysis of the fractions by SDS-PAGE revealed a striking difference between the two gradients (Figure 6.10 B). The distinct bands of the Optiprep gradient were separated in fractions 3 and 4. The ratio of VP3 and VP7 in fractions 1-3 was indicative of the formation of core-like particles. Fraction 4, however, contained far more VP3 than VP7, indicating that this fraction consisted mainly of subcore-like particles. These two species of particles were clearly separated in the Optiprep, but not the sucrose gradient. Here, subcore- and core-like particles were present throughout the collected fractions, with higher density fractions appearing to contain more CLPs, and lower density fractions having a higher proportion of VP3, i.e. SCLPs.

Both Optiprep and sucrose gradients efficiently separate BTV particles from plant material, which is retained at the top of the gradient. However, Optiprep appears to be much better suited to the separation of different particle species. This was also reflected in a parallel experiment with BTV virus-like particles (data not shown).

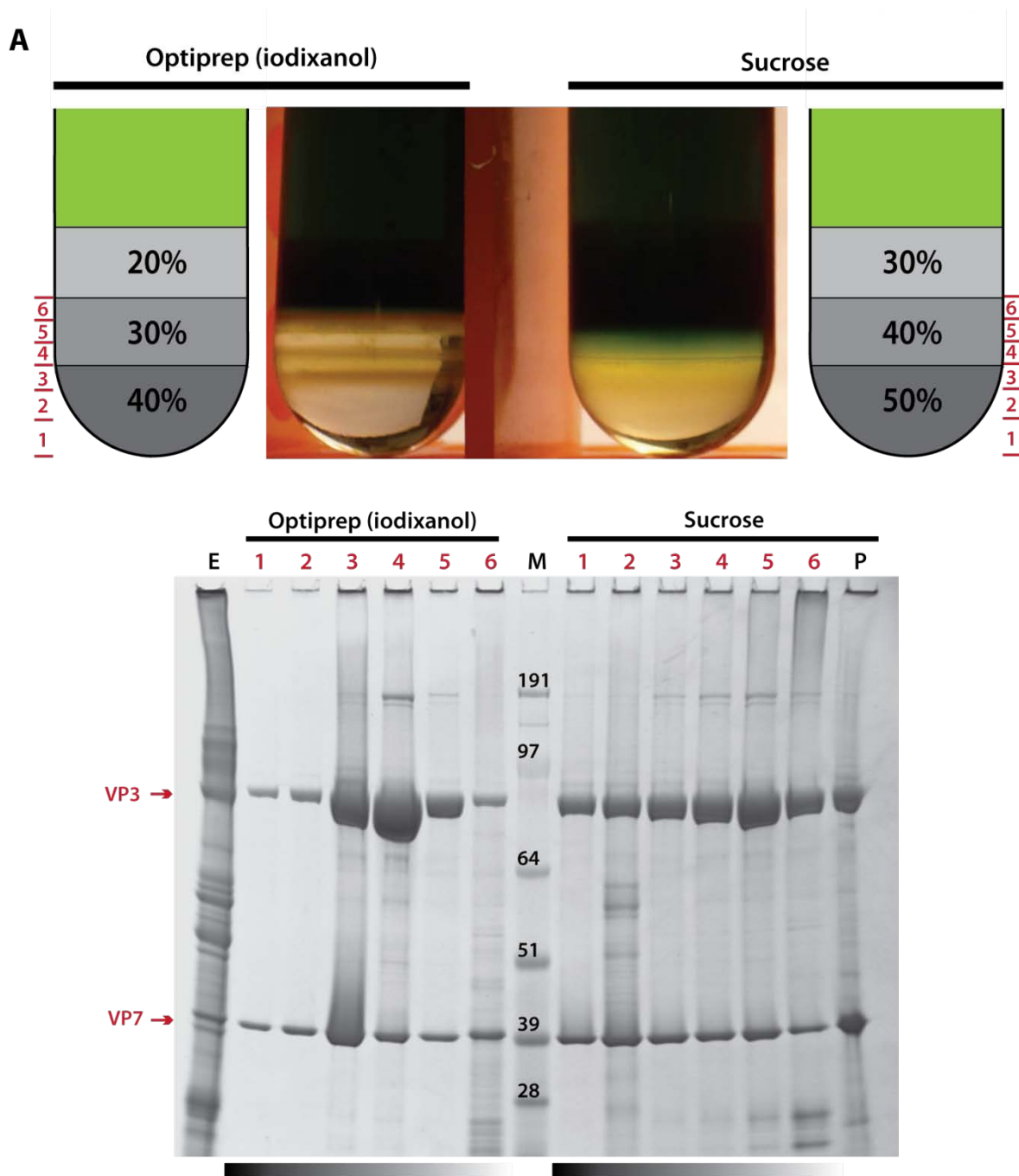


Figure 6.10: Iodixanol gradients are more suited to the separation of BTV particle species than sucrose gradients.

Leaves were infiltrated with pEAQex-BTV8.7-BTV8.3 and harvested 9 dpi. (A) Pooled clarified extract was distributed between two step density gradients (20 - 40% iodixanol and 30 - 50% sucrose) and imaged after ultracentrifugation. Fractions were collected from the bottom as indicated in red. (B) Fractions were separated by SDS-PAGE and Coomassie blue stained. E = clarified extract; M = SeeBlue +2 Marker; P = resuspended pellet.

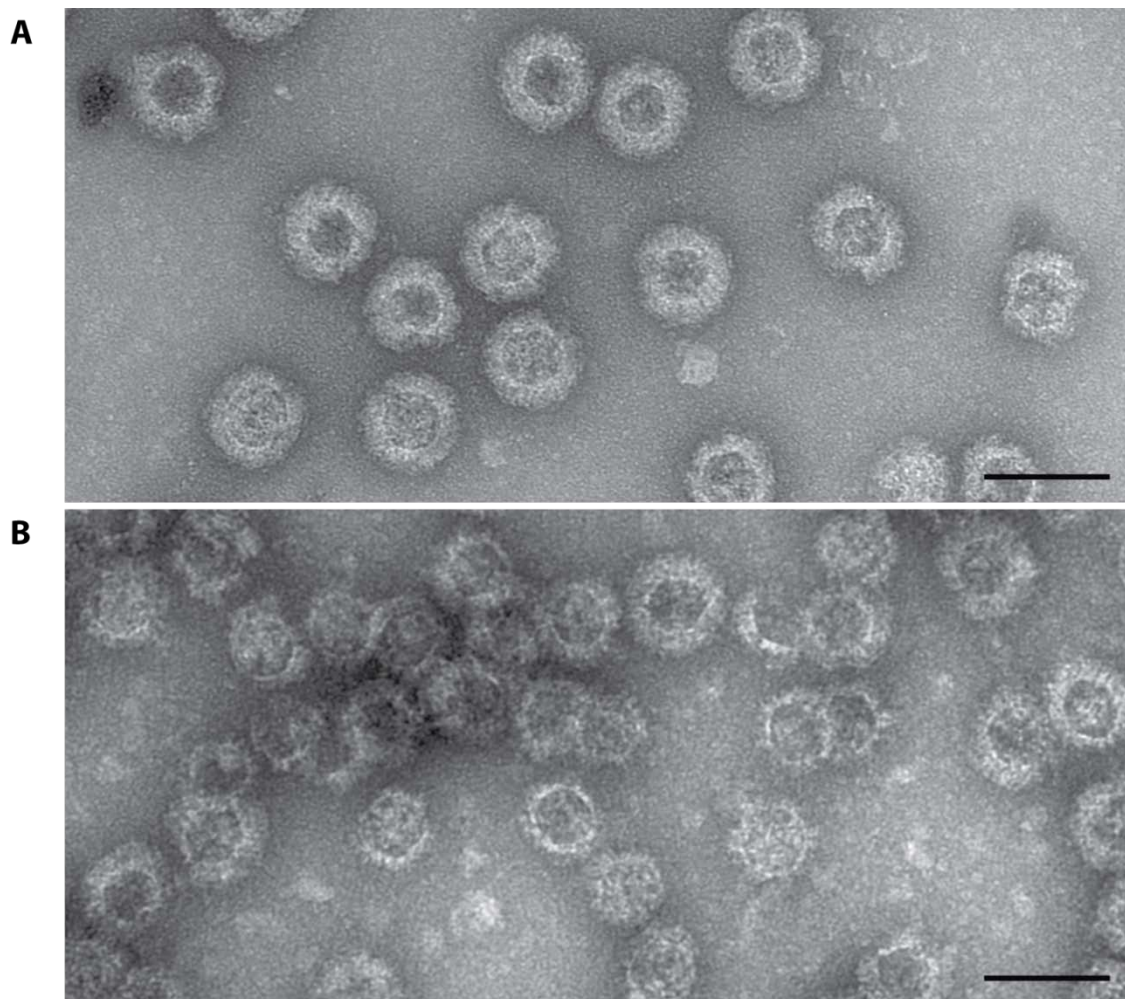


Figure 6.11: VLP integrity preservation is better in TEM grids prepared from sucrose fractions than iodixanol fractions.

Leaves were co-infiltrated with pEAQex-BTV8co-7HT-3 and pEAQex-BTV8.5co-BTV8.2co and harvested 8 dpi. Pooled clarified extract was distributed between two discontinuous density gradients: (A) 30 - 60% sucrose; (B) 20 - 50% iodixanol. VLP containing fractions were pooled and purified on a second round of density gradient centrifugation. VLP containing fractions were adsorbed to carbon-coated grids, rinsed with deionized water (3x), stained with 2% UA and imaged using TEM.

Analysis of the ratio of structural proteins in a gradient fraction provides a good indication of the composition of the sample and the particle species therein. However, no method surpasses TEM in providing confidence about the integrity of a sample intended for such critical experiments as animal studies. When preparing virus-like particles, samples which had been separated on sucrose gradients consistently showed higher particle integrity under TEM than those prepared with iodixanol (Figure 6.11). This effect may be an artefact of the harsh grid preparation and staining techniques involved in TEM. However, the quality of the sucrose-prepared particles, as well as the widely

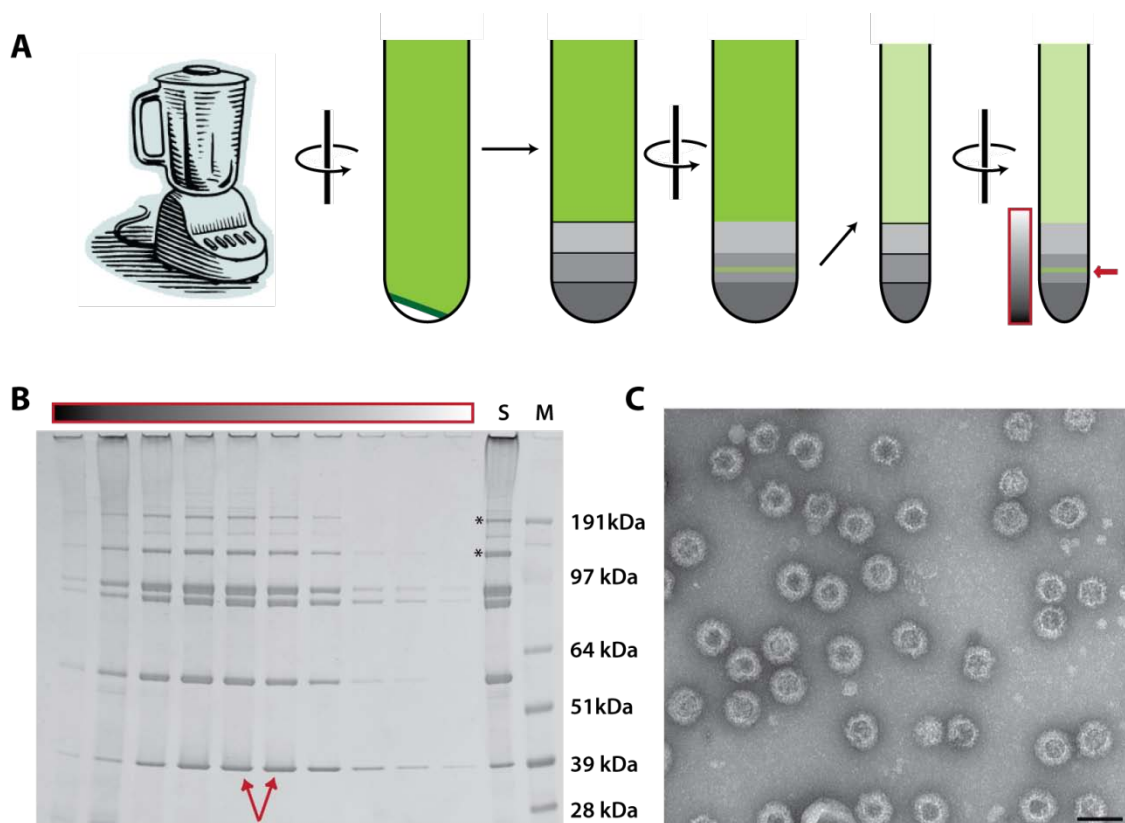


Figure 6.12: Purification of BTV-8 VLP intended for immunogenicity studies.

(A) Schematic representation of the key steps of the followed purification protocol for BTV-8 VLP and CLP: homogenization, clarification, sucrose gradient 1, fractionation, sucrose gradient 2, fractionation. (B) Leaves were co-infiltrated with pEAQex-BTV8co-7HT-3 and pEAQex-BTV8.5co-BTV8.2co and harvested 8 dpi. Clarified extract was purified on two sequential 30 - 60% sucrose gradients as described. Fractions were separated by 4-12% SDS-PAGE and Coomassie stained. Asterisk denotes bands that were submitted for mass spectrometry. Arrows indicate samples pooled for TEM analysis. S = starting material for second gradient spin; M = SeeBlue +2 marker; asterisks = bands confirmed by mass spectrometry to be VP5. (C) TEM of pooled purified samples as indicated by arrows in (B). Scale bar = 100 nm.

documented use of sucrose in preparation of BTV particle samples for immunogenicity trials, were reason to favour this medium for the preparation of particles intended for efficacy trials in sheep.

After much optimisation, the final purification procedure for obtaining BTV particles from *N. benthamiana* leaf tissue is schematically illustrated in Figure 6.12 A. Infiltrated leaf tissue was homogenised with three volumes of extraction buffer (BTV CLP or BTV VLP extraction buffers, as required), then filtered through Miracloth before centrifugation. The

clarified extract was applied to a 30 – 60 % sucrose step gradient, fractions of which were tested for the presence and ratio of BTV proteins by Coomassie-stained SDS-PAGE. Fractions of high quality were pooled, diluted, and subjected to a second round of density gradient centrifugation, containing only buffer and salt. Fractions were again tested for protein presence and ratios by SDS-PAGE analysis (Figure 6.12 B). The prominent bands in the high MW range were identified as VP5 multimers by mass spectrometry. The shown gel represents 1/400th of the total fractions obtained from 24 g of leaf tissue co-infiltrated with pEAQex-BTV8co-7HT-3 and pEAQex-BTV8.5co-BTV8.2co. Those fractions indicated by red arrows represent the fractions of optimal protein ratio, which were pooled and imaged using TEM (Figure 6.12 C). It is thus confirmed that a majority of particles in the preparation resemble VLPs, with a smaller proportion of CLPs present as expected. The amount of total BTV particles in this pooled sample was estimated from the intensity of Coomassie blue staining, and was later confirmed to be approximately 1.6 mg, corresponding to a recovery of 67 mg purified VLPs per kg FWT. However, this represents only a fraction of total BTV proteins produced, as a majority of assembled and unassembled proteins were discarded in gradient fractions deemed to have a poorer ratio of structural proteins or a high contamination with plant proteins and chlorophyll. Thus, a conservative estimate of total particulate BTV protein yield from *N. benthamiana* using the CPMV system is 200 mg / kg FWT. Further optimisation of extraction protocols may boost the relative recovery of pure VLPs from this total yield.

During TEM analysis of a purified VLP sample which had been stored at 4 °C for over two months, some virus-like particles were identified which appeared to interact with a contaminant, giving them the appearance of having another layer (Figure 6.13 A). Interestingly, while most of the VLPs in the sample resembled CLPs due to a loss of the outer VP5 and VP2 shell, the few particles found to have a 'halo' structure appeared to be remarkably intact. This suggests that these particles were protected from disassembly during storage and/or during TEM grid preparation. The same staining procedure and the same aliquot of uranyl acetate were used to stain other particle samples of BTV CLPs and Hepatitis B; however similar structures were not observed in these samples. This indicates that the 'halo' effect is not an artefact of staining, but specific to this BTV VLP sample.

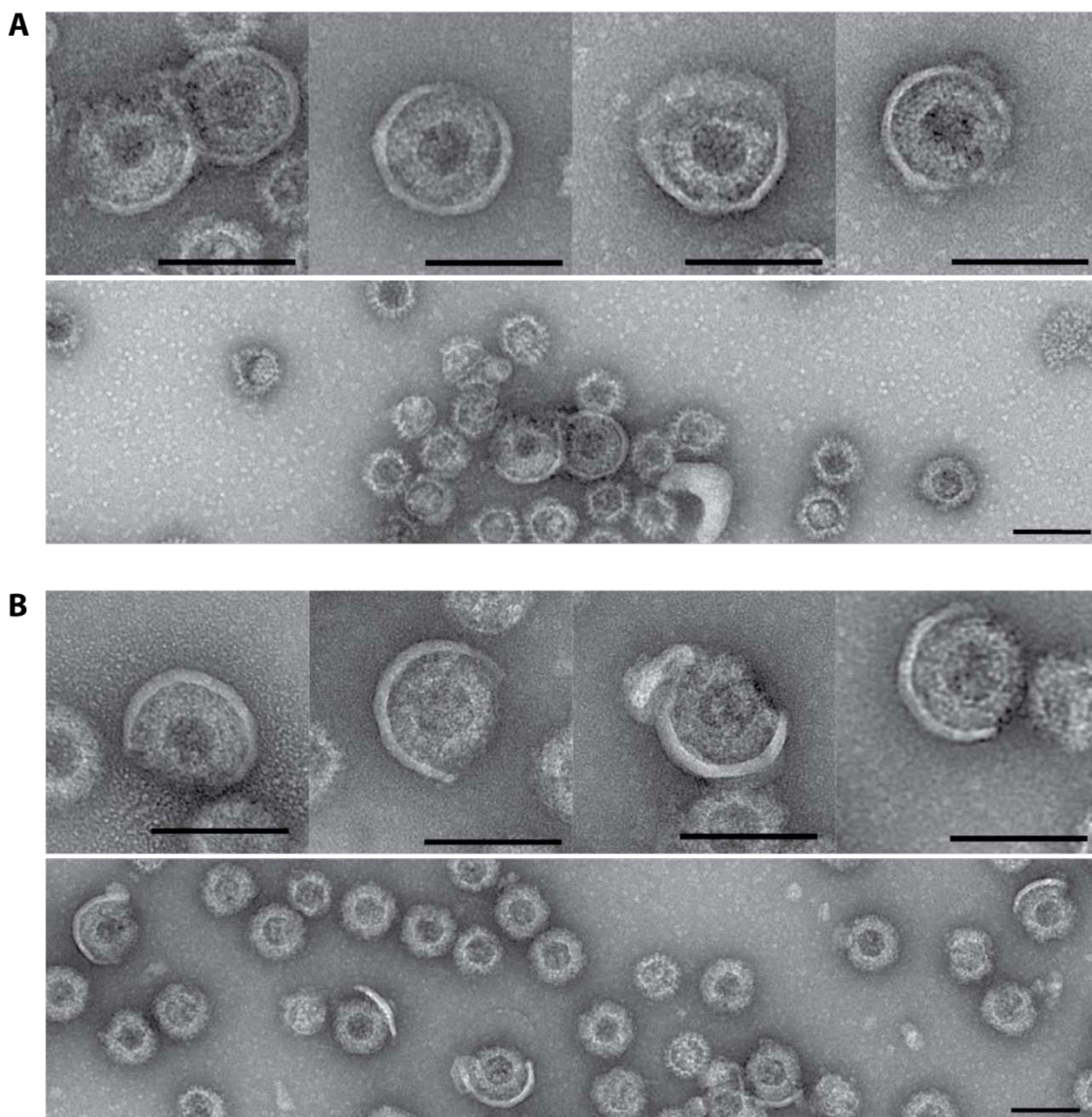


Figure 6.13: Preparations of purified BTV-8 VLPs contain some particles with associated halos.

BTV-8 virus-like particles were expressed in leaf tissue and subjected to two rounds of sucrose density gradients to purify. Particles were stored in ca. 40% sucrose fractions containing 20 mM Tris-HCl, 20 mM NaCl, pH 8.0. Samples were adsorbed to carbon-coated TEM grids, rinsed with water and stained with 2% uranyl acetate prior to imaging. Scale bars = 100 nm. (A) Sample was stored at 4°C for 2 months prior to imaging. (B) Independently prepared sample stored for two days prior to imaging.

In order to determine whether the halo structures were an artefact of the particular virus-like particle sample examined, a fresh VLP sample was prepared by following the same purification procedure. Having only been stored for a short period of time, the new sample had a higher proportion of full virus-like particles, as expected (Figure 6.13 B). Similar halo structures were also observed in this sample and appeared to be slightly

more abundant. The reproducibility of the structures indicates that there is, in fact, an interaction between full VLPs and these structures under the extraction and purification conditions employed. The thickness of approximately 8 nm is consistent with the thickness of the cellular membrane (Buchanan et al., 2000). Although BTV is not an enveloped virus, the outer shell of the particles has been shown to interact with membranes, both during entry and egress of the particles (Hassan et al., 2001; Hassan and Roy, 1999). It is conceivable, that plant-produced BTV VLPs could interact with cell membrane debris before or during purification. The disuse of detergents in the later stages of particle preparation may allow these membrane fragments to become stably associated with some particles. Since uranyl acetate stain was able to penetrate into these particles, it is clear that they are not entirely encased during grid preparation. However, the tight association of the structures with the particles does offer an explanation why the associated particles appear to be more intact than most other particles in the older sample (Figure 6.13 A). The time constraints of this project did not allow for these structures to be studied further.

The optimisation of extraction and purification procedures for BTV particles from plants has yielded a protocol which allows for consistently high quality BTV VLP preparations to be prepared. The purification procedure from the time of harvest requires less than two working days, with a recovery of 67 mg of purified VLP-rich particles per kilogram of fresh weight tissue.

6.4 DISCUSSION

Following the successful expression of BTV-10 CLPs (Chapter 5), in this chapter I have shown that it is possible to achieve high-level BTV-8 virus-like particle expression in plants using the CPMV-*HT* system in conjunction with the pEAQ vectors (Chapter 3). This provides a potentially cheaper alternative production system for an effective inherently safe Bluetongue vaccine against BTV-8.

High yields of full BTV-like particles were obtained upon expression of serotype 8 codon-optimized and wild-type genes, implying that efficiency of plant-based expression of BTV particles is serotype-dependent. It would, however, be interesting to determine whether codon-optimization of BTV-10 genes would allow recovery of full VLPs of this serotype as well. The high degree of variability in the outer shell proteins of BTV serotypes may lead to differences in protein stability. Codon usage may also affect the expression levels of BTV proteins. In fact, it was found that codon-optimization of BTV-8 genes for expression in *N. benthamiana* resulted in increased expression levels for all structural proteins, when compared with the wild-type genes. However, codon-optimization for *N. benthamiana* expression is not a universal guarantee of higher expression levels in plants, and ideally several codon usages should be tested for yield optimization (Maclean et al., 2007).

The problems encountered in the expression of complex heteromeric protein structures such as BTV VLPs clearly show that maximization of overall protein yield is not necessarily the best route to ensuring product quality. The BTV-like particle consists of 1440 subunits composed of a complex stoichiometric ratio of four different structural proteins (Stuart and Grimes, 2006). Each particle contains 120 copies of VP3 and 6.5 times as many copies of VP7, in addition to the other two structural proteins. The situation is further complicated by differences in mRNA and protein stability which inevitably influence the relative expression levels of different proteins. Thus, to maximize the amount of fully assembled particles in a preparation, it is necessary to modulate the expression levels of these four structural proteins.

In previous experiments, it was found that co-expression of two proteins in plant cells was more efficient when genes were cloned onto a single T-DNA construct, such as that of pEAQexpress (Section 3.3.6). Co-expression of all of the structural proteins of a virus in the same cell is of utmost importance for the assembly of the virus particle. Hence, the

genes for the structural proteins of BTV were combined in sets of two with pEAQexpress constructs, and later combined to form a single T-DNA for the simultaneous expression of four BTV genes in addition to P19 (section 6.3.5.2). Though this approach only resulted in a marginal improvement in protein ratios of the purified particles, it provided a great improvement to upstream processes such as the preparation of inoculum and the syringe agro-infiltration. Co-expression of four BTV genes and P19 from five separate constructs at an optical density of 0.3 requires the preparation of an inoculum of $OD_{600} = 1.5$, a very thick solution which is difficult to infiltrate and negatively impacts plant health. The efficient expression of all five genes from a 16 kb T-DNA region also represents the greatest number of genes expressed simultaneously from a single construct using the CPMV-*HT* system, and is thereby a good test of the expression system as well as the pEAQ vectors.

The use of long T-DNAs for expression of multiple proteins has previously presented a problem when used for the recovery of transgenic plants. T-DNA transfer occurs from the right border to the left border. Breakage of the T-DNA resulted in recovered transformants lacking the genes located closer to the left border (van Engelen et al., 1995). This is not a problem when using *Agrobacterium*-mediated T-DNA transfer for transient expression, as any breakages will not be detected. The results presented here show that high-level expression of BTV-8 VP5 can be achieved even when its cassette is cloned closest to the left border of a 16.1 kb T-DNA. Since the employed system provides each gene in the context of its own promoter and terminator sequences, expression may still be possible in the case of T-DNA breaks.

An efficient way of maximising the relative yield of fully assembled VLPs, as opposed to CLPs and SCLPs, is through the restriction of the availability of core proteins. The stoichiometry of structural proteins found in early BTV particle preparations was indicative of an overrepresentation of core-like particles (section 6.3.4). It was thought that a solution to this problem could be the use of the wild-type genes for VP3 and VP7 to limit the production of CLPs while maintaining high levels of VP5 and VP2 through the use of codon-optimized sequences. This approach did lead to a reduction of VP3 levels in particle preparations (section 6.3.5.1), showing that this strategy was valid. However, the ratio of proteins produced still indicated an over-representation of core- and subcore-like particles. It is known that the structural proteins VP2, VP5 and VP7 cannot assemble into particles in the absence of VP3 (Roy and Noad, 2006). Hence, the above strategy was refined by drastically limiting the expression of VP3 while maintaining high expression

levels of the other proteins to ensure that VP3 became the limiting factor in VLP assembly. This was achieved by cloning the codon-optimized VP3 gene behind the wild-type, rather than the *HyperTrans* CPMV RNA-2 leader (section 6.3.5.3). The results indicate that this is the best strategy for the preparation of VLPs as it limits the accumulation of core- and subcore-like particles. Virus-like particles produced in this way were deemed to be of very high integrity (Dr. Peter Mertens, Institute for Animal Health Pirbright, personal communication). The work presented here is the first use of combinations of *HT* and wild-type leaders of CPMV RNA-2 to modulate relative expression levels of heterologous proteins in this way.

The stoichiometry problems encountered during BTV VLP expression in plants are not limited to this expression system. Though the relative amounts of the four proteins are not discussed in great detail in publications about the insect cell-produced VLPs, close analysis of the literature does reveal that these problems are general. The first report of BTV VLP assembly presents Coomassie blue-stained gels clearly showing a lower proportion of VP5 than is expected of full virus preparations (French et al., 1990). The bands for VP3 and VP2 were not resolved, hence no conclusion can be drawn about the relative levels of VP2. Recently, the expression of all four structural proteins from a single baculovirus construct has been reported (Stewart et al., 2010). Discussions with the author revealed that one reason for doing this was to ensure efficient co-expression of all four proteins in every infected cell, a strategy that was also reported in Section 6.3.5.2. However, the gels and TEM images published in this article still show disproportionate levels of the four structural proteins in purified VLP preparations. The experiments reported in this chapter to modulate expression levels and achieve higher VLP homogeneity represent the first such attempts in the field.

The instability of the outer shell is integral to virion function during cell entry, and is not a phenomenon restricted to VLP production. In fact, the elucidation of the multi-shell composition of BTV virions was aided by the finding of two distinct particles in virus preparations: BTV-D (core) and BTV-L (virus; Martin and Zweerink, 1972). It was later found that virus particles are more easily labelled with anti-VP7 antibody after sedimentation through a sucrose gradient, indicating that gradient centrifugation damages the outer shell of particles (Hyatt and Eaton, 1988). Thus, it might be impossible to produce pure VLP preparations without contaminating CLPs and SCLPs. It is likely that the heterogeneity observed in particle preparations throughout the published literature is an

indication of incomplete assembly within cells, as much as damage during downstream-processing.

Despite the difficulties of handling an inherently instable virus, it was possible to produce VLP preparations of high quality for use in other applications. Sucrose fractions of purified VLPs and CLPs, produced as described in Section 6.3.6, have been frozen in aliquots, in preparation for preliminary immunogenicity and efficacy trials in sheep. Other samples prepared in Optiprep have been sent to Dr. Ann Meyers (University of Cape Town) for the purpose of raising antibodies. The antisera obtained will be an important tool for any future BTV work in both groups. Some critical next experiments include the use of the antiserum to detect BTV-8 proteins in a sample of commercial inactivated BTV vaccine, and to determine whether plant-made BTV-8 VLPs are able to raise neutralizing antibodies against authentic BTV-8. Plant-produced BTV-8 VLPs have also been provided to the Division of Structural Biology at the University of Oxford, where they were frozen in vitreous ice ready for cryoEM analysis (performed in collaboration with Dr. Alistair Siebert and Dr. Robert Gilbert). Structural information obtained from CEM would provide final proof of the integrity of the plant-produced VLPs.

During the purification of virus-like particles, crescent-shaped structures were observed to be associated with some of the particles in the final sucrose fractions (Figure 6.13). References to such structures could not be found in the literature. The thickness and lack of staining of the crescents leads me to speculate that these may be membrane fragments. It is known that both outer shell proteins associate with membranes: VP2 has a receptor-binding domain and a sialic acid-binding hub and functions in cell attachment during infection (Hassan and Roy, 1999; Zhang et al., 2010); VP5 is associated with lipid rafts and is involved in membrane permeabilization (Bhattacharya and Roy, 2008; Hassan et al., 2001). It is therefore conceivable that some lipids may associate with the VLPs before or during extraction, despite the presence of a detergent in the extraction buffer since the final stages of purification were performed without detergent. Interestingly, those particles associated with the crescent structures were the most intact VLPs in a sample which had been stored for several months. This may be an indication of a stabilizing effect of these structures on the VLPs. It would be interesting to test whether the addition of lipids to purified VLPs might aid in stabilizing these particles during storage. If it were possible to maintain efficacy while stabilizing VLPs in this way, this could be part of a solution to the problem of vaccine stability during storage and shipping.

Recently, it has been shown that a subunit vaccine consisting of plant-produced VP6 of Rotavirus induces passive protection of mice when administered orally (Zhou et al., 2010). At a yield of 1.54 mg / kg FWT and a 125 ug dose per mouse, this approach is far from economical. However, the proof of efficacy of an oral *Reoviridae* subunit vaccine, as well as recent findings that BTV-8 can be transmitted orally, indicate that it may be feasible to achieve immunogenicity from an orally administered plant-produced BTV vaccine in the future (Backx et al., 2009; Calvo-Pinilla et al., 2010). The high yields of over 200 mg BTV-8 proteins per kg FWT achieved using the CPMV-*HT* system certainly make this approach more economical.

During expression trials, an attempt was made to express the innermost structural protein VP3 on its own. Publications report that it is not possible to produce subcore-like particles by expressing BTV VP3 alone in insect cells (Hewat et al., 1992; Loudon and Roy, 1992). It is, however, possible to produce subcore-like particles of Broadhaven Virus, a related Orbivirus, in this way (Moss and Nuttall, 1994), indicating that self-assembly of BTV VP3 might be possible. Upon expression of VP3 alone in *N. benthamiana*, subcore-like particles could indeed be purified. These particles resemble those produced by removal of VP7 from baculovirus-produced CLPs (Hewat et al., 1992). This provides proof that BTV VP3 can, in fact, self-assemble into icosahedral particles without the need for interaction with other BTV proteins.

In this chapter, I have shown that the CPMV-*HT* system, in conjunction with the pEAQ vectors, can be used for high-level expression of BTV-8 SCLP, CLP and VLP in plants. The high yield of 67 mg purified VLP per kg FWT, and the good stoichiometric ratio of the produced proteins indicates that plants could rival insect cells as a production platform for BTV VLPs. Evidence of the self-assembly of VP3 in plants is indicative of the excellent capacity of plant cells to fold foreign proteins properly. This finding, as well as the evidence that C-terminally His-tagged BTV-10 VP3 retains its ability to form stable particles (Section 5.3.2) led me to investigate whether the plant-expression system would enable me to produce full BTV particles encapsidating large polypeptides, such as GFP (Chapter 7).

7 EXPRESSION AND USE OF FLUORESCENT BTV-LIKE PARTICLES

7.1 INTRODUCTION

The discovery of green fluorescent protein in 1962 and its later development as a biomarker have revolutionized many areas of biology by allowing proteins to be visualized *in vivo* (Chalfie et al., 1994; Shimomura et al., 1962). Recent advances in microscopy have enabled researchers to track individual fluorescent molecules, thereby making it possible to study the dynamics of protein movement within cells (reviewed by Greber and Way, 2006; Patterson et al., 2010). These new technologies provide an exciting new approach to the study of viruses.

Fluorescent tags and proteins have been used only relatively recently in the field of virology to study virus entry, movement and egress. In 1998, the report of fluorescent labelling of the structural proteins of a virus allowed researchers to track adenovirus cell attachment and internalization into tissue culture cells (Leopold et al.). Viruses can be labelled with fluorophores either directly by covalent bonding with the viral capsids, or indirectly by use of a virus-specific antibody (Bartlett and Samulski, 1998). Such labelled viruses have been used successfully in single molecule tracking experiments to visualize the infection pathway of an adeno-associated virus in real time (Seisenberger et al., 2001).

Despite their large size, the genetic fusion of fluorescent protein sequences to viral genes has provided another means of labelling some viruses. As described previously, it is possible to fuse GFP to the immunodominant loop of Hepatitis B core antigen, while maintaining its ability to form stable particles (Chapter 4; Kratz et al., 1999). Though these fusions have been explored mainly as a proof of principle for the insertion of large sequences for vaccine production, the formation of fluorescent HB cores opens up the possibility for the further study of HB particle assembly. It has already been shown that some enveloped viruses are amenable to budding in the presence of a fluorescent tag. In fact, it has been possible to produce fluorescent enveloped viruses, such as HIV-like particles, for the study of viral infection processes (Müller et al., 2004). More recently, Klingenstein et al. (2008) have been able to produce infectious double-labelled Rabies virus particles with a green fluorescent core and red fluorescent envelope. This was achieved

by fusion of RFP to the transmembrane domains of rabies virus G protein, and simultaneous expression of a GFP-fused nucleoprotein (Finke et al., 2004).

In the case of non-enveloped viruses, the labelling of the outside surface of the virus with a fluorescent protein or dye invariably alters the surface properties of the particles to some extent. This may impact biophysical properties, as seen in Chapter 4, and may influence binding, uptake and infectivity of the particle (Leopold et al., 1998). A possible solution to this problem is the encapsidation of a fluorophore on the inside of the particle, the exterior of which would resemble the authentic virus. A method for the non-covalent anchoring of EGFP to the inside of Cowpea Chlorotic Mottle Virus (CCMV) has recently been described (Minten et al., 2009). However, due to the small size of CCMV, it is necessary to produce mosaic particles which only contain a small number of GFP molecules in order to allow for efficient folding of the fluorophore and assembly of the particles.

Both Bluetongue Virus and Rotavirus have been shown to accommodate 120 copies of EGFP on the inside of core- and virus-like particles (Charpilienne et al., 2001; Kar et al., 2005). The *Reoviridae* subcore structure, with its large internal cavity encased by only 120 subunits of the same structural protein, makes it particularly suited to the encapsidation of large protein extensions. In 2001, an N-terminally truncated version of rotavirus VP2 (equivalent to BTV VP3) was fused to GFP via a flexible SRGS linker (Charpilienne et al., 2001). Co-expression of this construct with VP6 (equivalent to BTV VP7) in insect cells allowed rotavirus core-like particles to assemble, which resembled authentic cores. Furthermore, some evidence was provided for the assembly of the outer shell proteins VP4 and VP7 on this core-like structure, providing particles with distinct cell-binding characteristics. GFP- and DsRed-containing particles were used to study the internalization of rotavirus by kidney cell cultures.

GFP-tagging of Bluetongue Virus structural protein VP3 has enabled researchers to show that its intracellular localization changes when it is co-expressed with other structural proteins (Kar et al., 2005). When expressed individually in mammalian BSR cells, VP3 was localized to the host cell proteasome. However, co-expression with its structural partner VP7 and other BTV proteins caused VP3 to be concentrated in the vicinity of the nucleus, within virus inclusion bodies, where it assembled into stable core-like particles. Though it was clearly shown that GFP-VP3 is able to assemble into fluorescent CLP, no indication was given for the assembly into full virus-like particles in the presence of VP2

and VP5. Moreover, the baculovirus-produced fluorescent BTV CLPs (Kar et al., 2005) do not appear to have been utilized further in the study of BTV cell entry.

7.1.1 AIMS OF THIS CHAPTER

In order to allow the potential of fluorescent BTV particles to be exploited for the study of virus functions, it is essential to produce pure preparations of full fluorescent VLP (fVLP) resembling authentic virus. The work presented in this chapter describes the successful plant-based production of core-like and full virus-like particles of BTV with three different fluorophores contained on the inside. The modular nature of the gene construct allows for easy fusion of other proteins to VP3. Preliminary mammalian cell binding and entry study results are also presented.

7.2 SPECIFIC MATERIALS AND METHODS

7.2.1 CLONING

To construct pEAQ-HT-GFP:BTV8.3co, three fragments were ligated: (1) The *egfp* gene of pEAQ-HT-EGFP was amplified with M13F and GFP-BspEI-rev, then digested with *PacI* and *BspEI*; (2) The codon-optimized BTV-8 VP3 gene of pEAQ-HT-BTV8.3co (Chapter 6) was amplified with BTV8.3co-BspEI-fwd and C3, then digested with *BspEI* and *AvrII*; (3) pEAQ-HT-BTV8.3co was digested with *AvrII* and *PacI*.

A GFP: VP3co fusion construct with a wild-type CPMV RNA-2 5'UTR was cloned and named pEAQ-GFP:BTV8.3co. To produce this, three fragments were ligated: (1) pEAQ-GFP (a version with the wild-type 5'UTR of CPMV RNA-2) was digested with *XhoI*-*DraI* to obtain a pEAQ vector backbone with wild-type 5'UTR; (2-3) pEAQ-HT-BTV8-GFP:VP3co was digested with *XhoI*-*DraIII*-*EcoRI* and the *XhoI*-*DraIII* and *DraIII*-*DraIII* fragments were purified. Due to the interrupted palindromic recognition sequence of *DraIII*, the two sites cut by this enzyme produced different sticky ends, thereby ensuring directional ligation.

mRuby and mT-Sapphire were cloned into pEAQ-HT by amplification with respective end-tailoring primers (Table 7.1), digestion with *AgeI* and *XhoI*, and ligation with digested

vector to form pEAQ-HT-mRuby and pEAQ-HT-mT-Sapphire. N-terminal VP3 fusions with mRuby and mT-Sapphire were produced by amplification of these pEAQ-HT clones with C1 and the respective *Bsp*El end-tailoring primers and digestion with *Nru*I and *Bsp*El. The vector pEAQ-GFP:BTv8.3co was equally digested and the mRuby and mT-Sapphire fragments ligated. Constructs are listed in Appendix A.

Table 7.1: Oligonucleotides used in cloning of fluorescent BTV constructs.

Name	Sequence ^a	Function
BTv8.3co-BspEl-fw	CCTCCGGAGGCatggctgctcaaaat gagc	Primer for end-tailoring of <i>Bsp</i> El site to BTv-8 VP3co; sense
C1	aacgttgatcagatcgtgcttcggcacc	Universal sequencing primer from CPMV RNA-2 5'UTR; sense
C3	ctgaagggacgacctgtaaacaggag	Universal sequencing primer from CPMV RNA-2 3'UTR; antisense
GFP-BspEl-rev	agctccgattgtatagttcatccatgcc atg	Primer for end-tailoring of <i>Bsp</i> El site to EGFP; antisense
M13-F	acgttgtaaacgacggccag	Universal sequencing primer
mRuby_AgeI_F	CGACCGGTatgaacagcctgatcaaa g	Primer for end-tailoring of <i>Age</i> I site to mRuby; sense
mRuby_BspEl-R	AGTCCGGAccctccgcccaggcc	Primer for end-tailoring of <i>Bsp</i> El site to mRuby; antisense
mRuby_XhoI_R	ATCTCGAGttaccctccgcccaggcc	Primer for end-tailoring of <i>Xho</i> I site to mRuby; antisense
mT-Sapphire_BspEl_R	ATTCCGGActtgtagctcgctccatgc c	Primer for end-tailoring of <i>Bsp</i> El site to mT-Sapphire; antisense
mT-Sapphire_XhoI_R	ATCTCGAGttacttgtagctcgctcca tgc	Primer for end-tailoring of <i>Xho</i> I site to mT-Sapphire; antisense
SEQ_BTv8_VP3co_R	cctaaccttctgcataatc	Sequencing primer from BTv8.3co; antisense

^a END-TAILORING is shown in uppercase, restriction enzyme recognition sites are underlined.

7.2.2 PARTICLE PURIFICATION

Optimal fluorescent particle purification was achieved with the protocols used for BTv-8 VLP and CLP purification, as detailed in Section 6.2.2.

7.2.3 UPTAKE STUDIES

Experiments to track the internalization of GFP fVLP into mammalian cells were carried out in collaboration with Drs. Sarah Gold and Terry Jackson at the Institute for Animal Health, Pirbright.

Baby Hamster Kidney cells (BHK-21; European Cell Culture Collection) were maintained in Glasgow Minimum Essential Medium (GMEM) containing 10 % foetal bovine serum (FBS), 2 mM glutamine, 100 U/ml penicillin, 100 µg/ml streptomycin, 5 % (v/v) tryptose phosphate broth solution (Sigma). Cells were plated onto 13 mm borosilicate coverslips in 24-well tissue culture plates and maintained at 37 °C, 5 % CO₂, to be used when 40 - 60 % confluent.

To bind BTV fVLP, BHK cells were kept and washed three times with cold serum-free medium on ice before adding 200 µg/ml BTV -8 GFP fVLP and incubating on ice for 40 minutes. Unbound VLP was removed by washing twice with cold serum-free medium, then cells were warmed by washing three times with 37°C warm serum-free medium. Cells were incubated at 37 °C, 5 % CO₂ and replicates removed at 0, 15, 30 and 60 minute time points to monitor uptake. To stop internalization, cells were placed on ice and washed twice with cold serum-free medium before fixing with 4% paraformaldehyde for 40 minutes.

To detect VP5 and prepare cells for confocal microscopy, coverslips were washed three times with PBS before permeabilisation with 0.1% Triton X-100 for 20 minutes. After washing twice with PBS, non-specific binding was blocked using block buffer (100 ml TBS [10 ml of 1M Tris pH 7.5 in 500 ml 0.85% saline] supplemented with 1mM CaCl₂, 0.5mM MgCl₂, 10% Normal Goat Serum [Harlan Lab Sera] and 1% Teleostean Gelatin [Sigma]) for 30 minutes. Guinea-pig anti-BTV-1 VP5 antibody was added and incubated for one hour, washed three times with PBS and incubated with anti-guinea pig Alexa-Fluor-labelled secondary antibody (Molecular Probes) for one hour. After washing three times with PBS, cells were stained with 4',6'-Diamidino-2-Phenylindole (DAPI; Sigma) at 1:10 000 dilution in water for 10 minutes, then washed with PBS. Coverslips were then mounted in Vectashield mounting medium (Vector Laboratories) on a glass slide and sealed with clear nail varnish. Slides were stored at 4 °C

7.3 RESULTS

7.3.1 CONSTRUCTION OF pEAQ-HT-GFP:BTv8.3co

A fusion of EGFP to the N-terminus of BTV-8 VP3 was prepared as described in Section 7.2.1 (Figure 7.1). The good results achieved in expression and assembly of GFP-displaying Hepatitis B Tandem cores (Section 4.3.5) provided reason to design the GFP:VP3 fusion in such a way as to include a flexible serine-glycine-glycine linker between the GFP and VP3 proteins. This was achieved by end-tailoring PCR, which also introduced a unique *BspEI* site between the fused GFP and VP3 sequences. The unique *NruI* and *BspEI* sites flanking the *egfp* gene in pEAQ-HT-GFP:BTv8.3co allow for a simple substitution of *egfp* with any other gene of interest to produce new VP3 fusion proteins. This was done to produce mRuby and mT-Sapphire fusion proteins.

Fusion of the 27 kDa GFP protein to VP3 was designed to result in the assembly of particles with 120 copies of this fluorescent protein on the inside. To obtain a sense of the relative size of GFP and VP3, the published crystal structures of the two proteins were assembled into a single image using Pymol software (Figure 7.1 C). The face of each VP3 molecule measures 135 Å by 75 Å (Stuart and Grimes, 2006), making it far larger than the compact β -barrel structure of GFP, measuring only 30 Å in diameter (Ormo et al., 1996). This illustrates the availability of sufficient space to allow GFP to fold and fluoresce from the inside of BTV particles.

7.3.2 EXPRESSION OF GFP:VP3 AND ASSOCIATION WITH BTV STRUCTURAL PROTEINS

The pEAQ-HT-GFP:BTv8.3co construct was co-infiltrated with other BTV structural protein constructs in various combinations to establish whether the GFP:VP3 fusion protein could be expressed in plants and to determine whether it could form particles in the presence of other BTV structural proteins. GFP:VP3 was co-infiltrated with VP7 to obtain fluorescent core-like particles (fCLP), and with VP7, VP5 and VP2 for fluorescent virus-like particles (fVLP). Taking into account the possibility that fluorescent particle formation may only be possible in the form of mosaics with untagged VP3, leaf tissue was infiltrated with both GFP:VP3 and VP3 constructs at half of the optical density used for

VP7 (½ fCLP). As a control for assembly, VP3 and VP7 (pEAQ-*HT*-BTV8.3co and pEAQ-*HT*-BTV8.7co) without GFP tag were co-infiltrated (CLP). Leaves infiltrated with the GFP:VP3 were found to fluoresce under UV illumination, whereas the control infiltration did not produce fluorescence (Figure 7.2 A). The expression of the GFP:VP3 fusion protein did not appear to affect tissue health when compared with VP3.

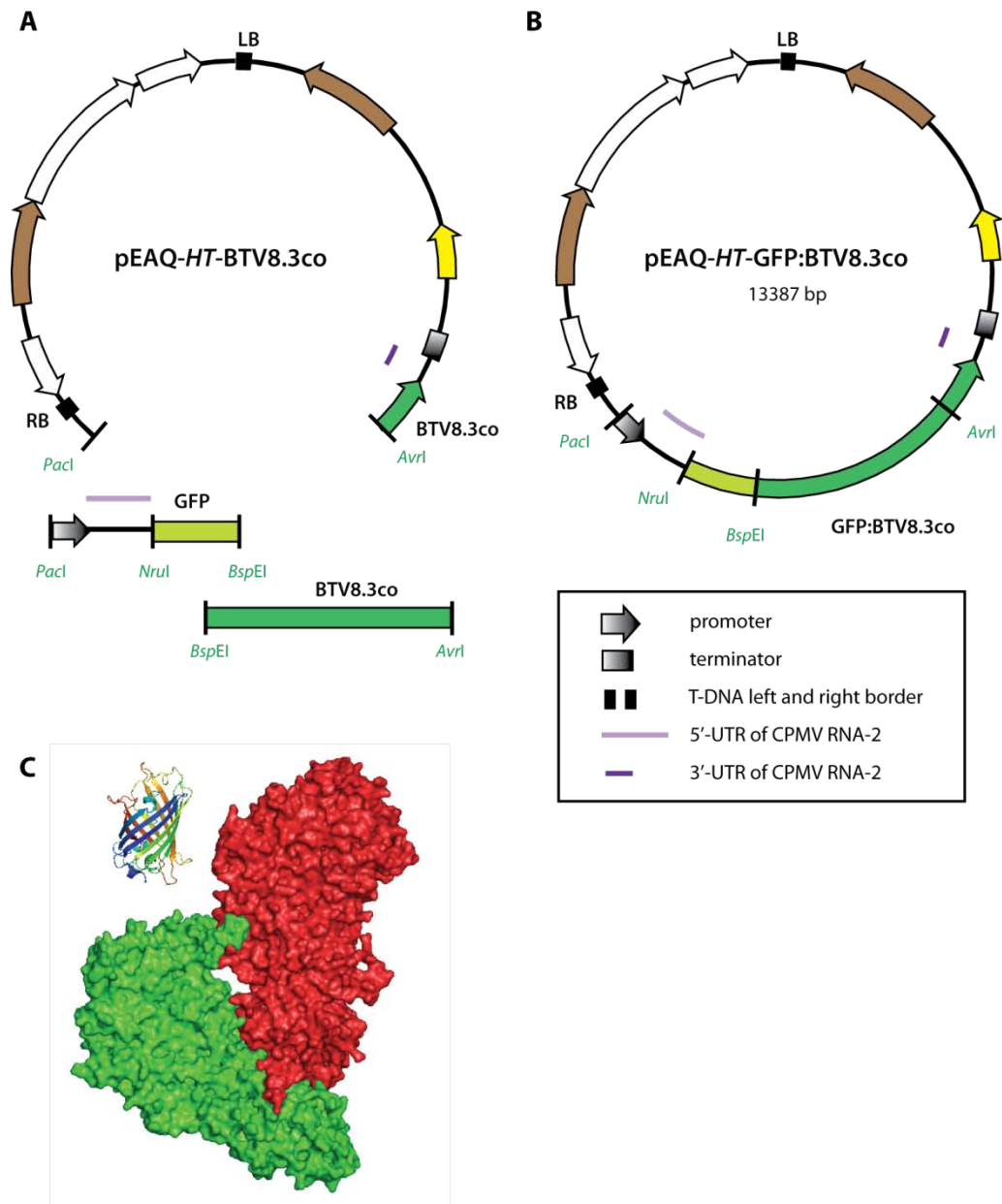


Figure 7.1: Design of a GFP:VP3 fusion construct.

(A) Schematic representation of the three fragments used in the construction of the clone. (B) Schematic representation of pEAQ-*HT*-GFP:BTV8.3co. Restriction sites and functional elements critical to the cloning strategy are labelled. (C) Illustration of the relative sizes of GFP and VP3. GFP is shown as a ribbon; VP3 dimer is shown as a space filling model. The image was produced with Pymol programme using published structural data.

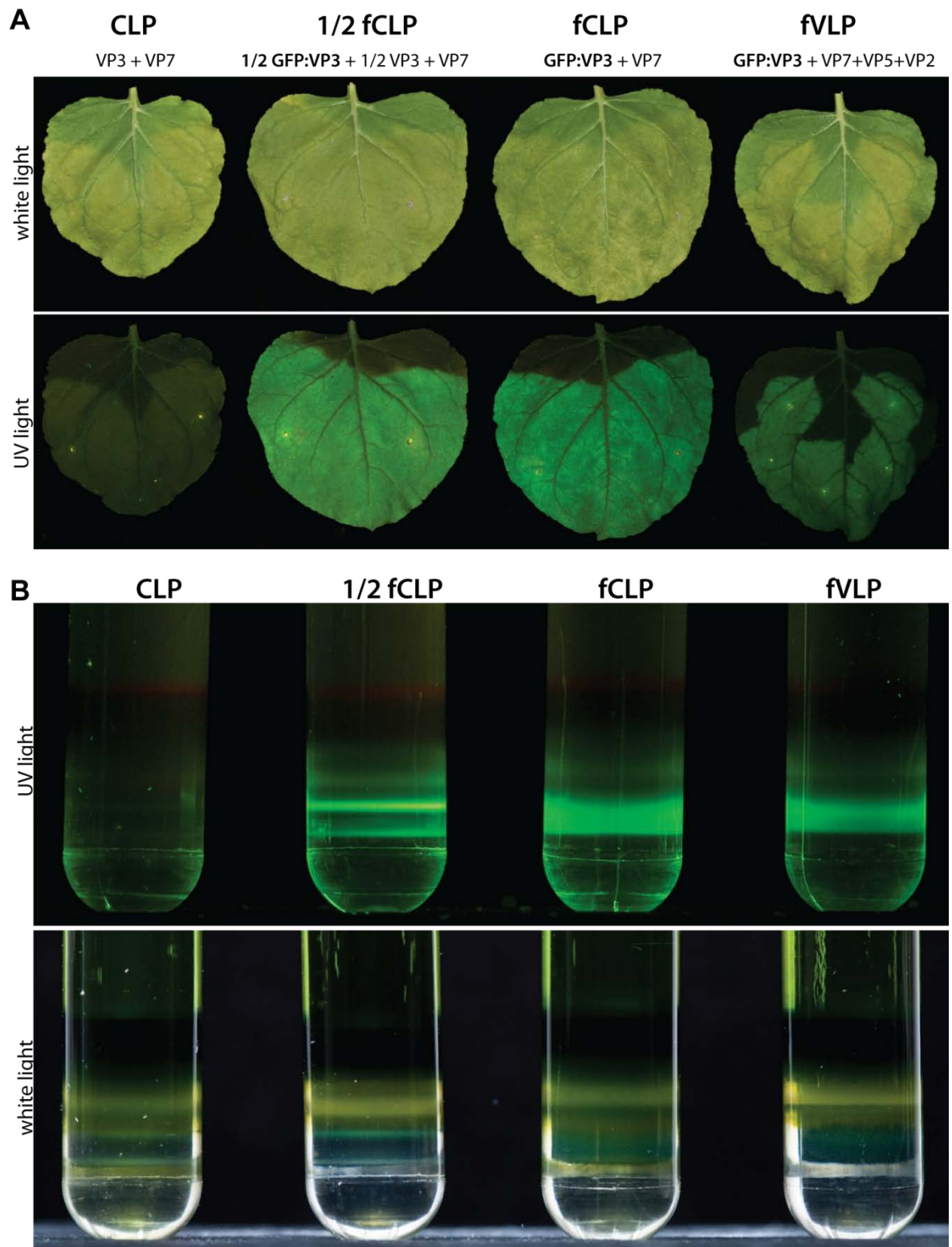


Figure 7.2: GFP:VP3 fusion protein is expressed in *N. benthamiana* leaf tissue and sediments in sucrose gradients.

Leaves were co-infiltrated with codon-optimized BTV8 constructs as indicated. 1/2 fCLP = infiltrations with GFP:VP3 and VP3 at half of the normal optical density each (i.e. OD₆₀₀ = 0.2). (A) Leaves were harvested 9 dpi and imaged under white and UV light to visualize GFP fluorescence. (B) Leaf tissue was extracted in low-salt SSB and clarified extract separated on 15 - 45 % iodixanol step gradients. Gradient tubes were imaged under white and UV light illumination to visualize GFP bands.

Clarified leaf extracts derived from the above infiltrations were separated on iodixanol step gradients to determine whether particles were being formed. After ultracentrifugation, fluorescence was detected only in the lower part of the gradients, indicating that the expressed GFP was efficiently incorporated into large structures (Figure 7.2 B). Both samples containing untagged VP3 produced two distinct thin bands at the bottom of the gradient, visible in white light. Under UV illumination, these bands were found to fluoresce in the $\frac{1}{2}$ fCLP sample. In contrast, the fCLP and fVLP samples produced a broader, greenish and fluorescent band spanning the same density range of the gradient. It was previously determined that co-expression of BTV-8 VP3 and VP7 constructs efficiently produces core-like particles in plants, and that these sediment to the in the range of 30 - 40% iodixanol (Section 6.3.4). Hence, the presence of fluorescent bands in this part of the gradient and a lack of fluorescence in other parts of the gradient indicated efficient fluorescent particle formation.

Gradients were fractionated from the bottom and the most fluorescent fractions separated on SDS-PAGE to determine their composition (Figure 7.3). As shown previously (Section 7.3.3), co-expression of VP3 and VP7 yielded both proteins in all fractions, with a peak in fraction 4, indicating core-like particle assembly. As seen previously (Section 6.3.5), an excess of VP3 was present in some fractions, indicating the presence of subcore-like particles. This fraction likely corresponds to the upper of the two distinct bands seen in the gradients (Figure 7.2 B). The fractions obtained from the $\frac{1}{2}$ CLP gradient contained similar amounts and patterns of VP3 and VP7 as the CLP fractions. However, in addition to the 103 kDa VP3 band, there was an intense band of lower electrophoretic motility, corresponding to GFP:VP3 (131 kDa). This indicates the presence of fluorescent core- or subcore-like particles. These fractions may contain a mixture of fluorescent and non-fluorescent particles, or mosaic particles, or both.

The ability of GFP:VP3 to form core-like particles containing 120 copies of GFP was finally proven by analysis of the fCLP fractions (Figure 7.3). These contained intense bands for both GFP:VP3 and VP7, indicating particle assembly. Crucially, there was no evidence of degradation products (i.e. free GFP and VP3), showing that all of the VP3 associated with the sedimenting particles was attached to GFP. The first evidence of the association of VP5 and VP2 with fluorescent BTV CLPs was found in the fractions of the fVLP gradient. Though the ratio of the outer shell proteins to core proteins was not indicative of a high proportion of VLP, the presence of VP2 and VP5 in the gradient fractions showed that the

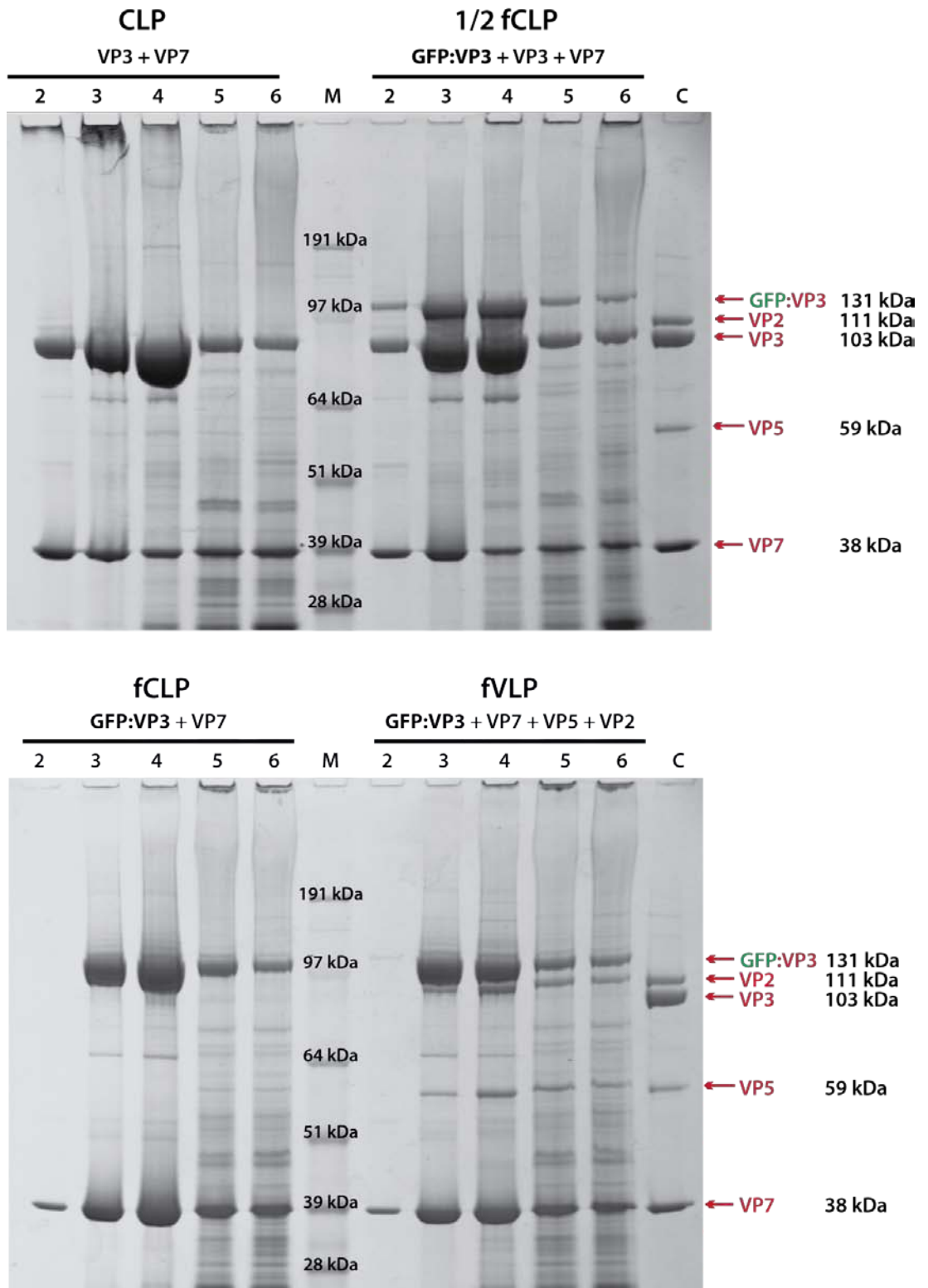


Figure 7.3: C-terminal fusion of GFP to VP3 does not significantly affect the gradient sedimentation pattern of co-expressed BTV-8 structural proteins.

Leaves were co-infiltrated with codon-optimized BTV8 constructs as indicated. 1/2 fCLP = infiltrations with GFP:VP3 and VP3-carrying *Agrobacteria* at half of the normal optical density each (i.e. $OD_{600} = 0.2$). Leaves were harvested 9 dpi, extracted in low-salt SSB and clarified extract separated on 15 - 45 % iodixanol step gradients. Key fractions were separated on 4 - 12 % SDS-PAGE gels and Coomassie blue stained. M = SeeBlue + 2 protein marker; C = purified BTV-8 VLP preparation.

outer shell proteins can associate with fluorescent core-like particles in the absence of untagged VP3.

7.3.3 OPTIMIZATION OF fVLP YIELD AND INTEGRITY

In order to study the uptake of Bluetongue virus by mammalian cells, it was important to produce particle preparations with a high proportion of fluorescent virus-like particles and few contaminating fCLP and fSCLP. Though the result presented above (Figure 7.3) shows that it is possible to produce fluorescent BTV particles with VP5 and VP2 attached, the ratio of BTV proteins is indicative of a mixture of fVLP, fCLP and fSCLP.

The best strategy for optimization of VLP yield has been found to be the use of a wild-type CPMV RNA-2 5'-UTR in the VP3 construct to down-regulate its expression relative to the other structural proteins (Section 6.3.5.3). Following this strategy, a new vector was prepared to replace the *HyperTrans* 5' UTR with the wild-type leader, thereby producing pEAQ-GFP:BTV8.3co. The effect of this change on the stoichiometry of BTV-8 protein expression was determined by production of fluorescent VLP with the *HT* and non-*HT* constructs for GFP:VP3 (Figure 7.4). As seen previously, the use of *HyperTrans* constructs results in an overproduction of VP3, resulting in an excess of GFP:VP3 and VP7 (Figure 7.4 A, lanes 7 + 8). BTV cores have a higher sedimentation rate than full virus, which explains why the excess of VP7 and GFP:VP3 is seen in the denser parts of the gradient. The BTV structural proteins in lanes 9-11 produce bands of similar intensity, as is expected for preparations of intact virus-like particles. The replacement of the *HyperTrans* leader of the GFP:VP3 construct results in similarly good fractions 9-11, indicating intact fVLP in these fractions (Figure 7.4 B). However, the over-representation of GFP:VP3 and VP7 in fractions 7 and 8 is greatly reduced. This indicates that, overall, leaves expressing GFP:VP3 from the wild-type leader construct have a higher proportion of fully assembled fVLP.

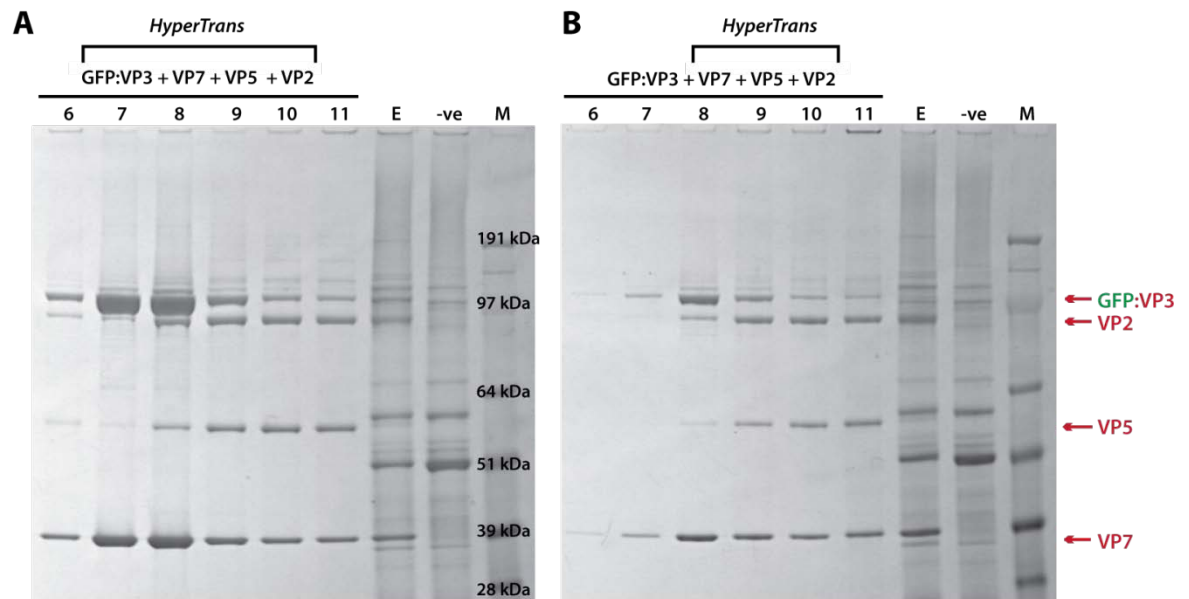


Figure 7.4: Lower expression levels of GFP:VP3 with a wild-type leader result in a reduced over-representation of fCLP in fVLP preparations.

Leaves were co-infiltrated with codon-optimized BTV8 constructs as indicated. GFP:VP3 was provided either in the context of a *HyperTrans* leader (A) or a wild-type leader (B). Leaves were harvested 8 dpi, extracted using BTV VLP extraction buffer and clarified extracts sedimented through discontinuous Optiprep gradients. Relevant fractions were separated on 4 - 12 % SDS-PAGE. M = SeeBlue + 2 protein marker; E = clarified extract; -ve = empty vector control extract.

In order to conclusively show that the fusion of GFP to VP3 does not inhibit the formation of virus-like particles, purified fVLP were imaged using negative staining and TEM (Figure 7.5). Images showed a high proportion of fully assembled fVLP, interspersed with some partially disassembled particles and fCLP. Fluorescent virus-like particles were morphologically indistinguishable from VLP (compare Figure 7.5 A and B). However, the internal cavity of fVLP did not appear to be as distinct, suggesting that the negative stain was less able to penetrate these particles. However, due to the variability of negative staining and TEM grid preparation, this distinction is not always clear.

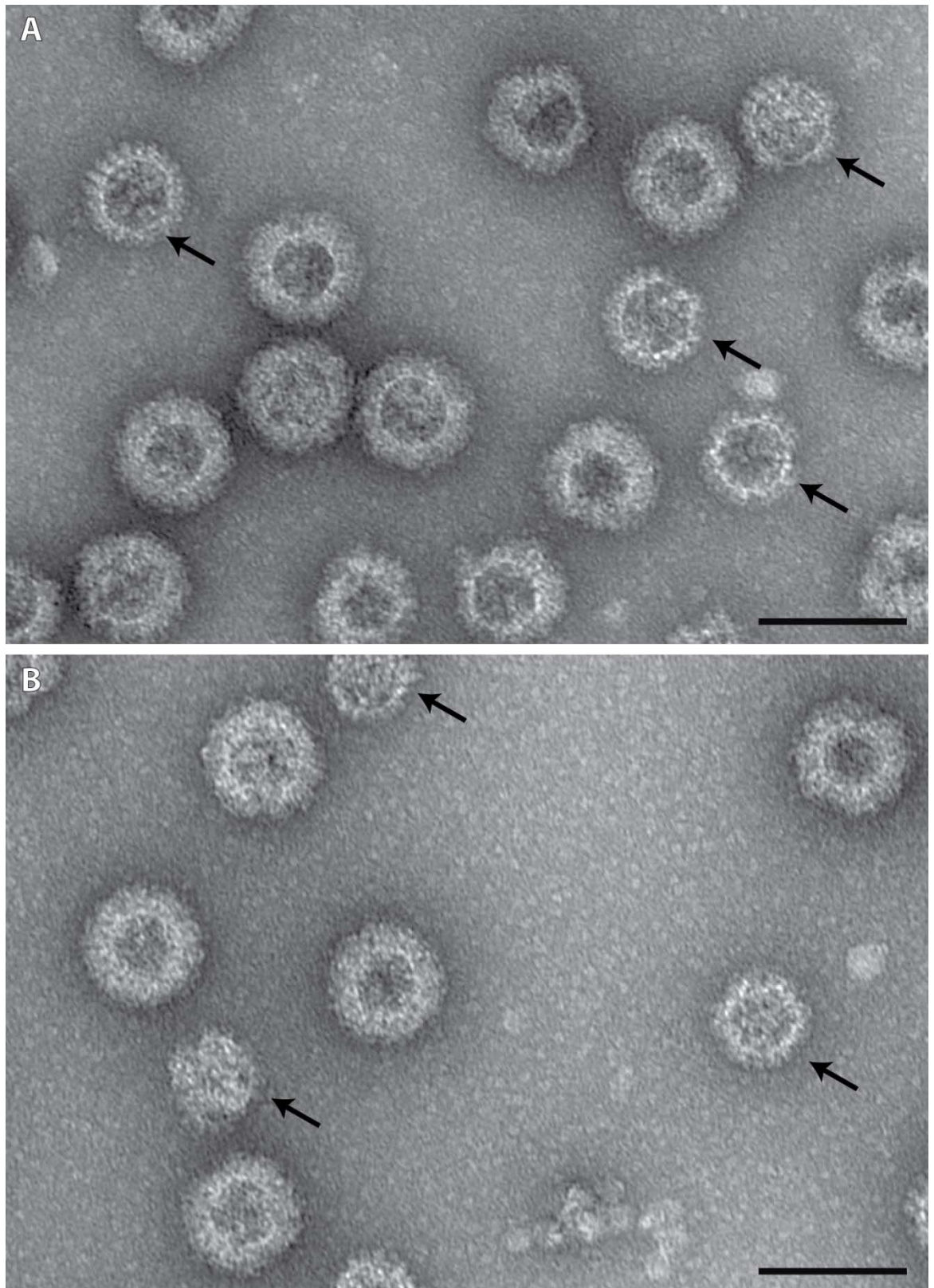


Figure 7.5: Purified fluorescent VLP are morphologically indistinguishable from normal VLP.

Virus-like particles were produced by co-expression of BTV-8 VP2, VP5 and VP7 with either VP3 to generate VLP (A) or GFP:VP3 to generate fVLP (B). Purified particle-containing sucrose fractions were imaged using negative staining (2% UA) and TEM. Arrows indicate particles which appear to have lost the outer shell. Scale bar = 100 nm.

7.3.4 INTERNALIZATION OF FLUORESCENT BTV-LIKE PARTICLES BY MAMMALIAN CELLS

One of the many potential uses of fluorescent Bluetongue VLPs is in the study of BTV cell entry. To determine whether plant-produced BTV fVLP bind mammalian cells, and to monitor their internalization, a confocal microscopy experiment with BHK cells was designed and carried out in collaboration with Dr. Sarah Gold and Dr. Terry Jackson (Institute for Animal Health, Pirbright).

In short, GFP fVLP were incubated with BHK cells on ice to allow binding of the virus to the cell membrane. After removal of unbound fVLP, uptake was initiated by incubation at 37 °C. Cells were fixed at time points of 0, 15, 30, and 60 minutes to monitor binding and uptake of virus. Permeabilization of the cells allowed VP5 to be labelled with a red Alexa Fluor dye by immunocytochemistry. The nuclei of the cells were stained with DAPI and fluorescent signals were imaged using confocal microscopy (Figures 7.6 and 7.7).

Before initiation of uptake (0 minute time point), signals for GFP:VP3 (green) and VP5 (red) were detected around the perimeter of the cells (Figure 7.6). The merged image showed co-localization (yellow) of the two signals, indicating that VP5 and GFP:VP3 were closely associated as is the case in virus-like particles. The binding of fVLP to BHK cells shows that the necessary binding motifs of VP5 and VP2 are present and in the correct conformation to allow interaction with the cell membrane and/or receptors.

After incubation at 37 °C for 15 minutes, the localization of GFP:VP3 and VP5 changed drastically. By this time, most of the fVLP had been internalized, resulting in punctate signals throughout the cytoplasm (Figure 7.6). The merged image showed that most of the GFP:VP3 and VP5 was still co-localized. This result shows that plant-produced fVLP are internalized efficiently by BHK cells, and that the core and outer shell of the particles is still in close proximity within the cells, 15 minutes after internalization.

At later time points, the signal for GFP:VP3 was gradually lost. Thirty minutes after initiation of uptake, both GFP:VP3 and VP5 signals were still detected throughout the cytoplasm (Figure 7.7). However, the merged image revealed that only a minority of foci showed co-localization of the two signals. The abundance of red foci within the cells indicated that VP5 was detected in these locations, whereas GFP:VP3 was not. This trend continued, and 60 minutes after internalization the vast majority of detected foci was red.

The gradual loss of GFP signal was not expected, but can be explained in two ways. One possibility is that the internalized particles partially disassembled after internalization, and that the fluorescent core-like particles were released from the early endosomes as is expected. If the core-like particles were spread out throughout the cytoplasm, the signal would be very dilute and hence not clearly detected. Another explanation for the loss of GFP signal is the fact that GFP fluorescence is pH-sensitive. From pH 7, EGFP fluorescence decreases rapidly with decreasing pH and is undetectable below pH 4.0 (Haupts et al., 1998). The pH of the early endosome has been found to be approximately pH 6, lowering to pH 5 upon fusion with lysosomes (Murphy et al., 1984). Such a pH shift may well be the cause of the loss of GFP signal at later time points.

The experiment presented here demonstrates the binding and internalization of plant-produced BTV-8 fVLP by BHK cells. However, to enable further study of the uncoating and intracellular movement of BTV by fluorescence tracking, it is essential to fuse VP3 to a fluorescent protein which fluoresces strongly at low pH.

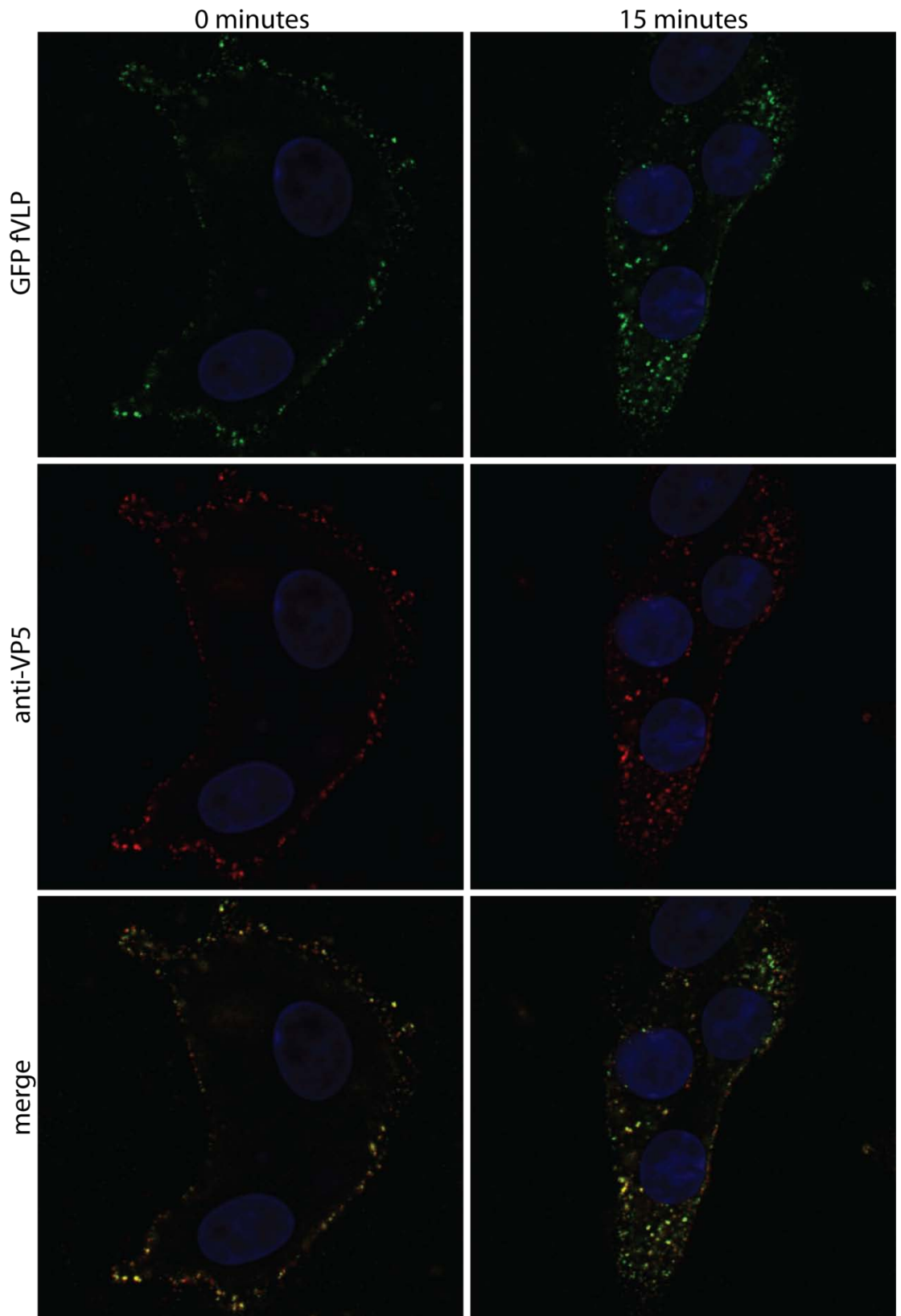


Figure 7.6: Plant-produced BTV-8 fVLP bind BHK cells and are internalized.

BTV-8 GFP fVLP were labelled with PM10 anti-VP5 antibody, then bound to BHK cells on ice 40 minutes, washed off, and uptake initiated by addition of pre-warmed medium. Uptake was stopped after 0 and 15 minutes and cells imaged using confocal microscopy to visualize DAPI-stained nuclei (blue), GFP (green), anti-VP5 antibody (red), and to determine co-localization (merge). Experiment performed in collaboration with Dr. Sarah Gold (IAH-P).

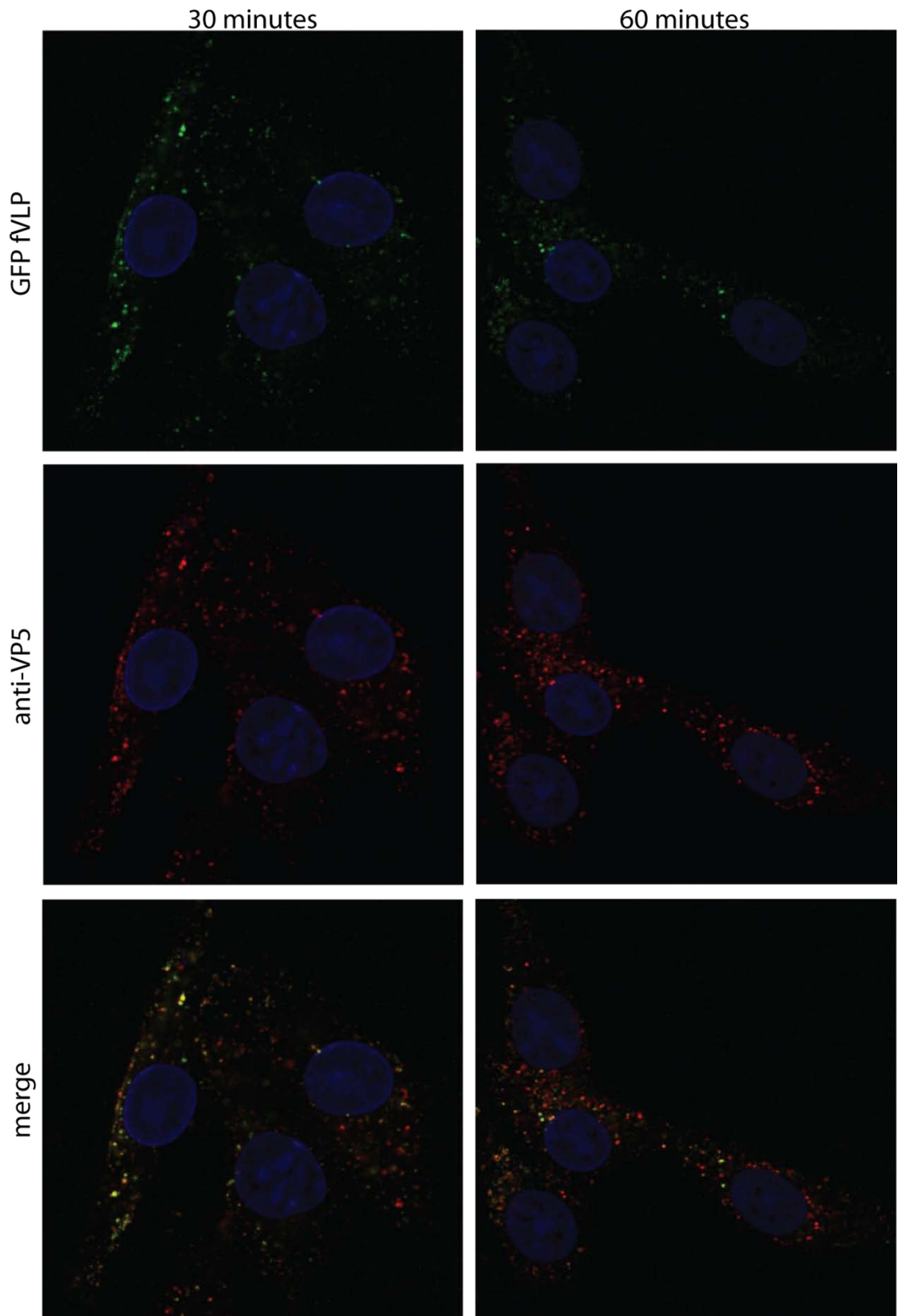


Figure 7.7: Plant-produced BTV-8 fVLP bind BHK cells and are internalized (Part 2).

BTV-8 GFP fVLP were labelled with PM10 anti-VP5 antibody, then bound to BHK cells on ice 40 minutes, washed off, and uptake initiated by addition of pre-warmed medium. Uptake was stopped after 30 and 60 minutes and cells imaged using confocal microscopy to visualize DAPI-stained nuclei (blue), GFP (green), anti-VP5 antibody (red), and to determine co-localization (merge). Experiment performed in collaboration with Dr. Sarah Gold (IAH-P).

7.3.5 RUBY + SAPPHIRE

The most likely explanation for the loss of GFP fluorescence upon internalization of GFP fVLP into BHK cells is the sensitivity of GFP to low pH. To widen the toolbox of fluorescent BTV particles, two other fluorescent protein variants were fused to the N-terminus of VP3 as previously described (section 6.2.1). mT-Sapphire is a green fluorescent protein with a pK_a of 4.9, making it more suited than EGFP to use in low pH environments (Zapata-Hommer and Griesbeck, 2003). mRuby is a monomeric far-red fluorescent protein with a pK_a of 4.4 and a higher fluorescence intensity than EGFP (Kredel et al., 2009). The constructs used for expression were called pEAQ-Sapphire:BTv8.3co and pEAQ-mRuby:BTv8.3co, respectively, and contained the wild-type CPMV RNA-2 leader sequence.

mRuby and mT-Sapphire fCLP (and fVLP) were produced by co-infiltration of the above constructs with *HyperTrans*, codon-optimized constructs for BTv-8 VP7 (and, when VLPs were required, also with VP5 and VP2). Upon separation of clarified extracts on sucrose density gradients, the Sapphire:VP3 fusion produced fluorescent bands similar to those seen for GFP:VP3-containing particles (Figure 7.8 A). As expected, the mRuby:VP3 extracts did not fluoresce green, but gradients showed a reddish band in the same area as the fluorescent band of GFP:VP3 gradients. The excitation wavelength of mRuby (558 nm) is not covered by the UV lamp used in these experiments, explaining the lack of intense far-red fluorescence.

Particle-containing fractions of the gradients were easily identified using a hand-held UV lamp. The most intensely fluorescent fractions were separated by SDS-PAGE and Coomassie-stained (Figure 7.8 B). The ratios of structural proteins detected in the fCLP and fVLP fractions did not differ significantly between the mRuby, mT-Sapphire and GFP particles. Fluorescent CLP fractions contained the respective VP3 fusion protein and VP7, with band intensities being similar, as expected for a molar ratio of 2 : 13. In the case of fluorescent virus-like particle fractions, VP2 and VP5 were also present. In the case of mRuby and mT-Sapphire fVLP, fraction 4 of the gradient appeared to contain an excess of the VP3 fusion protein, indicating contaminating fSCLP.

Fraction 3 of each gradient was deemed to contain the optimal stoichiometry of structural proteins for the respective species of fluorescent particle, and these fractions were imaged using negative staining and TEM (Figure 7.8 C). When compared with non-

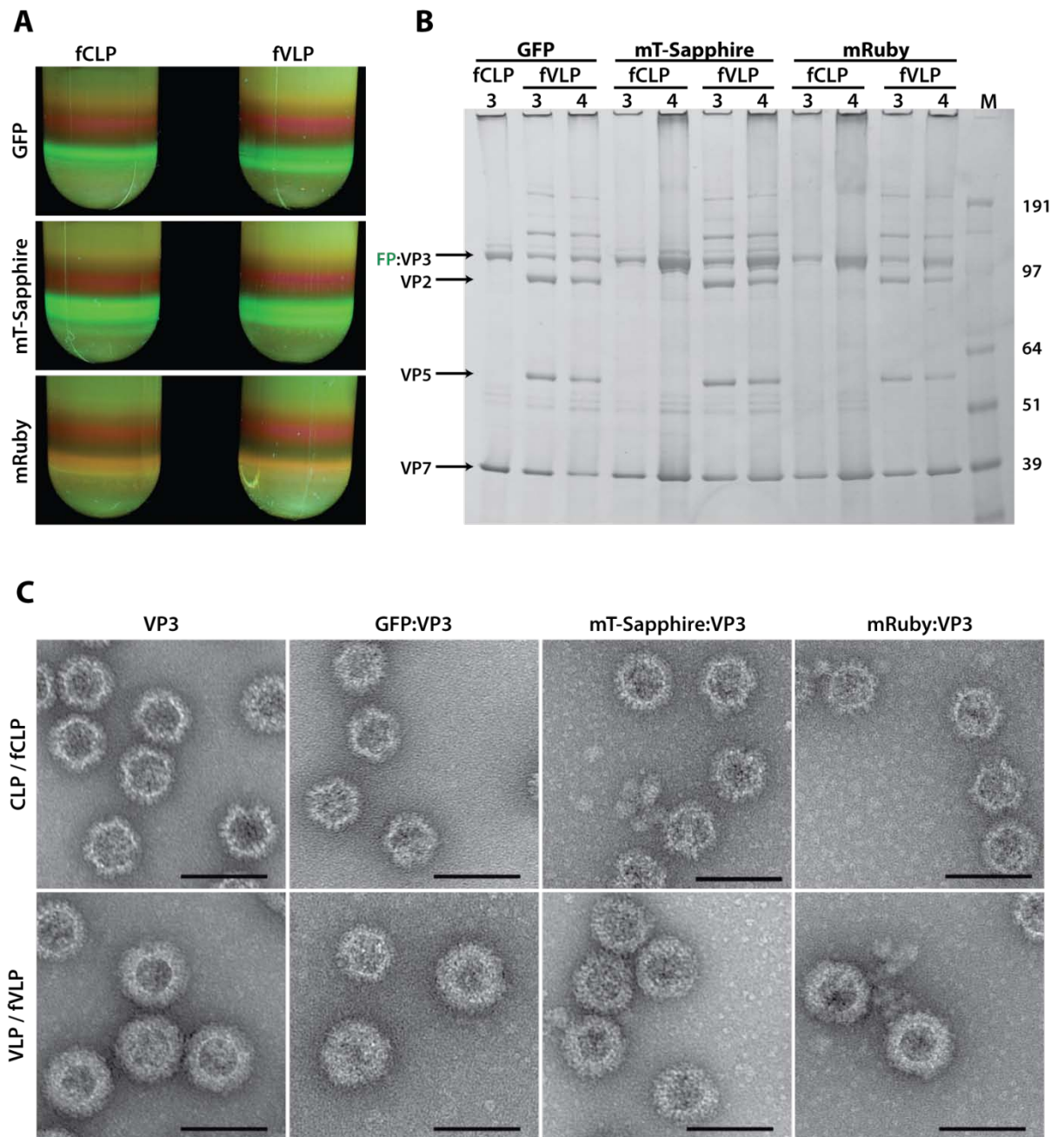


Figure 7.8: Production of fluorescent BTV-8 CLP and VLP with three different fluorophores.

fCLP (and fVLP) were produced by co-expression of BTV-8 VP7 (and VP5 and VP2) with one of three different VP3 versions: GFP:VP3, mRuby:VP3 or mT-Sapphire:VP3. (A) Clarified extracts were separated on sucrose density gradients and photographed under UV illumination. (B) The most fluorescent fractions were separated on 4 - 12 % SDS-PAGE and Coomassie blue-stained. (C) Fraction 3 of each gradient was imaged using negative staining and TEM. For comparison, CLP and VLP produced from regular VP3 are included. Scale bars = 100 nm.

fluorescent plant-produced CLP, the fluorescent CLP looked similar, with a distinctive spiky appearance owing to the VP7 trimers on their surface. Likewise, the fluorescent VLP were indistinguishable from the non-fluorescent VLP. As usual, some partially disassembled particles were present in the fVLP and VLP TEM grid preparations.

To determine whether the insertion of 120 fluorescent proteins on the inside of BTV-8 particles influences particle size, TEM images were used to measure particle diameters (Figure 7.9). At first glance, it appears as though virus-like particles containing GFP or mT-Sapphire are slightly smaller (ca. 6 nm) than either empty or mRuby-containing VLP. However, core-like particles derived from all four versions of VP3 have are very similar in size. Due to the instability of the outer shell of BTV, it is possible that the measured VLP size is variable and largely dependent on TEM grid preparation. Core-like particles are more stable and thus provide a more reliable measurement of relative particle size. In order to obtain more reliable data for VLP, it would be necessary to increase the sample number and to include data from multiple TEM grids for every particle species. Due to time constraints, this was not undertaken. The mRuby and mT-Sapphire particles have been supplied to my collaborators for use in further uptake studies to see whether they are less pH-sensitive, as expected.

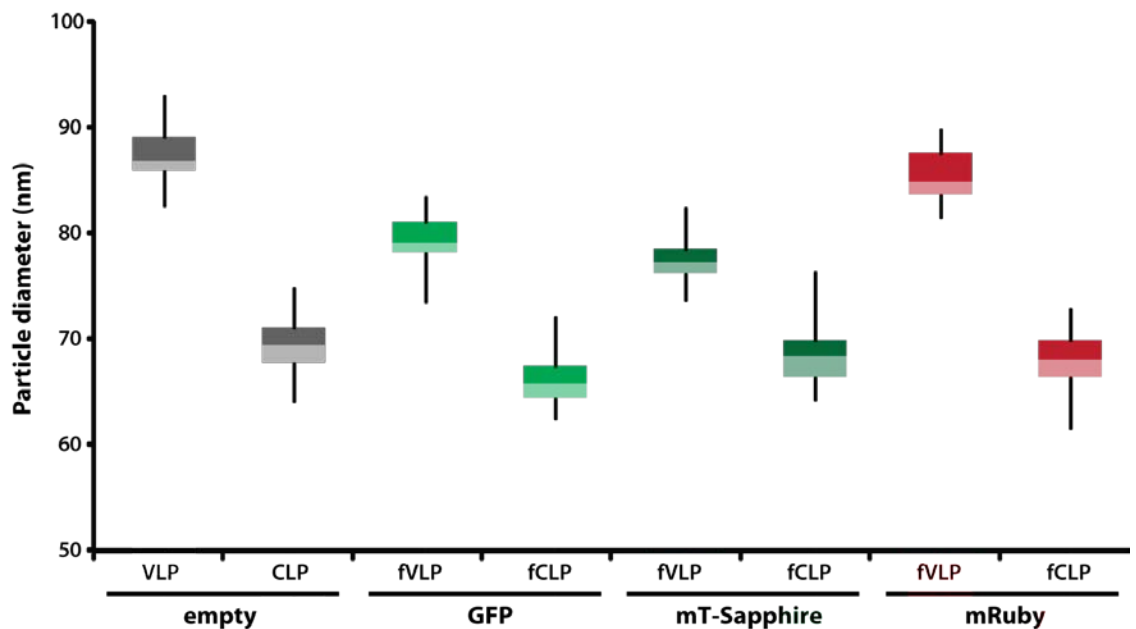


Figure 7.9: Core-like and virus-like particle size is not significantly influenced by fusion to fluorescent proteins.

Box plot analysis of the size distribution of different BTV-8 particles in TEM images. At least 25 particles were measured for each particle species using Adobe Photoshop. Data were analyzed with Microsoft Excel.

7.3.6 INTRACELLULAR LOCALIZATION OF GFP:VP3 IN PLANT CELLS

Tagging of VP3 with a fluorescent protein makes it possible to visualize the intracellular localization of VP3 and associated particle structures in the plant cells in which they are being expressed. In order to determine whether plant-expressed GFP:VP3 is found throughout the cytoplasm or in distinct foci, plants were infiltrated with combinations of GFP:VP3 and other BTV-8 structural protein constructs, and viewed using confocal microscopy.

Though GFP:VP3 is likely produced throughout the cytoplasm, fluorescence signals were detected only in distinct areas of the cell (Figure 7.10). Tissue expressing GFP:VP3 either on its own (fSCLP) or with VP7 (fCLP), contained large foci of fluorescence, usually in a single area of each cell. In contrast, tissue co-infiltrated with all four structural proteins of BTV contained cells with multiple, distinctly circular foci of fluorescence. As a control, pEAQ-HT-GFP was agroinfiltrated and tissue showed fluorescence throughout the cytoplasm of the cell. These preliminary results indicate that VP3 localizes to distinct areas of the cell upon expression, and that the presence of other BTV structural proteins influences the intracellular localization of VP3.

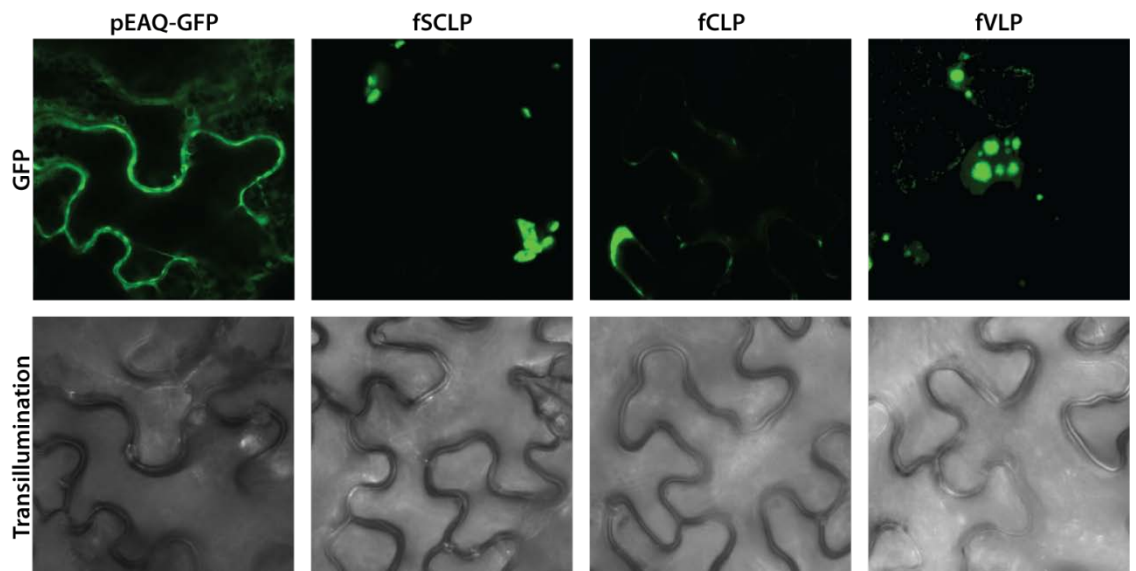


Figure 7.10: Intracellular localization of GFP:VP3 is influenced by co-expression of other structural proteins.

Plants were agro-infiltrated with constructs as indicated. GFP fluorescence in the lower epidermis was imaged at 8 dpi by confocal microscopy. fSCLP = GFP:VL3; fCLP = GFP:VP3 + VP7; fVLP = GFP:VP3 + VP7 + VP2 + VP5.

Given the necessary time, this experiment could be improved in several ways. To determine whether GFP:VP3 is associated with specific subcellular compartments, a combination of different vital stains could be used to visualize the nucleus (DAPI), cellular membranes (FM4-64) or mitochondria (MitoTracker). When visualizing individual cells, it is crucial to ensure that all proteins are efficiently co-expressed in each cell. Previous experiments have demonstrated that co-infiltration is not an effective means of ensuring efficient co-expression in every cell (Section 3.3.6). Thus, it is important to repeat this experiment with constructs containing all BTV structural proteins on the same T-DNA, as done in Section 6.3.5.2.

7.4 DISCUSSION

During the past decade, fluorescent particles of many different viruses have been produced for use in the study of virus function, or as a proof of principle for the encapsidation or display of large epitopes (reviewed by Brandenburg and Zhuang, 2007). However, the compact, multimeric structure of simple icosahedral viral capsids poses the problem of steric hindrance for the tagging of these viruses with functional fluorescent proteins. For instance, a small viral capsid composed of 240 subunits of one structural protein, e.g. the Hepatitis B core, will display 240 copies of the fused fluorescent protein. In Chapter 4 I have shown how the development of tandem HBcAg has enabled the display of a large polypeptide on every second *c/e1* loop, thereby reducing the steric hindrance. The display of foreign protein structures has focussed mainly on the outside of viral capsids where there is more space for folding.

Bluetongue virus and other *Reoviridae* have internal capsid structures which allow relatively few (120) foreign proteins to be assembled within a relatively large central cavity of up to 46 nm diameter (Fauquet et al., 2005, p. 467). The encapsidation of foreign proteins on the inside of a virus-like particle can have several key advantages: (1) Inside the particle, a foreign peptide is protected from the cellular protein degradation machinery. (2) If the linker between the structural protein and the foreign peptide is unstable, the detached foreign protein will remain trapped within the assembled particle.

(3) With the outer surface of the particle resembling the native virus, biophysical properties such as surface charge and isoelectric point will be largely unchanged, thereby allowing these particles to be purified using established protocols. (4) Structures on the outer surface of the particles which play a crucial role in receptor binding, cell attachment, cell entry, intracellular trafficking or localization will be present in their native conformation and will not be obscured by the foreign polypeptide. Depending on the application, however, the display of polypeptides on the outside may be necessary (e.g. targeting, receptor-ligand interaction).

Although the assembly of BTV particles containing GFP in insect cells was reported over five years ago, the huge potential of this tool for basic research of BTV and for biotechnological applications has not been exploited (Kar et al., 2005). The reasons for this may include low yield, instability of the linker between GFP and VP3, and most crucially the inability to form stable full virus-like particles with a complement of VP2 and VP5.

Here, an attempt was made to express GFP-tagged BTV-8 VP3 in plants, and to purify fluorescent BTV particles as was previously done using the baculovirus system (Kar et al., 2005). The instability of the GFP:VP3 fusion protein reported in the latter publication was addressed by the insertion of a flexible SGG linker between the two proteins, based on the good results achieved with such a linker during the expression of GFP-tagged tandem HBcAg (Chapter 4). This GFP:VP3 fusion protein was successfully expressed in leaf tissue on its own allowing assembly of fluorescent subcore-like particles (data not shown) and was found to assemble into fluorescent core-like particles when co-expressed with VP7 (Figure 7.2). The presence of a high proportion of untagged VP3 in fluorescent particles prepared using the baculovirus expression system (Kar et al., 2005) led authors to speculate that GFP-tagged VP3 can only assemble into chimaeric particles containing a proportion of untagged VP3 (Kar et al., 2005). This was disproved by the finding that fCLP produced from GFP:VP3 in plants contain only the fusion protein, with cleaved VP3 undetectable in these preparation. This shows that all 120 copies of VP3 in a particle can accommodate a large N-terminal extension.

While fluorescent BTV core-like particles have been produced previously, fluorescent virus-like particles have not been reported. However, similar experiments with GFP-tagged VP2 of the closely related rotavirus have resulted in virus-like particles consisting of all four structural proteins (Charpilienne et al., 2001). Though this publication did not

provide direct proof in the form of TEM images or SDS-PAGE gels, the indirect evidence of the assembly of the outer shell provides a good indication that it may be possible to produce full Bluetongue virus-like particles. In this chapter I have shown that GFP:VP3 does, in fact, assemble into fVLP when co-expressed with VP7, VP5 and VP2. Though the first attempts provided only a poor recovery of outer shell proteins, the stoichiometry was greatly improved by limiting of GFP:VP3 expression through the use of a wild-type 5'UTR as described in Chapter 6. Transmission electron microscopy confirmed that the fluorescent virus-like particles closely resembled normal VLP. To my knowledge, no TEM images of fluorescent *Reoviridae* particles have been published.

Purified plant-produced fluorescent BTV particles have already been supplied to several research groups for use in their experiments. At the John Innes Centre, an attempt has been made by Dr. Allister Crow to crystallize fCLP in order to obtain structural data for the encapsidated fluorescent protein. A positive outcome of this proof of principle experiment would open the door to the crystallization of other “difficult” proteins by proxy. The BTV particle scaffold would ensure solubility of the cargo protein and should allow standardized crystallization conditions to be employed. The design of the VP3 fusion construct allows for easy substitution of the *gfp* gene with any other gene of interest. It is questionable, however, whether the flexible linker inserted between VP3 and the cargo protein would allow for good crystallographic data to be obtained. Another possibility to obtain structural data for a cargo protein is provided by cryo electron microscopy. A sample of fVLP has been frozen in vitreous ice at the Division of Structural Biology, University of Oxford, and is awaiting CEM analysis by the research group of Dr. Robert Gilbert. These structural studies would also provide evidence for the structural integrity of plant-produced BTV VLP.

The most obvious application for fluorescent BTV particles is in the study of viral movement into and within cells. Purified fCLP have been supplied to Dr. Tom Wileman (University of East Anglia) for use in microinjection studies to track the movement of virus structures within cells. A collaborative project has been set up with Drs. Terry Jackson and Sarah Gold at the Institute for Animal Health, Pirbright, to study the binding and internalization of BTV in mammalian and insect cells. The results of preliminary experiments have been presented here. Plant-produced fVLP were shown to bind BHK cells *in vitro*, and the particles were internalized efficiently. In these experiments, the BTV core was visualized by excitation of the encapsidated GFP, while the outer shell was detected by immunocytochemistry using an antibody against VP5. This allowed

visualization of the co-localization of the inner and outer shells of the virus-like particles. It was expected that the signals for VP3 and VP5 would separate upon release of the core-like particle into the cytoplasm, thereby providing proof of the uncoating of the VLP upon endocytosis. However, the signal for GFP was lost unexpectedly, soon after uptake of the fVLP. This result mirrors the finding that trypsinized fluorescent rotavirus VLP are not detectable after uptake by MA104 cells (Charpilienne et al., 2001). The most logical explanation for this would be the quenching of fluorescence due to a rapid lowering of pH in the early endosome (Murphy et al., 1984; Patterson et al., 1997).

In an attempt to produce fluorescent BTV particles which are not quenched by the low pH of the endosome, GFP was replaced by two pH-stable fluorescent proteins, mRuby and mT-Sapphire (Kredel et al., 2009; Zapata-Hommer and Griesbeck, 2003). Expression and purification of these new fluorescent particles was done using the same protocols optimized for non-fluorescent BTV VLP (Chapter 6), and resulted in a similar yield. The transferability of purification methods to particles encapsidating foreign proteins provides an indication that expression of a foreign sequence on the inside of a particle leaves the biophysical surface properties of the particle largely unchanged. This is in stark contrast to the insertion of GFP on the outside of tandem Hepatitis B core-like particles, which were thereby rendered completely insoluble and required many changes to extraction conditions to allow recovery of even a small proportion of soluble particles (Chapter 4).

TEM analysis of the size and shape of fluorescent and non-fluorescent BTV CLP and VLP revealed that the presence of a foreign polypeptide on the inside of the BTV particles does not significantly affect their morphology. The four species of core-like particle (GFP-, mT-Sapphire-, mRuby-fused or wild-type) were similar in size, with fluorescent particles, if anything, appearing to be slightly smaller than wild-type particles. Though this finding was not statistically significant, it is consistent with the observation that empty BTV core-like particles are slightly larger than dsRNA-containing authentic core particles (Hewat et al., 1992). It would be interesting to compare structural data for authentic cores, core-like and fluorescent core-like particles to determine whether the packing of density on the inside of the particles causes subtle changes in particle structure.

In addition to the applications in structural studies and virus uptake discussed above, fluorescent BTV particles have the potential to be exploited for several other purposes. The functional cell attachment domains of the outer shell proteins could be studied by

co-expression of mutant versions of these proteins with fluorescent cores, followed by analyses of the effects on binding and uptake efficiency. It might be possible to co-express the mRuby fluorescent cores with a mT-Sapphire-tagged VP2, thereby producing dual-labelled VLP for real-time detection of the dissociation of BTV protein shells during infection (Bhattacharya et al., 2007). The GFP:VP3 fusion protein has already been used to study the localization of virus assembly, and this could be expanded upon (Kar et al., 2005). Fluorescent, fully assembled virus-like particles could also be used to shed light on the non-lytic virus egress by interaction with the cell membrane-associated non-structural protein NS3 in insect cells. It could also be possible to feed *Culicoides* species with fluorescent VLP in an effort to elucidate the viral infection process in the insect host.

During the many rounds of expression and particle purification performed as part of this project, the fluorescence of the particles was found to greatly facilitate the tracking of particles throughout the purification process. By simply shining UV light onto gradients, gel filtration columns and buffer exchange columns, it was possible to monitor which fractions contained BTV particles and to see whether significant loss of particles had occurred due to aggregation. If Bluetongue VLPs are to be developed as a vaccine, extraction and purification conditions will have to be further optimized for large-scale production. For these purposes, fluorescent particles may provide the ideal tool for the rapid analysis of the effect of changes to the established protocols. Furthermore, particle stability in a variety of pH, salt and temperature conditions as well as after long-term storage could be easily assessed using fluorescent particles.

The design of the developed GFP:VP3 construct allows other genes to be substituted for *gfp* through use of unique restriction sites. Thus, other proteins can be easily fused and tested for particle assembly within several days by transient expression using the CPMV-*HT* system. This provides a great advantage over the slower baculovirus expression system. It has been shown that immunization with BTV and rotavirus particles displaying an antigenic sequence on the inside induces an immune response against the inserted foreign peptide (Charpilienne et al., 2001; Tanaka et al., 1995). The apparent superior stability of the GFP:VP3 fusion protein seen here opens up the possibility for using plant-produced BTV particles as epitope carriers in the development of vaccines against other agents. It would be interesting to attempt the production of chimeric BTV CLP containing several different VP3 fusion proteins. As a proof of principle, this could be achieved by co-expression of GFP:VP3 and mRuby:VP3, followed by confocal microscopy of a dilute solution of purified particles to show co-localization of the green and red signals. Another

possibility would be the insertion of peptides with an affinity for certain drugs or metals. The large pores of the BTV CLP should allow the particles to be loaded with drug molecules, enabling the use of BTV as a vehicle for drug delivery, as envisaged for other viruses (Franzen and Lommel, 2009; Lee and Wang, 2006).

In conclusion, the work presented here shows that it is possible to produce high yields of fully assembled fluorescent Bluetongue Virus-like particles in plants which may find uses in basic research, downstream processing optimization, biotechnological and biomedical applications in the future.

8 DISCUSSION AND OUTLOOK

The overall aim of this thesis was to push the boundaries of virus-like particle production in plants by making use of recent advances in transient expression technology. Two of the main applications of VLPs, i.e. their use as vaccines in their own right, and their function as carriers of foreign epitopes, have been addressed by the expression of Bluetongue and Hepatitis B particles. Furthermore, a toolbox of small binary vectors has been created, which are uniquely suited to exploit the benefits of the CPMV-*HT* system for the transient expression of complex, heteromeric BTV-like particles – the largest and most complex biopharmaceutical protein structures to have been expressed in plants to date.

The CPMV-*HT* system achieves high expression levels by enhanced translation, not replication, and it has been shown to be ideally suited to the co-expression of up to three GOI by co-infiltration (Sainsbury and Lomonossoff, 2008). However, for the efficient cloning and co-expression of four BTV structural proteins as well as P19 within the same cell, the existing, outdated vector system had to be changed. In fact, I have shown that co-infiltration is not an efficient means of ensuring consistent cellular co-expression of as few as two foreign proteins, let alone five. The pEAQ vector series was developed to bring the CPMV-*HT* cloning system up to date and to allow for consistent co-expression of multiple proteins from a single T-DNA construct (Sainsbury et al., 2009). The pEAQ vectors are the first binary vectors to include an expression cassette for a suppressor of gene silencing, ideal for transient expression. Gateway-compatible versions of the vectors allow the CPMV-*HT* system to be used for high-throughput screening of new constructs, and allow it to be tested in parallel with other Gateway-compatible expression systems. In fact, Gateway cloning has allowed me to test the CPMV-*HT* leader sequences for expression of GFP in insect cells using the baculovirus system, which has provided a first indication of the functionality of CPMV-*HT* in heterologous systems (data not shown here). To date, in excess of 100 research groups and companies have used the pEAQ vectors, and they are one of the main expression platforms of the EU Framework 7 PLAPROVA project, showing that they are a widely used toolbox for various protein expression projects beyond the scope of this thesis. In particular, these vectors have been supplied to Medicago Inc., a company which is using the CPMV-*HT* system to produce influenza vaccines for human clinical trials.

For the purposes of my project, the pEAQ vectors were first used to express a relatively simple VLP, the hepatitis B tandem core. While wild type HBcAg particles have been produced successfully in many expression systems, including the CPMV system in plants (Mechtcheriakova et al., 2006; Sainsbury and Lomonossoff, 2008), tandem HBcAg particles have proved difficult to produce. Collaborators at the University of Leeds and Iqur Ltd, who developed the tandem core technology to overcome steric hindrance limitations in the use of wild type HBcAg as an epitope display platform, have expressed tHBcAg in *E. coli* and yeast systems. While empty tandem core particles can be produced efficiently using these systems, the attachment of GFP as a model epitope yielded a heterogeneous mixture of particle sizes which were not amenable to purification and structural analyses. This irregularity in particle structure presents a major hurdle in the adoption of tandem core technology for the development of human vaccines, due to strict quality assurance guidelines associated with regulatory approval of biopharmaceuticals. The challenge to produce more homogeneous tandem core particles with large inserts in a plant system was taken up.

In Chapter 4 I have shown that tHBcAg particles presenting active GFP on the outer surface can be expressed efficiently in plants using the pEAQ vectors. These particles are very regular in size and shape, allowing them to be used in structural studies using cryo-electron microscopy. The three-dimensional reconstruction obtained by CEM clearly shows the regular shape of the hepatitis B tandem core particle with a surrounding layer of density corresponding to the displayed GFP.

This proof of concept opens the door to allow the tandem core technology to be used for the display of other, more medically relevant epitopes and proteins. In fact, I have shown that a range of other tHBcAg constructs can be expressed using the CPMV-*HT* system. Constructs for the display of two model epitopes, namely GFP and a 40 aa fragment of the Hepatitis B surface antigen, exploit the unique propensity of tHBcAg to accommodate two different foreign sequences. Such particles could be used as bivalent vaccines, as first suggested by Brown et al (1991), or could include a targeting peptide to allow for targeted delivery of the tHBcAg particles to specific cell types. However, the display of foreign peptides on the outside of VLPs profoundly changes their surface properties, and this has led to the problem of aggregation of most of the tHBcAg constructs expressed during the work reported in this thesis. If tandem core technology is to be exploited commercially, it will be important to invest in the development of downstream processing protocols and buffers that are tailored for every new construct.

The finding that tHBcAg particles displaying GFP assemble more reliably in plant cells than they do in *E. coli* or yeast is another indication that plant-based pharmaceutical production systems have some key benefits over other traditional systems. As discussed previously, plants have the benefits of other eukaryotic systems, allowing for superior folding with the help of chaperones, and post-translational processing such as glycosylation and disulfide bond formation. In fact, transgenic plant systems are being developed which allow for near-human glycosylation patterns of antibodies and other biopharmaceuticals (Gomord et al., 2010). In comparison with mammalian cell production systems, plants have the added advantages of no risk of contamination with animal viruses and potentially far lower production costs. In fact, even the cost of cGMP plant production facilities are 3-4 times lower than the cost of mammalian cell culture facilities (Gleba, 2009). The development of new products using viral vector-based transient expression is also extremely fast, as demonstrated recently by the development of a plant-based VLP vaccine against the new H1N1 “swine flu” strain of influenza within three weeks of the release of the genetic sequence (D'Aoust et al., 2010). However, with big pharma slow to adopt this new technology, acceptance of plant-based expression systems may be raised by the development of a veterinary vaccine, such as Bluetongue virus-like particles, as a less tightly regulated stepping stone.

The pEAQ vectors have been a particularly useful and essential tool in the production of BTV-like particles. I have shown that it is possible to produce assembled virus-, core- and subcore-like particles of two BTV serotypes in plants, making this the second production platform successfully used for this purpose (after insect cells). Interestingly, it has been possible to produce SCLP by expression and self-assembly of VP3 alone, contradicting previous reports that SCLP can only be produced by removal of the outer layers of CLPs and VLPs (Hewat et al., 1992; Loudon and Roy, 1992). This is another indication of the superior ability of plants to produce the correct tertiary and quaternary structures of heterologous proteins.

The complexity of the BTV VLP arises from the stoichiometry of the structural proteins, the multi-layered structure, and the differing stabilities of the layers. The ratio of the four structural proteins comprising each BTV particle is 2 : 13 : 4 : 6 (VP3 : VP7 : VP2 : VP5), in stark contrast to the simple tHBcAg particle consisting of only one structural protein, or even CPMV or FMDV particles which have two or three structural proteins, respectively, at equimolar ratios. Expression of these four proteins at the required ratios is further complicated by the fact that expression levels attained for any given protein are

dependent on many factors such as mRNA stability, codon-usage, protein stability, protein toxicity, etc. Since BTV particles can exist in at least three different forms (SCLP, CLP, VLP), it is inevitable that particle preparations will contain a mixture of different particles. Close scrutiny of TEM images of Bluetongue virions and virus-like particles in published literature reveals a mixed population in most cases (French et al., 1990; Hewat et al., 1994; Roy et al., 1992). However, for the purposes of vaccine production, it is essential to produce the most homogeneous preparation of full VLPs possible, since the outer shell proteins VP5 and VP2 are the main immunogenicity determinants of BTV and are essential for vaccine efficacy. In Chapter 6, three strategies were employed to tackle the stoichiometry problem: (1) reduced relative expression of core proteins from non-codon-optimized constructs; (2) cloning of all four BTV genes and P19 onto the same T-DNA to ensure efficient co-expression; (3) reduced expression levels of the innermost protein (VP3) by selective combinatorial use of delRNA-2 with CPMV-*HT*. The third, and most effective approach made VP3 expression the limiting factor in particle assembly, allowing any VP3 particles the highest chance of acquiring a full complement of VP7, VP5 and VP2. Optimization of extraction and purification conditions enabled the recovery of highly pure and homogeneous VLP preparations using this approach.

The ability to modulate the relative expression levels of multiple proteins may have implications for other biotechnological applications. In the case of metabolic pathway engineering, individual enzymes may be needed at lower levels than others to ensure efficient conversion of a substrate to a desired product. The CPMV expression system is already being used for metabolic pathway engineering, for instance for production of the plant defense compound avenacin (Mugford et al., 2009). Another example would be the production of multiple proteins from a polyprotein by co-expression of a protease, where only relatively low levels of the protease enzyme may be needed. Proteases are often toxic when expressed at high levels, hence a lower expression level may be essential. In the case of the work presented here, it would be good to attempt the expression of relatively low levels of BTV-8 NS3 together with the structural proteins in order to reduce the necrosis associated with NS3 and to allow assembled VLPs to egress from the cells.

The pEAQ vectors can be used for simultaneous co-expression of at least five different genes of interest by transient expression. Though such a construct has not so far been tested for the regeneration of stable transformants, it is likely to make the recovery of homozygous lines for the expression of multiple proteins much easier.

Work on the expression of BTV particles was complicated by the lack of commercially available antibody and positive controls. Obtaining functional antibodies would allow several key experiments to be performed in the future, including Western blots, immunogold labelling of VP2 and VP5 to prove that VLP contain both outer shell proteins, and ELISA to quantify the produced proteins and particles. Antibody production in sheep is underway using the plant-produced VLP described in Chapter 6. I hope that the resulting antisera will be used to show production of virus-neutralizing antibodies, a key indication of efficacy as a vaccine. These will also be an invaluable tool for further BTV research by collaborators in South Africa. Furthermore, an efficacy trial using sheep has been planned by a company in South Africa to test both the plant-produced VLP and CLP for induction of protective immunity against Bluetongue disease. Particle aliquots are ready and awaiting shipping permit approval. The particles produced here are morphologically and stoichiometrically equivalent to insect cell-produced VLP, and I expect them to be just as effective. It may be worth investigating a possible oral vaccination strategy which would greatly facilitate immunization of large animal herds.

The ability to produce relatively homogeneous BTV VLP preparations using the CPMV-*HT* system led me to consider other applications for these particles, in addition to their use as a vaccine. It had already been shown that fluorescent CLPs of BTV could be produced in insect cells by way of fusing GFP to the N-terminus of VP3 (Kar et al., 2005). This fusion protein was used to track the intracellular localization of VP3 in insect cells expressing other BTV proteins. However, the fluorescent particles have not been used in basic research into the infection cycle of BTV. This is likely due to the instability of these particles and the inability to produce full fVLP with an intact VP2 and VP5 layer. Using the CPMV-*HT* system, it has been possible to produce such fluorescent VLP, which resemble the wild type VLPs in size and appearance under the TEM. Particles which contain the pH stable fluorescent proteins T-Sapphire and mRuby have also been produced. These particles are being used in a collaborative project with Drs. Terry Jackson and Sarah Gold at the Institute for Animal Health (Pirbright, UK) to study BTV cell attachment, internalization and disassembly in mammalian cells. By labelling the outer shell with a fluorescent dye, it should be possible to track virus entry as well as the disassembly of the outer shell and egress of the core particle into the cytoplasm of the infected cell. Such a system would allow easy monitoring of any effects of selective mutation of host or virus factors playing a role in internalization, thereby providing new insight into the process of BTV infection. This may also be applied to the insect vector. In the plant system, it would also be interesting to co-express a tonoplast-targeted BTV NS3 protein with the

fluorescent particles, which may allow the particles to “egress” into the plant cell vacuole. If this were possible, it could be used as a model system to study the factors involved in viral egress.

Encapsidation of epitopes on the inside of BTV core-like particles has been shown to elicit an immune response against these foreign peptides (Tanaka et al., 1995). The design of the GFP:VP3 fusion construct used here allows the *gfp* sequence to be easily replaced by other genes. Therefore, it should be straightforward to produce BTV particles with other foreign epitopes or whole proteins encapsidated on the inside, for use as vaccines. Such chimaeric virus-like particles with a full complement of VP5 and VP2 would likely be stronger immunogens than the core-like particles produced previously, due to their ability to bind mammalian cells and to be internalized. With the recent publication of detailed structural data for VP2 and VP5 (Zhang et al., 2010), it may be possible to design fusion proteins for the display of targeting peptides on the outer surface of BTV particles, further increasing their versatility.

The experiments with GFP-tagged VP3 presented here show that the display of GFP on the inside of BTV does not greatly alter the BTV particle surface properties, allowing them to be purified using the established protocols for untagged particles. This is in stark contrast to the GFP-displaying tHBcAg particles which required protocol optimization to allow recovery of even a small fraction of the particles. The ability to use a universal downstream-processing procedure for the purification of an array of different epitope-displaying VLPs is a great advantage. Assuming that BTV-like particles can elicit a strong, protective immune response against a foreign peptide displayed on their inside, I would argue that these particles could rival hepatitis B cores in their use as a versatile epitope carrier.

The work presented in this thesis provides a significant step forward in the establishment of plants as an alternative platform for VLP production. VLPs are a newly established vaccine technology, and though their efficacy and superior safety are widely accepted, the high cost of production associated with the cell culture systems used in their production has limited their use to economically important human diseases. Here, I have shown that the CPMV-*HT* system in conjunction with the newly developed pEAQ vectors is the ideal system for the production of highly complex heteromeric VLPs in plant tissue, showing that the system can rival traditionally used insect cell systems in its versatility. If acceptance of plant-based expression systems as a cheaper alternative can

be raised, the presented system has the potential to make VLP technology a more widely viable vaccine strategy to combat other human and veterinary diseases.

REFERENCES

- Aljabali, A.A.A., Sainsbury, F., Lomonossoff, G.P., and Evans, D.J. (2010). Cowpea mosaic virus unmodified empty virus-like particles loaded with metal and metal oxide. *Small* 6, 818-821.
- Backx, A., Heutink, R., van Rooij, E., and van Rijn, P. (2009). Transplacental and oral transmission of wild-type bluetongue virus serotype 8 in cattle after experimental infection. *Veterinary Microbiology* 138, 235-243.
- Bahnemann, H.G. (1976). Inactivation of viruses in serum with binary ethyleneimine. *Journal of Clinical Microbiology* 3, 209-210.
- Bandurska, K., Brodzik, R., Spitsin, S., Kohl, T., Portocarrero, C., Smirnov, Y., Pogrebnyak, N., Sirko, A., Koprowski, H., and Golovkin, M. (2008). Plant-produced hepatitis B core protein chimera carrying anthrax protective antigen domain-4. *Hybridoma* 27, 241-247.
- Bartlett, J.S., and Samulski, R.J. (1998). Fluorescent viral vectors: A new technique for the pharmacological analysis of gene therapy. *Nature Medicine* 4, 635-637.
- Basak, A.K., Grimes, J.M., Gouet, P., Roy, P., and Stuart, D.I. (1997). Structures of orbivirus VP7: Implications for the role of this protein in the viral life cycle. *Structure* 5, 871-883.
- Batten, C.A., Maan, S., Shaw, A.E., Maan, N.S., and Mertens, P.P.C. (2008). A European field strain of bluetongue virus derived from two parental vaccine strains by genome segment reassortment. *Virus Research* 137, 56-63.
- Baulcombe, D. (2004). RNA silencing in plants. *Nature* 431, 356-363.
- Bedoya, L., Martínez, F., Rubio, L., and Daròs, J.A. (2010). Simultaneous equimolar expression of multiple proteins in plants from a disarmed potyvirus vector. *J Biotechnol.*
- Bevan, M. (1984). Binary *Agrobacterium* vectors for plant transformation. *Nucleic Acids Res* 12, 8711-8721.
- Bevan, M.W., Flavell, R.B., and Chilton, M.D. (1983). A chimaeric antibiotic-resistance gene as a selectable marker for plant-cell transformation. *Nature* 304, 184-187.
- Bhattacharya, B., Noad, R.J., and Roy, P. (2007). Interaction between bluetongue virus outer capsid protein VP2 and vimentin is necessary for virus egress. *Virology Journal* 4, -.
- Bhattacharya, B., and Roy, P. (2008). Bluetongue virus outer capsid protein VP5 interacts with membrane lipid rafts via a SNARE domain. *J Virol* 82, 10600-10612.
- Birnbaum, F., and Nassal, M. (1990). Hepatitis B virus nucleocapsid assembly - primary structure requirements in the core protein. *J Virol* 64, 3319-3330.
- Böttcher, B., Wynne, S.A., and Crowther, R.A. (1997). Determination of the fold of the core protein of hepatitis B virus by electron cryomicroscopy. *Nature* 386, 88-91.
- Boyce, M., Wehrfritz, J., Noad, R., and Roy, P. (2004). Purified recombinant bluetongue virus VP1 exhibits RNA replicase activity. *J Virol* 78, 3994-4002.

- Brandenburg, B., and Zhuang, X.W. (2007). Virus trafficking - learning from single-virus tracking. *Nature Reviews Microbiology* 5, 197-208.
- Brown, A.L., Francis, M.J., Hastings, G.Z., Parry, N.R., Barnett, P.V., Rowlands, D.J., and Clarke, B.E. (1991). Foreign epitopes in immunodominant regions of hepatitis B core particles are highly immunogenic and conformationally restricted. *Vaccine* 9, 595-601.
- Brunel, F.M., Lewis, J.D., Destito, G., Steinmetz, N.F., Manchester, M., Stuhlmann, H., and Dawson, P.E. (2010). Hydrazone ligation strategy to assemble multifunctional viral nanoparticles for cell imaging and tumor targeting. *Nano Letters* 10, 1093-1097.
- Buchanan, B.B., Gruissem, W., and Jones, R.L. (2000). *Biochemistry & Molecular Biology of Plants* (Rockville, Md., American Society of Plant Physiologists).
- Bundy, B.C., Franciszkowicz, M.J., and Swartz, J.R. (2008). *Escherichia coli*-based cell-free synthesis of virus-like particles. *Biotechnology and Bioengineering* 100, 28-37.
- Burke, K.L., Dunn, G., Ferguson, M., Minor, P.D., and Almond, J.W. (1988). Antigen chimeras of poliovirus as potential new vaccines. *Nature* 332, 81-82.
- Burrell, C.J., Mackay, P., Greenaway, P.J., Hofschneider, P.H., and Murray, K. (1979). Expression in *Escherichia coli* of hepatitis B virus DNA sequences cloned in plasmid pBR322. *Nature* 279, 43-47.
- Calvo-Pinilla, E., Nieto, J.M., and Ortego, J. (2010). Experimental oral infection of bluetongue virus serotype 8 in IFNAR(-/-) mice. *J Gen Virol in press*.
- Cañizares, M.C., Liu, L., Perrin, Y., Tsakiris, E., and Lomonosoff, G.P. (2006). A bipartite system for the constitutive and inducible expression of high levels of foreign proteins in plants. *Plant Biotechnol J* 4, 183-193.
- Carpenter, S., Wilson, A., and Mellor, P.S. (2009). *Culicoides* and the emergence of bluetongue virus in northern Europe. *Trends in Microbiology* 17, 172-178.
- Castilla, J., Pintado, B., Sola, I., Sánchez-Morgado, J.M., and Enjuanes, L. (1998). Engineering passive immunity in transgenic mice secreting virus-neutralizing antibodies in milk. *Nature Biotechnology* 16, 349-354.
- Celma, C.C.P., and Roy, P. (2009). A viral nonstructural protein regulates bluetongue virus trafficking and release. *J Virol* 83, 6806-6816.
- Chalfie, M., Tu, Y., Euskirchen, G., Ward, W.W., and Prasher, D.C. (1994). Green fluorescent protein as a marker for gene expression. *Science* 263, 802-805.
- Charpilienne, A., Nejmeddine, M., Berois, M., Parez, N., Neumann, E., Hewat, E., Trugnan, G., and Cohen, J. (2001). Individual rotavirus-like particles containing 120 molecules of fluorescent protein are visible in living cells. *Journal of Biological Chemistry* 276, 29361-29367.
- Chen, Q.J., Zhou, H.M., Chen, J., and Wang, X.C. (2006). A Gateway-based platform for multigene plant transformation. *Plant Molecular Biology* 62, 927-936.
- Clarke, B.E., Newton, S.E., Carroll, A.R., Francis, M.J., Appleyard, G., Syred, A.D., Highfield, P.E., Rowlands, D.J., and Brown, F. (1987). Improved immunogenicity of a peptide epitope after fusion to hepatitis B core protein. *Nature* 330, 381-384.

- Cohen, B.J., and Richmond, J.E. (1982). Electron-microscopy of hepatitis B core antigen synthesized in *Escherichia coli*. *Nature* 296, 677-678.
- Comellas-Aragonès, M., Engelkamp, H., Claessen, V.I., Sommerdijk, N.A.J.M., Rowan, A.E., Christianen, P.C.M., Maan, J.C., Verduin, B.J.M., Cornelissen, J.J.L.M., and Nolte, R.J.M. (2007). A virus-based single-enzyme nanoreactor. *Nature Nanotechnology* 2, 635-639.
- Cramer, C.L., Boothe, J.G., and Oishi, K.K. (1999). Transgenic plants for therapeutic proteins: Linking upstream and downstream strategies. In *Plant Biotechnology-Bk*, pp. 95-118.
- Crawford, S.E., Labbe, M., Cohen, J., Burroughs, M.H., Zhou, Y.J., and Estes, M.K. (1994). Characterization of virus-like particles produced by the expression of rotavirus capsid proteins in insect cells. *J Virol* 68, 5945-5952.
- Crowther, R.A., Kiselev, N.A., Böttcher, B., Berriman, J.A., Borisova, G.P., Ose, V., and Pumpens, P. (1994). Three-dimensional structure of hepatitis B virus core particles determined by electron cryomicroscopy. *Cell* 77, 943-950.
- D'Aoust, M.A., Couture, M.M.J., Charland, N., Trepanier, S., Landry, N., Ors, F., and Vezina, L.P. (2010). The production of hemagglutinin-based virus-like particles in plants: a rapid, efficient and safe response to pandemic influenza. *Plant Biotechnol J* 8, 607-619.
- D'Aoust, M.A., Lavoie, P.O., Couture, M.M.J., Trépanier, S., Guay, J.M., Dargis, M., Mongrand, S., Landry, N., Ward, B.J., and Vézina, L.P. (2008). Influenza virus-like particles produced by transient expression in *Nicotiana benthamiana* induce a protective immune response against a lethal viral challenge in mice. *Plant Biotechnol J* 6, 930-940.
- Dafny-Yelin, M., and Tzfira, T. (2007). Delivery of multiple transgenes to plant cells. *Plant Physiol* 145, 1118-1128.
- Dane, D.S., Cameron, C.H., and Briggs, M. (1970). Virus-like particles in serum of patients with Australia antigen-associated hepatitis. *Lancet* 1, 695-698.
- Daniell, H. (2006). Production of biopharmaceuticals and vaccines in plants via the chloroplast genome. *Biotechnol J* 1, 1071-1079.
- Decker, E.L., and Reski, R. (2007). Moss bioreactors producing improved biopharmaceuticals. *Curr Opin Biotechnol* 18, 393-398.
- Delchambre, M., Gheysen, D., Thines, D., Thiriart, C., Jacobs, E., Verdin, E., Horth, M., Burny, A., and Bex, F. (1989). The GAG precursor of simian immunodeficiency virus assembles into virus-like particles. *EMBO Journal* 8, 2653-2660.
- Dietrich, C., and Maiss, E. (2003). Fluorescent labelling reveals spatial separation of potyvirus populations in mixed infected *Nicotiana benthamiana* plants. *Journal of General Virology* 84, 2871-2876.
- Doran, P.M. (2000). Foreign protein production in plant tissue cultures. *Curr Opin Biotechnol* 11, 199-204.
- Douglas, T., and Young, M. (1998). Host-guest encapsulation of materials by assembled virus protein cages. *Nature* 393, 152-155.

- Drake, J.W., and Holland, J.J. (1999). Mutation rates among RNA viruses. *Proc Natl Acad Sci U S A* 96, 13910-13913.
- Earley, K.W., Haag, J.R., Pontes, O., Opper, K., Juehne, T., Song, K.M., and Pikaard, C.S. (2006). Gateway-compatible vectors for plant functional genomics and proteomics. *Plant Journal* 45, 616-629.
- El Amrani, A., Barakate, A., Askari, B.M., Li, X.J., Roberts, A.G., Ryan, M.D., and Halpin, C. (2004). Coordinate expression and independent subcellular targeting of multiple proteins from a single transgene. *Plant Physiol* 135, 16-24.
- Engler, C., Gruetzner, R., Kandzia, R., and Marillonnet, S. (2009). Golden gate shuffling: a one-pot DNA shuffling method based on type IIs restriction enzymes. *PLoS One* 4, e5553.
- Engler, C., Kandzia, R., and Marillonnet, S. (2008). A one pot, one step, precision cloning method with high throughput capability. *PLoS One* 3, e3647.
- Evans, D.J., McKeating, J., Meredith, J.M., Burke, K.L., Katrak, K., John, A., Ferguson, M., Minor, P.D., Weiss, R.A., and Almond, J.W. (1989). An engineered poliovirus chimera elicits broadly reactive HIV-1 neutralizing antibodies. *Nature* 339, 385-388.
- Fauquet, C., Mayo, M., Maniloff, J., Desselberger, U., and Ball, L., eds. (2005). *Virus Taxonomy: 8th Report of the International Committee on Taxonomy of Viruses* (San Diego, Elsevier Academic Press).
- Fenner, F. (1988). *Smallpox and its eradication* (Geneva, World Health Organization).
- Finke, S., Brzozka, K., and Conzelmann, K.K. (2004). Tracking fluorescence-labeled rabies virus: Enhanced green fluorescent protein-tagged phosphoprotein P supports virus gene expression and formation of infectious particles. *J Virol* 78, 12333-12343.
- Flavell, R.B. (1994). Inactivation of gene expression in plants as a consequence of specific sequence duplication. *Proc Natl Acad Sci U S A* 91, 3490-3496.
- Forzan, M., Marsh, M., and Roy, P. (2007). Bluetongue virus entry into cells. *J Virol* 81, 4819-4827.
- Forzan, M., Wirblich, C., and Roy, P. (2004). A capsid protein of nonenveloped bluetongue virus exhibits membrane fusion activity. *Proc Natl Acad Sci U S A* 101, 2100-2105.
- Franzen, S., and Lommel, S.A. (2009). Targeting cancer with 'smart bombs': equipping plant virus nanoparticles for a 'seek and destroy' mission. *Nanomedicine* 4, 575-588.
- French, T.J., Marshall, J.J.A., and Roy, P. (1990). Assembly of double-shelled, virus-like particles of bluetongue virus by the simultaneous expression of 4 structural proteins. *J Virol* 64, 5695-5700.
- French, T.J., and Roy, P. (1990). Synthesis of bluetongue virus (BTV) corelike particles by a recombinant baculovirus expressing the 2 major structural core proteins of BTV. *J Virol* 64, 1530-1536.
- Frisch, D.A., Harrishaller, L.W., Yokubaitis, N.T., Thomas, T.L., Hardin, S.H., and Hall, T.C. (1995). Complete sequence of the binary vector Bin 19. *Plant Molecular Biology* 27, 405-409.
- Frolova, O.Y., Petrunia, I.V., Komarova, T.V., Kosorukov, V.S., Sheval, E.V., Gleba, Y.Y., and Dorokhov, Y.L. (2010). Trastuzumab-binding peptide display by tobacco mosaic virus. *Virology*.

- Fuller, S.D. (1987). The T=4 envelope of sindbis virus is organized by interactions with a complementary T=3 capsid. *Cell* 48, 923-934.
- Gallina, A., Bonelli, F., Zentilin, L., Rindi, G., Muttini, M., and Milanesi, G. (1989). A recombinant hepatitis B core antigen polypeptide with the protamine-like domain deleted self-assembles into capsid particles but fails to bind nucleic acids. *J Virol* 63, 4645-4652.
- Gehin, A., Gilbert, R., Stuart, D., and Rowlands, D. (2004). Hepatitis B core antigen fusion proteins. accessed 2010 (<http://www.freepatentsonline.com/y2004/0223965.html>)
- Ghosh, M.K., Borca, M.V., and Roy, P. (2002a). Virus-derived tubular structure displaying foreign sequences on the surface elicit CD4(+) Th cell and protective humoral responses. *Virology* 302, 383-392.
- Ghosh, M.K., Dériaud, E., Saron, M.F., Lo-Man, R., Henry, T., Jiao, X.N., Roy, P., and Leclerc, C. (2002b). Induction of protective antiviral cytotoxic T cells by a tubular structure capable of carrying large foreign sequences. *Vaccine* 20, 1369-1377.
- Gilbert, N. (2009). Europe prepares for drugs from GM plants. Nature Publishing Group. accessed August, 2010 (<http://www.nature.com/news/2009/090807/full/news.2009.630.html>)
- Giritch, A., Marillonnet, S., Engler, C., van Eldik, G., Botterman, J., Klimyuk, V., and Gleba, Y. (2006). Rapid high-yield expression of full-size IgG antibodies in plants coinfecting with noncompeting viral vectors. *Proc Natl Acad Sci U S A* 103, 14701-14706.
- Gleba, Y. (2009). Plant-based vaccines and antibodies: How will they contribute to human health? In *Plant-based Vaccines and Antibodies* (Verona, Italy).
- Gleba, Y., Klimyuk, V., and Marillonnet, S. (2005). Magniffection - a new platform for expressing recombinant vaccines in plants. *Vaccine* 23, 2042-2048.
- Gleba, Y., Marillonnet, S., and Klimyuk, V. (2004). Engineering viral expression vectors for plants: the 'full virus' and the 'deconstructed virus' strategies. *Curr Opin Plant Biol* 7, 182-188.
- Gold, S., Monaghan, P., Mertens, P., and Jackson, T. (2010). A clathrin independent macropinocytosis-like entry mechanism used by bluetongue virus-1 during infection of BHK cells. *PLoS One* 5, -.
- Gomord, V., Fitchette, A.C., Menu-Bouaouiche, L., Saint-Jore-Dupas, C., Plasson, C., Michaud, D., and Faye, L. (2010). Plant-specific glycosylation patterns in the context of therapeutic protein production. *Plant Biotechnol J* 8, 564-587.
- Goodin, M.M., Zaitlin, D., Naidu, R.A., and Lommel, S.A. (2008). *Nicotiana benthamiana*: Its history and future as a model for plant-pathogen interactions. *Molecular Plant-Microbe Interactions* 21, 1015-1026.
- Gopinath, K., Wellink, J., Porta, C., Taylor, K.M., Lomonossoff, G.P., and van Kammen, A. (2000). Engineering cowpea mosaic virus RNA-2 into a vector to express heterologous proteins in plants. *Virology* 267, 159-173.
- Greber, U.F., and Way, M. (2006). A superhighway to virus infection. *Cell* 124, 741-754.
- Griesbeck, C., Kobl, I., and Heitzer, M. (2006). *Chlamydomonas reinhardtii*: a protein expression system for pharmaceutical and biotechnological proteins. *Molecular Biotechnology* 34, 213-223.

- Grimes, J., Basak, A.K., Roy, P., and Stuart, D. (1995). The crystal structure of bluetongue virus VP7. *Nature* 373, 167-170.
- Grimes, J.M., Burroughs, J.N., Gouet, P., Diprose, J.M., Malby, R., Zientara, S., Mertens, P.P.C., and Stuart, D.I. (1998). The atomic structure of the bluetongue virus core. *Nature* 395, 470-478.
- Gurunathan, S., Klinman, D.M., and Seder, R.A. (2000). DNA vaccines: Immunology, application, and optimization. *Annual Review of Immunology* 18, 927-974.
- Halpin, C., Cooke, S.E., Barakate, A., El Amrani, A., and Ryan, M.D. (1999). Self-processing 2A-polyproteins - a system for co-ordinate expression of multiple proteins in transgenic plants. *The Plant Journal* 17, 453-459.
- Hartley, J.L., Temple, G.F., and Brasch, M.A. (2000). DNA cloning using *in vitro* site-specific recombination. *Genome Research* 10, 1788-1795.
- Hassan, S.H., Wirblich, C., Forzan, M., and Roy, P. (2001). Expression and functional characterization of bluetongue virus VP5 protein: Role in cellular permeabilization. *J Virol* 75, 8356-8367.
- Hassan, S.S., and Roy, P. (1999). Expression and functional characterization of bluetongue virus VP2 protein: Role in cell entry. *J Virol* 73, 9832-9842.
- Haupts, U., Maiti, S., Schwille, P., and Webb, W.W. (1998). Dynamics of fluorescence fluctuations in green fluorescent protein observed by fluorescence correlation spectroscopy. *Proc Natl Acad Sci U S A* 95, 13573-13578.
- Hellens, R.P., Allan, A.C., Friel, E.N., Bolitho, K., Grafton, K., Templeton, M.D., Karunairetnam, S., Gleave, A.P., and Laing, W.A. (2005). Transient expression vectors for functional genomics, quantification of promoter activity and RNA silencing in plants. *Plant Methods* 1, 13.
- Hellens, R.P., Edwards, E.A., Leyland, N.R., Bean, S., and Mullineaux, P.M. (2000). pGreen: a versatile and flexible binary Ti vector for *Agrobacterium*-mediated plant transformation. *Plant Molecular Biology* 42, 819-832.
- Hewat, E.A., Booth, T.F., Loudon, P.T., and Roy, P. (1992). 3-Dimensional reconstruction of baculovirus expressed bluetongue virus core-like particles by cryoelectron microscopy. *Virology* 189, 10-20.
- Hewat, E.A., Booth, T.F., and Roy, P. (1994). Structure of correctly self-assembled bluetongue virus-like particles. *Journal of Structural Biology* 112, 183-191.
- Hiatt, A., Cafferkey, R., and Bowdish, K. (1989). Production of antibodies in transgenic plants. *Nature* 342, 76-78.
- Hobman, T.C., Lundstrom, M.L., Mauracher, C.A., Woodward, L., Gillam, S., and Farquhar, M.G. (1994). Assembly of rubella virus structural proteins into virus-like particles in transfected cells. *Virology* 202, 574-585.
- Hoekema, A., Hirsch, P.R., Hooykaas, P.J.J., and Schilperoort, R.A. (1983). A binary plant vector strategy based on separation of *vir*-region and T-region of the *Agrobacterium tumefaciens* Ti-plasmid. *Nature* 303, 179-180.

- Holness, C.L., Lomonosoff, G.P., Evans, D., and Maule, A.J. (1989). Identification of the initiation codons for translation of cowpea mosaic virus middle component RNA using site-directed mutagenesis of an infectious cDNA clone. *Virology* 172, 311-320.
- Houdebine, L.M. (2000). Transgenic animal bioreactors. *Transgenic Res* 9, 305-320.
- Huang, Y.H., Liang, W.Q., Wang, Y.J., Zhou, Z.A., Pan, A.H., Yang, X.H., Huang, C., Chen, J.X., and Zhang, D.B. (2005). Immunogenicity of the epitope of the foot-and-mouth disease virus fused with a hepatitis B core protein as expressed in transgenic tobacco. *Viral Immunology* 18, 668-677.
- Huang, Z., Chen, Q., Hjelm, B., Arntzen, C., and Mason, H. (2009). A DNA replicon system for rapid high-level production of virus-like particles in plants. *Biotechnology and Bioengineering* 103, 706-714.
- Huang, Z., Santi, L., LePore, K., Kilbourne, J., Arntzen, C.J., and Mason, H.S. (2006). Rapid, high-level production of hepatitis B core antigen in plant leaf and its immunogenicity in mice. *Vaccine* 24, 2506-2513.
- Hyatt, A.D., and Eaton, B.T. (1988). Ultrastructural distribution of the major capsid proteins within bluetongue virus and infected cells. *Journal of General Virology* 69, 805-815.
- Hyatt, A.D., Gould, A.R., Coupar, B., and Eaton, B.T. (1991). Localization of the nonstructural protein NS3 in bluetongue virus-infected cells. *Journal of General Virology* 72, 2263-2267.
- Janssen, B.J., and Gardner, R.C. (1989). Localized transient expression of GUS in leaf disks following cocultivation with *Agrobacterium*. *Plant Molecular Biology* 14, 61-72.
- Kapila, J., De Rycke, R., Van Montagu, M., and Angenon, G. (1997). An *Agrobacterium*-mediated transient gene expression system for intact leaves. *Plant Science* 122, 101-108.
- Kar, A.K., Ghosh, M., and Roy, P. (2004). Mapping the assembly pathway of bluetongue virus scaffolding protein VP3. *Virology* 324, 387-399.
- Kar, A.K., Iwatani, N., and Roy, P. (2005). Assembly and intracellular localization of the bluetongue virus core protein VP3. *J Virol* 79, 11487-11495.
- Karimi, M., Inzé, D., and Depicker, A. (2002). GATEWAY™ vectors for *Agrobacterium*-mediated plant transformation. *Trends in Plant Science* 7, 193-195.
- Kearney, C.M., Donson, J., Jones, G.E., and Dawson, W.O. (1993). Low-level of genetic drift in foreign sequences replicating in an RNA virus in plants. *Virology* 192, 11-17.
- Kim, Y., Chang, K.O., Kim, W.Y., and Saif, L.J. (2002). Production of hybrid double- or triple-layered virus-like particles of group A and C rotaviruses using a baculovirus expression system. *Virology* 302, 1-8.
- Klein, T.M., Wolf, E.D., Wu, R., and Sanford, J.C. (1987). High-velocity microprojectiles for delivering nucleic acids into living cells. *Nature* 327, 70-73.
- Klingen, Y., Conzelmann, K.K., and Finke, S. (2008). Double-labeled rabies virus: Live tracking of enveloped virus transport. *J Virol* 82, 237-245.

- Kratz, P.A., Böttcher, B., and Nassal, M. (1999). Native display of complete foreign protein domains on the surface of hepatitis B virus capsids. *Proc Natl Acad Sci U S A* *96*, 1915-1920.
- Kredel, S., Oswald, F., Nienhaus, K., Deuschle, K., Röcker, C., Wolff, M., Heilker, R., Nienhaus, G.U., and Wiedenmann, J. (2009). mRuby, a bright monomeric red fluorescent protein for labeling of subcellular structures. *PLoS One* *4*, e4391.
- Laguía-Becher, M., Martín, V., Kraemer, M., Corigliano, M., Yacono, M.L., Goldman, A., and Clemente, M. (2010). Effect of codon optimization and subcellular targeting on *Toxoplasma gondii* antigen SAG1 expression in tobacco leaves to use in subcutaneous and oral immunization in mice. *BMC Biotechnol* *10*, 52.
- Lee, L.A., and Wang, Q. (2006). Adaptations of nanoscale viruses and other protein cages for medical applications. *Nanomedicine* *2*, 137-149.
- Lee, L.Y., and Gelvin, S.B. (2008). T-DNA binary vectors and systems. *Plant Physiol* *146*, 325-332.
- Lee, S.Y., Choi, J.W., Royston, E., Janes, D.B., Culver, J.N., and Harris, M.T. (2006). Deposition of platinum clusters on surface-modified tobacco mosaic virus. *Journal of Nanoscience and Nanotechnology* *6*, 974-981.
- Leopold, P.L., Ferris, B., Grinberg, I., Worgall, S., Hackett, N.R., and Crystal, R.G. (1998). Fluorescent virions: Dynamic tracking of the pathway of adenoviral gene transfer vectors in living cells. *Human Gene Therapy* *9*, 367-378.
- Lico, C., Chen, Q., and Santi, L. (2008). Viral vectors for production of recombinant proteins in plants. *J Cell Physiol* *216*, 366-377.
- Liu, L., Grainger, J., Cañizares, M.C., Angell, S.M., and Lomonosoff, G.P. (2004). Cowpea mosaic virus RNA-1 acts as an amplicon whose effects can be counteracted by a RNA-2-encoded suppressor of silencing. *Virology* *323*, 37-48.
- Loudon, P.T., Hirasawa, T., Oldfield, S., Murphy, M., and Roy, P. (1991). Expression of the outer capsid protein VP5 of two bluetongue viruses, and synthesis of chimeric double-shelled virus-like particles using combinations of recombinant baculoviruses. *Virology* *182*, 793-801.
- Loudon, P.T., and Roy, P. (1991). Assembly of 5 bluetongue virus proteins expressed by recombinant baculoviruses - inclusion of the largest protein VP1 in the core and virus-like particles. *Virology* *180*, 798-802.
- Loudon, P.T., and Roy, P. (1992). Interaction of nucleic acids with core-like and subcore-like particles of bluetongue virus. *Virology* *191*, 231-236.
- Ma, J.K.C., Hiatt, A., Hein, M., Vine, N.D., Wang, F., Stabila, P., Vandolleweerd, C., Mostov, K., and Lehner, T. (1995). Generation and assembly of secretory antibodies in plants. *Science* *268*, 716-719.
- Maclean, J., Koekemoer, M., Olivier, A.J., Stewart, D., Hitzeroth, I.I., Rademacher, T., Fischer, R., Williamson, A.L., and Rybicki, E.P. (2007). Optimization of human papillomavirus type 16 (HPV-16) L1 expression in plants: comparison of the suitability of different HPV-16 L1 gene variants and different cell-compartment localization. *Journal of General Virology* *88*, 1460-1469.

- Marillonnet, S., Giritch, A., Gils, M., Kandzia, R., Klimyuk, V., and Gleba, Y. (2004). In planta engineering of viral RNA replicons: Efficient assembly by recombination of DNA modules delivered by *Agrobacterium*. *Proc Natl Acad Sci U S A* *101*, 6852-6857.
- Martin, J., Odoom, K., Tuite, G., Dunn, G., Hopewell, N., Cooper, G., Fitzharris, C., Butler, K., Hall, W.W., and Minor, P.D. (2004). Long-term excretion of vaccine-derived poliovirus by a healthy child. *J Virol* *78*, 13839-13847.
- Martin, S.A., and Zweerink, H.J. (1972). Isolation and characterization of 2 types of bluetongue virus particles. *Virology* *50*, 495-506.
- Martinez-Costas, J., Sutton, G., Ramadevi, N., and Roy, P. (1998). Guanylyltransferase and RNA 5'-triphosphatase activities of the purified expressed VP4 protein of bluetongue virus. *Journal of Molecular Biology* *280*, 859-866.
- Mason, H.S., Ball, J.M., Shi, J.J., Jiang, X., Estes, M.K., and Arntzen, C.J. (1996). Expression of norwalk virus capsid protein in transgenic tobacco and potato and its oral immunogenicity in mice. *Proc Natl Acad Sci U S A* *93*, 5335-5340.
- Mason, H.S., Lam, D.M.K., and Arntzen, C.J. (1992). Expression of hepatitis B surface antigen in transgenic plants. *Proc Natl Acad Sci U S A* *89*, 11745-11749.
- Matzke, M., Kanno, T., Claxinger, L., Huettel, B., and Matzke, A.J.M. (2009). RNA-mediated chromatin-based silencing in plants. *Current Opinion in Cell Biology* *21*, 367-376.
- McLachlan, A. (1991). *Molecular Biology of the Hepatitis B Virus* (Boca Raton, Fla., CRC Press).
- Mechtcheriakova, I.A., Eldarov, M.A., Nicholson, L., Shanks, M., Skryabin, K.G., and Lomonosoff, G.P. (2006). The use of viral vectors to produce hepatitis B virus core particles in plants. *J Virol Methods* *131*, 10-15.
- Mehlhorn, H., Walldorf, V., Klimpel, S., Jahn, B., Jaeger, F., Eschweiler, J., Hoffmann, B., and Beer, M. (2007). First occurrence of *Culicoides obsoletus*-transmitted bluetongue virus epidemic in Central Europe. *Parasitology Research* *101*, 219-228.
- Mertens, P.P.C., Burroughs, J.N., and Anderson, J. (1987). Purification and properties of virus particles, infectious subviral particles, and cores of bluetongue virus serotype 1 and serotype 4. *Virology* *157*, 375-386.
- Mikhailov, M., Monastyrskaya, K., Bakker, T., and Roy, P. (1996). A new form of particulate single and multiple immunogen delivery system based on recombinant bluetongue virus-derived tubules. *Virology* *217*, 323-331.
- Milich, D.R., Schödel, F., Hughes, J.L., Jones, J.E., and Peterson, D.L. (1997). The hepatitis B virus core and e antigens elicit different Th cell subsets: Antigen structure can affect Th cell phenotype. *J Virol* *71*, 2192-2201.
- Minigo, G., Scholzen, A., Tang, C.K., Hanley, J.C., Kalkanidis, M., Pietersz, G.A., Apostolopoulos, V., and Plebanski, M. (2007). Poly-L-lysine-coated nanoparticles: A potent delivery system to enhance DNA vaccine efficacy. *Vaccine* *25*, 1316-1327.
- Minor, P.D., John, A., Ferguson, M., and Icenogle, J.P. (1986). Antigenic and molecular evolution of the vaccine strain of type 3 poliovirus during the period of excretion by a primary vaccinee. *Journal of General Virology* *67*, 693-706.

- Minten, I.J., Hendriks, L.J.A., Nolte, R.J.M., and Cornelissen, J.J.L.M. (2009). Controlled encapsulation of multiple proteins in virus capsids. *Journal of the American Chemical Society* 131, 17771-17773.
- Møller-Larsen, A., and Christensen, T. (1998). Isolation of a retrovirus from multiple sclerosis patients in self-generated iodixanol gradients. *J Virol Methods* 73, 151-161.
- Monger, W., Alamillo, J.M., Sola, I., Perrin, Y., Bestagno, M., Burrone, O.R., Sabella, P., Plana-Duran, J., Enjuanes, L., Garcia, J.A., *et al.* (2006). An antibody derivative expressed from viral vectors passively immunizes pigs against transmissible gastroenteritis virus infection when supplied orally in crude plant extracts. *Plant Biotechnol J* 4, 623-631.
- Monie, A., Hung, C.F., Roden, R., and Wu, T.C. (2008). Cervarix: a vaccine for the prevention of HPV 16, 18-associated cervical cancer. *Biologics* 2, 97-105.
- Monie, A., Hung, C.F., and Wu, T.C. (2007). Preventive and therapeutic HPV vaccines. *Current Opinion in Investigational Drugs* 8, 1038-1050.
- Moore, I., Samalova, M., and Kurup, S. (2006). Transactivated and chemically inducible gene expression in plants. *Plant Journal* 45, 651-683.
- Mor, T.S., Moon, Y.S., Palmer, K.E., and Mason, H.S. (2003). Geminivirus vectors for high-level expression of foreign proteins in plant cells. *Biotechnology and Bioengineering* 81, 430-437.
- Morikawa, Y., Goto, T., and Sano, K. (1999). *In vitro* assembly of human immunodeficiency virus type 1 GAG protein. *Journal of Biological Chemistry* 274, 27997-28002.
- Moss, S.R., and Nuttall, P.A. (1994). Subcore-like and core-like particles of broadhaven virus (BRDV), a tick-borne Orbivirus, synthesized from baculovirus-expressed VP2 and VP7, the major core proteins of BRDV. *Virus Research* 32, 401-407.
- Mugford, S.T., Qi, X.Q., Bakht, S., Hill, L., Wegel, E., Hughes, R.K., Papadopoulou, K., Melton, R., Philo, M., Sainsbury, F., *et al.* (2009). A serine carboxypeptidase-like acyltransferase is required for synthesis of antimicrobial compounds and disease resistance in oats. *Plant Cell* 21, 2473-2484.
- Müller, B., Daecke, J., Fackler, O.T., Dittmar, M.T., Zentgraf, H., and Kräusslich, H.G. (2004). Construction and characterization of a fluorescently labeled infectious human immunodeficiency virus type 1 derivative. *J Virol* 78, 10803-10813.
- Murphy, R.F., Powers, S., and Cantor, C.R. (1984). Endosome pH measured in single cells by dual fluorescence flow cytometry - rapid acidification of insulin to pH 6. *Journal of Cell Biology* 98, 1757-1762.
- Naqvi, S., Farré, G., Sanahuja, G., Capell, T., Zhu, C., and Christou, P. (2009). When more is better: multigene engineering in plants. *Trends in Plant Science*.
- Nason, E.L., Rothagel, R., Mukherjee, S.K., Kar, A.K., Forzan, M., Prasad, B.V.V., and Roy, P. (2004). Interactions between the inner and outer capsids of bluetongue virus. *J Virol* 78, 8059-8067.
- Nassal, M., Skamel, C., Vogel, M., Kratz, P.A., Stehle, T., Wallich, R., and Simon, M.M. (2008). Development of hepatitis B virus capsids into a whole-chain protein antigen display platform: New particulate Lyme disease vaccines. *International Journal of Medical Microbiology* 298, 135-142.

- Nawrath, C., Poirier, Y., and Somerville, C. (1994). Targeting of the polyhydroxybutyrate biosynthetic pathway to the plastids of *Arabidopsis thaliana* results in high-levels of polymer Accumulation. *Proc Natl Acad Sci U S A* 91, 12760-12764.
- Neuhaus, G., and Spangenberg, G. (1990). Plant transformation by microinjection techniques. *Physiologia Plantarum* 79, 213-217.
- Nuttall, P.A., Jacobs, S.C., Jones, L.D., Carey, D., and Moss, S.R. (1992). Enhanced neurovirulence of tick-borne Orbiviruses resulting from genetic modulation. *Virology* 187, 407-412.
- Ormo, M., Cubitt, A.B., Kallio, K., Gross, L.A., Tsien, R.Y., and Remington, S.J. (1996). Crystal structure of the *Aequorea victoria* green fluorescent protein. *Science* 273, 1392-1395.
- Owens, R.J., Limn, C., and Roy, P. (2004). Role of an arbovirus nonstructural protein in cellular pathogenesis and virus release. *J Virol* 78, 6649-6656.
- Park, N.H., Song, I.H., and Chung, Y.-H. (2006). Chronic hepatitis B in hepatocarcinogenesis. *Postgraduate Medical Journal* 82, 507-515.
- Pasek, M., Goto, T., Gilbert, W., Zink, B., Schaller, H., Mackay, P., Leadbetter, G., and Murray, K. (1979). Hepatitis B virus genes and their expression in *Escherichia coli*. *Nature* 282, 575-579.
- Patterson, G., Davidson, M., Manley, S., and Lippincott-Schwartz, J. (2010). Superresolution imaging using single-molecule localization. *Annual Review of Physical Chemistry*, Vol 61 61, 345-367.
- Patterson, G.H., Knobel, S.M., Sharif, W.D., Kain, S.R., and Piston, D.W. (1997). Use of the green fluorescent protein and its mutants in quantitative fluorescence microscopy. *Biophysical Journal* 73, 2782-2790.
- Pawley, J.B. (2006). *Handbook of Biological Confocal Microscopy*, 3rd edn (New York, NY, Springer).
- Porta, C., and Lomonosoff, G.P. (1996). Use of viral replicons for the expression of genes in plants. *Molecular Biotechnology* 5, 209-221.
- Porta, C., Spall, V.E., Findlay, K.C., Gergerich, R.C., Farrance, C.E., and Lomonosoff, G.P. (2003). Cowpea mosaic virus-based chimaeras - Effects of inserted peptides on the phenotype, host range, and transmissibility of the modified viruses. *Virology* 310, 50-63.
- Porta, C., Spall, V.E., Loveland, J., Johnson, J.E., Barker, P.J., and Lomonosoff, G.P. (1994). Development of cowpea mosaic virus as a high-yielding system for the presentation of foreign peptides. *Virology* 202, 949-955.
- Prunkard, D., Cottingham, I., Garner, I., Bruce, S., Dalrymple, M., Lasser, G., Bishop, P., and Foster, D. (1996). High-level expression of recombinant human fibrinogen in the milk of transgenic mice. *Nature Biotechnology* 14, 867-871.
- Quan, F.S., Huang, C.Z., Compans, R.W., and Kang, S.M. (2007). Virus-like particle vaccine induces protective immunity against homologous and heterologous strains of influenza virus. *J Virol* 81, 3514-3524.
- Rabindran, S., and Dawson, W.O. (2001). Assessment of recombinants that arise from the use of a TMV-based transient expression vector. *Virology* 284, 182-189.

- Radloff, C., Vaia, R.A., Brunton, J., Bouwer, G.T., and Ward, V.K. (2005). Metal nanoshell assembly on a virus bioscaffold. *Nano Letters* 5, 1187-1191.
- Rao, A.Q., Bakhsh, A., Kiani, S., Shahzad, K., Shahid, A.A., Husnain, T., and Riazuddin, S. (2009). The myth of plant transformation. *Biotechnology Advances* 27, 753-763.
- Ratcliff, F., Harrison, B.D., and Baulcombe, D.C. (1997). A similarity between viral defense and gene silencing in plants. *Science* 276, 1558-1560.
- Raz, E., Carson, D.A., Parker, S.E., Parr, T.B., Abai, A.M., Aichinger, G., Gromkowski, S.H., Singh, M., Lew, D., Yankauckas, M.A., *et al.* (1994). Intradermal gene immunization - the possible role of DNA uptake in the induction of cellular immunity to viruses. *Proc Natl Acad Sci U S A* 91, 9519-9523.
- Rehermann, B., and Nascimbeni, M. (2005). Immunology of hepatitis B virus and hepatitis C virus infection. *Nature Reviews Immunology* 5, 215-229.
- Richards, H.A., Halfhill, M.D., Millwood, R.J., and Stewart, C.N. (2003). Quantitative GFP fluorescence as an indicator of recombinant protein synthesis in transgenic plants. *Plant Cell Reports* 22, 117-121.
- Riedel, S. (2005). Edward Jenner and the history of smallpox and vaccination. *Proc Bayl Univ Med Cent* 18, 21-25.
- Rose, R.C., Bonnez, W., Reichman, R.C., and Garcea, R.L. (1993). Expression of human papillomavirus type-11 L1 protein in insect cells - *In vivo* and *in vitro* assembly of virus-like particles. *J Virol* 67, 1936-1944.
- Roy, P., Bishop, D.H.L., Leblois, H., and Erasmus, B.J. (1994). Long-lasting protection of sheep against bluetongue challenge after vaccination with virus-like particles - evidence for homologous and partial heterologous protection. *Vaccine* 12, 805-811.
- Roy, P., French, T., and Erasmus, B.J. (1992). Protective efficacy of virus-like particles for bluetongue disease. *Vaccine* 10, 28-32.
- Roy, P., and Noad, R. (2006). Bluetongue virus assembly and morphogenesis. *Reoviruses: Entry, Assembly and Morphogenesis* 309, 87-116.
- Roy, P., and Noad, R. (2008). Virus-like particles as a vaccine delivery system - Myths and facts. *Human Vaccines* 4, 5-12.
- Roy, P., Urakawa, T., Vandijk, A.A., and Erasmus, B.J. (1990). Recombinant virus-vaccine for bluetongue disease in sheep. *J Virol* 64, 1998-2003.
- Ryan, M.D., and Drew, J. (1994). Foot-and-mouth disease virus 2A oligopeptide mediated cleavage of an artificial polyprotein. *EMBO Journal* 13, 928-933.
- Rybicki, E.P. (2010). Plant-made vaccines for humans and animals. *Plant Biotechnol J* 8, 620-637.
- Sainsbury, F., Lavoie, P.O., D'Aoust, M.A., Vezina, L.P., and Lomonossoff, G.P. (2008). Expression of multiple proteins using full-length and deleted versions of cowpea mosaic virus RNA-2. *Plant Biotechnol J* 6, 82-92.

- Sainsbury, F., and Lomonosoff, G.P. (2008). Extremely high-level and rapid transient protein production in plants without the use of viral replication. *Plant Physiol* 148, 1212-1218.
- Sainsbury, F., Thuenemann, E.C., and Lomonosoff, G.P. (2009). pEAQ: versatile expression vectors for easy and quick transient expression of heterologous proteins in plants. *Plant Biotechnol J* 7, 682-693.
- Saldaña, S., Guadarrama, F.E., Flores, T.D.O., Arias, N., López, S., Arias, C., Ruiz-Medrano, R., Mason, H., Mor, T., Richter, L., *et al.* (2006). Production of rotavirus-like particles in tomato (*Lycopersicon esculentum* L.) fruit by expression of capsid proteins VP2 and VP6 and immunological studies. *Viral Immunology* 19, 42-53.
- Salfeld, J., Pfaff, E., Noah, M., and Schaller, H. (1989). Antigenic determinants and functional domains in core antigen and e antigen from hepatitis B Virus. *J Virol* 63, 798-808.
- Sambrook, J.F., EF; Maniatis, T. (1989). *Molecular Cloning: A Laboratory Manual*, 2nd edn (Cold Spring Harbour, NY, Cold Spring Harbour Press).
- Santi, L., Huang, Z., and Mason, H. (2006). Virus-like particles production in green plants. *Methods* 40, 66-76.
- Saunders, K., Sainsbury, F., and Lomonosoff, G.P. (2009). Efficient generation of cowpea mosaic virus empty virus-like particles by the proteolytic processing of precursors in insect cells and plants. *Virology* 393, 329-337.
- Saxena, P., Hsieh, Y., Alvarado, V., Sainsbury, F., Saunders, K., Lomonosoff, G., and Scholthof, H. (2010). Improved foreign gene expression in plants using a virus-encoded suppressor of RNA silencing modified to be developmentally harmless. *Plant Biotechnol J in press*.
- Schödel, F., Moriarty, A.M., Peterson, D.L., Zheng, J., Hughes, J.L., Will, H., Leturcq, D.J., Mcgee, J.S., and Milich, D.R. (1992). The position of heterologous epitopes inserted in hepatitis B virus core particles determines their immunogenicity. *J Virol* 66, 106-114.
- Schödel, F., Peterson, D., Hughes, J., Wirtz, R., and Milich, D. (1996). Hybrid hepatitis B virus core antigen as a vaccine carrier moiety: I. Presentation of foreign epitopes. *J Biotechnol* 44, 91-96.
- Seisenberger, G., Ried, M.U., Endreß, T., Büning, H., Hallek, M., and Bräuchle, C. (2001). Real-time single-molecule imaging of the infection pathway of an adeno-associated virus. *Science* 294, 1929-1932.
- Sheikholeslam, S.N., and Weeks, D.P. (1987). Acetosyringone promotes high-efficiency transformation of *Arabidopsis thaliana* explants by *Agrobacterium tumefaciens*. *Plant Molecular Biology* 8, 291-298.
- Shimomura, O., Saiga, Y., and Johnson, F.H. (1962). Purification and properties of aequorin, a bio-(chemi-) luminescent protein from jelly fish, *Aequorea aequorea*. *Federation Proceedings* 21, 401-&.
- Sijmons, P.C., Dekker, B.M., Schrammeijer, B., Verwoerd, T.C., van den Elzen, P.J., and Hoekema, A. (1990). Production of correctly processed human serum albumin in transgenic plants. *Biotechnology (N Y)* 8, 217-221.

- Silhavy, D., Molnár, A., Lucioli, A., Szittyá, G., Hornyik, C., Tavazza, M., and Burgyán, J. (2002). A viral protein suppresses RNA silencing and binds silencing-generated, 21- to 25-nucleotide double-stranded RNAs. *EMBO Journal* 21, 3070-3080.
- Simons, J.P., McClenaghan, M., and Clark, A.J. (1987). Alteration of the quality of milk by expression of sheep β -lactoglobulin in transgenic mice. *Nature* 328, 530-532.
- Sivakumar, G. (2006). Bioreactor technology: a novel industrial tool for high-tech production of bioactive molecules and biopharmaceuticals from plant roots. *Biotechnol J* 1, 1419-1427.
- Soto, C.M., Martin, B.D., Sapsford, K.E., Blum, A.S., and Ratna, B.R. (2008). Toward single molecule detection of staphylococcal enterotoxin B: Mobile sandwich immunoassay on gliding microtubules. *Analytical Chemistry* 80, 5433-5440.
- Soto, C.M., and Ratna, B.R. (2010). Virus hybrids as nanomaterials for biotechnology. *Curr Opin Biotechnol*.
- Spök, A., Twyman, R.M., Fischer, R., Ma, J.K.C., and Sparrow, P.A.C. (2008). Evolution of a regulatory framework for pharmaceuticals derived from genetically modified plants. *Trends in Biotechnology* 26, 506-517.
- Stahl, S.J., and Murray, K. (1989). Immunogenicity of peptide fusions to hepatitis B virus core antigen. *Proc Natl Acad Sci U S A* 86, 6283-6287.
- Stäuber, N., MartinezCostas, J., Sutton, G., Monastyrskaya, K., and Roy, P. (1997). Bluetongue virus VP6 protein binds ATP and exhibits an RNA-dependent ATPase function and a helicase activity that catalyze the unwinding of double-stranded RNA substrates. *J Virol* 71, 7220-7226.
- Steinmetz, N.F. (2010). Viral nanoparticles as platforms for next-generation therapeutics and imaging devices. *Nanomedicine*.
- Steinmetz, N.F., Calder, G., Lomonosoff, G.P., and Evans, D.J. (2006). Plant viral capsids as nanobuilding blocks: Construction of arrays on solid supports. *Langmuir* 22, 10032-10037.
- Stewart, M., Bhatia, Y., Athmaran, T.N., Noad, R., Gastaldi, C., Dubois, E., Russo, P., Thiery, R., Sailleau, C., Breard, E., *et al.* (2010). Validation of a novel approach for the rapid production of immunogenic virus-like particles for bluetongue virus. *Vaccine* 28, 3047-3054.
- Stuart, D.I., and Grimes, J.M. (2006). Structural studies on Orbivirus proteins and particles. *Reoviruses: Entry, Assembly and Morphogenesis* 309, 221-244.
- Sugiyama, K., Bishop, D.H.L., and Roy, P. (1982). Analyses of the genomes of bluetongue viruses recovered from different states of the United States and at different times. *American Journal of Epidemiology* 115, 332-347.
- Sutter, G., and Moss, B. (1992). Nonreplicating vaccinia vector efficiently expresses recombinant genes. *Proc Natl Acad Sci U S A* 89, 10847-10851.
- Sutter, G., Wyatt, L.S., Foley, P.L., Bennink, J.R., and Moss, B. (1994). A recombinant vector derived from the host range-restricted and highly attenuated MVA strain of vaccinia virus stimulates protective immunity in mice to influenza virus. *Vaccine* 12, 1032-1040.

- Szmaragd, C., Wilson, A.J., Carpenter, S., Wood, J.L.N., Mellor, P.S., and Gubbins, S. (2010). The spread of bluetongue virus serotype 8 in Great Britain and its control by vaccination. *PLoS One* 5, -.
- Tan, B.H., Nason, E., Staeuber, N., Jiang, W.R., Monastyrskaya, K., and Roy, P. (2001). RGD tripeptide of bluetongue virus VP7 protein is responsible for core attachment to *Culicoides* cells. *J Virol* 75, 3937-3947.
- Tanaka, S., Mikhailov, M., and Roy, P. (1995). Synthesis of bluetongue virus chimeric VP3 molecules and their interactions with VP7 protein to assemble into virus core-like particles. *Virology* 214, 593-601.
- Taylor, K.M., Porta, C., Lin, T.W., Johnson, J.E., Barker, P.J., and Lomonossoff, G.P. (1999). Position-dependent processing of peptides presented on the surface of cowpea mosaic virus. *Biological Chemistry* 380, 387-392.
- Thompson, C., and Buck, C. (2007). Purification of papillomavirus capsids using agarose gel filtration. <http://home.ccr.cancer.gov/lco/gelfiltration.htm>. accessed May, 2010
- Tissot, A.C., Renhofa, R., Schmitz, N., Cielens, I., Meijerink, E., Ose, V., Jennings, G.T., Saudan, P., Pumpens, P., and Bachmann, M.F. (2010). Versatile virus-like particle carrier for epitope based vaccines. *PLoS One* 5, -.
- Toth, R.L., Chapman, S., Carr, F., and Cruz, S.S. (2001). A novel strategy for the expression of foreign genes from plant virus vectors. *Febs Letters* 489, 215-219.
- Tsuda, S., Yoshioka, K., Tanaka, T., Iwata, A., Yoshikawa, A., Watanabe, Y., and Okada, Y. (1998). Application of the human hepatitis B virus core antigen from transgenic tobacco plants for serological diagnosis. *Vox Sanguinis* 74, 148-155.
- Tzfira, T., Tian, G.W., Lacroix, B., Vyas, S., Li, J.X., Leitner-Dagan, Y., Krichevsky, A., Taylor, T., Vainstein, A., and Citovsky, V. (2005). pSAT vectors: a modular series of plasmids for autofluorescent protein tagging and expression of multiple genes in plants. *Plant Molecular Biology* 57, 503-516.
- Usha, R., Rohll, J.B., Spall, V.E., Shanks, M., Maule, A.J., Johnson, J.E., and Lomonossoff, G.P. (1993). Expression of an animal virus antigenic site on the surface of a plant virus particle. *Virology* 197, 366-374.
- Valenzuela, P., Medina, A., and Rutter, W.J. (1982). Synthesis and assembly of hepatitis B virus surface antigen particles in yeast. *Nature* 298, 347-350.
- van Bokhoven, H., Le Gall, O., Kasteel, D., Verver, J., Wellink, J., and van Kammen, A.B. (1993). *Cis*-acting and *trans*-acting elements in cowpea mosaic virus RNA replication. *Virology* 195, 377-386.
- van Engelen, F.A., Molthoff, J.W., Conner, A.J., Nap, J.P., Pereira, A., and Stiekema, W.J. (1995). pBINPLUS: an improved plant transformation vector based on pBIN19. *Transgenic Res* 4, 288-290.
- Vaquero, C., Sack, M., Chandler, J., Drossard, J., Schuster, F., Monecke, M., Schillberg, S., and Fischer, R. (1999). Transient expression of a tumor-specific single-chain fragment and a chimeric antibody in tobacco leaves. *Proc Natl Acad Sci U S A* 96, 11128-11133.

- Venters, C., Graham, W., and Cassidy, W. (2004). Recombivax-HB: perspectives past, present and future. *Expert Review of Vaccines* 3, 119-129.
- Voinnet, O., Pinto, Y.M., and Baulcombe, D.C. (1999). Suppression of gene silencing: A general strategy used by diverse DNA and RNA viruses of plants. *Proc Natl Acad Sci U S A* 96, 14147-14152.
- Voinnet, O., Rivas, S., Mestre, P., and Baulcombe, D. (2003). An enhanced transient expression system in plants based on suppression of gene silencing by the p19 protein of tomato bushy stunt virus. *Plant Journal* 33, 949-956.
- Walker, A., Skamel, C., Vorreiter, J., and Nassal, M. (2008). Internal core protein cleavage leaves the hepatitis B virus capsid intact and enhances its capacity for surface display of heterologous whole chain proteins. *Journal of Biological Chemistry* 283, 33508-33515.
- Warzecha, H., Mason, H.S., Lane, C., Tryggvesson, A., Rybicki, E., Williamson, A.L., Clements, J.D., and Rose, R.C. (2003). Oral immunogenicity of human papillomavirus-like particles expressed in potato. *J Virol* 77, 8702-8711.
- Whitacre, D.C., Lee, B.O., and Milich, D.R. (2009). Use of hepadnavirus core proteins as vaccine platforms. *Expert Review of Vaccines* 8, 1565-1573.
- WHO (2008). Fact Sheet Number 204: Hepatitis B. accessed 3 September, 2010 (<http://www.who.int/mediacentre/factsheets/fs204/en/>)
- WHO (2010a). Live-attenuated vaccines. accessed 30th August, 2010 (http://www.who.int/vaccine_research/diseases/tb/vaccine_development/live_attenuated/en/index.html)
- WHO (2010b). Polio vaccines and polio immunization in the pre-eradication era: WHO position paper. In *WHO Weekly epidemiological record*, pp. 213-228.
- Wittmann, E.J., and Baylis, M. (2000). Climate change: Effects on *Culicoides*-transmitted viruses and implications for the UK. *Veterinary Journal* 160, 107-117.
- Wolff, J.A., Malone, R.W., Williams, P., Chong, W., Acsadi, G., Jani, A., and Felgner, P.L. (1990). Direct gene-transfer into mouse muscle *in vivo*. *Science* 247, 1465-1468.
- Wynne, S.A., Crowther, R.A., and Leslie, A.G.W. (1999). The crystal structure of the human hepatitis B virus capsid. *Molecular Cell* 3, 771-780.
- Xiang, C.B., Han, P., Lutziger, I., Wang, K., and Oliver, D.J. (1999). A mini binary vector series for plant transformation. *Plant Molecular Biology* 40, 711-717.
- Xiang, S.D., Selomulya, C., Ho, J., Apostolopoulos, V., and Plebanski, M. (2010). Delivery of DNA vaccines: an overview on the use of biodegradable polymeric and magnetic nanoparticles. *Wiley Interdisciplinary Reviews-Nanomedicine and Nanobiotechnology* 2, 205-218.
- Xu, H.T., Fan, B.L., Yu, S.Y., Huang, Y.H., Zhao, Z.H., Lian, Z.X., Dai, Y.P., Wang, L.L., Liu, Z.L., Fei, J., *et al.* (2007). Construct synthetic gene encoding artificial spider dragline silk protein and its expression in milk of transgenic mice. *Animal Biotechnology* 18, 1-12.

- Ye, X.D., Al-Babili, S., Klöti, A., Zhang, J., Lucca, P., Beyer, P., and Potrykus, I. (2000). Engineering the provitamin A β (-carotene) biosynthetic pathway into (carotenoid-free) rice endosperm. *Science* 287, 303-305.
- Yin, J.C., Li, G.X., Ren, X.F., and Herrler, G. (2007). Select what you need: A comparative evaluation of the advantages and limitations of frequently used expression systems for foreign genes. *J Biotechnol* 127, 335-347.
- Zapata-Hommer, O., and Griesbeck, O. (2003). Efficiently folding and circularly permuted variants of the Sapphire mutant of GFP. *Bmc Biotechnology* 3, -.
- Zhang, X., Boyce, M., Bhattacharya, B., Schein, S., Roy, P., and Zhou, Z.H. (2010). Bluetongue virus coat protein VP2 contains sialic acid-binding domains, and VP5 resembles enveloped virus fusion proteins. *Proc Natl Acad Sci U S A* 107, 6292-6297.
- Zheng, J., Schödel, F., and Peterson, D.L. (1992). The structure of hepadnaviral core antigens - Identification of free thiols and determination of the disulfide bonding pattern. *Journal of Biological Chemistry* 267, 9422-9429.
- Zhou, B., Zhang, Y., Wang, X., Dong, J., Wang, B., Han, C., Yu, J., and Li, D. (2010). Oral administration of plant-based rotavirus VP6 induces antigen-specific IgAs, IgGs and passive protection in mice. *Vaccine* 28, 6021-6027.

APPENDIX A: TABLE OF CONSTRUCTS

	Name	Encoded proteins	GW	Binary	5'-UTR	Notes
Chapter 3	pENTR-ET2	GFP	x		<i>HT</i>	
	pDEST-BINPLUS	none	x	x	n/a	
	pDEST-BINPLUS-GFP	GFP	x	x	wt	Co-infiltrate pBIN61-P19
	pDEST-BINPLUS-GFP-HT	GFP	x	x	<i>HT</i>	Co-infiltrate pBIN61-P19
	pBINPLUS-GFP	GFP		x	wt	Co-infiltrate pBIN61-P19
	pBINPLUS-GFP-HT	GFP		x	<i>HT</i>	Co-infiltrate pBIN61-P19
	pBD-FSC2-GFP-HT	GFP		x	<i>HT</i>	Co-infiltrate pBIN61-P19
	pEAQbeta	GFP		x	<i>HT</i>	Co-infiltrate pBIN61-P19
	pEAQ-GFP-HT	GFP		x	<i>HT</i>	Co-infiltrate pBIN61-P19
	pEAQ-HT	(NPTII, P19)		x	<i>HT</i>	
	pEAQexpress-GFP-HT	GFP (P19)		x	<i>HT</i>	"pEAQex"
	pEAQselectK-GFP-HT	GFP (NPTII)		x	<i>HT</i>	Co-infiltrate pBIN61-P19
	pEAQspecialK-GFP-HT	GFP (NPTII, P19)		x	<i>HT</i>	
	pEAQ-HT-DEST-1	(NPTII, P19)	x	x	<i>HT</i>	untagged
	pEAQ-HT-DEST-2	(NPTII, P19)	x	x	<i>HT</i>	N-term His
	pEAQ-HT-DEST-3	(NPTII, P19)	x	x	<i>HT</i>	C-term His
	pEAQ-GW-GFP	GFP (NPTII, P19)	x	x	<i>HT</i>	
	pEAQ-GW-HisGFP	His-GFP (NPTII, P19)	x	x	<i>HT</i>	
	pEAQ-GW-GFPHis	GFP-His (NPTII, P19)	x	x	<i>HT</i>	
	pEAQ-GW-GFP-Stop	GFP (NPTII, P19)	x	x	<i>HT</i>	
	pEAQ-HT-EYFP	YFP (NPTII, P19)		x	<i>HT</i>	
	pEAQ-HT-ECFP	CFP (NPTII, P19)		x	<i>HT</i>	
	pEAQex-EYFP-ECFP	YFP, CFP (P19)		x	<i>HT</i>	
Chapter 4	pEAQ-HT-HBcΔ176	HBcΔ176 (NPTII, P19)		x	<i>HT</i>	
	pEAQ-HT-CoHe7e-empty	CoHe7e-empty (NPTII, P19)		x	<i>HT</i>	
	pEAQ-GW-CoHo7e-empty	CoHo7e-empty (NPTII, P19)	x	x	<i>HT</i>	
	pEAQ-GW-CoHe7e-sAg	CoHe7e-sAg (NPTII, P19)	x	x	<i>HT</i>	
	pEAQ-HT-CoHo7e-sAg	CoHo7e-sAg (NPTII, P19)		x	<i>HT</i>	

	Name	Encoded proteins	GW	Binary	5'-UTR	Notes
Chapter 4 – Hepatitis B	pEAQ-GW-CoHe7e-sAg,eGFP	CoHe7e-sAg,eGFP (NPTII, P19)	x	x	HT	
	pEAQ-GW-CoHo7e-sAg,eGFP	CoHo7e-sAg,eGFP (NPTII, P19)	x	x	HT	
	pEAQ-HT-CoHe7e-eGFPs	CoHe7e-eGFPs (NPTII, P19)		x	HT	
	pEAQ-HT-CoHe7e-eGFPs	CoHe7e-eGFPs (NPTII, P19)		x	HT	
	pDEST-BD-CoHe7e-eGFPL	CoHe7e-eGFPL (NPTII)	x	x	HT	Co-infiltrate pBIN61-P19
	pDEST-BD-CoHo7e-HAVP1	CoHo7e-HAVP1 (NPTII)	x	x	HT	Co-infiltrate pBIN61-P19
Chapter 5 – BTV-10	pDEST-BD-BTV10.3	BTV-10 VP3 (NPTII)	x	x	HT	Co-infiltrate pBIN61-P19
	pDEST-BD-BTV10.7	BTV-10 VP7 (NPTII)	x	x	HT	Co-infiltrate pBIN61-P19
	pDEST-BD-BTV10.3-His	BTV-10 VP3-His (NPTII)	x	x	HT	Co-infiltrate pBIN61-P19
	pDEST-BD-BTV10.7-His	BTV-10 VP7-His (NPTII)	x	x	HT	Co-infiltrate pBIN61-P19
	pEAQ-HT-BTV10.2	BTV-10 VP2 (NPTII, P19)		x	HT	
	pEAQ-HT-BTV10.2-His	BTV-10 VP2-His (NPTII, P19)		x	HT	
	pEAQ-HT-BTV10.5	BTV-10 VP5 (NPTII, P19)		x	HT	
	pEAQ-HT-BTV10.5-His	BTV-10 VP5-His (NPTII, P19)		x	HT	
	pEAQ-HT-BTV10.NS1	BTV-10 NS1 (NPTII, P19)		x	HT	
pEAQ-HT-BTV10.NS1-His	BTV-10 NS1-His (NPTII, P19)		x	HT		
Chapter 6 – BTV-8	pEAQ-HT-BTV8.2	BTV-8 VP2 (NPTII, P19)		x	HT	
	pEAQ-HT-BTV8.2co	BTV-8 VP2co (NPTII, P19)		x	HT	codon optimized
	pEAQ-HT-BTV8.3	BTV-8 VP3 (NPTII, P19)		x	HT	
	pEAQ-HT-BTV8.3co	BTV-8 VP3co (NPTII, P19)		x	HT	codon optimized
	pEAQ-HT-BTV8.5	BTV-8 VP5 (NPTII, P19)		x	HT	
	pEAQ-HT-BTV8.5co	BTV-8 VP5co (NPTII, P19)		x	HT	codon optimized
	pEAQ-HT-BTV8.7co	BTV-8 VP7co (NPTII, P19)		x	HT	codon optimized
	pEAQ-GW-BTV8.NS3	BTV-8 NS3 (NPTII, P19)	x	x	HT	
	pEAQex-BTV8.5co-BTV8.2co	BTV-8 VP5co, BTV-8 VP2co (P19)		x	HT	codon optimized
	pEAQex-BTV8.7co-BTV8.3co	BTV-8 VP7co, BTV-8 VP3co (P19)		x	HT	codon optimized
	pEAQex-BTV8.7-BTV8.3	BTV-8 VP7, BTV-8 VP3 (P19)		x	HT	

	Name	Encoded proteins	GW	Binary	5'-UTR	Notes
Chapter 6	pEAQex-BTV8-52co73	BTV-8 VP5co, BTV-8 VP2co, BTV-8 VP7, BTV-8 VP3 (P19)		x	<i>HT</i>	½ codon optimized, ½ wild-type
	pEAQex-BTV8co-7HT-3	BTV-8 VP7co, BTV-8 VP3co (P19)		x	→	VP7 is <i>HT</i> , VP3 is <i>wt</i>
Chapter 7 – fluorescent BTV	pEAQ-HT-GFP:BTV8.3co	BTV8 GFP:VP3co fusion (NPTII, P19)		x	<i>HT</i>	
	pEAQ-GFP:BTV8.3co	BTV8 GFP:VP3co fusion (NPTII, P19)		x	<i>wt</i>	
	pEAQ-mRuby:BTV8.3co	BTV8 mRuby:VP3co fusion (NPTII, P19)		x	<i>wt</i>	
	pEAQ-Sapphire:BTV8.3co	BTV8 mT-Sapphire:VP3co fusion (NPTII, P19)		x	<i>wt</i>	
	pEAQ-GFP	GFP (NPTII, P19)		x	<i>wt</i>	

APPENDIX B: SEQUENCES OF CODON-OPTIMIZED BTV8 GENES

The following sequences were codon-optimized for expression in *N. benthamiana* and synthesized by GeneArt AG. Start codons are highlighted in green, stop codons are highlighted in red. The restriction sites used for cloning into pEAQ-HT, namely AgeI and XhoI, are underlined in orange and blue, respectively.

BTV-8 VP2co

```

1   TTAATTAATC GCGACCGGTA TGGAAGAACT CGCTATCCCA ATCTACACTA
51  ACGTTTTCCC AGCTGAGCTT CTTGATGGAT ACGATTACAT CATCGATGTT
101 TCTTCTAGGG TTGAAGAAGA AGGCGACGAG CCAGTTAAGA GGCATGATGT
151 GACTGAGATT CCTAGGAACT CCATGTTCTGA TATCAAGGAT GAGCACATCA
201 GGGATGCTAT TATCTACAAG CCAGTGAACA ACGATGGATA CGTTTTGCCA
251 AGGGTGCTCG ATATTACTCT CAAGGCTTTC GATGATAGGA AGCGTGTTGT
301 TCTTAACGAT GGACACTCTG AGTTTCACAC TAAGACTAAC TGGGTGCAGT
351 GGATGATTGA TGATGCTATG GATGTGCAGC CACTCAAAGT TGATATTGCT
401 CACACTAGGT CTAGGATTTT TCACGCTCTC TTCAATTGCA CTGTGAGGCT
451 TCATTCTAAG AAGGCTGATA CTGCTTCTTA TCACGTTGAG CCAGTGGAAA
501 TTGAATCTTG GGGATGCAAT CACACTTGGC TTTCTAGGAT TCACCACCTT
551 GTTAACGTTG AGCTTTTCCA CTGTTCTCAA GAGGCTGCTT ACACTCTTAA
601 GCCAACTTAC AAGATCATTT CCAACGCTGA AAGGGCTTCT ACTTCCGATT
651 CTTTCAACGG AACTATGATC GAGCTTGGTA GGAATCATCA GATCCAGATG
701 GGAGATCAAG GATACCAGAA GCTTAAAGAG GGACTTGTTT AGGTTAGAAT
751 CGAGGGAAAG ACTCCACTTG TTATCCAGGA AGAGATCACT GCTCTCAACA
801 AGATTCGTGA GCAATGGATT GCTAGGAATT TCGATCAGCG TGAGATTAAG
851 GTTTTGGATT TGTGCAGGCT TCTTTCAACT ATCGGTAGGA AGATGTGCAA
901 TACTGAAGAG GAACCTAAGA ACGAGGCTGA TCTTTCTGTT AAGTTCAGA
951 TGGAACTCGA TGAGATTTTC AGGCCAGGAA ATAACGAGAG GACTAACATT
1001 ATGGGAGGTG GAGTTCATAG AAAGAACGAG GACAGGTTCT ACGTGCTCAT
1051 TATGATTGCT GCTTCCGATA CAAACAAGGG AAGGATTTGG TGGTCTAATC
1101 CATATCCATG TCTTAGGGGT GCTCTTATTG CTGCTGAGGT TCAGCTTGGA
1151 GATGTGTACA ACCTTCTCCG TAATTGGTTC CAATGGTCTG TTAGGCCAAC
1201 TTACGTTCCA TACGATAGGA ACAGAGAGTC CGATAAGTAC ATCTACTCCA
1251 GGATCAACCT TTTCGATTCT ACTCTTAGGC CAGGTGATAA GATTGTGCAC
1301 TGGGAGTACA AGCTTTTGAA CGAGGTTAGA GAGGTGTCAA TCAACAAGGG
1351 AAACGAGTGT GATTTGTTCC CAGAGGATGA AGAGTTCACT ACTAAGTTCC
1401 ATGAGGCTAG GTATACTGAG ATGAAGAACC AGATTATTCA GTCTGGATGG
1451 AACCAGAGGG ATTTCAAGAT GCACAAGATC CTTGAGGATG GTGCTAACGT
1501 GCTCACAATC GATTTTGAGA AGGATGCTCA CATTGGAAC TGGATCTGCTC
1551 TTTCTCTCCC TGATTACTAC AACAAGTGGA TTATCGCTCC AATGTTCAAC
1601 GCTAAGCTCA GGATTACTGA GGTGTGTGATT GGAAGTCTC ACACTGATGA
1651 TCCAGCTGTT GGAAGATCTG CTAAGGCTTT CACTCACGAT CCATTTCGATC
1701 TTCAAAGGTA CTGTCTCGCT AGGTATTATG ATGTTAGGCC AGGAATGATG
1751 GGTAGAGCTT TGTCTAAGCA GCAGAATATG TCCTCCATGA CTGATAAGCT
1801 TTCCAAGCAA GAGGATTACG CTGGAATTGT GTCAGAAGG CTTGAGTACA
1851 AAGAGAGAGA GAACCGTTGT CTTACTGAGA CTGCTCAGTA CGTTTTCGAA
1901 AAGACTTGCC TCTACGTTTT GGAGCTTCTT TCTAGGCATA CAATGCCATC
1951 TGAGGATTCT GAAGTGAAGT TCGAGCACCC AACTATTGAT CCATCTGTGG

```

2001 ATATCGAGAC TTGGAAGATC ATTGATGTGT CCCAGCTCAT TATCTTCGTG
 2051 TTCGATTACC TTTTCGAGAA CCGTAAGATC GTTAGGGATA CAACTGAAGC
 2101 TAGGTGGACT CTTTTCAAGA TTAGGTCTGA GGTTGGAAGG GCTAGGATTG
 2151 ATGCTATCGA GATGACTTTT CCAAGGTTCC GAAGGATGCT TAGGAATGCT
 2201 TCTCAGGCTA AGATCAACCA GGATATCGCT TGCCTTAACT TCCTTCCACT
 2251 CCTCTTCATT ATCGGTGATA ACATCTCTTA CGCTCATAGG CAATGGTCTA
 2301 TTCCAGTGCT TCTTTACGCT CACGATATCA GGATTATCCC ACTTGAGGTT
 2351 GGAGCTTACA ATAACAGGTT CGGACTTACT TCTTACCTTG AGTACATGGC
 2401 TTTCTTCCCA TCTTATGCTA CTAGGGTGGC AAAGATTGAT GAGTCCATCA
 2451 AAGAGTGCGC TATTGCTATG GCTGAGTTCT ACATGAACAC TGATATTCAC
 2501 TCTGGATCCG TGATGTCTAA CGTGATCACT ACTAAGAGGC TTCTCTACGA
 2551 GACTTACCTT GCTTCTCTTT GCGGTGGATA CTCTGATGGA CTTCTCTGGT
 2601 ACTTGCCAAT TACTCACCCA TCTAAGTGCC TTGTTGCTTT CGAAGTTGCT
 2651 GATGATGTTG TGCCACTTTC TGTTAGAAGA GAGAGGATTC TTTCTAGGTT
 2701 CCCACTTTCT TCAAGGCACG TGAAGGGAAT TGCTCTTATT TCCGTGGATA
 2751 GGAACCAGAA AGTTTCTGTT CAGACTGAGG GAATTGTGAC TCATAGGCTC
 2801 TGCAAGAAGA ACCTTCTCAA GTACGTTTGT GATGTGATCC TCTTCAAGTT
 2851 CTCTGGTCAC GTTTTCGGAA ACGATGAGAT GCTTACTAAG CTCCTCAACG
 2901 TTTGACTCGA GGCCTGGCGC GCC

BTv-8 VP3co

1 TTAATTAATC GCGACCGGTA TGGCTGCTCA AAATGAGCAA AGGCCAGAGA
 51 GGATTAAGAC TACTCCATAC CTTGAGGGTG ATGTGCTTTC TTCTGATTCT
 101 GGACCACTTC TTTCTGTTTT CGCTCTCCAA GAGATTATGC AGAAGGTTAG
 151 GCAAGTTCAG GCTGATTACA TGACTGCTAC TAGGGAAAGTT GATTTCACTG
 201 TTCCAGATGT GCAGAAAATC CTCGATGATA TCAAGGCTCT TGCTGCTGAG
 251 CAAGTGTACA AGATTGTGAA GGTGCCATCC ATTTCTTTCA GGCACATTGT
 301 GATGCAATCT AGGGATAGGG TTCTCAGAGT GGATACTTAC TACGAAGAGA
 351 TGTCTCAGGT TGGAGATGTG ATTACTGAAG ATGAGCCAGA GAAGTTCTAC
 401 TCCACTATCA TCAAGAAGGT GAGATTCATT AGGGGAAAGG GATCTTTCAT
 451 TCTCCACGAT ATCCCAACTA GAGATCACAG AGGAATGGAA GTTGCTGAGC
 501 CAGAAGTTCT TGGAGTTGAG TTCAAGAAATG TGCTTCCAGT TCTTACTGCT
 551 GAACACAGGG CTATGATTCA GAATGCTCTC GATGGATCTA TTATCGAGAA
 601 CGGAAACGTT GCAACTAGGG ATGTGGATGT GTTTATTGGA GCTTGCTCTG
 651 AGCCAATCTA CAGGATCTAC AACAGGCTTC AGGGATATAT TGAGGCTGTT
 701 CAGCTTCAAG AACTCAGGAA CTCTATTGGT TGGCTTGAAA GGCTTGGACA
 751 GAGGAAGAGG ATTACTTACT CTCAAGAGGT GCTCACTGAT TTTAGAAGGC
 801 AGGATACAAT TTGGGTTTTG GCTCTCCAGC TTCCAGTTAA CCCACAAGTT
 851 GTTTGGGATG TTCCAAGGTC CTCTATTGCT AACCTCATCA TGAACATTGC
 901 TACTTGCCCTT CCAACTGGTG AGTACATTGC TCCAAACCCA AGGATTTCTT
 951 CCATTACTCT CACTCAGAGG ATCACTACTA CTGGACCATT CGCTATTCTT
 1001 ACTGGATCTA CTCCAAGTGC TCAGCAGCTT AACGATGTGA GGAAGATCTA
 1051 CCTTGCTCTT ATGTTCCCAG GACAGATTAT TCTCGATCTC AAGATCGATC
 1101 CAGGTGAAAG AATGGATCCA GCTGTTAGAA TGTTTGCTGG TGTTGTTGGA
 1151 CACCTTCTTT TTAGTGCTGG TGGAAGGTTT ACTAACCTCA CACAGAATAT
 1201 GGCTAGGCAG CTTGATATTG CTCTCAACGA TTACCTCCTC TATATGTACA
 1251 ACACTAGGGT TCAGGTTAAC TATGGACCAA CTGGTGAACC ACTCGATTTT
 1301 CAGATTGGTA GGAACCAGTA CGATTGCAAT GTTTTTCAGGG CTGATTTTCGC
 1351 TACTGGAACT GGATACAATG GATGGGCTAC TATTGATGTG GAGTACAGAG
 1401 ATCCAGCTCC ATATGTTTCA TCTCAGCGTT ACATTAGGTA CTGCGGAATT
 1451 GATTCTAGGG AACTCATCAA CCCAACTACT TACGGAATCG GAATGACTTA
 1501 CCACTGCTAC AATGAGATGC TTAGGATGCT TGTTGCTGCT GGAAAGGATT

1551 CTGAGGCTGC T TACTTCAGA TCTATGCTCC CATTCCACAT GGTTAGGTTC
 1601 GCTAGGATTA ACCAGATCAT CAACGAGGAT CTTCACTCTG TTTTCTCCCT
 1651 CCCTGATGAT ATGTTCAACG CTCTCCTTCC TGATCTTATT GCTGGTGCTC
 1701 ATCAGAATGC TGATCCAGTT GTGCTTGATG TGTCTTGAT TTCTCTCTGG
 1751 TTCGCTTTCA ACAGATCTTT CGAGCCAAC TATAGGAATG AGATGTTGGA
 1801 GATTGCTCCA CTTATTGAGT CTGTGTACGC TTCTGAGCTT TCTGTTATGA
 1851 AGGTGGACAT GAGGCACCTT TCACTTATGC AAAGGCGTTT CCCAGATGTT
 1901 CTTATTCAAG CTAGGCCATC CCATTTTTGG AAGGCTGTGC TTAATGATTC
 1951 TCCAGAGGCT GTTAAGGCTG TGATGAACCT TTCTCACTCC CACAACCTCA
 2001 TCAACATCAG GGATATGATG AGATGGGTTC TCCTTCCATC TCTTCAACCA
 2051 TCTCTTAAGC TTGCTCTTGA AGAAGAAGCT TGGGCTGCTG CTAATGATTT
 2101 CGAGGATCTC ATGCTTACTG ATCAGGTTTA CATGCACAGG GATATGCTTC
 2151 CAGAACCCTAG GCTTGATGAT ATTGAGAGGT TCAGGCAAGA GGGATTCTAC
 2201 TACACTAACA TGCTTGAAGC TCCACCAGAA ATTGATAGGG TGGTGCAGTA
 2251 CACTTATGAG ATTGCTAGGC TCCAAGCTAA TATGGGACAA TTCAGGGCTG
 2301 CTCTTAGGCG TATTATGGAT GATGATGATT GGGTTAGGTT CGGAGGTGTT
 2351 CTTAGAACTG TGAGGGTGAA GTTTTTTGAT GCTAGGCCAC CAGATGATAT
 2401 TCTTCAGGGA CTCCCATTCT CTTACGATAC AAACGAGAAG GGTGGACTTT
 2451 CTTACGCTAC TATCAAGTAC GCTACTGAGA CTACTATCTT CTACCTCATC
 2501 TACAACGTGG AGTTCTCTAA CACTCCAGAT TCTCTCGTGC TCATCAACCC
 2551 TACTTACACT ATGACTAAGG TGTTTCATCAA CAAGAGAATT GTGGAGAGAG
 2601 TTAGGGTTGG ACAGATTCTT GCTGTGCTTA ACAGGCGTTT CGTTGCTTAT
 2651 AAGGGAAAGA TGAGGATCAT GGATATTACT CAGTCCCTCA AGATGGGAAC
 2701 TAAGCTTGCT GCTCCAACCTG TT **TAACTCGA** GGCCTGGCGC GCC

BTV-8 VP5co

1 TTAATTAATC GCG **ACCGGTA** TGGGAAAGAT TATTAAGTCC CTCTCAAGGT
 51 TCGGAAAGAA GGTGGAAAC GCTCTTACTT CCAACACTGC TAAGAAGATC
 101 TACTCCACTA TTGGAAAGGC TGCTGAGAGA TTTGCTGAGT CTGAGATTGG
 151 ATCCGCTGCT ATTGATGGAC TTGTTTCAAGG ATCTGTGCAC TCTCTTATGA
 201 CTGGTGAGTC TTACGGTGAG TCTGTAAAGC AAGCTGTGCT TCTTAACGTT
 251 ATGGGATCTG GTGAAGAACT TCCAGATCCA CTTTCTCCAG GTGAAAGGGG
 301 AATGCAGACT AAGATTCGTG AACTTGAGGA TGAACAGAGG AACGAGCTTA
 351 TTAGGCTCAA GTACAACGAT AAGATCAAGC AGAAGTTCGG AAAAGAGCTT
 401 GAAGAGGTTT ACGAGTTCAT GAACGGTGTT GCTAAGCAAG AGGAAGATGA
 451 AGAGAAGCAC TACGATGTGC TTAAGAAGGC TGTTAACTCC TACGATAAGA
 501 TCCTTACTGA GGAAGAGAAG CAGATGAGGA TTCTTGCTAC TGCTCTCCAG
 551 AAAGAGGTGA AAGAAAGGAC TGGAACCTGAG GCTGTTATGG TGAAAGAGTA
 601 CAGGAACAAG ATCGACGCTC TCAAAGAGGC TATTGAGGTT GAAAGGGATG
 651 GAATGCAGGA AGAAGCTATC CAAGAGATCG CTGGAATGAC TGCTGATGTT
 701 CTTGAAGCTG CTTCTGAAGA GGTTCCTACTT ATTGGAGCTG GAATGGCTAC
 751 TGCTGTTGCT ACTGGAAGGG CTATTGAGGG AGCTTACAAG CTTAAGAAGG
 801 TGATCAACGC TCTTTCTGGA ATTGATCTCA CTCACCTCAG GACTCCAAAG
 851 ATTGAGCCAA CTATCGTGTC TACTGTGCTC GATCACAAAG TCAAGGATAT
 901 CCCAGATGAG ATGCTTGCTG TGTCTGTGCT TTCTAAGAAT AGGGCTATCG
 951 AAGAGAACCA CAAAGAGATC ATCCACCTCA AGAACGAAAT TCTCCCAAGG
 1001 TTCAAGAAAG CTATGGATGA AGAGAAAGAG ATTTGCGGAA TCGAGGATAA
 1051 GAAGATCCAC CCAAAGGTTA TGATGAAGTT CAAGATCCCA AGGACTCAAC
 1101 AACACAGAT TCACATCTAT TCCGCACCTT GGGATTCTGA TGATGTGTTT
 1151 TTCTTCCACT GCATTTCTCA TCATCACGCT AACGAGTCTT TCTTCATCGG
 1201 ATTCGATCTT GGAATTGATT TGGTGCCTA CGAGGATCTT ACTGCTCATT
 1251 GGCATGCTCT TGGAGCTGCT CAAGCTGCTG TTGGAAGATC TCTTAACGAG

1301 GTGTACAAAG AGTTCCTTAA CCTCGCTATC AACAACTT ACTCCTCTCA
 1351 AATGCACGCT AGAAGGATGA TTAGGTCCAA GACTGTTCAC CCAATCTACC
 1401 TTGGATCTCT CCACTACGAT ATCTCATTCT CTACTCTCAG GTCTAATGCT
 1451 CAGAGGATTG TGTACGATGA GGAACCTCAG ATGCACATTC TTAGGGGACC
 1501 ACTTCATTTT CAGAGAAGGG CTATTCTCGG AGCTATTAAG CACGGTGTGA
 1551 AGATTCTTGG AACTGAAGTG GATATTCCAC TCTTCCTTAG GAACGCTTGA
 1601 CTCGAGGCCT GCGCGGCC

BTV-8 VP7co

1 TTAATTAATC GCGACCGGTA TG GATAACAAT TGCTGCTAGG GCTCTTACTG
 51 TTATGAGAGC TTGCGCTACT CTTCAAGAGG CTAGGATTGT GCTTGAGGCT
 101 AACGTGATGG AAATTCTCGG AATCGCTATC AATAGGTACA ACGGACTTAC
 151 TCTTAGGGGT GTTACTATGA GGCCAACTTC TCTTGCTCAG AGGAACGAGA
 201 TGTTCCTTCAT GTGCCTCGAT ATGATGCTTT CTGCTGCTGG TATTAACGTG
 251 GGACCAATCT CTCCAGATTA CACTCAGCAC ATGGCTACTA TTGGAGTTCT
 301 TGCTACTCCA GAGATCCCTT TTACTIONTGA GGCTGCTAAT GAGATTGCTA
 351 GGGTGACAGG TGAAACTTCT ACTTGGGGAC CAGCTAGACA ACCATACGGA
 401 TTTTCTTGG AGACTGAAGA GACTTTTCAA CCAGGACGTT GGTTTATGAG
 451 AGCTGCTCAA GCTGTTACTG CTGTTGTTTG CGGACCAGAT ATGATTCAGG
 501 TGTCCTTAA TGCTGGTGCT AGAGGTGATG TTCAGCAGAT TTTCCAGGGT
 551 AGGAACGATC CAATGATGAT CTACCTTGTG TGGAGAAGGA TTGAGAATTT
 601 CGCTATGGCT CAGGGAAATT CTCAACAAAC TCAGGCTGGT GTTACTGTTT
 651 CTGTTGGAGG TGTGATATG AGAGCTGGAA GGATTATTGC TTGGGATGGA
 701 CAAGCTGCAC TTCATGTTCA TAACCCAACT CAGCAGAATG CTATGGTTCA
 751 GATTCAGGTG GTGTTCTACA TCTCTATGGA TAAGACTCTC AACCAGTACC
 801 CAGCTCTTAC TGCTGAGATC TTCAACGTTT ACTCCTTCAG GGATCATACT
 851 TGGCATGGAC TCAGGACTGC TATTCTCAAC AGGACTACTC TTCCAAATAT
 901 GCTCCCACCA ATCTTCCCAC CAAACGATAG GGATTCTATC CTTACTTTGC
 951 TCCTTCTTAG CACTCTTGCT GATGTGTACA CTGTTCTTAG GCCAGAGTTC
 1001 GCTATTCATG GTGTTAATCC AATGCCAGGA CCACTTACTA GAGCTATTGC
 1051 TAGGGCTGCT TATGTGTGAC TCGAGGCCTG GCGCGGCC

APPENDIX C: PUBLICATION OF pEAQ VECTORS

The pEAQ vector series developed as part of this thesis has been published:

Sainsbury, F.*, Thuenemann, E.C.*, and Lomonosoff, G.P. (2009). pEAQ: versatile expression vectors for easy and quick transient expression of heterologous proteins in plants. *Plant Biotechnology Journal* **7**, 682-693.

* These authors contributed equally to the work.